2023

Marine and Human Environmental Factors Influence *Vibrio parahaemolyticus* and *Vibrio vulnificus In Vitro* Biofilm Processes on Plastics

Ryan Eric Leighton

Marine and Human Environmental Factors Influence *Vibrio parahaemolyticus* and *Vibrio vulnificus In Vitro* Biofilm Processes on Plastics

by

Ryan Eric Leighton

Bachelor of Arts
University of North Carolina, 2017

Master of Science
University of North Carolina, 2018

Submitted in Partial Fulfillment of the Requirements

For the Degree of Doctor of Philosophy in

Environmental Health Sciences

Arnold School of Public Health

University of South Carolina

2023

Accepted by:

Alan Decho, Major Professor

Sean Norman, Committee Member

Geoff Scott, Committee Member

John Ferry, Committee Member

Rachel Noble, Committee Member

Ann Vail, Dean of the Graduate School

DEDICATION

I would like to dedicate this work to my family. Without their support, none of this would have been possible. I would also like to dedicate this work to all the coffee shops and breweries in Columbia that I spent writing this work. They gave me the caffeine or beer that fueled the countless hours of writing, revising, organizing, and analyzing. I would lastly like to thank the countless music artists that kept me company and made all this work possible.

ACKNOWLEDGEMENTS

I would like to acknowledge the following people and organizations who made this study possible:

First, I would like to thank everyone in the Decho and Norman Labs, especially Karlen Correa Vélez, Samantha Case and Savannah Chandler for their expertise, help, attention to detail and support. I also want to thank my undergraduate research assistants, whose dedication made my lab work and life easier – Addison Creech, Gracie Anderson, Karishma Amirichetty and Grace Astarita.

I would also like to thank Dr. Guoshuai Cai and his student Liyan Xiong for their expertise in statistics and helping to explain and conduct the statistical analyses. I would have been very lost without you both!

I would like to acknowledge the incredible support of my dissertation committee: Dr. Alan Decho, Dr. Sean Norman, Dr. Geoff Scott, Dr. John Ferry and Dr. Rachel Noble. I am extremely grateful for my research advisor and mentor, Dr. Alan Decho. Dr. Decho, thank you so much for your years of patience, support, feedback, expertise and allowing me to grow as a researcher and scientist.

I would lastly like to thank the Center for Oceans and Human Health and Climate Change Interactions for funding my work and the entire Environmental Health Sciences Administrative Team for all their help. Great science can't happen without great support!

ABSTRACT

Marine bacteria often exist in biofilms as communities attached to surfaces, like plastic. Growing concerns exist regarding marine plastics acting as potential vectors of pathogenic *Vibrio*, especially in a changing climate. It has been generalized that *Vibrio vulnificus* and *Vibrio parahaemolyticus* often attach to plastic surfaces. Different strains of these *Vibrios* exist having different growth and biofilm forming properties. This work evaluated how temperature and strain variability affect *V. parahaemolyticus* and *V. vulnificus* biofilm formation and characteristics on glass (GL), low-density polyethylene (LDPE), polypropylene (PP), and polystyrene (PS). This work also evaluated how human body related factors like temperature, pH, nutrient availability, and media composition such as Human Plasma-Like Media (HPLM), Simulated Gastric Fluid (SGF) and Simulated Intestinal Fluid (SIF) affect *in vitro* biofilm dispersal processes by human isolated *V. parahaemolyticus* and *V. vulnificus*, especially from microplastics. Taken together, these studies suggest that different strains of *V. parahaemolyticus* and *V. vulnificus* can rapidly form biofilms with high cell densities and rapidly disperse from different plastic types *in vitro*. However, these biofilm processes are highly variable and are species-, strain-specific, and dependent on plastic type, especially under different temperatures, pH, nutrients, and fluid compositions. These studies also suggest that different species of *Vibrio* can rapidly respond to different environmental conditions, especially those related to human digestion.

TABLE OF CONTENTS

LIST OF TABLES

LIST OF FIGURES

LIST OF ABBREVIATIONS

ANOVA ..... Analysis of Variance

CFU ..... Colony Forming Units

EPS ..... Extracellular Polymeric Substance(s)

GL ..... Glass

HAB ..... Harmful Algal Bloom

HPLM ..... Human Plasma-Like Medium

LDPE ..... Low-Density Polyethylene

MPs ..... Microplastics

MSYE ..... Modified Seawater Yeast Extract

MS ..... Modified Seawater

OD ..... Optical Density

PBS ..... Phosphate Buffer Saline

PP ..... Polypropylene

PS ..... Polystyrene

RFU ..... Relative Fluorescence Unit

SD ..... Standard Deviation

SGF ..... Simulated Gastric Fluid

SIF ..... Simulated Intestinal Fluid

TE ..... Tris-EDTA

INTRODUCTION

Growing concerns exist regarding marine plastics acting as potential vectors of pathogenic *Vibrio*, especially in a changing climate. This dissertation is a collection of studies that focus on the effect of temperature, strain variability, pH, nutrient availability and media composition on *in vitro* biofilm production and dispersal by *V. parahaemolyticus* and *V. vulnificus* on low-density polyethylene, polypropylene, and polystyrene. The dissertation is organized accordingly, with the primary body of literature related to marine and human environmental factors that affect biofilm formation and dispersal and supporting work on modeling environmental factors' effects on *V. parahaemolyticus* and *V. vulnificus* planktonic and biofilm growth reported in the appendix. The format reflects publications (submitted or published). A total of three publications are anticipated from this body of work: three reporting original research.

Chapter 1 is a study that examined how strain variability and temperature affected biofilm processes on low-density polyethylene, polypropylene, and polystyrene. In this study we reported that all strains of both *Vibrio* species attached to GL (which was used as the control) and all plastics at all temperatures tested. As a species, *V. vulnificus* produced more biofilm on PS compared to GL, and biofilm biomass was enhanced at lower temperature compared to higher temperatures. However, all individual strains' biofilm biomass and cell densities varied greatly at all temperatures tested. It was also determined that total dry biofilm biomass for both species was greater on plastics

compared to GL. It was found that extracellular polymeric substance (EPS) chemical characteristics were similar on all plastics of both species, with extracellular proteins mainly contributing to the composition of EPS. All strains were hydrophobic at all temperatures tested, further illustrating both species' affinity for potential attachment to plastics. Taken together, this study suggests that different strains of *V. parahaemolyticus* and *V. vulnificus* can rapidly form biofilms with high cell densities on different plastic types *in vitro*. However, the biofilm process is highly variable and is species-, strain-specific, and dependent on plastic type, especially under different temperatures. This work was published in *Frontiers in Microbiology* (2023).

Chapter 2 is a study that examined how sudden exposure to changes in temperature, pH, nutrient availability, and media composition that mimic the human environment affect biofilm dispersal from LDPE, PP, and PS MPs. Both species were able to adequately disperse from all types of plastics under most exposure conditions. *V. parahaemolyticus* was able to tolerate and survive lower pH that resembles the gastric environment compared to *V. vulnificus.* pH had a positive effect on overall *V. parahaemolyticus* biofilm biomass in microplates and cell colonization from PP and PS. pH also had a positive effect on *V. vulnificus* cell colonization from LDPE and PP. However, most biofilm biomass, biofilm cell and dispersal cell densities of both species greatly varied after exposure to elevated temperature, pH and nutrient starvation. It was also found that certain exposures to simulated human medias affected both *V. parahaemolyticus* and *V. vulnificus* biofilm biomass and biofilm cell densities on LDPE, PP and PS compared to exposure to traditional media of similar pH. Cyclic-di-GMP was higher in biofilm cells compared to dispersal cells, but exposure to more stressful

conditions increased signal concentrations in both biofilm and dispersal states. Taken together, this study suggests that human pathogenic strains of *V. parahaemolyticus* and *V. vulnificus* can rapidly disperse with high cell densities from different plastic types *in vitro*. However, the biofilm dispersal process is highly variable and is species specific and dependent on plastic type, especially under different human body related environmental exposures. This work was published in *Frontiers in Microbiology* (2023).

The appendices are supplementary materials for the two chapters and a related study I contributed to with Dr. Norman's group at the University of South Carolina. Appendix A is composed of supplementary data and figures for Chapter 1 while Appendix B is composed of supplementary data and figures for Chapter 2. Appendix C is a study that used modeling of environmental variables like temperature and pH to determine the effects on planktonic and biofilm growth of *V. parahaemolyticus* and *V. vulnificus*. My role in this work was to determine biofilm biomass of several strains of both species at various pH levels at different temperatures at different timepoints. This study found different optimal conditions for *Vibrio* planktonic and biofilm lifecycles. In addition, this study showed that temperature and pH can impact *Vibrio* growth both within and between species. This work was published in *GeoHealth* (2023).

CHAPTER 1

VIBRIO PARAHAEMOLYTICUS AND *VIBRIO VULNIFICUS IN VITRO* COLONIZATION ON PLASTICS INFLUENCED BY TEMPERATURE AND STRAIN VARIABILITY[1]

[1] Leighton RE, Correa Vélez KE, Xiong L, Creech AG, Amirichetty KP, Anderson GK, Cai G, Norman RS and Decho AW (2023), *Vibrio parahaemolyticus* and *Vibrio vulnificus in vitro* colonization on plastics influenced by temperature and strain variability. Frontiers in Microbiology 13:1099502. 10.3389/fmicb.2022.1099502

1.1 Abstract

Marine bacteria often exist in biofilms as communities attached to surfaces, like plastic. Growing concerns exist regarding marine plastics acting as potential vectors of pathogenic *Vibrio*, especially in a changing climate. It has been generalized that *Vibrio vulnificus* and *Vibrio parahaemolyticus* often attach to plastic surfaces. Different strains of these *Vibrios* exist having different growth and biofilm forming properties. This study evaluated how temperature and strain variability affect *V. parahaemolyticus* and *V. vulnificus* biofilm formation and characteristics on glass (GL), low-density polyethylene (LDPE), polypropylene (PP), and polystyrene (PS). All strains of both species attached to GL and all plastics at 25, 30 and 35°C. As a species, *V. vulnificus* produced more biofilm on PS ($p \leq 0.05$) compared to GL, and biofilm biomass was enhanced at 25°C compared to 30° ($p \leq 0.01$) and 35°C ($p \leq 0.01$). However, all individual strains' biofilm biomass and cell densities varied greatly at all temperatures tested. Comparisons of biofilm forming strains for each species revealed a positive correlation ($r = 0.58$) between their dry biomass weight and OD_{570} values from crystal violet staining, and total dry biofilm biomass for both species was greater ($p \leq 0.01$) on plastics compared to GL. It was also found that extracellular polymeric substance (EPS) chemical characteristics were similar on all plastics of both species, with extracellular proteins mainly contributing to the composition of EPS. All strains were hydrophobic at 25, 30 and 35°C, further illustrating both species' affinity for potential attachment to plastics. Taken together, this study suggests that different strains of *V. parahaemolyticus* and *V. vulnificus* can rapidly form biofilms with high cell densities on different plastic types *in vitro*. However, the biofilm

process is highly variable and is species-, strain-specific, and dependent on plastic type, especially under different temperatures.

1.2 Introduction

Vibrio parahaemolyticus and *Vibrio vulnificus* are two known marine pathogens that naturally exist in the marine environment and can infect both marine animals and humans (Baker-Austin et al., 2018). They are a major concern to human health as they commonly infect humans through consumption of raw seafood (Elmahdi et al., 2018). The Centers for Disease Control and Prevention (CDC) estimates that pathogenic *Vibrio* cause approximately 80,000 illnesses in the United States each year, with 52,000 of these cases likely being attributed to ingestion of contaminated seafood (Control & Prevention, 2019). However, exact number of cases of vibriosis are unknown due to underreporting in clinical settings, as a typical infection can present as symptoms like other common health problems (Baker-Austin et al., 2010; Bell & Bott, 2021). Symptoms of both *V. parahaemolyticus* and *V. vulnificus* infections include cramps, nausea, fever, and bloody diarrhea. *V. vulnificus* skin infections can be more severe and lead to rapid septicemia and death if an open wound encounters salt or brackish water (Control & Prevention, 2019). Most bacterial diseases in humans are caused by biofilm infections, which are bacteria embedded within a self-secreted matrix that offers protection from the outside environment (Jamal et al., 2018).

Marine bacteria, including potentially pathogenic *Vibrio* species, often exist in biofilms, where communities of microbes are enclosed in a protective, self-secreted matrix of extracellular polymeric substances (EPS) and attached to a surface or as suspended aggregates (Decho & Gutierrez, 2017). The EPS matrix consists of organic

polymers such as polysaccharides, proteins and eDNA (extracellular DNA), and protects bacteria from environmental stresses like desiccation, changes in temperature and pH, competition and predation, sunlight exposure and from low nutrient conditions (De Kievit et al., 2001; Stewart & William Costerton, 2001; Donlan, 2002; Zettler, Mincer & Amaral-Zettler, 2013; Decho & Gutierrez, 2017; Lami, 2019). This matrix also contributes to enhanced protection of pathogenic strains from antibiotics and enhances virulence (Schroeder, Brooks & Brooks, 2017). In the past, most studies of bacteria have focused on analyses of individual planktonic cells in the water column. However, many natural marine bacteria, like *Vibrio*, often exist in biofilm states. Biofilms commonly occur on a variety of substrates in marine environments including animal carapaces, algae, ship hulls, and specifically plastics (Zettler, Mincer & Amaral-Zettler, 2013; De Tender et al., 2015; Dang & Lovell, 2016; Lage & Graca, 2016; de Carvalho, 2018). Growth of biofilms can be influenced by environmental factors including temperature.

Temperature is a primary environmental variable that influences *Vibrio* planktonic and biofilm lifecycles, and contributes greatly to growth and habitat range (Gilbert et al., 2012; Tiruvayipati & Bhassu, 2016; Ward et al., 2017; Hernández-Cabanyero et al., 2020). This presents a possibility that bacterial cells enclosed in the biofilm matrix on plastic surfaces may be responding to environmental changes by exhibiting different growth and activity patterns compared to their planktonic counterparts (Guzmán-Soto et al., 2021). Most cases of vibriosis occur during summer months due to warmer sea surface temperatures in which the bacteria thrive. However, *V. parahaemolyticus* and *V. vulnificus* infections are increasing in prevalence due to climate change contributing to rising seawater temperatures and extending the length of time of

warm sea surface temperatures (Parry et al., 2007; Whitehead et al., 2009; Baker-Austin et al., 2013; Baker-Austin et al., 2016; Vezzulli et al., 2016; Deeb et al., 2018; Control & Prevention, 2019). Since these two *Vibrio* species are known to form biofilms and have been shown to be early colonizers of plastic surfaces, it follows that plastics could increase *Vibrio* exposure to humans (Kesy et al., 2021; Tavelli et al., 2022). Attached biofilms could contribute to higher bacterial concentrations in contaminated seafood, leading to increased levels of bacterial exposure to humans if consumed raw (Keswani et al., 2016; Kesy et al., 2021).

The hydrophobic or hydrophilic nature of the bacterial cell surface also plays a major role in bacteria's ability to colonize and form biofilms on abiotic surfaces like plastics (Rosenberg, 1984; Reifsteck, Wee & Wilkinson, 1987). More hydrophobic cells adhere more strongly to hydrophobic surfaces like plastic, while more hydrophilic cells adhere more strongly to hydrophilic surfaces like glass (Kochkodan et al., 2008; Giaouris, Chapot-Chartier & Briandet, 2009). It is generally accepted that the lifecycles of pathogenic *Vibrios*, like *V. parahaemolyticus* and *V. vulnificus* include natural environmental and host-associated stages (Kamp et al., 2013; Tiruvayipati & Bhassu, 2016; Ghenem et al., 2017; Hernández-Cabanyero & Amaro, 2020). It has been suggested that within marine environments exposure to changes in temperature may increase chances of survival and infectivity of *V. parahaemolyticus* and *V. vulnificus* within host-associated stages (Motes et al., 1998; Strom & Paranjpye, 2000; Froelich & Noble, 2016; Sullivan & Neigel, 2018). While studies have identified genotypic and phenotypic traits that allow these bacteria to survive within each environment, the ability to form biofilms on plastics, which could help the bacteria transition between the two

environments by ingestion, is not well understood (Reidl & Klose, 2002; Oberbeckmann, Lder & Labrenz, 2015; Hernández-Cabanyero et al., 2019). There is an underlying knowledge gap regarding hydrophobicity of different strains of *V. parahaemolyticus* and *V. vulnificus* and their interactions with different types of plastics.

Bacterial colonization and biofilm development on surfaces involve multiple processes, one of which is material type surface characteristics (Flemming et al 2016). This means that hydrophobicity, hydrophilicity, and chemical composition of a surface like plastic can influence bacterial attachment and development (Nakanishi et al., 2021). There are several major types of plastic, which include polyethylene (PE), polypropylene (PP) polystyrene (PS). There are increased probabilities that these plastic types end up in marine environments due to their high production and usage (Andrady, 2003; Brien, 2007; Andrady, 2011; Eriksen et al., 2014; Lusher, Hollman & Mendoza, 2017). Contamination of marine habitats by large pieces of plastics (macroplastics) have raised environmental concerns due to their possible transfer to animals that may coincidently or selectively ingest plastic particles that have been mistaken for food, leading to health complications and death (Gregory, 2009). In addition, plastics poorly degrade in marine environments, and this degradation leads to smaller particulates, deemed “microplastics,” which are classified as plastic particles smaller than 5 millimeters in size (Arthur, Baker & Bamford, 2009; Eriksen et al., 2014; GESAMP, 2016). There are growing concerns that both macro- and microplastics can travel large distances and act as transport vectors for attached bacterial pathogens (Zettler, Mincer & Amaral-Zettler, 2013; Oberbeckmann, Lder & Labrenz, 2015; Debroas, Mone & Ter Halle, 2017; Kesy et al., 2019; Bowley et al., 2021).

Recent studies conducted in marine environments have found microbial communities associate and live on plastic surfaces. These plastic-associated communities have been termed the "Plastisphere," and has raised serious implications for both marine life and human health (Ward & Kach, 2009; Zettler, Mincer & Amaral-Zettler, 2013). *Vibrio* have been found to be a major community member on marine plastic particles, but *Vibrio* concentrations on plastic surfaces have appeared lower compared to natural marine particles (Bryant et al., 2016; Curren & Leong, 2019; Amaral-Zettler, Zettler & Mincer, 2020). However, since *Vibrio* biofilms have still been found on numerous macro and microplastic substate surface types in several marine surface waters, this implies that plastic particles could act as transport vectors of potentially pathogenic *Vibrio* to new areas outside of their native range and to marine animals that may accidently or selectively ingest the biofilm-associated plastic particles coincidently with food particles (Goldstein, Carson & Eriksen, 2014; Reisser et al., 2014; Kirstein et al., 2016; Viršek et al., 2017; Bowley et al., 2021). In addition, since these bacteria are in close proximity to each other in biofilms on plastics, there is high potential for horizontal transfer of antibiotic-resistance genes, compounding the exposure risk to both marine and human health (Arias-Andres et al., 2018; Laverty et al., 2020).

In this study, we examined the effect of temperature on *in vitro* biofilm production by *V. parahaemolyticus* and *V. vulnificus* on different types of plastics, which included low-density polyethylene, polypropylene, and polystyrene. We compared biofilm production of both species, from three strains isolated from different sources (human, animal, and water), a total of six different strains. We hypothesized that all strains from both *Vibrio* species would produce greater amounts of biofilm on all plastic

types compared to a glass (control) due to the increased hydrophobic properties of plastic, which make it a more suitable substrate for colonization. Higher temperatures for *V. parahaemolyticus* and lower temperatures for *V. vulnificus* should also lead to increased biofilm formation on plastics due to previous studies that have examined both species biofilm production under different temperature conditions. We also postulated that human isolated strains of both species would produce the greatest amount of biofilm on all plastic types compared to animal and seawater isolated strains due to the harsher survival conditions in human hosts compared to the marine environment.

1.3 Materials and Methods

Bacterial Strains and Growth Conditions

Two clinical and two animal strains were obtained from the American Type Culture Collection (ATCC, Manassas, VA, United States). One seawater strain was gifted from the National Oceanic Atmospheric Administration (NOAA) Charleston, SC, United States and was originally isolated from the marine environment (methods in Supplementary Material, Vickery et al., 2007) in South Carolina, and one other seawater strain for this study was also directly isolated from the marine environment (methods in Supplementary Material, Kim et al., 2015) in South Carolina (Table 1.1). *V. parahaemolyticus* strains are commonly classified by their species marker (*tlh*) and capacity to infect humans through production of thermostable direct hemolysin (*tdh*) or thermostable direct hemolysin-related hemolysin (*trh*) virulence factors (Honda & Iida, 1993; Broberg, Calder & Orth, 2011). In our study, human isolated strain ATCC17802 contained *tlh* and *trh*, mollusk isolated strain ATCC43996 contained *tlh* and *tdh*, while the seawater isolate strain vpC12 only contained the species marker *tlh*. While *V.*

vulnificus strains can also be classified by virulence factors, *V. vulnificus* can also be classified by 16S rRNA typing, which reveals if they are more clinically- (type B, higher possible human infectivity) or more environmentally- (type A, higher possible marine vertebrate infectivity) associated. In our study, the human isolate strain ATCC27562 and seawater isolate strain are type B while eel isolate strain (ATCC33147) is type A.

One clinical, one animal and one seawater isolated strain of both *V. vulnificus* and *V. parahaemolyticus* were tested for biofilm formation at different temperatures on different substrate surfaces. All strains were maintained in 25% (vol/vol) glycerol at −80°C to be used in further experiments. A single colony of each bacteria was inoculated in 5 mL modified seawater with yeast extract (MSYE, ATCC medium 804, Oliver & Colwell, 1973) broth supplemented with calcium chloride (1.8 g/L), as calcium chloride contributes to biofilm formation (Tischler et al., 2018), and incubated overnight at 35°C with shaking (180 rpm). After incubation, the broth culture was adjusted to 10^7 cells (OD_{600}) using a SpectraMax M3 plate reader after calibrating the instrument's absorbance values to cell counts from spread plating (Molecular Devices, San Jose, CA, United States).

Biofilm Formation

Biofilm formation experiments were adapted from Hamanaka et al., 2012 and Valquier-Flynn et al., 2017. Disc coupons (Table 1.2, BioSurface Technologies, Boseman, MT, USA) were chemically sterilized (70% ethanol for GL and PP, 70% isopropanol for LDPE and PS) for 24 hours and were then placed in sterile petri dishes in a biosafety cabinet until residual alcohol evaporated. Then the coupons were placed in 24-well sterile non-treated microplates (Costar®, Corning, NY, USA) or sterilized slide

coupons (Biosurface Technol.) in sterile petri dishes (Falcon®, Corning, NY, USA), and then were filled with 990 μL (24-well microplate) or 14.85 mL (petri dish) of fresh MSYE broth supplemented with calcium chloride medium. The plates were then inoculated with 10 μL of the bacterial cultures for 24 well plates and 150 μL for petri dishes (10^7 cells) to achieve a final cell density of 10^5 cells per well/dish. Then, the 24-well plates were incubated at 25, 30, 35°C with low shaking (125 rpm) to form biofilms in 24 hours, and petri dishes incubated at 30°C with low shaking (85 rpm) to form biofilms in 48 hours, with spent media in petri dishes being replaced with 15 mL fresh media after 24 hours. Low shaking conditions, instead of static, were chosen to introduce shear stress to the biofilms, to better resemble the marine environment. Borosilicate glass coupons were chosen as the substrate type controls and used as the substrate reference for statistical analyses. Wells/dishes containing MSYE broth supplemented with calcium chloride without inoculation and with coupons were used as blank and group controls. Biofilm biomass on each disc coupon experimental and control group had biological triplicates and each experiment was conducted three times independently. Biofilm biomass on each slide coupon experimental group was pooled from 10 biological replicates one time. All plates/dishes were sealed with Parafilm™ (Bemis, Neenah, WI, USA) to reduce evaporative loss of media.

Crystal Violet Staining Assay

Biofilms of both *V. parahaemolyticus* and *V. vulnificus* were quantified by crystal violet staining according to O'Toole, 2011 and Valquier-Flynn et al., 2017 with some modifications. Following 24-hour incubation, planktonic cells were removed from the 24-well microplates before gently washing with 1X phosphate buffer saline (PBS, Molecular

Biologicals International, Irvine, CA, USA) three times. 500 µL of 100% methanol (Sigma-Aldrich)) was then added to the plates to fix the biofilms to the glass and plastics and incubated at room temperature for 20 minutes. Then, the methanol was removed, and residual methanol allowed to evaporate off disc coupon surfaces. The biofilms were stained with 700 µL of 0.1% (wt/vol) crystal violet (Sigma-Aldrich) for 15 minutes at room temperature. The staining solution was removed, and then 1X PBS was used to remove the non-bound dye four times. The glass and plastic coupons were then transferred to a new 24-well non-treated microplate and the stained and washed biofilms were air dried overnight. Lastly, 600 µL of 30% acetic acid (Fisher Scientific) was added to dissolve the bound crystal violet and incubated at room temperature for 15 minutes. Optical densities of each well were measured by absorbance (570 nm) using a SpectraMax M3 plate reader (Molecular Devices). Mean OD_{570} values were then divided by the surface area (405 mm^2) of the disc coupons tested to obtain final biofilm biomass values per mm of the surface type.

Biofilm Removal and Determination of Colony Counts

Total colony counts were determined from biofilm suspensions according to Portillo et al., 2013 and Bjerkan, Witsø & Bergh, 2009 with some modifications. Following 24-hour incubation, planktonic cells were removed from the 24-well non-treated microplate wells before washing disc coupons with 700 µL 1X PBS gently, four times. Then, disc coupons were placed individually in 10 mL 1X PBS in a conical tube (Falcon®) and vortexed using a Vortex Genie 2® (Fisher Sci.) at the highest setting for 1 minute. Then, coupons and 1X PBS solution were individually transferred to borosilicate glass culture tubes (VWR International, Radnor, PA, USA) and placed in a Branson

M2800 ultrasonication water bath (Branson Ultrasonics, Brookfield, CT, USA) and sonicated for 5 minutes at 40 kHZ. The coupons and 1X PBS solution were then transferred back to conical tubes, and vortexed again for 1 minute. Then, the biofilm suspension in 1X PBS was serially diluted in 1X PBS in conical tubes and 10^{-4} to 10^{-7} serial dilutions were spread onto prewarmed MSYE supplemented with calcium chloride agar plates. Plates were incubated at 30°C for 20-24 hours. The viability of cells was determined in terms of colony forming units (CFU) per coupon. Biofilm cell densities of each disc coupon experimental and control group had biological triplicates and each experiment was conducted three times independently. Mean CFU values were then log transformed and divided by the surface area (405 mm^2) of the disc coupons tested to obtain final CFU values per mm of the surface type.

EPS Extraction and Measurements of Dry Cell and EPS Biomass Concentrations

The strains of both *Vibrio* species that exhibited greatest biofilm biomass, on average, combined on all plastic disc surface types were used for measuring cell and EPS concentrations. *V. parahaemolyticus* strain ATCC17802 (human) and *V. vulnificus* strain vv155 (seawater) exhibited the greatest mean combined biomass per mm^2 of all plastic disc surfaces at 30°C (OD_{570} / 405mm^2 ~ 4.17E-03). EPS extraction was conducted according to Bramhachari et al., 2007 with some modifications. Following 48-hour incubation at 30°C, planktonic cells were removed from petri dishes before washing slide coupon with 10 mL 0.85% saline gently two times. Then, the slide coupon was placed in 30 mL 0.85% saline in a conical tube and vortexed at highest setting for one minute for plastics, and low setting for glass. Then, coupon and 0.85% saline solution were transferred to borosilicate glass test tube, and placed in water sonication bath, and

sonicated for five minutes at 40 kHz. The coupon and saline solution were then transferred back to conical tube, and vortexed again for one minute. Lastly, the coupon was then scraped on all sides with a cell scraper (Falcon®, Corning, NY, USA), scraper submerged in solution, and coupon removed. This was repeated 9 more times to pool 10 slide coupons' total cell and EPS contents in 0.85% saline solution. Then, the 30 mL 0.85% saline biofilm suspension was centrifuged (4,000 x g) to pellet cells. Cell pellet was then resuspended in same solution, centrifuged again, and this process repeated two more times. Cell pellet was saved at 4°C while supernatant (EPS solution) was then immediately mixed with 75% total volume cold ethanol (VWR) overnight to precipitate the EPS. Total EPS and ethanol solution was then centrifuged to pellet EPS, the supernatant removed, and the remaining EPS saved. The cell pellet and crude EPS was then freeze dried using a FreeZone® 6 system (Labconco, Kansas City, MO, USA) and weighed.

EPS Chemical Composition Analysis

The total carbohydrate content was measured after first dialyzing the EPS solution in SnakeSkin™ membrane with a 10,000 molecular weight cut-off (Fisher Sci.) in a borosilicate glass beaker of deionized water for 24 hours at 4°C. Then the EPS solution was mixed with 75% total volume cold ethanol (VWR) overnight to precipitate the EPS. Total EPS and ethanol solution were then centrifuged to pellet EPS, the supernatant removed, and the remaining EPS saved. The EPS was then freeze-dried and weighed. This was repeated three times for each plastic type for (1) carbohydrate, (2) protein and (3) eDNA quantification. (1) Dried crude EPS was prepared and carbohydrate content quantified according to Dubois et al., 1951 using a Total Carbohydrate Assay Kit with

glucose as the calibration standard according to manufacturer's instructions (Cell Biolabs, San Diego, CA, USA). The measurement was carried out using absorbance (490 nm) (Molecular Devices, San Jose, CA, USA). (2) Dried crude EPS was prepared by using a Compat-Able™ Protein Assay Preparation Reagent kit (Fisher Sci.) according Jiao et al., 2010 and manufacturer's instructions. Then the protein content was measured using a Bradford assay kit with bovine serum albumin (BSA) as the calibration standard according to manufacturer's instructions (Fisher Sci.). Absorbance measurements were conducted (595 nm). (3) Dried crude EPS was prepared according to Grande et al., 2015. EPS was resuspended in 1 mL 1X TE buffer (Fisher Sci.) and DNA was quantified using the Invitrogen Quant-iT™ PicoGreen™ dsDNA reagent kit (Molecular Probes, Eugene, OR, USA), with λ-DNA as the calibration standard according to manufacturer's instructions. Fluorescence was measured using a SpectraMax M3 plate reader (excit/emiss = 480/520 nm). % EPS by weight was calculated by standardization of each mean concentration of proteins, carbohydrates and eDNA to µg/mL, then divided by total starting weight of pooled crude EPS from 10 samples.

Hydrophobicity Assay

Microbial adherence to hydrocarbons was determined using p-xylene according to the MATH test method (Rosenberg, 1984; Kwaszewska, Brewczynska & Szewczyk, 2006; Mizan et al., 2016) with slight modifications. Briefly, overnight cultures of all strains in MSYE broth supplemented with calcium chloride were diluted to 10^5 cells and then grown at 25, 30 and 35°C for 24 hours at 125 rpm. The cells were harvested by centrifugation (4,000 x g) for 10 minutes, washed twice with 1X PBS, and then resuspended in 1X PBS to an OD_{600} ~0.3 – 0.6 (A0). One mL of p-xylene (Beantown

Chemical, Hudson, NH, USA) was added to a conical tube containing four mL of the adjusted bacterial/PBS suspension and the mixture was then vortexed vigorously at the highest setting for two minutes and incubated for 20 minutes at room temperature to allow separation of the two phases. The supernatant (aqueous hydrocarbon phase) was then carefully removed using glass Pasteur pipettes and cellular absorbance was measured (OD_{600}) in PBS suspension (A1). Hydrophobicity was calculated as the percentage of planktonic cells partitioning into the hydrocarbon phase. The percentage of p-xylene partitioning was estimated using the following formula: $([A0 – A1]/A0) \times 100$ (Rivas et al. 2008). A mean adherence to p-xylene ≤ 30% indicated that the strains were hydrophilic; values > 30% signified hydrophobic strains. Highly hydrophobic strains exhibited values ≥ 70% (Kwaszewska, Brewczynska & Szewczyk, 2006). Each experimental and control group was completed in biological triplicate and each experiment conducted independently three times.

Statistical Analyses

The experimental data for biomass CFUs, and hydrophobicity were expressed as the mean ± standard deviation. Biomass dry weights from slide coupons were expressed as mean total pooled biomass from 10 biological replicates. Biochemical characteristic weights of EPS were expressed as a percentage of the total pooled EPS weight of plastic type. Two-way analysis of variance (ANOVA) models were calculated using Rstudio software to compare value differences ($\alpha = 0.05$). Strain, temperature and surface type were the variables for all models. Glass was selected as the reference surface and 25°C was selected as the reference temperature for all analyses. Also, *V. parahaemolyticus* strain ATCC17802 was selected as the reference strain for all *V. parahaemolyticus* strains

while *V. vulnificus* strain ATCC27562 was selected as the reference strain for all *V. vulnificus* strains. Bonferroni correction was calculated and applied to p-values to control for type 1 error. A t-test ($\alpha = 0.05$) was calculated for comparison between mean total dry biomass weights between all plastics and glass and a Pearson correlation coefficient was calculated for comparison between mean total dry biomass weight and mean biofilm biomass absorbance data using Excel's data analysis toolpak.

1.4 Results

Plastics Enhance *V. parahaemolyticus* and *V. vulnificus* Biofilm Formation Compared to Glass

Experiments were conducted to test the effect of temperature (25, 30, and 35 °C) on biofilm biomass production and biofilm cell viability on glass (GL), low density polyethylene (LDPE), polypropylene (PP), and polystyrene (PS) by three different strains of both *V. parahaemolyticus* and *V. vulnificus* for 24 hours. The vortex/sonication method as described previously was first tested to confirm efficacy of biofilm removal from all substate surfaces while also preserving cell viability (Supplemental Figure A.1 – A.3, Table A.14, A.15). Raw mean data are presented in Supplemental Tables A.1 and A.6.

The crystal violet staining assay reflects total bacterial biomass formed on the substate surface types. The biofilm removal and colony count assay reflects biofilm cell densities (expressed as colony forming units, CFUs) on the substate surface types. From these two assays, it was shown that at a species level, both *V. parahaemolyticus* and *V. vulnificus* appeared to have greater biofilm biomass and CFU concentrations at all temperatures tested on all combined plastic types compared to GL (Figure 1). *V. parahaemolyticus* formed greater biofilms and had slightly greater biofilm CFU

concentrations at 30°C and 35°C on all combined plastic types, while *V. vulnificus* formed greater biofilm biomass at 25°C, but had slightly greater biofilm CFU concentrations at 30°C and 35°C. The comparison of biofilm biomass between *Vibrio* species revealed high biomass variability between substrate surface composition types (glass vs. plastic) at different temperatures, as indicated by high standard deviation bars. Comparison of biofilm biomass between combined species isolate types (human, animal, water) also revealed high biomass variability between all substrate surfaces at different temperatures (Supplemental Figure A.4). However, these high standard deviation bars are due to high variability between species and strain types.

Surface Material and Temperature Influences *V. parahaemolyticus* and *V. vulnificus* Biofilm Formation

Examining biofilm formation on individual plastic types of LDPE, PP and PS at different temperatures (25, 30 35°C) revealed that as a species *V. parahaemolyticus* appeared to form the greatest biofilms, on average, on LDPE and PP at 30°C and 35°C and had higher CFU concentrations across all plastics compared to GL (Figure 1.2). *V. parahaemolyticus* biofilm formation on PS was only marginally higher than GL at all temperatures yet still had an overall higher CFU concentration compared to GL. *V. parahaemolyticus* formed the greatest biofilms across all temperatures on LDPE and PP, which have a specific density lower than seawater (~1.02), compared to PS and GL which have a higher specific density than seawater. Comparatively, as a species *V. vulnificus* appeared to form greater biofilms, on average, on all plastic types at 25°C. Also, compared to *V. parahaemolyticus*, *V. vulnificus* biofilm formation was greatest on PS at 25°C. *V. vulnificus* formed greater biofilms on LDPE at 35°C compared to 30°C,

but this trend was opposite for PS as biofilm formation was greater at 30°C than 35°C. *V. vulnificus* biofilm biomass and CFU concentrations on LDPE and PS were also higher than GL across all temperatures. *V. vulnificus* biofilm formation on PP was only slightly higher than GL at higher temperatures (30, 35°C), and had lower biofilm biomass at 25°C and lower CFU concentrations on PP at 25 and 30°C compared to GL.

ANOVA revealed certain significant differences ($\alpha = 0.05$) in the amount of biofilm formation on each plastic type compared to glass at the species level (Figure 1.2, Supplemental Tables A.3 – A.5, A.8 – A.10). *V. parahaemolyticus* did not produce significantly more biofilm or significantly more CFUs on any plastic surface ($p = 0.99$) compared to GL. Temperature was also not a significant factor in contributing to *V. parahaemolyticus* biofilm biomass (30° $p = 0.99$, 35°C $p = 0.99$) or CFUs (30°C $p = 0.99$, 35°C $p = 0.99$). However, *V. vulnificus* produced significantly more biofilm, but not CFUs, on PS ($p \leq 0.05$) compared to GL. *V. vulnificus* biofilm biomass production was also significantly enhanced at 25°C compared to 30° ($p \leq 0.01$) and 35°C ($p \leq 0.01$).

Strain Type Influences *V. parahaemolyticus* and *V. vulnificus* Colonization and Biofilm Biomass and Cell Viability

At a strain level, the highest biofilm formation with a mean OD_{570} per mm^2 (OD_{570} / $405mm^2$) of 5.92E-03 was obtained on LDPE and PP by *V. parahaemolyticus* strain ATCC17802 at 30°C, and the lowest biofilm formation with a mean OD_{570} per mm^2 of 7.41E-05 was obtained on PP by *V. parahaemolyticus* strain vpC12 at 30°C. This further highlights the variability of biofilm formation between different strains of the same species (Figure 1.3A, Table A.1). All strains of both *Vibrio* species also had high concentrations of biofilm CFUs on GL and the three types of plastic over 24 hours and

under all temperature conditions. The highest CFU concentration was obtained on LDPE by *V. vulnificus* strain vv155 at 35°C, while the lowest CFU concentration was obtained on GL by *V. vulnificus* strain ATCC33147 at 30°C (Figure 1.3B, Supplemental Table A.6). Further comparison of the individual strains revealed significant differences ($p \leq 0.05$) in biofilm formation and CFUs between strains on different surfaces and temperatures (Figure 1.3A, B, Supplemental Table A.1, A.6).

V. parahaemolyticus animal isolate (ATCC43996) and seawater isolate vpC12 produced significantly lower biofilm biomass ($p \leq 0.001$) and CFUs ($p \leq 0.01$) than human isolate ATCC17802 (Supplemental Table A.2, A.7). Human isolated strain ATCC17802 had significantly greater biofilm formation ($p \leq 0.05$) and CFU concentrations ($p \leq 0.01$) on all plastic surfaces compared to glass. This strain also produced significantly greater biofilms and had greater CFU concentrations at 30 and 35°C ($p \leq 0.05$) compared to 25°C. Animal isolated strain ATCC43996 also had significantly greater ($p \leq 0.01$) biofilm formation on all plastic surfaces compared to GL. However, elevated temperatures (30, 35°C) significantly decreased ($p \leq 0.01$) the amount of overall biofilm produced by this strain compared to 25°C, but an increase in temperature had no significant effect (30°C, $p = 0.2$; 35°, $p = 0.12$) on CFU concentrations. Seawater isolate strain vpC12 did not have significantly greater ($p > 0.05$) biofilm biomass or CFU concentrations on any plastic surface compared to GL, however elevated temperature (30°C) did lead to a significant decrease ($p \leq 0.05$) in overall biofilm production compared to 25°C.

V. vulnificus animal isolate ATCC33147 had no significant differences in biofilm biomass ($p = 0.99$) or CFU concentrations ($p = 0.99$) compared to human isolate

ATCC27562 (Supplemental Table A.2, A.7). However, water isolate vv155 surprisingly produced significantly greater biofilm biomass ($p \leq 0.001$) and had significantly higher CFU concentrations ($p \leq 0.05$) than ATCC27562. Human isolated strain ATCC27562 did not have significantly greater ($p > 0.05$) biofilm biomass or CFU concentrations on any plastic surface compared to GL, however elevated temperature (30, 35°C) did lead to a significant decrease ($p \leq 0.01$) in overall biofilm production. Animal isolated strain ATCC33147 had significantly greater ($p \leq 0.05$) biofilm formation on PS compared to GL, and significantly greater ($p \leq 0.05$) CFUs on LDPE compared to GL. However, elevated temperature (30, 35°C) also led to a significant decrease ($p \leq 0.05$) in overall biofilm production, but not in CFU concentrations, compared to 25°C. Seawater isolated strain vv155 had significantly greater ($p \leq 0.05$) biofilm formation on PS compared to GL, but an increase in temperature had no significant effect ($p > 0.05$) on overall biofilm biomass and CFU concentrations.

Comparison of biofilm biomass between combined species isolate sources (human, animal, water) revealed high biomass and CFU variability between surface types at different temperatures as indicated by high standard deviations (Supplemental Figure A.3). While it appeared human isolated strains tended to produce, on average, greater biofilms and CFUs on LDPE and PP at higher temperatures (30, 35°C), *V. parahaemolyticus* strain ATCC17802 mainly accounted for this high biofilm mean due to it being the greatest biofilm former at higher temperatures compared to *V. vulnificus* strain ATCC27562 that formed greater biofilms at 25°C across all surface types (Figure 1.3A, B, Supplemental Table A.1, A.6). The other strain sources (animal and water) of

both species formed greater biofilms, on average, at 25°C across all surface types than at higher temperatures (30, 35°C).

Comparison of biofilm biomass between isolates and plastic surface types revealed differences in mean percent change compared to GL (Table 1.3). 41/54 total means of biofilm biomass on plastic across all temperatures had a mean positive percent change in biofilm biomass compared to GL. The greatest mean positive percent change compared to GL was observed with strain ATCC17802 on LDPE and PP at 25°C and 30°C. Strains vpC12 and ATCC27562 accounted for 9/12 of the negative mean percent changes in biomass across all temperatures, meaning they formed greater biofilms on GL, on average, compared to plastic in these cases. However, most of these negative percent changes were attributed to LDPE and PP compared to GL, as both strains had a mean positive percent change on PS compared to GL.

Comparison of biofilm CFU concentrations between isolates and plastic surface types at all temperatures tested revealed differences in % change compared to GL (Table 1.4). 42/54 total means of biofilm CFU concentrations on plastic across all temperatures had a mean positive % change in biofilm CFU concentrations compared to GL. The greatest mean positive % change compared to GL was observed with strain ATCC33137 at 30°C on LDPE. Strains vpC12 and ATCC27562 accounted for 8/12 of the negative mean % changes in biofilm CFUs across all temperatures, meaning they had greater mean biofilm CFUs on GL compared to specific plastic types in these cases. However, strain vpC12 had a mean positive % change in CFU concentrations at 25°C on all plastic types and strain ATCC27562 had a mean positive % change in CFU concentrations at 35°C on

all plastic types. At 35°C, 5/6 strains had a mean positive % change in biofilm CFUs on all plastic types compared to glass and lower temperatures.

Differences in Substrate Type Affect Biofilm Cell and Extracellular Polymeric Substance Concentration and Composition

Across all strains, *V. parahaemolyticus* strain ATCC17802 and *V. vulnificus* strain vv155 had the highest mean combined biomass per mm^2 of all plastics at 30°C (OD_{570} / $405mm^2$ ~ 4.17E-03). These strains were chosen to be further analyzed for cell and EPS weight and EPS biochemical characterization. Comparison of ATCC17802 and vv155 strains combined total dry biomass on glass compared to plastic revealed significantly greater total dry biomass weights on all plastic types compared to glass ($p \leq 0.01$) (Table 1.5). Further comparison revealed a moderately positive Pearson correlation coefficient ($r = 0.58$) between mean total dry biofilm biomass weights (mg) and mean biofilm biomass from crystal violet staining (OD_{570}) of all surfaces of both strains.

Biochemical characterization of both *Vibrio* species EPS revealed that extracellular proteins were the main component of the EPS, followed by carbohydrates and eDNA on all plastic types (Figure 1.4, Supplemental Table A.11). *V. parahaemolyticus* extracellular proteins accounted for 75, 77, 76% of total EPS mass on LDPE, PP, and PS respectively. *V. parahaemolyticus* extracellular carbohydrates made up 16, 21, 18% of total EPS mass on LDPE, PP, and PS respectively, and eDNA made up ~1% of total EPS mass on each plastic type. *V. vulnificus* extracellular proteins accounted for 80, 83, 70% of total EPS mass on LDPE, PP, and PS respectively. *V. vulnificus* extracellular carbohydrates accounted for 17, 13, 26% of total EPS on LDPE, PP, and PS respectively and eDNA also made up ~1% of total EPS mass on each plastic type.

Temperature and Strain Variability Influences Planktonic Cell Hydrophobicity

The MATH method, which is based on the degree of adherence to the hydrocarbon-p-xylene interface, showed that all strains were moderately (values > 30%) to strongly (values ≥ 70%) adhesive to p-xylene, and thus considered hydrophobic, at all temperatures tested (Figure 1.5). Raw mean hydrophobicity data are presented in Table A.12 in the Supplementary Data. Most strains (5/6) became slightly less hydrophobic as temperature increased from 25°C to 35°C. *V. parahaemolyticus* strain ATCC43996 was highly hydrophobic at 25 and 30°C while all *V. vulnificus* strains were highly hydrophobic at 25°C, with strain ATCC33147 also being highly hydrophobic at 30 and 35°C. At a species level, *V. vulnificus* was, on average, more hydrophobic than *V. parahaemolyticus* at all temperatures tested, especially at 30 and 35°C (19% and 16% more hydrophobic, respectively; Supplemental Table A.13).

1.5 Discussion

While plastic pollution in the marine environment remains a global concern, their role as substrates for microbial habitats and subsequently vectors for the dispersion of pathogenic or non-pathogenic bacteria must be further evaluated, especially under evolving climate change scenarios (Zettler, Mincer & Amaral-Zettler, 2013; Kirstein et al., 2016). *V. parahaemolyticus* and *V. vulnificus* are potential pathogenic bacteria that can infect both marine animals and humans. In past decades, *Vibrio* habitat range has increased and coincided with an increase in plastic production and growth. This expansion of *Vibrio* coupled with their potential to colonize and live on numerous plastic types will increase the potential risk of both marine animal and human exposure to *Vibrio* species. To better understand the emerging environmental and public health risks

associated with bacterial colonization of plastic particles, studies are needed to determine how this process is affected by different substrate types under different environmental conditions, such as temperature. This study focused on how different bacterial strains from distinct isolation sources of both *V. parahaemolyticus* and *V. vulnificus* interact with common marine plastics, such as low-density polyethylene, polypropylene, and polystyrene, under different temperatures.

Bacterial cells have been shown to attach quicker and to grow and develop biofilms more rapidly on hydrophobic surfaces like plastics compared with hydrophilic surfaces like glass (Donlan, 2002). Our study further suggests this as plastic was found to be a more favorable substrate on average than glass for both *Vibrio* species at all temperatures tested under 24 hours *in vitro* (Figure 1.1). Our study also indicates and further strengthens the assumption that *Vibrio* are early colonizers of plastics, especially LDPE, PP and PS, as both *V. parahaemolyticus* and *V. vulnificus* were able to colonize and develop biofilms on these plastics within 24 hours (Harrison et al., 2014; Kesy et al., 2021). Interestingly, most individual isolates besides *V. parahaemolyticus* ATCC17802 produced greater biofilm formation at lower temperature (25°C) compared to higher temperatures (30, 35°C). This is in accordance with studies that have reported both *V. parahaemolyticus* and *V. vulnificus* biofilm growth in 96-well microplates under different temperature conditions (Han et al., 2016; Çam, Brinkmeyer & Schwarz, 2019; Billaud et al., 2022). This suggests that *Vibrio* may produce greater amounts of biofilm as a survival mechanism in response to lower temperatures in the marine environment. However, when environmental conditions become more suitable and warmer, cells might be dispersing from these biofilms and contributing to higher planktonic cell concentrations (Townsley

& Yildiz, 2015; Guilhen, Forestier & Balestrino, 2017; Sheikh et al., 2022). In the context of climate change and public health, warming waters could be contributing to potentially higher exposure risk by this increased *Vibrio* biofilm dispersal leading to higher planktonic cell concentrations (Deeb et al., 2018).

The genus *Vibrio* has been reported to have "feast or famine" growth strategies, and the introduction of a new surface into a marine environment may provide a colonization opportunity niche which *Vibrio* rapidly respond to (Gilbert et al., 2012; Takemura, Chien & Polz, 2014; Westrich et al., 2016). However, while it did appear from our study that specific surface type could influence the colonization and biofilm development over a 24-hour period, our study only observed *V. parahaemolyticus* and *V. vulnificus* colonization and biofilm development over 24-hours on each individual plastic, so this process might be more undirected and driven by the colonization opportunity of a new surface. As there were visually observed differences in substrate flotation behavior and the substrates tested were confirmed to be different in specific density (Table 1.2), floatation behavior could also influence the adhesion of *Vibrio* species and, consequently, the production of biofilm on these substrates, especially in the context of *in situ* marine environments. This is important to note, as many studies have focused mainly on lower specific density plastics on the surface of marine environments as these plastic types are more easily observed, and not on plastics with higher specific density properties or on plastics that have lost buoyancy due to biofouling that are found at greater depths and in sediment (Zettler, Mincer & Amaral-Zettler, 2013; Cózar et al., 2014; Van Sebille et al., 2015 Kirstein et al., 2016; Laverty et al., 2020; Delacuvellerie et al., 2022). While these two *Vibrio* species have been found in the 'Plastisphere' on the commonly occurring

marine plastics assessed in the present study, studies on other *Vibrio* species colonization and biofilm development on different plastics, synthetic and organic polymers, and other substrate surfaces are still lacking both *in vitro* and *in vivo*.

There is high strain variability within *Vibrio* species in growth and biofilm formation. Strain variability has not been closely examined in plastic colonization (Whiting & Golden, 2002; Han et al., 2016; Odeyemi & Ahmad, 2017; Song et al., 2017; Çam & Brinkmeyer, 2020). *V. parahaemolyticus* human isolated strain ATCC17802 had the significantly greatest ($p \leq 0.01$) biofilm formation on LDPE and PP compared to GL and compared to the other *V. parahaemolyticus* strains tested, especially at 30 and 35°C. Song et al., 2017 has also reported that pathogenic strains of *V. parahaemolyticus* form greater biofilms than non-pathogenic strains. This strain is positive for the *trh* gene, a known virulence factor, signifying that known *V. parahaemolyticus* human pathogenic strains can adequately colonize, and have considerable biofilm formation on plastics in a 24-hour period, especially in warmer temperatures. Interestingly, without adjusting the CFUs per mm^2 of surface type, it was also found that all *V. parahaemolyticus* isolates' CFU concentrations on all plastic types had above the threshold dose needed to be infectious in humans ($\geq 10^5$ CFUs) at all temperatures tested (Marx, Hockberger & Walls, 2013).

V. vulnificus seawater isolated strain vv155 had the highest biofilm formation on all plastics at 25°C and was significantly greater on PS compared to GL and compared to the other *V. vulnificus* strains tested. While seawater isolates are expected to be strong biofilm producers to survive harsh marine environmental conditions, the result that *V. vulnificus* human isolate ATCC27562 was not the highest biofilm former was surprising.

It was expected that human isolates would have the highest biofilm production between all isolate sources due to being isolated from the more stressful environment of the human host. However, research conducted by Çam & Brinkmeyer, 2020 revealed that both clinical and environmental strains of *V. vulnificus* formed greater biofilms at lower temperatures. While the *V. vulnificus* human isolated strain ATCC27562 did not have the highest biofilm formation on plastics compared to this *V. vulnificus* water isolate, it cannot be ruled out that potential human pathogenic strains have higher colonization ability of plastic materials. This is especially apparent as the vv155 strain has a 16S rRNA designated type B genotype, which has a strong association with clinical strains, meaning it may have a high level of virulence in humans (Nilsson et al., 2003). While type A strains are more environmentally associated, infections in humans from type A have still been reported, and been shown to be more virulent in mice (LD_{50}= 10^5 - 10^6 CFU) when compared to type B strains (LD_{50}= 10^8 CFU) (Amaro, 1992; Amaro & Biosca, 1996; Nilsson et al., 2003; Drake, DePaola & Jaykus, 2007; Jones & Oliver, 2009; Çam, Brinkmeyer & Schwarz, 2019; Wu et al., 2022). Only the *V. vulnificus* ATCC33147 type B strain CFUs on LDPE and PS had above the considered threshold LD_{50} dose of 10^5 - 10^6 CFUs (without adjusting the CFUs per mm^2 of surface type) needed to be lethal in animals at all temperatures tested (Amaro & Biosca, 1996; Jeong & Satchell, 2012; Marx, Hockberger & Walls, 2013).

Biofilm biomass on substrate surfaces consists of the bacteria cells and their self-secreted extracellular polymeric substances (EPS) which are mainly comprised of biopolymers such as polysaccharides, proteins, and extracellular DNA (eDNA) (Flemming, 2016; Decho & Gutierrez, 2017). These three major components of the EPS

matrix contribute specific roles in biofilm formation, such as attachment and structural integrity (Dragoš & Kovács, 2017). The biofilm component dry mass, biochemical characteristics and concentrations of EPS varies depending on the bacterial species and the environment in which the biofilm was grown/formed (Vu et al., 2009; Wagner et al., 2009; Villeneuve, Bouchez & Montuelle, 2011; Kavita, Mishra & Jha, 2013). It is important to note that the dry cell and crude EPS mass and EPS biochemical concentrations obtained in this study might be underestimations of the total amount on the substrates tested, as portions of the weights and concentrations obtained from substrates might be lost during processing, and largely depend on the biofilm removal method, its removal efficiency, and EPS biochemical characterization treatments. Regardless, our study still observed a moderately positive correlation between the mean pooled dry biofilm biomass weight recovered from slide coupons and biofilm biomass from crystal violet staining of disc coupons, strengthening the assumption that crystal violet staining is an accurate method in estimating total biofilm biomass on substrates. Understanding the role of biochemical components in EPS may provide a further understanding of biofilm formation mechanisms of *V. parahaemolyticus* and *V. vulnificus* in their attachment to plastic substrates.

The quantitative analysis of the EPS from *V. parahaemolyticus* and *V. vulnificus* showed that extracellular proteins were the main component of EPS by mass of the mature biofilms on all plastic types, followed by carbohydrates then eDNA (Figure 1.4). These results suggested that extracellular proteins and carbohydrates were the main key components of the biofilm matrix of both species on plastics. These results are consistent with Li et al., 2020, which found extracellular proteins and carbohydrates were

the main components of mature *V. parahaemolyticus* biofilms. To the best of our knowledge, this is one of the first studies to quantify and characterize *V. vulnificus* EPS and its overall biochemical characteristics, especially on plastics, compared to previous studies that focused more on genes that were correlated with biofilm formation (Joseph & Wright, 2004; Grau et al., 2008; Kim et al., 2011; Lee et al., 2013). However, as these three biochemical components did not quite equal 100% of the dry EPS mass of both species across all substrate types, there might be other smaller components that may be part of the EPS like metals, and further analysis is needed to confirm this in addition to identifying specific proteins and carbohydrates that make up both species EPS on plastics (Jiao et al., 2010).

The hydrophobicity of bacteria may differ between the strains of a species and may change in response to changes in environmental conditions (temperature, nutrient availability, etc.), growth phases and growth state (planktonic vs biofilm) (Nwanyanwu et al., 2012). The present results also indicate this, as both *V. parahaemolyticus* and *V. vulnificus* strains possess wide differences in their hydrophobicity in the planktonic state at different temperatures. Both *Vibrio* species were considered hydrophobic, with *V. vulnificus* being more hydrophobic than *V. parahaemolyticus* at all temperatures tested, especially at 30 and 35°C (19% and 16% more hydrophobic, respectively) based on their adhesion to p-xylene, a hydrocarbon (Supplemental Table A.6). All individual strains were considered hydrophobic at all temperatures tested (Figure 1.5). Only one *V. parahaemolyticus* strain (ATCC43996) had strong adhesion to p-xylene and thus was considered highly hydrophobic at 25 and 30°C, while all *V. vulnificus* strains had strong adhesion to p-xylene at 25°C, and *V. vulnificus* strain ATCC33147 exhibited strong

adhesion to hydrocarbons at all temperatures tested (Figure 1.5). These results confirm the high variability of the hydrophobicity of *Vibrio* species and strains' planktonic cells, and that different temperatures can influence the degree of hydrophobicity (Lee & Yii, 1996; Wong & Chang, 2005; Mizan et al., 2016). The development of specific adaptive mechanisms of *Vibrio* to the toxicity and low bioavailability of these plastic substrates could contribute to the modification of its cell surface hydrophobicity to permit direct hydrophobic-hydrophobic interactions with these plastic substrates in initial colonization. This could lead to potential biodegradation of plastics as it has been reported that adequate hydrophobic/hydrophilic properties of bacteria can contribute to degradation of hydrocarbons (Krasowska & Sigler, 2014.

Taken together, these results indicate that different strain types of *V. parahaemolyticus V. vulnificus* can rapidly and adequately form biofilms with high viable cell concentrations on different plastic material types *in vitro*. However, this colonization process is highly variable and depends on species, strain, and plastic type, especially under different temperatures. Further studies are needed to compare these *Vibrio in vitro* plastic colonization processes to those found in the natural marine environment. While seawater surface temperature is monitored as it is predictive for *Vibrio* growth, this monitoring only accounts for planktonic cell growth and biofilms must also be included in monitoring. Seafood is already screened and tested for potential *Vibrio* contamination, but additional screening for plastic particles in seafood must also be considered as humans are likely being frequently exposed to plastics particles as they been found in high concentrations in commercially harvested seafood (Wu et al., 2019; Curren et al., 2020; Nicole, 2021). The present results highlight the ability of *Vibrio* species to form

biofilms on plastics, and may need to be incorporated into forecast models for *Vibrio* risk to better predict potential human exposure to pathogenic *Vibrios*, especially under climate change scenarios (Jacobs et al., 2014; Deeb et al., 2018; Ferchichi et al., 2021). Lastly, as both *V. parahaemolyticus* and *V. vulnificus* have been demonstrated to rapidly colonize plastics, their ability to utilize and degrade LDPE, PP, and PS also needs to be further explored (Obuekwe, Al-Jadi & Al-Saleh, 2009; Heipieper, Cornelissen & Pepi, 2010; Harrison et al., 2014; Raghul et al., 2014).

1.6 References

Amaral-Zettler, L. A., E. R. Zettler and T. J. Mincer (2020). "Ecology of the plastisphere." Nature Reviews Microbiology **18**(3): 139-151.

Amaro, C. (1992). "Comparative study of phenotypic and virulence properties in *Vibrio vulnificus* biotype 1 and 2 obtained from a European eel farm experiencing mortalities." Diseases of Aquatic Organisms **13**: 29-35.

Amaro, C. and E. G. Biosca (1996). "*Vibrio vulnificus* biotype 2, pathogenic for eels, is also an opportunistic pathogen for humans." Applied and Environmental Microbiology **62**(4): 1454-1457.

Arias-Andres, M., U. Klümper, K. Rojas-Jimenez and H.-P. Grossart (2018). "Microplastic pollution increases gene exchange in aquatic ecosystems." Environmental Pollution **237**: 253-261.

Arthur, C., J. Baker and H. Bamford (2009). Proceedings of the International Research Workshop on the Occurrence, Effects, and Fate of Microplastic Marine Debris, September 9-11, 2008.

Baker-Austin, C., J. D. Oliver, M. Alam, A. Ali, M. K. Waldor, F. Qadri and J. Martinez-Urtaza (2018). "*Vibrio* spp. infections." Nature Reviews Disease Primers **4**(1): 1-19.

Baker-Austin, C., L. Stockley, R. Rangdale and J. Martinez-Urtaza (2010). "Environmental occurrence and clinical impact of *Vibrio vulnificus* and *Vibrio parahaemolyticus*: a European perspective." Environmental Microbiology Reports **2**(1): 7-18.

Baker-Austin, C., J. A. Trinanes, S. Salmenlinna, M. Löfdahl, A. Siitonen, N. G. Taylor and J. Martinez-Urtaza (2016). "Heat wave–associated vibriosis, Sweden and Finland, 2014." Emerging Infectious Diseases **22**(7): 1216.

Baker-Austin, C., J. A. Trinanes, N. G. Taylor, R. Hartnell, A. Siitonen and J. Martinez-Urtaza (2013). "Emerging *Vibrio* risk at high latitudes in response to ocean warming." Nature Climate Change **3**(1): 73-77.

Bell, A. and M. Bott (2021). "Vibriosis:: What You and Your Patients Need To Know." Delaware Journal of Public Health **7**(1): 14-21.

Billaud, M., F. Seneca, E. Tambutté and D. Czerucka (2022). "An Increase of Seawater Temperature Upregulates the Expression of *Vibrio parahaemolyticus* Virulence Factors Implicated in Adhesion and Biofilm Formation." Frontiers in Microbiology **13**.

Bjerkan, G., E. Witsø and K. Bergh (2009). "Sonication is superior to scraping for retrieval of bacteria in biofilm on titanium and steel surfaces in vitro." Acta Orthopaedica **80**(2): 245-250.

Bowley, J., C. Baker-Austin, A. Porter, R. Hartnell and C. Lewis (2021). "Oceanic Hitchhikers – Assessing Pathogen Risks from Marine Microplastic." Trends in Microbiology **29**(2): 107-116.

Bramhachari, P., P. K. Kishor, R. Ramadevi, B. R. Rao and S. K. Dubey (2007). "Isolation and characterization of mucous exopolysaccharide (EPS) produced by *Vibrio* furnissii strain VB0S3."

Broberg, C. A., T. J. Calder and K. Orth (2011). "*Vibrio parahaemolyticus* cell biology and pathogenicity determinants." Microbes and infection **13**(12-13): 992-1001.

Çam, S. and R. Brinkmeyer (2020). "The effects of temperature, pH, and iron on biofilm formation by clinical versus environmental strains of *Vibrio vulnificus*." Folia Microbiologica **65**(3): 557-566.

Çam, S., R. Brinkmeyer and J. R. Schwarz (2019). "Quantitative PCR enumeration of vcgC and 16S rRNA type A and B genes as virulence indicators for environmental and clinical strains of *Vibrio vulnificus* in Galveston Bay oysters." Canadian Journal of Microbiology **65**(8): 613-621.

Control, C. f. D. and Prevention (2019). *Vibrio* species causing vibriosis.

Cózar, A., F. Echevarría, J. I. González-Gordillo, X. Irigoien, B. Úbeda, S. Hernández-León, Á. T. Palma, S. Navarro, J. García-de-Lomas and A. Ruiz (2014). "Plastic debris in the open ocean." Proceedings of the National Academy of Sciences **111**(28): 10239-10244.

Curren, E., C. P. Leaw, P. T. Lim and S. C. Y. Leong (2020). "Evidence of Marine Microplastics in Commercially Harvested Seafood." Frontiers in bioengineering and biotechnology **8**: 562760-562760.

Dang, H. and C. R. Lovell (2016). "Microbial Surface Colonization and Biofilm Development in Marine Environments." Microbiology and Molecular Biology Reviews **80**(1): 91-138.

de Carvalho, C. C. C. R. (2018). "Marine Biofilms: A Successful Microbial Strategy With Economic Implications." Frontiers in Marine Science **5**(126).

De Kievit, T. R., R. Gillis, S. Marx, C. Brown and B. H. Iglewski (2001). "Quorum-Sensing Genes in *Pseudomonas aeruginosa* Biofilms: Their Role and Expression Patterns." Applied and Environmental Microbiology **67**(4): 1865.

De Tender, C. A., L. I. Devriese, A. Haegeman, S. Maes, T. Ruttink and P. Dawyndt (2015). "Bacterial Community Profiling of Plastic Litter in the Belgian Part of the North Sea." Environmental Science & Technology **49**(16): 9629-9638.

Debroas, D., A. Mone and A. Ter Halle (2017). "Plastics in the North Atlantic garbage patch: A boat-microbe for hitchhikers and plastic degraders." Science of The Total Environment **599-600**: 1222-1232.

Decho, A. W. and T. Gutierrez (2017). "Microbial Extracellular Polymeric Substances (EPSs) in Ocean Systems." Frontiers in Microbiology **8**(922).

Deeb, R., D. Tufford, G. I. Scott, J. G. Moore and K. Dow (2018). "Impact of Climate Change on *Vibrio vulnificus* Abundance and Exposure Risk." Estuaries and coasts : Journal of the Estuarine Research Federation **41**(8): 2289-2303.

Delacuvellerie, A., A. Géron, S. Gobert and R. Wattiez (2022). "New insights into the functioning and structure of the PE and PP plastispheres from the Mediterranean Sea." Environmental Pollution **295**: 118678.

Donlan, R. M. (2002). "Biofilms: microbial life on surfaces." Emerging infectious diseases **8**(9): 881-890.

Dragoš, A. and Á. T. Kovács (2017). "The peculiar functions of the bacterial extracellular matrix." Trends in Microbiology **25**(4): 257-266.

Drake, S. L., A. DePaola and L.-A. Jaykus (2007). "An Overview of *Vibrio vulnificus* and *Vibrio parahaemolyticus*." Comprehensive Reviews in Food Science and Food Safety **6**(4): 120-144.

Dubois, M., K. Gilles, J. Hamilton, P. Rebers and F. Smith (1951). "A colorimetric method for the determination of sugars." Nature **168**(4265): 167-167.

Elmahdi, S., S. Parveen, S. Ossai, L. V. DaSilva, M. Jahncke, J. Bowers and J. Jacobs (2018). "*Vibrio parahaemolyticus* and *Vibrio vulnificus* Recovered from Oysters during an Oyster Relay Study." Applied and Environmental Microbiology **84**(3): e01790-01717.

Eriksen, M., L. Lebreton, H. Carson, M. Thiel, C. Moore, J. Borerro, F. Glagani, P. Ryan and J. Reisser (2014). "Plastic pollution in the world's oceans." PLoS ONE **9**.

Ferchichi, H., A. St-Hilaire, T. B. M. J. Ouarda and B. Lévesque (2021). "Impact of the future coastal water temperature scenarios on the risk of potential growth of pathogenic *Vibrio* marine bacteria." Estuarine, Coastal and Shelf Science **250**: 107094.

Flemming, H.-C. (2016). "EPS—then and now." Microorganisms **4**(4): 41.

Froelich, B. A. and R. T. Noble (2016). "*Vibrio* bacteria in raw oysters: managing risks to human health." Philosophical Transactions Royal Society London B Biological Sciences **371**(1689).

Ghenem, L., N. Elhadi, F. Alzahrani and M. Nishibuchi (2017). "*Vibrio parahaemolyticus*: A Review on Distribution, Pathogenesis, Virulence Determinants and Epidemiology." Saudi Journal of Medicine & Medical sSiences **5**(2): 93-103.

Giaouris, E., M.-P. Chapot-Chartier and R. Briandet (2009). "Surface physicochemical analysis of natural *Lactococcus lactis* strains reveals the existence of hydrophobic and low charged strains with altered adhesive properties." International Journal of Food Microbiology **131**(1): 2-9.

Gilbert, J. A., J. A. Steele, J. G. Caporaso, L. Steinbrück, J. Reeder, B. Temperton, S. Huse, A. C. McHardy, R. Knight and I. Joint (2012). "Defining seasonal marine microbial community dynamics." The ISME journal **6**(2): 298-308.

Goldstein, M. C., H. S. Carson and M. Eriksen (2014). "Relationship of diversity and habitat area in North Pacific plastic-associated rafting communities." Marine Biology **161**(6): 1441-1453.

Grande, R., M. C. Di Marcantonio, I. Robuffo, A. Pompilio, C. Celia, L. Di Marzio, D. Paolino, M. Codagnone, R. Muraro, P. Stoodley, L. Hall-Stoodley and G. Mincione (2015). "*Helicobacter pylori* ATCC 43629/NCTC 11639 Outer Membrane Vesicles (OMVs) from Biofilm and Planktonic Phase Associated with Extracellular DNA (eDNA)." Frontiers in Microbiology **6**(1369).

Grau, B. L., M. C. Henk, K. L. Garrison, B. J. Olivier, R. M. Schulz, K. L. O'Reilly and G. S. Pettis (2008). "Further characterization of *Vibrio vulnificus* rugose variants and identification of a capsular and rugose exopolysaccharide gene cluster." Infection and immunity **76**(4): 1485-1497.

Gregory, M. R. (2009). "Environmental implications of plastic debris in marine settings--entanglement, ingestion, smothering, hangers-on, hitch-hiking and alien invasions." Philosophical transactions of the Royal Society of London. Series B, Biological sciences **364**(1526): 2013-2025.

Guilhen, C., C. Forestier and D. Balestrino (2017). "Biofilm dispersal: multiple elaborate strategies for dissemination of bacteria with unique properties." Molecular Microbiology **105**(2): 188-210.

Guzmán-Soto, I., C. McTiernan, M. Gonzalez-Gomez, A. Ross, K. Gupta, E. J. Suuronen, T.-F. Mah, M. Griffith and E. I. Alarcon (2021). "Mimicking biofilm formation and development: Recent progress in in vitro and in vivo biofilm models." iScience **24**(5): 102443.

Hamanaka, D., M. Onishi, T. Genkawa, F. Tanaka and T. Uchino (2012). "Effects of temperature and nutrient concentration on the structural characteristics and removal of vegetable-associated *Pseudomonas* biofilm." Food Control **24**(1): 165-170.

Han, N., M. Mizan, I. Jahid and S.-D. Ha (2016). "Biofilm formation by *Vibrio parahaemolyticus* on food and food contact surfaces increases with rise in temperature." Food Control **70**: 161-166.

Harrison, J. P., M. Schratzberger, M. Sapp and A. M. Osborn (2014). "Rapid bacterial colonization of low-density polyethylene microplastics in coastal sediment microcosms." BMC Microbiology **14**(1): 232.

Heipieper, H. J., S. Cornelissen and M. Pepi (2010). Surface Properties and Cellular Energetics of Bacteria in Response to the Presence of Hydrocarbons. Handbook of

Hydrocarbon and Lipid Microbiology. K. N. Timmis. Berlin, Heidelberg, Springer Berlin Heidelberg**:** 1615-1624.

Hernández-Cabanyero, C. and C. Amaro (2020). "Phylogeny and life cycle of the zoonotic pathogen *Vibrio vulnificus*." Environmental Microbiology **22**(10): 4133-4148.

Hernández-Cabanyero, C., E. Sanjuán, B. Fouz, D. Pajuelo, E. Vallejos-Vidal, F. E. Reyes-López and C. Amaro (2020). "The Effect of the Environmental Temperature on the Adaptation to Host in the Zoonotic Pathogen *Vibrio vulnificus*." Frontiers in microbiology **11**: 489-489.

Hernández-Cabanyero, C., C. T. Lee, V. Tolosa-Enguis, E. Sanjuán, D. Pajuelo, F. Reyes-López, L. Tort and C. Amaro (2019). "Adaptation to host in *Vibrio vulnificus*, a zoonotic pathogen that causes septicemia in fish and humans." Environmental microbiology **21**(8): 3118-3139.

Honda, T. and T. Iida (1993). "The pathogenicity of *Vibrio parahaemolyticus* and the role of the thermostable direct haemolysin and related haemolysins." Reviews in Medical Microbiology **4**(2): 106-113.

Jacobs, J. M., M. Rhodes, C. W. Brown, R. R. Hood, A. Leight, W. Long and R. Wood (2014). "Modeling and forecasting the distribution of *Vibrio vulnificus* in Chesapeake Bay." Journal of Applied Microbiology **117**(5): 1312-1327.

Jeong, H.-G. and K. J. F. Satchell (2012). "Additive Function of *Vibrio vulnificus* MARTXVv and VvhA Cytolysins Promotes Rapid Growth and Epithelial Tissue Necrosis During Intestinal Infection." PLOS Pathogens **8**(3): e1002581.

Jiao, Y., G. D. Cody, A. K. Harding, P. Wilmes, M. Schrenk, K. E. Wheeler, J. F. Banfield and M. P. Thelen (2010). "Characterization of extracellular polymeric substances from acidophilic microbial biofilms." Applied and Environmental Microbiology **76**(9): 2916-2922.

Jones, M. K. and J. D. Oliver (2009). "*Vibrio vulnificus*: Disease and Pathogenesis." Infection and Immunity **77**(5): 1723-1733.

Joseph, L. A. and A. C. Wright (2004). "Expression of *Vibrio vulnificus* capsular polysaccharide inhibits biofilm formation." Journal of Bacteriology **186**(3): 889-893.

Kamp, H. D., B. Patimalla-Dipali, D. W. Lazinski, F. Wallace-Gadsden and A. Camilli (2013). "Gene fitness landscapes of *Vibrio cholerae* at important stages of its life cycle." PLoS Pathogons **9**(12): e1003800.

Kavita, K., A. Mishra and B. Jha (2013). "Extracellular polymeric substances from two biofilm forming *Vibrio* species: characterization and applications." Carbohydrate Polymers **94**(2): 882-888.

Keswani, A., D. M. Oliver, T. Gutierrez and R. S. Quilliam (2016). "Microbial hitchhikers on marine plastic debris: Human exposure risks at bathing waters and beach environments." Marine Environmental Research **118**: 10-19.

Kesy, K., M. Labrenz, B. S. Scales, B. Kreikemeyer and S. Oberbeckmann (2021). "*Vibrio* Colonization Is Highly Dynamic in Early Microplastic-Associated Biofilms as Well as on Field-Collected Microplastics." Microorganisms **9**(1): 76.

Kesy, K., S. Oberbeckmann, B. Kreikemeyer and M. Labrenz (2019). "Spatial Environmental Heterogeneity Determines Young Biofilm Assemblages on Microplastics in Baltic Sea Mesocosms." Frontiers in Microbiology **10**(1665).

Kim, H.-J., J.-O. Ryu, S.-Y. Lee, E.-S. Kim and H.-Y. Kim (2015). "Multiplex PCR for detection of the *Vibrio* genus and five pathogenic *Vibrio* species with primer sets designed using comparative genomics." BMC microbiology **15**: 239-239.

Kim, M., J.-M. Park, H.-J. Um, K.-H. Lee, H. Kim, J. Min and Y.-H. Kim (2011). "The antifouling potentiality of galactosamine characterized from *Vibrio vulnificus* exopolysaccharide." Biofouling **27**(8): 851-857.

Kirstein, I. V., S. Kirmizi, A. Wichels, A. Garin-Fernandez, R. Erler, M. Löder and G. Gerdts (2016). "Dangerous hitchhikers? Evidence for potentially pathogenic *Vibrio* spp. on microplastic particles." Marine Environmental Research **120**: 1-8.

Kochkodan, V., S. Tsarenko, N. Potapchenko, V. Kosinova and V. Goncharuk (2008). "Adhesion of microorganisms to polymer membranes: a photobactericidal effect of surface treatment with TiO2." Desalination **220**(1): 380-385.

Krasowska, A. and K. Sigler (2014). "How microorganisms use hydrophobicity and what does this mean for human needs?" Frontiers in Cellular and Infection Microbiology **4**: 112.

Kwaszewska, A. K., A. Brewczynska and E. M. Szewczyk (2006). "Hydrophobicity and biofilm formation of lipophilic skin corynebacteria." Polish Journal of Microbiology **55**(3): 189-193.

Lage, O. and A. P. Graca (2016). Biofilms: An Extra Coat on Macroalgae.

Lami, R. (2019). Chapter 3 - Quorum Sensing in Marine Biofilms and Environments. Quorum Sensing. G. Tommonaro, Academic Press**:** 55-96.

Laverty, A. L., S. Primpke, C. Lorenz, G. Gerdts and F. C. Dobbs (2020). "Bacterial biofilms colonizing plastics in estuarine waters, with an emphasis on *Vibrio* spp. and their antibacterial resistance." PLOS ONE **15**(8): e0237704.

Lee, K.-J., J.-A. Kim, W. Hwang, S.-J. Park and K.-H. Lee (2013). "Role of capsular polysaccharide (CPS) in biofilm formation and regulation of CPS production by quorum-sensing in *Vibrio vulnificus*." Molecular Microbiology **90**(4): 841-857.

Li, W., J. J. Wang, H. Qian, L. Tan, Z. Zhang, H. Liu, Y. Pan and Y. Zhao (2020). "Insights Into the Role of Extracellular DNA and Extracellular Proteins in Biofilm Formation of *Vibrio parahaemolyticus*." Frontiers in Microbiology **11**(813).

Marx, J., R. Hockberger and R. Walls (2013). Rosen's Emergency Medicine-Concepts and Clinical Practice E-Book: 2-Volume Set, Elsevier Health Sciences.

Mizan, M. F. R., I. K. Jahid, M. Kim, K.-H. Lee, T. J. Kim and S.-D. Ha (2016). "Variability in biofilm formation correlates with hydrophobicity and quorum sensing among *Vibrio parahaemolyticus* isolates from food contact surfaces and the distribution of the genes involved in biofilm formation." Biofouling **32**(4): 497-509.

Motes, M., A. DePaola, D. Cook, J. Veazey, J. Hunsucker, W. Garthright, R. Blodgett and S. Chirtel (1998). "Influence of water temperature and salinity on *Vibrio vulnificus* in northern gulf and atlantic coast oysters (Crassostrea virginica)." Applied Environmental Microbiology **64**(4): 1459-1465.

Nakanishi, E. Y., J. H. Palacios, S. Godbout and S. Fournel (2021). "Interaction between Biofilm Formation, Surface Material and Cleanability Considering Different Materials Used in Pig Facilities—An Overview." Sustainability **13**(11): 5836.

Nicole, W. (2021). "Microplastics in Seafood: How Much Are People Eating?" Environmental Health Perspectives **129**(3): 034001.

Nilsson, W. B., R. N. Paranjype, A. DePaola and M. S. Strom (2003). "Sequence polymorphism of the 16S rRNA gene of *Vibrio vulnificus* is a possible indicator of strain virulence." Journal of Clinical Microbiology **41**(1): 442-446.

Nwanyanwu, C., C. Alisi, C. Nweke and J. Orji (2012). "Cell surface properties of phenol-utilizing bacteria isolated from petroleum refinery wastewater." Journal of Research in Biology **2**: 383-391.

O'Toole, G. A. (2011). "Microtiter dish biofilm formation assay." Journal of Visualized Experiments : JoVE(47): 2437.

Oberbeckmann, S., M. G. J. Lder and M. Labrenz (2015). "Marine microplastic-associated biofilms a review." Environmental Chemistry 12(5): 551-562.

Obuekwe, C. O., Z. K. Al-Jadi and E. S. Al-Saleh (2009). "Hydrocarbon degradation in relation to cell-surface hydrophobicity among bacterial hydrocarbon degraders from petroleum-contaminated Kuwait desert environment." International Biodeterioration & Biodegradation **63**(3): 273-279.

Odeyemi, O. A. and A. Ahmad (2017). "Population dynamics, antibiotics resistance and biofilm formation of Aeromonas and *Vibrio* species isolated from aquatic sources in Northern Malaysia." Microbial Pathogenesis **103**: 178-185.

Oliver, J. D. and R. R. Colwell (1973). "Extractable lipids of gram-negative marine bacteria: phospholipid composition." Journal of Bacteriology **114**(3): 897-908.

Parry, M. L., O. F. Canziani, J. P. Palutikof, P. J. Van Der Linden and C. E. Hanson (2007). "IPCC, 2007: climate change 2007: impacts, adaptation and vulnerability. Contribution of working group II to the fourth assessment report of the intergovernmental panel on climate change." Cambridge University Press, Cambridge, UK.

Portillo, M. E., M. Salvadó, A. Trampuz, V. Plasencia, M. Rodriguez-Villasante, L. Sorli, L. Puig and J. P. Horcajada (2013). "Sonication versus vortexing of implants for diagnosis of prosthetic joint infection." Journal of Clinical Microbiology **51**(2): 591-594.

Raghul, S., S. Bhat, M. Chandrasekaran, V. Francis and E. Thachil (2014). "Biodegradation of polyvinyl alcohol-low linear density polyethylene-blended plastic film by consortium of marine benthic *Vibrio*s." International Journal of Environmental Science and Technology **11**(7): 1827-1834.

Reidl, J. and K. E. Klose (2002). "*Vibrio cholerae* and cholera: out of the water and into the host." FEMS Microbiology Reviews **26**(2): 125-139.

Reifsteck, F., S. Wee and B. Wilkinson (1987). "Hydrophobicity—hydrophilicity of staphylococci." Journal of Medical Microbiology **24**(1): 65-73.

Reisser, J., J. Shaw, G. Hallegraeff, M. Proietti, D. K. A. Barnes, M. Thums, C. Wilcox, B. D. Hardesty and C. Pattiaratchi (2014). "Millimeter-sized marine plastics: a new pelagic habitat for microorganisms and invertebrates." PloS one **9**(6): e100289-e100289.

Rosenberg, M. (1984). "Bacterial adherence to hydrocarbons: a useful technique for studying cell surface hydrophobicity." FEMS Microbiology Letters **22**(3): 289-295.

Schroeder, M., B. D. Brooks and A. E. Brooks (2017). "The Complex Relationship between Virulence and Antibiotic Resistance." Genes **8**(1): 39.

Sheikh, H. I., M. Najiah, A. Fadhlina, A. A. Laith, M. M. Nor, K. C. A. Jalal and N. A. Kasan (2022). "Temperature Upshift Mostly but not Always Enhances the Growth of *Vibrio* Species: A Systematic Review." Frontiers in Marine Science **9**.

Song, X., Y. Ma, J. Fu, A. Zhao, Z. Guo, P. K. Malakar, Y. Pan and Y. Zhao (2017). "Effect of temperature on pathogenic and non-pathogenic *Vibrio parahaemolyticus* biofilm formation." Food Control **73**: 485-491.

Stewart, P. S. and J. William Costerton (2001). "Antibiotic resistance of bacteria in biofilms." The Lancet **358**(9276): 135-138.

Strom, M. S. and R. N. Paranjpye (2000). "Epidemiology and pathogenesis of *Vibrio vulnificus*." Microbes and Infection **2**(2): 177-188.

Sullivan, T. J. and J. E. Neigel (2018). "Effects of temperature and salinity on prevalence and intensity of infection of blue crabs, Callinectes sapidus, by *Vibrio cholerae*, *V. parahaemolyticus*, and *V. vulnificus* in Louisiana." Journal of Invertebrate Pathology **151**: 82-90.

Takemura, A. F., D. M. Chien and M. F. Polz (2014). "Associations and dynamics of *Vibrionaceae* in the environment, from the genus to the population level." Frontiers in Microbiology **5**: 38.

Tavelli, R., M. Callens, C. Grootaert, M. F. Abdallah and A. Rajkovic (2022). "Foodborne pathogens in the plastisphere: Can microplastics in the food chain threaten microbial food safety?" Trends in Food Science & Technology **129**: 1-10.

Tiruvayipati, S. and S. Bhassu (2016). "Host, pathogen and the environment: the case of Macrobrachium rosenbergii, *Vibrio parahaemolyticus* and magnesium." Gut Pathogens **8**(1): 15.

Tischler, A. H., L. Lie, C. M. Thompson and K. L. Visick (2018). "Discovery of Calcium as a Biofilm-Promoting Signal for *Vibrio fischeri* Reveals New Phenotypes and Underlying Regulatory Complexity." Journal of Bacteriology **200**(15): e00016-00018.

Townsley, L. and F. H. Yildiz (2015). "Temperature affects c-di-GMP signalling and biofilm formation in *Vibrio cholerae*." Environmental Microbiology **17**(11): 4290-4305.

Valquier-Flynn, H., C. L. Wilson, A. E. Holmes and C. D. Wentworth (2017). "Growth Rate of *Pseudomonas aeruginosa* Biofilms on Slippery Butyl Methacrylate-Co-Ethylene Dimethacrylate (BMA-EDMA), Glass and Polycarbonate Surfaces." Journal of Biotechnology & Biomaterials **7**(4): 274.

Van Sebille, E., C. Wilcox, L. Lebreton, N. Maximenko, B. D. Hardesty, J. A. Van Franeker, M. Eriksen, D. Siegel, F. Galgani and K. L. Law (2015). "A global inventory of small floating plastic debris." Environmental Research Letters **10**(12): 124006.

Vezzulli, L., C. Grande, P. C. Reid, P. Hélaouët, M. Edwards, M. G. Höfle, I. Brettar, R. R. Colwell and C. Pruzzo (2016). "Climate influence on *Vibrio* and associated human diseases during the past half-century in the coastal North Atlantic." Proceedings of the National Academy of Sciences **113**(34): E5062-E5071.

Vickery, M. C., W. B. Nilsson, M. S. Strom, J. L. Nordstrom and A. DePaola (2007). "A real-time PCR assay for the rapid determination of 16S rRNA genotype in *Vibrio vulnificus*." Journal of Microbiological Methods **68**(2): 376-384.

Villeneuve, A., A. Bouchez and B. Montuelle (2011). "In situ interactions between the effects of season, current velocity and pollution on a river biofilm." Freshwater Biology **56**(11): 2245-2259.

Viršek, M. K., M. N. Lovšin, Š. Koren, A. Kržan and M. Peterlin (2017). "Microplastics as a vector for the transport of the bacterial fish pathogen species Aeromonas salmonicida." Marine Pollution Bulletin **125**(1): 301-309.

Vu, B., M. Chen, R. J. Crawford and E. P. Ivanova (2009). "Bacterial extracellular polysaccharides involved in biofilm formation." Molecules **14**(7): 2535-2554.

Wagner, M., N. P. Ivleva, C. Haisch, R. Niessner and H. Horn (2009). "Combined use of confocal laser scanning microscopy (CLSM) and Raman microscopy (RM): Investigations on EPS–Matrix." Water Research **43**(1): 63-76.

Ward, C. S., C.-M. Yung, K. M. Davis, S. K. Blinebry, T. C. Williams, Z. I. Johnson and D. E. Hunt (2017). "Annual community patterns are driven by seasonal switching between closely related marine bacteria." The ISME Journal **11**(6): 1412-1422.

Ward, J. E. and D. J. Kach (2009). "Marine aggregates facilitate ingestion of nanoparticles by suspension-feeding bivalves." Marine Environmental Research **68**(3): 137-142.

Westrich, J. R., A. M. Ebling, W. M. Landing, J. L. Joyner, K. M. Kemp, D. W. Griffin and E. K. Lipp (2016). "Saharan dust nutrients promote *Vibrio* bloom formation in marine surface waters." Proceedings of the National Academy of Sciences **113**(21): 5964-5969.

Whitehead, P. G., R. L. Wilby, R. W. Battarbee, M. Kernan and A. J. Wade (2009). "A review of the potential impacts of climate change on surface water quality." Hydrological Sciences Journal **54**(1): 101-123.

Whiting, R. C. and M. H. Golden (2002). "Variation among *Escherichia coli* O157:H7 strains relative to their growth, survival, thermal inactivation, and toxin production in broth." International Journal of Food Microbiology **75**(1): 127-133.

Wong, H.-C. and C.-N. Chang (2005). "Hydrophobicity, Cell Adherence, Cytotoxicity, and Enterotoxigenicity of Starved *Vibrio parahaemolyticus*." Journal of Food Protection **68**(1): 154-156.

Wu, W., Z. Jing, X. Yu, Q. Yang, J. Sun, C. Liu, W. Zhang, L. Zeng and H. He (2019). "Recent advances in screening aquatic products for *Vibrio* spp." TrAC Trends in Analytical Chemistry **111**: 239-251.

Wu, Z., Y. Wu, H. Gao, X. He, Q. Yao, Z. Yang, J. Zhou, L. Ji, J. Gao, X. Jia, Y. Dou, X. Wang and P. Shao (2022). "Identification and whole-genome sequencing analysis of *Vibrio vulnificus* strains causing pearl gentian grouper disease in China." BMC Microbiology **22**(1): 200.

Zettler, E., T. Mincer and L. Amaral-Zettler (2013). "Life in the "Plastisphere": Microbial Communities on Plastic Marine Debris." Environmental Science & Technology **47**.

Table 1.1 *Vibrio* strains used in this study.

Species	Isolation Source	Strain ID	Isolate Origin	Characteristics
V. parahaemolyticus	ATCC	ATCC17802	Human	*tlh / trh*
V. parahaemolyticus	ATCC	ATCC43996	Mollusk	*tlh / tdh*
V. parahaemolyticus	UofSC	vpC12	Seawater	*tlh*
V. vulnificus	ATCC	ATCC27562	Human	16S Type B
V. vulnificus	ATCC	ATCC33147	Eel	16S Type A
V. vulnificus	NOAA	vv155	Seawater	16S Type B

Table 1.2 Coupon types and characteristics used in this study.

Coupon Type	Chemical Formula	Density	Diameter or Length/Thickness	Surface Area	Usage
Borosilicate Glass	BH_6NaO_7Si	Disc coupon - 2.19 g/cm³ Slide coupon – 2.48 g/cm³	Disc coupon - 12.7mm/3.8mm Slide coupon - 75mm/1mm	Disc coupon – 405mm² Slide coupon – 2460mm²	Laboratory and kitchen glassware, industrial systems, electronics
Low-Density Polyethylene	$(C_2H_4)_n$	Disc coupon - 0.89 g/cm³ Slide coupon – 0.86 g/cm³	Disc coupon - 12.7mm/3.8mm Slide Coupon – 73mm/1.6mm	Disc coupon – 405mm² Slide coupon – 2501mm²	Plastic bags, six-pack rings, packaging film, bottles, netting

Polypropylene	$(C_3H_6)_n$	Disc coupon - 0.87 g/cm³ Slide coupon – 0.83 g/cm³	Disc coupon - 12.7mm/3.8mm Slide coupon - 75mm/1.6mm	Disc coupon – 405mm² Slide coupon – 2569mm²	Rope, bottle caps, packaging film, netting
Polystyrene	$(C_8H_8)_n$	Disc coupon - 1.05 g/cm³ Slide coupon – 1.18 g/cm³	Disc coupon - 12.7mm/3.8mm Slide coupon - 77mm/0.6mm	Disc coupon – 405mm² Slide coupon – 2451mm²	Plastic utensils, food containers

Table 1.3 Summary of biofilm biomass showing percent change (%) between all *V. parahaemolyticus* and *V. vulnificus* strains and plastic types at different temperatures compared to glass controls.

Strain	Plastic Type	25°C	30°C	35°C
ATCC17802	LDPE*	663%	774%	337%
	PP*	457%	782%	343%
	PS*	117%	195%	-13%
ATCC43996	LDPE*	220%	177%	236%
	PP*	118%	30%	83%
	PS*	148%	224%	234%
vpC12	LDPE	161%	-48%	-8%
	PP	83%	-74%	-23%
	PS	192%	42%	0%
ATCC27562	LDPE	-10%	-38%	116%
	PP	-17%	-69%	-18%

	PS	59%	60%	138%
ATCC33147	LDPE	2%	199%	378%
	PP	-40%	83%	35%
	PS*	104%	295%	318%
vv155	LDPE	61%	175%	121%
	PP	-22%	133%	21%
	PS*	75%	284%	62%

Green = (+), red = (-), yellow = no change. * = significantly greater overall biofilm formation on this surface compared to glass.

Table 1.4 Summary of biofilm CFUs showing percent change (%) between all *V. parahaemolyticus* and *V. vulnificus* strains and plastic types at different temperatures compared to glass controls.

Strain	**Plastic Type**	**25°C**	**30°C**	**35°C**
ATCC17802	LDPE*	97%	97%	93%
	PP*	91%	97%	93%
	PS*	94%	97%	81%
ATCC43996	LDPE	84%	42%	83%
	PP	65%	55%	78%
	PS	83%	-196%	30%
vpC12	LDPE	96%	70%	-116%
	PP	92%	-43%	-499%

	PS	94%	69%	-116%
ATCC27562	LDPE	-418%	-147%	94%
	PP	-164%	-622%	93%
	PS	8%	20%	87%
ATCC33147	LDPE*	93%	99%	95%
	PP	-1551%	3%	52%
	PS	91%	95%	95%
vv155	LDPE	-19%	13%	87%
	PP	74%	-324%	82%
	PS	6%	62%	80%

Green = (+), red = (-). * = significantly greater overall CFUs on this surface compared to glass.

Table 1.5 Estimated pooled cell and crude extracellular polymeric substance mean dry weight per slide coupon at 30°C after 48 hours.

Strain	Coupon Type	Mean Dry Cell Weight (mg)	Mean Dry Crude EPS Weight (mg)	Mean Total Dry Biomass Weight (mg)	Mean Biofilm Biomass (OD_{570})
ATCC17802	GL	0.03	0.04	0.07	0.27
	LDPE	0.09	0.09	0.18	2.42
	PP	0.07	0.1	0.17	2.44
	PS	0.04	0.05	0.09	0.81
vv155	GL	0.01	0.03	0.04	0.47

	LDPE	0.21	0.07	0.28	1.31
	PP	0.12	0.07	0.19	1.11
	PS	0.15	0.18	0.33	1.83
Significance (*p*), Correlation (*r*)				$p \leq 0.01$	$r = 0.58$

Significance (***p***) was calculated by comparison of the mean total dry biomass weight between glass and all plastics combined. Correlation (***r***) was calculated by comparison of mean total dry biomass weights to respective mean biofilm biomass OD_{570} values.

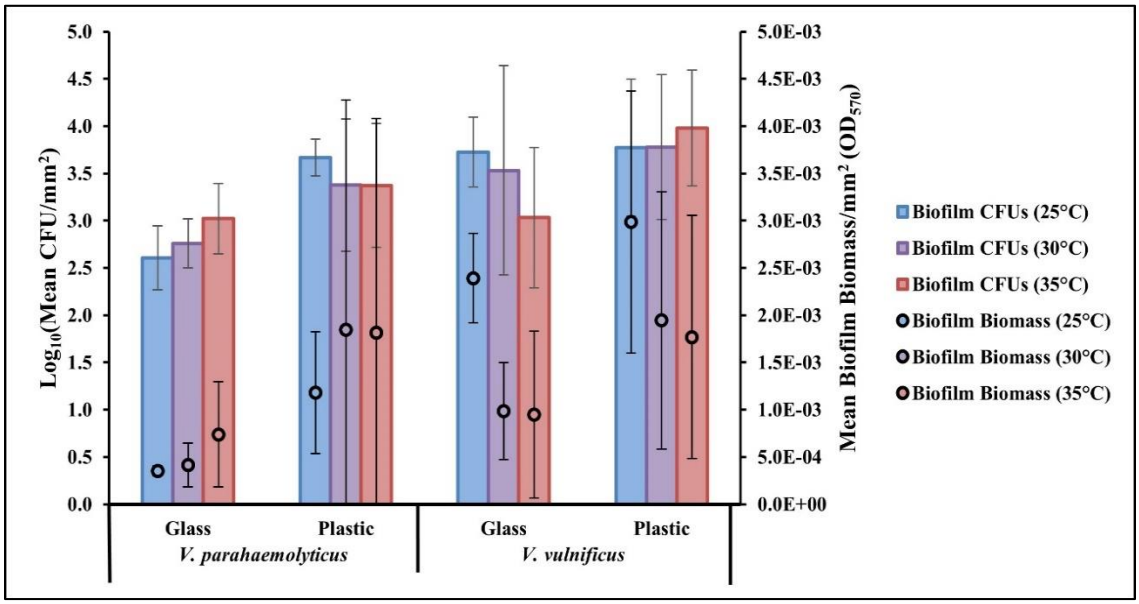

Figure 1.1 Plastics enhance *V. parahaemolyticus* and *V. vulnificus* biofilm formation compared to glass. Effect of temperature (°C) on mean biofilm biomass and CFUs (means ± SD) by *V. parahaemolyticus* and *V. vulnificus* between glass and all plastics after 24 hours (means of all biological triplicates and three independent experiments).

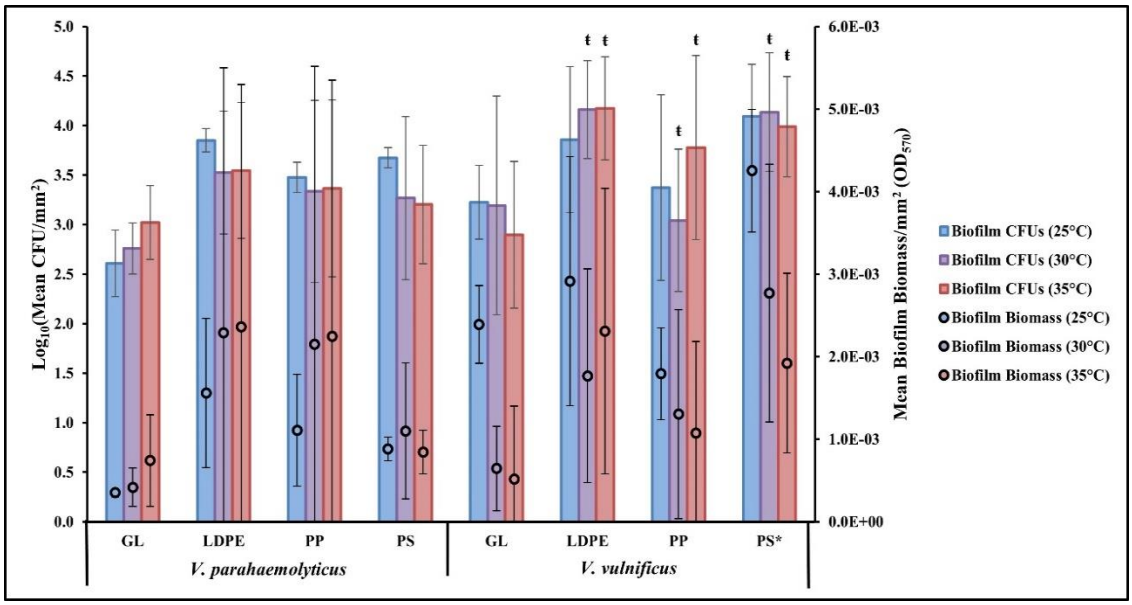

Figure 1.2 Surface material and temperature influences *V. parahaemolyticus* and *V. vulnificus* biofilm formation. Comparison of biofilm biomass and CFUs (means ± SD) by both *V. parahaemolyticus* and *V. vulnificus* between substate surface type at different temperatures after 24 hours (means of all experiments). * = Significantly greater biofilm biomass compared to GL, ŧ = significantly less overall biofilm biomass compared to 25°C

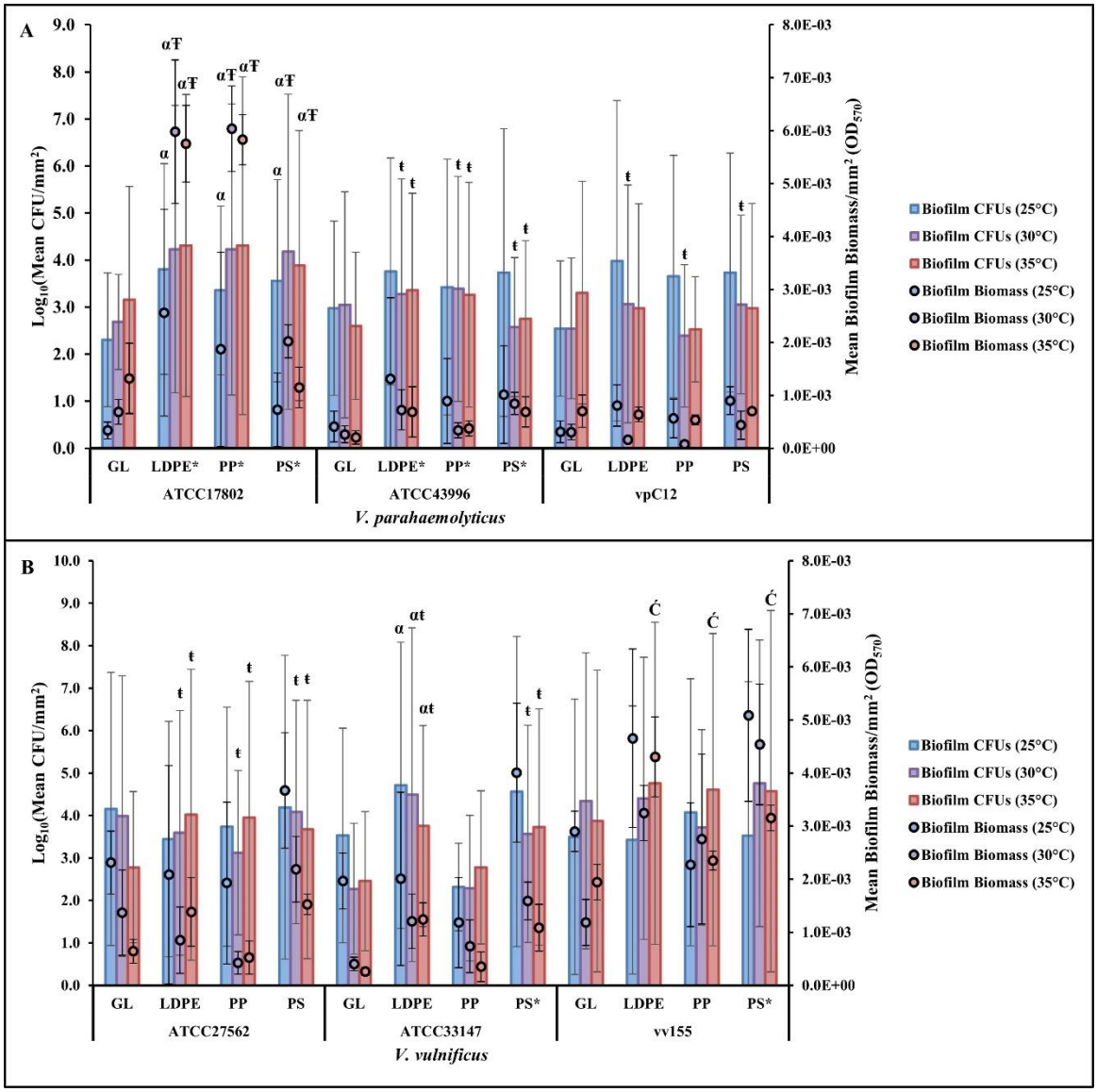

Figure 1.3 Strain type influences *V. parahaemolyticus* and *V. vulnificus* colonization and biofilm biomass and cell viability. Comparison of biofilm biomass and CFUs (means ± SD) by *V. parahaemolyticus* strains (**A**) and *V. vulnificus* strains (**B**) between glass and all plastic types at different temperatures after 24 hours (means of all biological triplicates and three independent experiments).* = significantly greater biofilm biomass compared to GL, α = significantly greater CFUs compared to GL, Ŧ = significantly greater overall biofilm biomass compared to 25°C, ŧ = significantly less overall biofilm biomass compared to 25°C, Ć = significantly greater overall CFUs compared to 25°C.

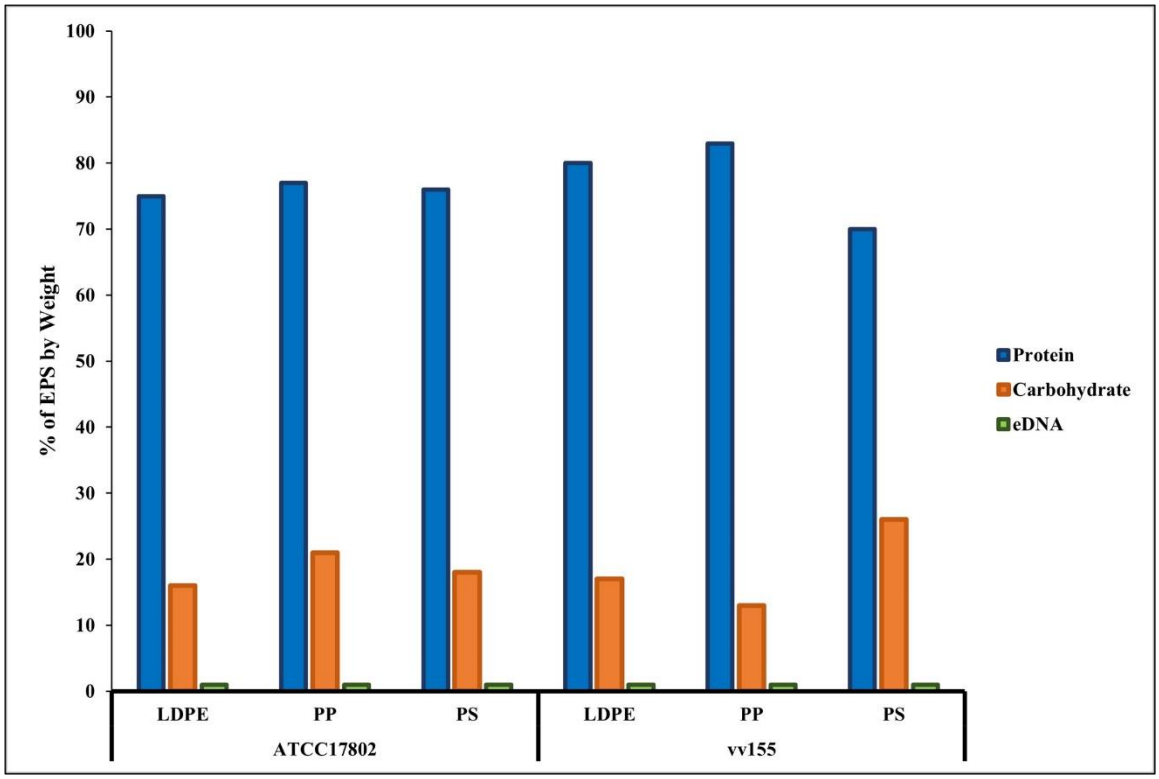

Figure 1.4 Proteins are the main component of *V. parahaemolyticus* and *V. vulnificus* extracellular polymeric substances on plastics. % EPS by weight of biochemical characteristics of *V. parahaemolyticus* (ATCC17802) and *V. vulnificus* (vv155) on all plastic types. % EPS by weight was calculated by standardization of each mean concentration of proteins, carbohydrates and eDNA to µg/mL, then divided by total starting weight of pooled crude EPS from 10 samples.

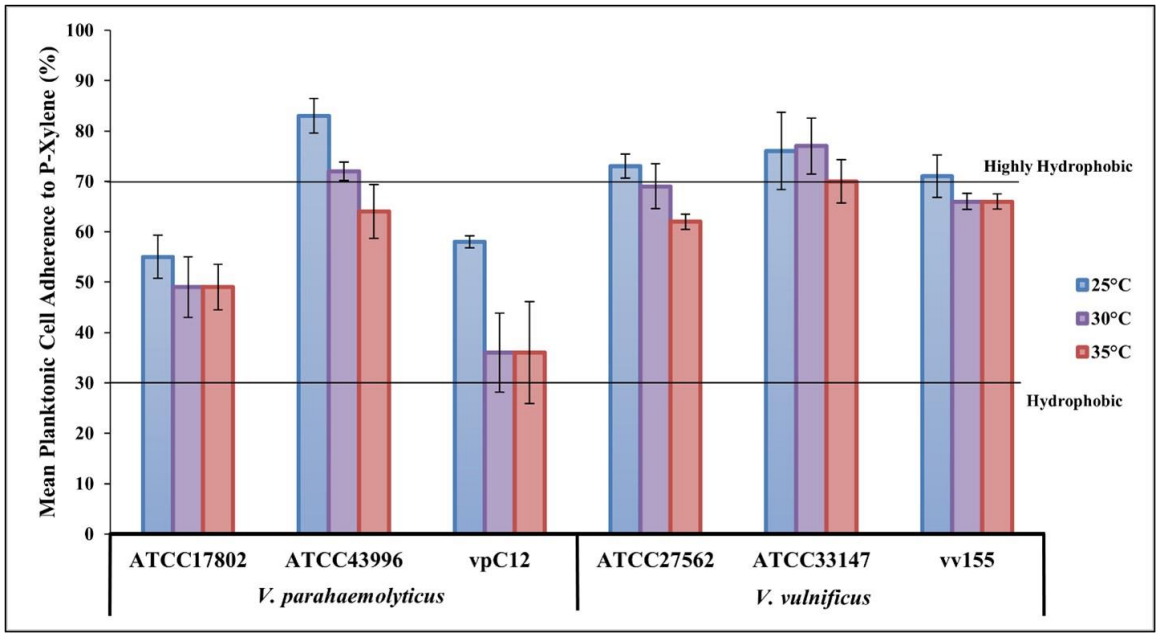

Figure 1.5 Lower temperatures increase *Vibrio* hydrophobicity. *V. parahaemolyticus* and *V. vulnificus* individual strain adherence (means ± SD) to p-xylene (%) at different temperatures (means of all biological triplicates and three independent experiments). Lines designate planktonic cell hydrophobicity from hydrophobic (30% adherence) to highly hydrophobic (70% adherence).

CHAPTER 2

VIBRIO PARAHAEMOLYTICUS AND *VIBRIO VULNIFICUS IN VITRO* BIOFILM DISPERSAL FROM MICROPLASTICS INFLUENCED BY SIMULATED HUMAN ENVIRONMENT[1]

[1] Leighton RE, Xiong L, Anderson GK, Astarita GM, Cai G, Norman RS and Decho AW (2023). *Vibrio parahaemolyticus* and *Vibrio vulnificus In Vitro* Biofilm Dispersal from Microplastics Influenced by Simulated Human Environment. Submitted to Frontiers in Microbiology.

2.1 Abstract

Growing concerns exist regarding human ingestion of contaminated seafood that contains *Vibrio* biofilms on microplastics (MPs). One of the mechanisms enhancing biofilm related infections in humans is due to biofilm dispersion, a process that triggers release of bacteria from biofilms into the surrounding environment, such as the gastrointestinal tract of human hosts. Dispersal of cells from biofilms can occur in response to environmental conditions such as sudden changes in temperature, pH and nutrient conditions, as the bacteria leave the biofilm to find a more stable environment to colonize. This study evaluated how brief exposures to nutrient starvation, elevated temperature, different pH levels and simulated human media affect *V. parahaemolyticus* and *V. vulnificus* biofilm dispersal and processes on and from low-density polyethylene (LDPE), polypropylene (PP), and polystyrene (PS) MPs. Both species were able to adequately disperse from all types of plastics under most exposure conditions. *V. parahaemolyticus* was able to tolerate and survive the low pH that resembles the gastric environment compared to *V. vulnificus.* pH had a significantly ($p \leq 0.05$) positive effect on overall *V. parahaemolyticus* biofilm production in microplates and cell colonization from PP and PS. pH also had a positive effect on *V. vulnificus* cell colonization from LDPE and PP. However, most biofilm biomass, biofilm cell and dispersal cell densities of both species greatly varied after exposure to elevated temperature, pH and nutrient starvation. It was also found that certain exposures to simulated human media affected both *V. parahaemolyticus* and *V. vulnificus* biofilm biomass and biofilm cell densities on LDPE, PP and PS compared to exposure to traditional media of similar pH. Cyclic-di-GMP was higher in biofilm cells compared to dispersal cells, but exposure to more stressful

conditions significantly increased signal concentrations in both biofilm and dispersal states. Taken together, this study suggests that human pathogenic strains of *V. parahaemolyticus* and *V. vulnificus* can rapidly disperse with high cell densities from different plastic types *in vitro*. However, the biofilm dispersal process is highly variable, species specific and dependent on plastic type, especially under different human body related environmental exposures.

2.2 Introduction

Vibrio parahaemolyticus and *Vibrio vulnificus* are two known pathogenic species that naturally exist in the marine environment and can infect both marine animals and humans. These Gram-negative pathogens commonly infect humans through consumption of contaminated raw seafood (Elmahdi et al., 2018). While human infections are rare, symptoms of both *V. parahaemolyticus* and *V. vulnificus* infections can include cramps, nausea, fever, and bloody diarrhea. *V. vulnificus* foodborne infections can be more severe, and is considered one of the most fatal foodborne pathogens in the United States, with a fatality rate of around 50% in susceptible human hosts (Jones & Oliver, 2009; Oliver, 2015; Control & Prevention, 2019). *V. vulnificus* can also infect humans and cause deadly skin infections through marine water contact with open wounds (Oliver et al., 2012). Both *V. parahaemolyticus* and *V. vulnificus* often exist in biofilms, which are bacterial communities enclosed in a protective, self-secreted matrix of extracellular polymeric substances (EPS). Both species have been found attached to biotic or abiotic surfaces, which can include carapaces, algae, and specifically microplastics (MPs) (Donlan, 2002; Zettler et al., 2013; Zettler, Mincer & Amaral-Zettler, 2013; De Tender et al., 2015; Dang & Lovell, 2016; Kirstein et al., 2016; Lage & Graca, 2016; Decho &

Gutierrez, 2017; de Carvalho, 2018; Lami, 2019). A biofilm's natural lifecycle consists of cell attachment to a surface, followed by growth and biofilm development, and lastly periodic detachment of cells, called passive dispersion (Flemming et al., 2007; Kaplan, 2010). Biofilms contribute to over 75% of microbial infections (Davies, 2003; Guilhen, Forestier & Balestrino, 2017). One of the mechanisms of biofilm related infections can be influenced by the environment, called active environmentally induced biofilm dispersion, which triggers the release of bacteria from biofilms into the hosts' body environment (Flemming, Neu & Wozniak, 2007; Wang et al., 2011; Marks et al., 2013 Jamal et al., 2018; Rumbaugh & Sauer, 2020).

Dispersion is often referred to as "seeding dispersal," which facilitates the transfer of bacteria to new sites for colonization to repeat their biofilm lifecycle (Purevdorj-Gage, Costerton & Stoodley, 2005). Active seeding dispersal of cells from biofilms can occur in response to detecting changes in environmental conditions such as sudden changes in temperature, pH and nutrient conditions. In such cases, the bacteria leave the biofilm to find a more stable environment to colonize (McDougald et al., 2012). Dispersed cells have a phenotype between that of biofilm and planktonic cells, and have been found to display higher motility, virulence, adherence, and altered antibiotic resistance compared to their own biofilm and planktonic cells (Chua et al., 2014; Rumbaugh & Sauer, 2020). Biofilm dispersal can be a major mechanism of ingested foodborne and waterborne bacterial infections in humans (Abdallah et al., 2014). This likely occurs as potential persister cells embedded in biofilms survive the sudden changes in temperature and pH in a new environment like the human gastrointestinal tract. When environmental conditions are more favorable, the cells become metabolically active and disperse from the

consumed abiotic or biotic surface, and lead to colonization of the gastrointestinal surfaces (Motta et al., 2021; Xiong et al., 2022). One of these abiotic surfaces can be MPs, and since *Vibrio* biofilms have been abundantly found on MPs, one implication is that MPs could act as transport vectors of pathogenic *Vibrio* species to marine animals that coincidently or selectively ingest biofilm-associated MP particles instead of food particles. Consequently, consumption of raw seafood contaminated with *Vibrio* that dispersed from, or living on MPs could lead to higher human exposure to potential pathogenic *Vibrio* species and thus higher infection rates (Goldstein et al., 2014; Reisser et al., 2014; Kirstein et al., 2016; Viršek et al., 2017).

MPs are considered plastics that are less than 5 millimeters in size. They enter marine environments through direct introduction from runoff or wastewater that contains the particles or generated from the weathering or degradation of macroplastics in the environment (Barnes et al., 2009; Lambert et al., 2014). Primary MPs are defined as MPs that are produced by industry and are released directly into the environment. Secondary MPs are those that have fragmented from macroplastics due to degradation factors, with the majority of macroplastic pollution in marine environments being generated from land (Koelmans et al., 2014; GESAMP, 2016). Potential sources of primary MPs include exfoliants for personal care products like hand cleaners and facial cleansers. Secondary MPs include synthetic textile fibers and tire abrasion particles (Browne et al., 2011; Dubaish & Liebezeit, 2013; Lassen et al., 2015; Duis & Coors, 2016).

However, it is difficult to determine and quantify the sources, and thus reliable estimates of MP particles. One conservative model has suggested there are at least 5.25 trillion plastic particles in the oceans, weighing 243,978 metric tons (Eriksen et al.,

2014). Since this is a conservative estimate, there could be many more plastic particles in the ocean, causing high levels of exposure on marine life from plastic particle ingestion (Hollman et al., 2013; Wright et al., 2013). MPs have been found in several seafood species including clams and shrimp, with fiber, film and sphere MPs being some of the most abundant types, and concentrations as high as an average of 7,000 particles per shrimp and low as 5 particles per gram of clams (Davidson & Dudas, 2016; Waite, Donnelly & Walters, 2018; Curren et al., 2020) Recent studies conducted in marine environments have found bacterial communities, including *V. parahaemolyticus* and *V. vulnificus,* associate and live on MP surfaces. This could have serious implications for both marine life and human health, as MPs could be contributing to higher pathogenic *Vibrio* concentrations in contaminated raw seafood and thus increased exposure to humans by ingestion, or increased exposure by physical contact with biofilm-associated MPs in marine environments (Ward & Kach, 2009; Zettler, Mincer & Amaral-Zettler, 2013; Keswani et al., 2016; Kesy et al., 2021).

Vibrio biofilms on MPs and their sudden response to conditions likely encountered in the human host by ingestion such as elevated temperature, nutrient starvation and decreased pH is not well understood (Reidl & Klose, 2002; Oberbeckmann, Lder & Labrenz, 2015; Hernández-Cabanyero et al., 2019). However, to better assess potential changes in bacterial responses to the human environment, the use of simulated human-like media also needs to be implemented in non-invasive studies and models. This mimics components of the digestive system like simulated gastric fluid (SGF) and simulated intestinal fluid (SIF), and simulated components of the circulatory system like Human Plasma-Like Medium (HPLM).

Synthetic human-like media have been recently developed to better model the human environment. Exposing different bacteria to these medias can improve our understanding of how pathogens respond to these simulated human conditions as a proxy for *in vivo* studies. For example, use of simulated gastric fluids (SGF) and simulated intestinal fluids (SIF) can improve our understanding of how pathogenic *Vibrio* may survive aspects of human digestion and then colonize the human host (Wang et al., 2019). Blood media/agar, which has consisted of some percentage of animal blood like sheep, horse or bovine, has been previously used as a model in culturing *Vibrio* species from infected patients to examine effects like potential hemolysis (Collins, 1967; Davis et al., 1980; Kaysner, DePaola & Jones, 2004; Egwuatu et al., 2014; Public Health England, 2015; Wong & Griffin, 2018; Bonnet et al., 2019). However, this blood "media" does not have the same reported salts, nutrients, or metabolites as human blood (Cantor et al., 2017; Cantor, 2019). HPLM was recently synthesized to closely mimic an adult human's metabolic and salt profile and content (Cantor et al., 2017). HPLM has been used for several studies that have examined specific human cell types in the medium and determined effects on cell growth and metabolism. The results of these studies have shown that HPLM improved the effects on cells compared to traditional human cell culture media (Cantor et al., 2017; Cantor, 2019; Leney-Greene, et al., 2020; Rossiter et al., 2021). While HPLM has been reported in a few studies that examined specific human cell type culture and shows promise in becoming a standard media for human cell culture, using this HPLM for assessing human bacterial pathogens has not yet been reported (Cantor, 2019; Leney-Greene, et al., 2020; Rossiter et al., 2021). Using HPLM to assess pathogenic *Vibrio* species *in vitro* biofilm response to conditions that mimic human

plasma and body temperature could lead to better optimization of noninvasive studies and models, especially in clinical settings. Human environmental factors can influence biofilm growth and viability, and can also affect intracellular communication, with signaling molecules like cyclic-di-GMP playing roles in *Vibrio* dispersion, pathogenicity, and virulence in human hosts.

Active, environmentally induced dispersion occurs due to sensing of intracellular dispersion cues. This is accomplished by a membrane-associated protein complex that relays signals via a series of post-transcriptional modifications that can change the concentration of the intracellular signaling molecule cyclic-di-GMP (c-di-GMP) (Rumbaugh & Sauer, 2020). C-di-GMP can control and trigger the motile and sessile forms of the biofilm cell lifecycle (Galperin, 2004; Flemming et al., 2007; Römling, Galperin & Gomelsky, 2013; Lami, 2019). Different concentrations of c-di-GMP in the cell lead to different actions, with high concentrations leading to biofilm formation and low concentrations leading to dispersion (Valentini & Filloux, 2016). Some of the mechanistic actions and cellular responses include: type IV pili retraction, surface adhesin, EPS production and biofilm dispersion, all of which can be major factors in potential pathogenicity and virulence (Yildiz, 2008; Kaplan, 2010; Römling, Galperin & Gomelsky, 2013). As mentioned previously, the biofilm lifecycle is considered a developmental process that consists of attachment to a surface, bacterial growth and maturation and then periodic dispersal of cells (O'Toole, Kaplan & Kolter, 2000; Chua et al., 2014; Sauer et al., 2022). C-di-GMP is likely a checkpoint in this development that enables cells to either reach further biofilm maturation, or revert to a previous stage in the biofilm lifecycle if certain conditions change (Hengge, 2009; Römling, Galperin &

Gomelsky, 2013). This type of cellular communication can determine a biofilm's growth and lifecycle on surfaces like MPs that are potentially ingested by the human host. There is an underlying knowledge gap regarding how sudden changes that mimic the human environment affect *V. parahaemolyticus* and *V. vulnificus* biofilm biomass and dispersal processes, especially on and from low-density polyethylene, polypropylene, and polystyrene MPs.

In this study, we examined the effect of temperature, pH, nutrient availability, and media composition on *in vitro* biofilm dispersal processes by human isolated *V. parahaemolyticus* and *V. vulnificus*. We evaluated overall biofilm dispersal and viability in microplates, and then dispersal from low-density polyethylene (LDPE), polypropylene (PP), and polystyrene (PS) MPs. We also examined how c-di-GMP production and concentration were impacted by media composition and cell state (biofilm vs dispersed cells). We hypothesized that both *Vibrio* species would have overall decreased biofilm formation and cell dispersion in microplates when suddenly exposed to lower pHs and higher temperatures, especially in nutrient starved conditions due to stress. We also hypothesized both *Vibrio* species would have greater overall biofilm formation and cell dispersion in microplates when suddenly exposed to higher pH and temperature as conditions become more favorable. Both *Vibrio* species should also disperse from all MP types tested when exposed to these same favorable conditions. We also hypothesized that both human isolated strains would produce greater amounts of biofilm when exposed to HPLM compared to traditional media and have increased cell dispersal as their infection response to simulated human conditions. Exposure to SGF should lead to decreased cell dispersion due to low pH while exposure to SIF should lead to increased

cell dispersion due to higher pH. C-di-GMP concentrations should be higher in the biofilm state compared to dispersal state, with higher concentrations in dispersal cells in more stressful conditions.

2.3 Materials and Methods

Bacterial Strains and Growth Conditions

Two clinical strains (one of *V. parahaemolyticus*, one of *V. vulnificus*) were obtained from the American Type Culture Collection (Table 1, ATCC, Manassas, VA, United States). *V. parahaemolyticus* strains are commonly classified by their species marker (*tlh*) and capacity to infect humans through production of thermostable direct hemolysin (*tdh*) or thermostable direct hemolysin-related hemolysin (*trh*) virulence factors (Honda & Iida, 1993; Broberg, Calder & Orth, 2011). In our study, human isolated strain ATCC17802 contained *tlh* and *trh* and its human estimated threshold mean infective dose (ID_{50}) is listed in Table 1. While *V. vulnificus* strains can also be classified by virulence factors, *V. vulnificus* can also be classified by 16S rRNA typing, which reveals if they are more clinically- (type B, higher possible human infectivity) or more environmentally- (type A, higher possible marine vertebrate infectivity) associated. In our study, the human isolate strain ATCC27562 is type B and its human estimated threshold mean infective dose (ID_{50}) is also listed in Table 1.

The two clinical strains were tested for biofilm formation and dispersal after exposure to different temperatures, pHs and nutrients and media compositions. All strains were maintained in 25% (vol/vol) glycerol at −80°C to be used in further experiments. A single colony of each bacteria was inoculated in 5 mL unadjusted modified seawater with yeast extract (MSYE, ATCC medium 804, Oliver & Colwell, 1973) broth supplemented

with calcium chloride (1.8 g/L), as calcium chloride contributes to biofilm formation (Tischler et al., 2018), and incubated overnight at 30°C with shaking at 180 revolutions/minute (rpm). After incubation, the broth culture was adjusted to 10^7 cells (OD_{600}) using a SpectraMax M3 plate reader after calibrating the instrument's absorbance values to cell counts from spread plating (Molecular Devices, San Jose, CA, United States), which was used for subsequent experiments. The pH of MSYE and MSYE without peptone and yeast extract (MS), was adjusted using 1M hydrochloric acid and 1M sodium hydroxide using a SevenExcellence™ pH probe (Mettler-Toledo, Columbus, OH, USA) after pH standard calibration. HPLM was obtained from Thermo Fisher (Waltham, USA) while SGF (supplemented with pepsin) and SIF (supplemented with trypsin and pancreatin) were obtained from Biochemazone™ (Ontario, Canada).

Biofilm Formation in Microplates

Biofilm formation experiments in microplates were adapted from O'Toole, 2011. In summary, adjusted cell densities (10^7 cells) were diluted 1:100 in fresh MSYE supplemented with calcium chloride media to reach a final density of 10^5 cells. Then 150µL of the diluted culture was pipetted into clear tissue-culture treated 96-well polystyrene microplates (Costar®, Corning, NY, United States) for OD_{600} and OD_{570} readings or black walled, clear bottom tissue-culture treated 96-well polystyrene microplates for fluorescence readings. Then, the 96-well plates were incubated at 25°C with low shaking (125 rpm) for 24 hours to form biofilms. Wells containing MSYE supplemented with calcium chloride without inoculation were used as blank and group controls. Low shaking conditions, instead of static, were chosen to introduce shear stress to the biofilms, to better resemble the marine and human environments in all microplate

biofilm formation and dispersal experiments. All plates in biofilm formation and dispersal experiments were sealed with Parafilm™ (Bemis, Neenah, WI, United States) to prevent evaporation of media.

Biofilm Dispersal Microplate Assay

Biofilms of both *V. parahaemolyticus* and *V. vulnificus* were dispersed according to Gjermansen et al., 2005 and Barraud et al., 2014 with some modifications. Briefly, after 24-hours planktonic cells were removed from the 96-well microplates before washing with 175µL 1X phosphate buffer saline (PBS, Molecular Biologicals International, Irvine, CA, United States) gently three times. Wells were then refilled (150 µL) with media and incubated under conditions outlined in Table 2. Wells containing media without inoculation were used as blank and group controls. The optical density of each well was measured at λ= 600nm using a SpectraMax M3 plate reader (Molecular Devices, San Jose, CA, United States) every 15 minutes for 2 hours at 25 or 37°C.

Crystal Violet Staining Microplate Assay

Biofilms of both *V. parahaemolyticus* and *V. vulnificus* in microplates were quantified by crystal violet staining according to O'Toole, 2011 and Valquier-Flynn et al., 2017 with some modifications. Following 2-hour exposures, planktonic cells were removed and then each well was gently washed with 175µL 1X phosphate buffer saline (PBS, Molecular Biologicals International, Irvine, CA, United States) three times. 175µL of 100% methanol (Sigma-Aldrich, St. Louis, MO, United States) was then added to the plates to fix the biofilms to the plates at room temperature for 20 minutes. Then, the methanol was removed, and residual methanol allowed to evaporate from plates in fume hood. Biofilms were stained with 150µL of 0.1% (wt/vol) crystal violet (Sigma-Aldrich,

St. Louis, MO, United States) for 15 minutes at room temperature. Staining solution was removed via pipette, and then 175µL 1X PBS was used to remove the non-bound dye three times. The stained and washed biofilms were air dried overnight in a fume hood, then 150µL of 30% acetic acid (Fisher Scientific, Hampton, NH, United States) was added to dissolve the bound crystal violet for 15 minutes. 125µL of the solubilized crystal violet acetic acid solution was then transferred to a new 96-well clear polystyrene microplate, and optical densities of each well were measured by absorbance (570 nm) using a SpectraMax M3 plate reader (Molecular Devices).

Biofilm Formation on MPs

Biofilm formation experiments on MPs were adapted from O'Toole, 2011, Hamanaka et al., 2012, Valquier-Flynn et al., 2017 and Leighton et al., 2023. In summary, MPs were generated from slide coupons of low-density polyethylene (LDPE), polypropylene (PP), and polystyrene (PS) (BioSurface Technologies, Boseman, MT, United States) by cutting the coupons to dimensions of 4mm x 1mm. Plastics were chemically sterilized (70% ethanol for PP, 70% isopropanol for LDPE and PS) for 24 hours and were then placed in sterile petri dishes in a biosafety cabinet until residual alcohol evaporated. Chemically sterilized MPs were then placed in 96-well sterile non-treated microplates (Costar®, Corning, NY, United States) and then adjusted cell densities (10^7 cells) were diluted 1:100 in fresh MSYE with calcium chloride media to reach a final density of 10^5 cells. Microplates containing MPs were filled with 150 µL of inoculum, then then microplates were incubated at 25°C with low shaking (125 rpm) to form biofilms in 24 hours. Wells containing media without inoculation and with MPs were used as blank and group controls.

Biofilm Dispersal Microplastic Assay

Biofilm dispersal experiments were adapted from Hamanaka et al., 2012 and Valquier-Flynn et al., 2017 with slight modifications. Following 24-hour incubation, MPs were washed three times with 175µL 1X PBS, and then MPs were transferred to new wells containing 150 µL media and incubated in conditions in Table 2. Wells containing media without inoculation were used as blank and group controls.

Crystal Violet Staining Microplastic Assay

Biofilms of both *V. parahaemolyticus* and *V. vulnificus* on MPs were quantified by crystal violet staining according to Leighton et al., 2023 with some modifications. After the remainder of the planktonic cells were removed, the MPs were gently washed three times in 175 µL 1X PBS, and then 175 µL of 100% methanol (Sigma-Aldrich, St. Louis, MO, United States) was added per well to fix the biofilms and incubated at room temperature for 20 minutes. Then, the methanol was removed, and residual methanol allowed to evaporate off MP surfaces in fume hood. The biofilms were stained with 150 µL of 0.1% (wt/vol) crystal violet (Sigma-Aldrich, St. Louis, MO, United States) for 15 minutes at room temperature. The staining solution was removed, and then 1X PBS was used to remove the non-bound dye three times. The MPs were then transferred to a new 96-well non-treated microplate and the stained and washed biofilms on both MPs and their respective microplates were air dried overnight in fume hood. Lastly, 150 µL of 30% acetic acid (Fisher Scientific, Hampton, NH, United States) was added to dissolve the bound crystal violet and incubated at room temperature for 15 minutes. The optical density of each well was measured at a wavelength of 570 nm using a SpectraMax M3 plate reader (Molecular Devices, San Jose, CA, United States). Mean OD_{570} values were

then divided by the surface area (24 mm^2 - PP & LDPE, 14 mm^2 - PS) of the plastics tested to obtain final biofilm biomass values per mm of the surface type.

Determination of Dispersed Biofilm Cell Densities from MPs

Total dispersed biofilm cell densities were determined after biofilms on MPs were exposed to different pHs, temperatures, nutrient availability, and media compositions. After incubation, 100 µL of each well was either taken and serially diluted (10^{-2} to 10^{-7}) in 900 µL 1X PBS in microcentrifuge tubes, or directly spread plated (10^{-1}) onto prewarmed MSYE supplemented with calcium chloride agar plates for determination of number of dispersed cells. Plates were incubated at 37°C for 20-24 hours. Biofilm dispersed cells were determined in terms of colony forming units (CFU) per MP and then log transformed to obtain final values.

Biofilm Removal and Determination of Colony Counts

Total colony counts were determined from biofilm suspensions according to Bjerkan, Witsø & Bergh, 2009, Portillo et al., 2013 and Leighton et al., 2023 with some modifications. Following 24-hour incubation, planktonic cells were removed from the 96-well non-treated microplate wells before washing MPs with 175 µL 1X PBS gently, three times. Then, plastics were placed individually in 1 mL 1X PBS in sterile borosilicate culture tubes (VWR International, Radnor, PA, USA) with a rubber cap and vortexed using a Vortex Genie 2® (Fisher Sci.) at the highest setting for 1 minute. The borosilicate glass tubes containing the plastics and 1X PBS solution were then placed in a Branson M2800 ultrasonication water bath (Branson Ultrasonics, Brookfield, CT, USA) and sonicated for 5 minutes at 40 kHZ. The glass tubes were vortexed again for 1 minute. Lastly, the biofilm suspension in 1X PBS was serially diluted in 1X PBS in

microcentrifuge tubes and 10^{-1} to 10^{-7} serial dilutions were spread onto prewarmed MSYE supplemented with calcium chloride agar plates. Plates were incubated at 37°C for 20-24 hours. The viability of cells was determined as CFUs per MP. The biofilm cell densities of each plastic group had biological triplicates and each experiment was conducted three times independently. Mean CFU values were then divided by the surface area (24 mm^2 - PP & LDPE, 14 mm^2 - PS) of the plastics tested to obtain CFU values per mm of the surface type. CFU values were then log-transformed to obtain final values.

Resazurin Viability Assay

The viability of both *V. parahaemolyticus* and *V. vulnificus* biofilms were examined after being exposed to different conditions (Table 2) by a resazurin metabolic assay according to Riss et al., 2004 with some modifications. After 24-hours, planktonic cells were removed from the black walled, clear bottom 96-well microplates before washing with 175µL 1X phosphate buffer saline (PBS, Molecular Biologicals International, Irvine, CA, United States) gently three times. Then, wells were refilled (150 µL) with media and incubated in conditions in Table 2 at 37°C. After incubation, the planktonic cells were removed and then each well was washed with 175µL 1X phosphate buffer saline (PBS, Molecular Biologicals International, Irvine, CA, United States) gently three times. Then each well was refilled with 150 µL of unadjusted MSYE supplemented with calcium chloride and 30 µL of filter sterilized resazurin (0.15 mg/mL in 1x PBS) was also added to each well. Fluorescence was read (excit/emiss =560/590nm) every 15 minutes for 4 hours at 37°C. Final RFU values were then normalized against their

corresponding OD_{600} values after exposure. Wells containing media without inoculation were used as blank and group controls.

Cyclic-di-GMP Assay

Estimation of c-di-GMP levels of both *V. parahaemolyticus* and *V. vulnificus* were examined after being exposed to MSYE, SIF and HPLM at 37°C for 2 hours by a cyclic-di-GMP assay kit (Lucerna, Brooklyn, NY, United States) according to manufacturer's instructions with some modifications. Briefly, after environmental exposure 100 µL of dispersed cells were diluted 1:10 in RNase-free water. Sterilized swabs were used to collect biofilms, then swabs were submerged and vortexed in 150 µL of RNase-free water, and 100 µL of biofilm cells were diluted 1:10 in RNase-free water. Then, 50 µL of diluted culture along with assay reagents and serially diluted c-di-GMP standards were set up for the assay, and then the c-di-GMP concentration was calculated according to the standard calibration curve. Appropriate sample dilution factors were multiplied to get the final c-di-GMP concentrations (in picograms per microliter).

Statistical Analyses

The experimental data for biofilm biomass, biofilm CFUs, cell colonization, dispersal CFUs and c-di-GMP concentrations were expressed as the mean ± standard deviation. Experimental data for biofilm viability were expressed as the mean and then normalized against corresponding mean OD_{600} values. Two-way analysis of variance (ANOVA) models were calculated using Rstudio software to compare value differences ($\alpha = 0.05$) in biofilm biomass, biofilm CFUs, cell colonization and dispersal CFUs. For the first set of models, temperature, pH and nutrient content were the variables in examining value differences between nutrient rich and nutrient starved conditions at

different temperature and pH intraspecies. 25°C was selected as the reference temperature, MSYE as the reference media and pH as a continuous variable for all analyses. For the second set of models, temperature and media composition were the variables in examining value differences between simulated human medias and MSYE intraspecies, and *Vibrio* species was a variable for examining value differences interspecies. 25°C was selected as the reference temperature, MSYE with similar pH to simulated human medias as the reference medias, and *V. parahaemolyticus* as the reference species for all analyses. One-way ANOVAs ($\alpha = 0.05$) were calculated for comparison between c-di-GMP levels within and between biofilm and dispersal cells after exposure to different medias using Excel's data analysis toolpak. Bonferroni corrections were calculated and applied to all p-values to control for type 1 errors.

2.4 Results

Experiments and statistical analyses were conducted to test the effect and differences in temperature (25, 37°C), pH (3, 4, 5, 6, 7, 7.4, 8.1), nutrient availability (MS) and simulated human media composition (HPLM, SGF, SIF) after 2-hour exposure on overall biofilm biomass, cell viability, dispersal and c-di-GMP concentrations in microplates and biofilm biomass, cell viability, dispersal and colonization on/from LDPE, PP and PS MPs by human isolated strains of *V. parahaemolyticus* and *V. vulnificus*. All raw means and statistical data are presented in Supplemental Tables S1 – S61.

The crystal violet staining assays reflected total bacterial biomass (expressed as OD_{570} values) on microplates, MP surface types, and subsequent microplate colonization from dispersal of these MP surfaces. Cell concentration assays reflected cell dispersal in

microplates (expressed as OD_{600} values), and biofilm cell and biofilm dispersal cell densities (expressed as colony forming units, CFUs) on/from the substate surface types. Resazurin metabolic assays reflected biofilm cell viability (expressed as RFUs). C-di-GMP assays reflected biofilm and cell dispersal state signaling molecule concentrations (expressed as pg/µL).

Elevated temperature, changes in pH, and nutrient starvation influence overall *V. parahaemolyticus* and *V. vulnificus* biofilm formation, cell dispersal and biofilm viability in microplates.

Overall, both *V. parahaemolyticus* and *V. vulnificus* appeared to have differences in their biofilm biomass and cell dispersal concentrations after being exposed to elevated temperatures, different pH levels and nutrient starvation (Figure 1; Supplemental Table S1, S2). Regarding *V. parahaemolyticus* in nutrient rich media, exposure to elevated temperature (37°C) had variable effects on biofilm biomass, but increased cell dispersal concentrations. However, in nutrient starved media, exposure to elevated temperature appeared to increase biofilm biomass but decrease cell dispersal concentrations, except at lower pH levels of 3 and 4 where cell dispersal concentrations increased. Exposure to lower pHs (3, 4) led to a decrease in biofilm biomass in both nutrient rich and nutrient starved conditions, with a greater negative effect on cell dispersal concentrations in nutrient rich conditions. Regarding *V. vulnificus* in nutrient rich media, exposure to elevated temperature (37°C) had variable effects on biofilm biomass, but increased cell dispersal concentrations. This same phenomenon was observed in nutrient starved media, with variable effects on biofilm biomass, but increased cell dispersal. However, *V. vulnificus* was greatly affected by nutrient starvation, as this led to a decrease in biofilm

biomass across all pHs at both 25 and 37°C compared to nutrient rich conditions. Exposure to lower pHs (3, 4) led to a greater decrease in biofilm biomass in nutrient rich conditions compared to nutrient starved.

ANOVA revealed certain significant differences ($p \leq 0.05$) in the amount of biofilm biomass and cell dispersal concentrations in microplates. Regarding *V. parahaemolyticus*, there was a significant positive effect of pH on *V. parahaemolyticus* overall biofilm biomass ($p \leq 0.05$) and cell dispersal concentrations ($p \leq 0.001$) in microplates (Supplemental Table S5). Meaning, when pH increased there was a significant increase in both *V. parahaemolyticus* biofilm biomass and cell dispersal concentrations in a short time (2 hours). However, temperature and nutrient starvation were not significant factors on either biofilm biomass or cell dispersal concentrations (Supplemental Table S3, S4). Regarding *V. vulnificus*, elevated temperature, pH, and nutrient starvation were not significant factors in either biofilm biomass or cell dispersal concentrations in microplates (Supplemental Table S3 – S5).

Biofilms of both *V. parahaemolyticus* and *V. vulnificus* were able to tolerate and survive in both nutrient rich and starved conditions at pH 4 – 8.1 for 2 hours, with similar metabolism characteristics across these conditions within both species (Figure 2; Supplemental Table S10, S11). Biofilm viability was impacted in pH of 3 and noticeably decreased for both species. However, *V. parahaemolyticus* biofilms still tolerated and survived a pH of 3 in both nutrient rich and starved conditions and biofilms recovered in growth once exposed to non-stressed conditions. Comparatively *V. vulnificus* was able to survive pH of 3 in nutrient rich conditions but did not recover as well and did not survive pH of 3 in nutrient starved conditions.

Elevated temperature, changes in pH and nutrient starvation influence *V. parahaemolyticus* biofilm biomass, biofilm cell concentrations, cell dispersal and cell colonization on and from LDPE, PP and PS Microplastics

Exposure to elevated temperature (37°C) had variable effects on *V. parahaemolyticus* biofilm biomass and biofilm cell concentrations on LDPE in nutrient rich conditions, (Figure 3, 1A; Supplemental Table S12, S13). However, biofilm biomass on LDPE was greater in nutrient rich compared to nutrient starved conditions across all pH levels and elevated temperature. In nutrient starved conditions, exposure to elevated temperature appeared to have variable effects on LDPE biofilm biomass, but elevated temperature decreased biofilm cell concentrations across all pH levels. Cell dispersal concentrations from LDPE were roughly the same at medium to higher pH (5 – 8.1) both in nutrient rich and nutrient starved conditions (Figure 3, 1B; Supplemental Table S14, S15). While small concentrations of biofilm cells survived at the lowest pH of 3 in both nutrient rich and starved conditions, no dispersal cells were detected at pH 3. Cell colonization was noticeably higher in nutrient rich conditions compared to nutrient starved. Elevated temperature contributed to greater cell colonization in nutrient rich conditions but decreased cell colonization in nutrient starved. ANOVA revealed certain significant differences ($p \leq 0.05$) in the amount of biofilm biomass on LDPE. There was a significant positive effect of pH ($p \leq 0.01$) on *V. parahaemolyticus* biofilm biomass on LDPE, meaning when pH increased, biofilm biomass on LDPE significantly increased (Supplemental Table S26).

Elevated temperature largely decreased *V. parahaemolyticus* biofilm biomass (except at pH 3) and biofilm cell concentrations (except at pH 7) on PP in nutrient rich

conditions (Figure 3, 2A; Supplemental Table S16, S17). In nutrient starved conditions, exposure to elevated temperature appeared to have variable effects on PP biofilm biomass, with little changes in biofilm cell concentrations except slight decreases in cell concentrations at pH of 4 and 8.1. Cell dispersal concentrations from PP were roughly the same at higher pH (7 – 8.1), in that cell dispersal in nutrient rich conditions was slightly higher at both 25°C and 37°C compared to nutrient starved (Figure 3, 2B; Supplemental Table S18, S19). Cell colonization was noticeably higher in nutrient rich conditions compared to nutrient starved, especially at elevated temperature (37°C) and at pH of 6 – 8.1. While small concentrations of biofilm cells survived at the lowest pH of 3 in nutrient rich conditions, no dispersal cells were detected at pH 3. ANOVA revealed certain significant differences ($p \leq 0.05$) in the amount of cell dispersal and colonization from PP. There was a significant positive effect of pH ($p \leq 0.05$) on *V. parahaemolyticus* cell dispersal from PP, meaning as pH increased, cell dispersal also significantly increased (Supplemental Table S26). There was also a significant positive effect of pH alone ($p \leq 0.01$) and a significant synergistic positive effect of pH and elevated temperature ($p \leq 0.001$) on *V. parahaemolyticus* cell colonization from dispersal of PP (Supplemental Table S26, S28). This means when just pH and a combination of pH and temperature increased, cell colonization also significantly increased. However, a combination of pH, elevated temperature and nutrient starvation led to a significant synergistic negative effect ($p \leq 0.01$) on *V. parahaemolyticus* cell colonization from dispersal of PP (Supplemental Table S30).

Elevated temperature decreased *V. parahaemolyticus* biofilm biomass but had variable effects on biofilm cell concentrations across all pH levels on PS in nutrient rich

conditions (Figure 3, 3A; Supplemental Table S20, S21). In nutrient starved conditions, exposure to elevated temperatures decreased biofilm biomass across all pH levels (except pH of 4), and decreased biofilm cell concentrations at pH 4 – 7. An increase in temperature increased cell dispersal concentrations from PS at pH 5 – 8.1 (Figure 3, 3B; Supplemental Table S22, S23). Cell colonization was noticeably higher in nutrient rich conditions compared to nutrient starved, especially at elevated temperature (37°C) and at pH 6 – 8.1. No concentrations of biofilm cells or dispersal cells were detected at pH 3. ANOVA revealed certain significant differences ($p \leq 0.05$) in the amount of cell colonization from PS. There was a significant positive effect of pH alone ($p \leq 0.05$) and a significant synergistic positive effect of pH and elevated temperature ($p \leq 0.01$) on *V. parahaemolyticus* cell colonization from dispersal of PS (Supplemental Tale S26, S28). This means when just pH and a combination of pH and temperature increased, cell colonization also significantly increased. However, a combination of pH, elevated temperature and nutrient starvation led to a significant synergistic negative effect ($p \leq 0.05$) on *V. parahaemolyticus* cell colonization from dispersal of PS (Supplemental Table S30).

Elevated temperature, changes in pH and nutrient starvation influence *V. vulnificus* biofilm biomass, biofilm cell concentrations, cell dispersal and cell colonization on and from LDPE, PP and PS Microplastics.

Exposure to elevated temperature (37°C) had variable effects on *V. vulnificus* biofilm biomass across all pH levels but decreased biofilm cell concentrations on LDPE in nutrient rich conditions at pH 6 – 8.1 (Figure 4, 1A; Supplemental Table S12, S13). In nutrient starved conditions, exposure to elevated temperature increased biofilm biomass

at pH 6 – 7.4 but had variable effects on biofilm cell concentrations on LDPE. An increase in temperature increased cell dispersal concentrations from LDPE at pH 5 – 8.1 in nutrient rich media (Figure 4, 2A; Supplemental Table S14, S15). While elevated temperature had variable effects on cell colonization from LDPE in nutrient rich media, colonization was noticeably higher compared to nutrient starved conditions. No concentrations of biofilm cells or dispersal cells were detected at pH 3. ANOVA revealed certain significant differences ($p \leq 0.05$) in the amount of cell colonization from LDPE. There was a significant positive effect of pH on *V. vulnificus* cell colonization from LDPE ($p \leq 0.05$) (Supplemental Table S26). This means as pH increased, there was a significant increase in the amount of cell colonization from LDPE.

Exposure to elevated temperature (37°C) increased *V. vulnificus* biofilm biomass at pH 6 – 7.4 but had variable effects on biofilm cell concentrations on PP in nutrient rich conditions (Figure 4, 1B; Supplemental Table S16, S17). Biofilm biomass on PP was greater in nutrient rich compared to nutrient starved conditions across all pH levels. In nutrient starved conditions, exposure to elevated temperature had variable effects on both biofilm biomass and cell concentrations. However, at pH of 4 biofilm cell concentrations were noticeably higher at 25°C and especially 37°C in nutrient starved conditions compared to nutrient rich. An increase in temperature increased cell dispersal concentrations from PP at pH 6 – 8.1 and increased cell colonization from PP at pH 5 – 7.4 in nutrient rich media (Figure 4, 2B; Supplemental Table S18, S19). Cell colonization was noticeably higher in nutrient rich conditions compared to nutrient starved, especially at elevated temperature (37°C) and at pH 6 – 7.4. However, at pH of 4 cell dispersal were noticeably higher at 25°C and especially 37°C in nutrient starved conditions compared to

nutrient rich. No concentrations of biofilm cells or dispersal cells were detected at pH 3. ANOVA revealed certain significant differences ($p \leq 0.05$) in the amount of cell colonization from PP. There was a significant positive effect of pH on *V. vulnificus* cell colonization from PP ($p \leq 0.05$) (Supplemental Table S26). This means as pH increased, there was a significant increase in the amount of cell colonization from PP.

Exposure to elevated temperature (37°C) had variable effects on *V. vulnificus* biofilm biomass across all pH levels, but increased cell biofilm concentrations on PS in nutrient rich conditions at pH 5 – 7.4 (Figure 4, 1C; Supplemental Table S20, S21). In nutrient starved conditions, exposure to elevated temperature increased biofilm biomass at pH 3 – 7.4, especially at pH 5 and 6 as biofilm biomass was greater at these pH levels in nutrient starved conditions compared to nutrient rich. However, elevated temperature decreased biofilm cell concentrations at pH 5 – 7.4 in nutrient starved conditions. An increase in temperature increased cell dispersal concentrations from PS at pH 5 – 8.1, with noticeable increases in cell colonization at pH 6 and 7.4 in nutrient rich media (Figure 4, 2C; Supplemental Table S22, S23). Cell colonization was noticeably higher in most pH levels (except pH of 4 and 6) in nutrient rich conditions compared to nutrient starved. An increase in temperature decreased cell dispersal at pH 6 – 8.1 in nutrient starved media. No concentrations of biofilm cells or dispersal cells were detected at pH 3. Elevated temperature and simulated human medias influence overall *V. parahaemolyticus* and *V. vulnificus* biofilm biomass, cell dispersal and biofilm viability in microplates.

Overall, both *V. parahaemolyticus* and *V. vulnificus* appeared to have differences in their biofilm biomass and cell dispersal concentrations after being exposed to elevated temperatures and simulated human media (Figure 5; Supplemental Table S31, S32).

Regarding *V. parahaemolyticus* in simulated human media, exposure to elevated temperature (37°C) decreased biofilm biomass in SIF and HPLM, but increased biofilm biomass in SGF. Elevated temperature also decreased cell dispersal concentrations in HPLM. *V. parahaemolyticus* biofilm biomass and cell dispersal concentrations were greatest in HPLM across all three simulated human medias. Biofilm biomass was lowest after exposure to SGF, with cell dispersal concentrations being mostly undetected in SGF and SIF. Regarding *V. vulnificus* in simulated human media, exposure to elevated temperature (37°C) increased biofilm biomass in SGF, SIF and HPLM. Elevated temperature also increased cell dispersal concentrations in HPLM. *V. vulnificus* biofilm biomass and cell dispersal concentrations were greatest in HPLM across all three simulated human medias. Biofilm biomass was comparable after exposure to SGF and SIF, with cell dispersal concentrations being mostly undetected.

Results of ANOVAs revealed certain significant differences ($p \leq 0.05$) in the amount of biofilm biomass concentrations in microplates. Regarding *V. parahaemolyticus*, there were no significant effects of temperature on biofilm biomass or cell dispersal concentrations in SGF, SIF or HPLM (Supplemental Table S33). There were also no significant effects on media composition on *V. parahaemolyticus* biofilm biomass or cell dispersal compared to similar pH MSYE (Supplemental Table S34). Regarding *V. vulnificus*, there were no significant effects of temperature on biofilm biomass or cell dispersal concentrations in SGF, SIF or HPLM (Supplemental Table S33). However, HPLM significantly enhanced *V. vulnificus* biofilm biomass ($p \leq 0.05$) compared to similar pH MSYE (Supplemental Table S34). There were no significant effects of SGF or SIF on biofilm biomass or cell dispersal concentrations compared to

similar pH MSYE (Supplemental Table S34). *V. vulnificus* had significantly less biofilm biomass after exposure to SGF ($p \leq 0.01$), SIF ($p \leq 0.01$), and HPLM ($p \leq 0.01$), compared to *V. parahaemolyticus* (Supplemental Table S36).

Biofilms of both *V. parahaemolyticus* and *V. vulnificus* were able to tolerate and survive in both HPLM and SIF for 2 hours (Figure 6, Supplemental Table S40). *V. parahaemolyticus* had similar metabolic characteristics after exposure to HPLM and SIF (Figure 6, A), but *V. vulnificus* biofilm cell metabolism was higher after exposure to HPLM compared to SIF (Figure 6, B). Biofilm viability was impacted in SGF and noticeably decreased for both species. However, *V. parahaemolyticus* biofilms still tolerated and survived exposure to SGF and biofilms recovered in growth once exposed to non-stressed conditions. Comparatively *V. vulnificus* was not able to survive exposure to SGF.

Elevated temperature and simulated human medias influence *V. parahaemolyticus* and *V. vulnificus* biofilm biomass, biofilm cell concentrations, cell dispersal and cell colonization on and from LDPE, PP and PS Microplastics

Exposure to elevated temperature decreased *V. parahaemolyticus* biofilm biomass and biofilm cell concentrations on LDPE in SGF, SIF and HPLM (Figure 7, 1A; Supplemental Table S41, S42). *V. parahaemolyticus* biofilm biomass on LDPE was greatest at both 25°C and 37°C in SIF compared to SGF and HPLM, but biofilm cell concentrations were greatest at both 25°C and 37°C in HPLM compared to SIF and SGF. Elevated temperature decreased *V. parahaemolyticus* cell dispersal concentrations from LDPE in SIF, but increased cell dispersal in HPLM (Figure 7, 2A, Supplemental Table S43, S44). This trend was opposite for cell colonization, as elevated temperature

increased cell colonization from LDPE in SIF but decreased cell colonization in HPLM. While no concentrations of biofilm cells or dispersal cells were detected after exposure to SGF, biofilm biomass and cell colonization was higher at both 25°C and 37°C compared to HPLM. Exposure to elevated temperature did not have noticeable effects on *V. vulnificus* biofilm biomass or biofilm cell concentrations on LDPE in SGF or SIF (Figure 7, 1A; Supplemental Table S41, S42). However, elevated temperature did increase biofilm biomass but slightly decreased biofilm cell concentrations in HPLM. Both biofilm biomass and biofilm cell concentrations were greatest in HPLM compared to SGF and SIF. Again, exposure to elevated temperature did not have detectable effects on *V. vulnificus* cell dispersal from LDPE in SGF or SIF (Figure 7, 2A; Supplemental Table S43, S44). However, elevated temperature did increase cell colonization from LDPE in SGF, SIF and HPLM, with slightly higher cell dispersal concentrations in HPLM. Both cell colonization and cell dispersal concentrations were greatest in HPLM compared to SGF and SIF. No detectable concentrations of *V. vulnificus* biofilm cells or dispersal cells were observed after exposures to SGF or SIF. ANOVA revealed certain significant differences ($p \leq 0.05$) in the amount of *V. vulnificus* biofilm cell concentrations on LDPE. HPLM significantly enhanced *V. vulnificus* biofilm cell concentrations on LDPE ($p \leq 0.05$) when compared to MSYE at a similar pH (Supplemental Table S53).

Exposure to elevated temperature decreased *V. parahaemolyticus* biofilm biomass on PP in SGF, SIF and HPLM (Figure 7, 1B; Supplemental Table S45, S46). *V. parahaemolyticus* biofilm biomass on PP was greatest at 25°C in SIF and 37°C in HPLM, but biofilm cell concentrations were greatest at both 25°C and 37°C in HPLM compared to SIF and SGF. An increase in temperature increased *V. parahaemolyticus* cell dispersal

concentrations from PP in HPLM, and SIF but decreased cell dispersal in SIF (Figure 7, 2B; Supplemental Table S47, S48). This trend was opposite for cell colonization, as elevated temperature increased cell colonization from PP in SIF but decreased cell colonization in HPLM. While no concentrations of *V. parahaemolyticus* biofilm cells or dispersal cells were detected after exposure to SGF, cell colonization was about the same at both 25°C and 37°C compared to HPLM. Exposure to elevated temperature did not have noticeable effects on *V. vulnificus* biofilm biomass or biofilm cell concentrations on PP in SGF or SIF (Figure 7, 1B, Supplemental Table S45, S46). However, elevated temperature did increase biofilm biomass and slightly increased biofilm cell concentrations in HPLM. Both biofilm biomass and biofilm cell concentrations were greatest in HPLM compared to SGF and SIF. Exposure to elevated temperature did not have noticeable effects on *V. vulnificus* cell dispersal from PP in SGF or SIF (Figure 7, 2A; Supplemental Table S47, S48). However, elevated temperature did increase cell colonization from PP in SGF, SIF and HPLM, with slightly greater cell dispersal concentrations in HPLM. Both cell colonization and cell dispersal concentrations were greatest in HPLM compared to SGF and SIF. No concentrations of *V. vulnificus* biofilm cells or dispersal cells were detected after exposure to SGF or SIF. ANOVA revealed certain significant differences ($p \leq 0.05$) in the amount of *V. vulnificus* biofilm biomass on PP. *V. vulnificus* had significantly less biofilm biomass on PP after exposure to SGF ($p \leq 0.05$), SIF ($p \leq 0.05$), and HPLM ($p \leq 0.05$), compared to *V. parahaemolyticus* (Supplemental Table S56).

Exposure to elevated temperature increased *V. parahaemolyticus* biofilm biomass on PS in SGF and SIF, but decreased biofilm biomass in HPLM (Figure 7, 1C;

Supplemental Table S49, S50). *V. parahaemolyticus* biofilm biomass and biofilm cell concentrations on PS were greatest at both 25°C and 37°C in HPLM compared to SIF and SGF. An increase in temperature decreased *V. parahaemolyticus* cell dispersal concentrations from PS in HPLM and SIF (Figure 7, 2C; Supplemental Table S51, S52). This trend was opposite for cell colonization, as elevated temperature increased cell colonization from PS in SIF and HPLM. While no concentrations of *V. parahaemolyticus* biofilm cells or dispersal cells were detected after exposure to SGF, cell colonization was about the same at both 25°C and 37°C compared to SIF. ANOVA revealed certain significant differences ($p \leq 0.05$) in the amount of *V. parahaemolyticus* biofilm biomass on PS. HPLM significantly enhanced *V. parahaemolyticus* biofilm biomass on PS (≤ 0.01) compared to MSYE with similar pH (Supplemental Table S53). Exposure to elevated temperature increased *V. vulnificus* biofilm biomass on PS in SIF and HPLM, but decreased biofilm biomass in SGF (Figure 7, 1C; Supplemental Table S49, S50). An increase in temperature increased biofilm cell concentrations in HPLM but decreased biofilm cell concentrations in SIF. Both biofilm biomass and biofilm cell concentrations were greatest in HPLM at elevated temperature compared to SGF and SIF. Exposure to elevated temperature did not have noticeable effects on *V. vulnificus* cell dispersal from PS in SGF or SIF (Figure 7, 2C; Supplemental Table S51, S52). However, elevated temperature did increase cell colonization from PS in SGF, SIF and HPLM, with slightly greater cell dispersal concentrations in HPLM. Both cell colonization and cell dispersal concentrations were greatest in HPLM compared to SGF and SIF. No concentrations of *V. vulnificus* biofilm cells or dispersal cells were detected after exposure to SGF or SIF. ANOVA revealed certain significant differences ($p \leq 0.05$) in the amount of *V. vulnificus*

biofilm biomass and biofilm cells on PS. HPLM ($p \leq 0.05$), SGF ($p \leq 0.01$) and SIF (≤0.01) significantly enhanced *V. vulnificus* biofilm biomass on PS compared to MSYE with similar pHs (Supplemental Table S53). Exposure to elevated temperature also significantly enhanced *V. vulnificus* biofilm biomass ($p \leq 0.001$) and biofilm cells (≤0.01) on PS in HPLM and significantly enhanced biofilm biomass on PS in SIF ($p \leq 0.05$) compared to MSYE of similar pHs (Supplemental Table S55). *V. vulnificus* had significantly less biofilm biomass on PS after exposure to HPLM ($p \leq 0.001$) compared to *V. parahaemolyticus* (Supplemental Table S58). There was also a significant synergistic effect of HPLM and elevated temperature on *V. vulnificus* biofilm biomass and cell concentrations ($p \leq 0.05$) on PS compared to *V. parahaemolyticus* (Supplemental Table S59).

Simulated human media and cell state influence *V. parahaemolyticus* and *V. vulnificus* c-di-GMP concentrations

Overall, both *V. parahaemolyticus* and *V. vulnificus* appeared to have differences in their c-di-GMP concentrations in both the biofilm and dispersal state after being exposed to MSYE, SIF and HPLM (Figure 8, Supplemental Table S60). There were greater c-di-GMP concentrations in *V. parahaemolyticus* biofilm state in MSYE, SIF and HPLM compared to dispersal state. Exposure to SIF led to greater c-di-GMP concentrations in both biofilm and dispersal states compared to exposure to MSYE and HPLM. ANOVA revealed certain significant differences ($p \leq 0.05$) in the concentrations of *V. parahaemolyticus* c-di-GMP concentrations between different media exposures. *V. parahaemolyticus* biofilm cells exposed to SIF had significantly enhanced c-di-GMP concentrations compared to biofilms exposed to MSYE ($p \leq 0.01$) and HPLM p (≤ 0.01)

(Supplemental Table S61). There were no significant differences in *V. parahaemolyticus* dispersal cell c-di-GMP concentrations in different medias (Supplemental Table S61). There were also no significant differences between the biofilm and dispersal state of *V. parahaemolyticus* cells after exposure to MSYE, SIF and HPLM (Supplemental Table S62). Regarding *V. vulnificus*, there were greater c-di-GMP concentrations in biofilm cells exposed to MSYE and HPLM. However, exposure to SIF led to greater concentrations of c-di-GMP in dispersal cells compared to biofilm cells. Exposure to SIF led to greater c-di-GMP concentrations in both biofilm and dispersal states compared to exposure to MSYE and HPLM. ANOVA revealed certain significant differences ($p \leq 0.05$) in the concentrations of *V. vulnificus* c-di-GMP concentrations between different media exposures and between biofilm and dispersal cell states. *V. vulnificus* biofilm and dispersal cells exposed to SIF had significantly enhanced c-di-GMP concentrations compared to their counterparts exposed to MSYE ($p \leq 0.01$) and HPLM ($p \leq 0.01$) (Supplemental Table S61). *V. vulnificus* biofilm cells also had significantly greater c-di-GMP concentrations compared to dispersal cells in MSYE ($p \leq 0.05$) and HPLM ($p \leq 0.001$), but there was no significant difference in biofilm and dispersal cell states when exposed to SIF ($p = 1.00$) (Supplemental Table S62).

2.5 Discussion

Biofilm formation facilitates the ability of pathogenic bacteria like *Vibrio* to colonize most environmental niches like MPs, which consequently enables the bacteria embedded in the biofilm to be translocated to marine animals, and then vectored to humans due to biofilm dispersal from MPs to animal tissues or the biofilms on MPs themselves by ingestion (Austin, 2010; Kaplan, 2010; Yang et al., 2020; Bowley et al.,

2021; Fabra et al., 2021). MPs' role as substrates for microbial habitats and subsequently vectors of pathogenic *Vibrio* to humans must be further evaluated, especially during the human ingestion process (Zettler, Mincer & Amaral-Zettler, 2013; Kirstein et al., 2016). *Vibrio*'s habitat range has increased likely due to climate change providing more optimal growth conditions, which has coincided with an increase in plastic production (Froelich & Daines, 2020; Maquart, Froehlich & Boyer, 2022). At the same time, an increase in temperature and carbon and nitrogen pollution has led to increased prevalence of cyanobacterial harmful algal blooms (HABs) (O'Neil et al., 2012; Visser et al., 2016). As HAB outbreaks have also been suggested to enhance *V. parahaemolyticus* and *V. vulnificus* growth, understanding how an increase in temperature and the presence of nutrients may affect *Vibrio* biofilm growth is also of importance (Greenfield et al., 2017). This expansion of *Vibrio* coupled with their inherent propensity to colonize, persist, and disperse from numerous plastic types will increase the future potential infection risks to humans, especially by ingestion of contaminated seafood (Keswani et al., 2016; Bowley et al., 2021; Cverenkárová et al., 2021). To better understand the emerging public health risks associated with bacterial dispersal from plastic particles, studies are needed to determine how this process on different substrate types is affected by human environmental conditions, such as simulated human body pH, temperature, nutrient availability, and fluid composition. This study focused on how both *V. parahaemolyticus* and *V. vulnificus* disperse from common marine plastics, such as low-density polyethylene, polypropylene, and polystyrene, under different simulated human body conditions, especially those related to digestion.

There were observable differences in substrate flotation behavior and the substrates tested were confirmed to differ in their specific densities (Table 2). Floatation behaviors could also influence the adhesion of *Vibrio* species and, consequently, the production and dispersal of biofilms on these substrates, especially in the context of *in situ* human environments (Gaylarde et al., 2023). While these two *Vibrio* species have been found in the 'plastisphere' of the commonly occurring marine plastics that were assessed in the present study, *in vitro* and *in vivo* studies on the colonization of other *Vibrio* species and their dispersal onto and off of different plastics, synthetic and organic polymers, and other substrate surfaces are still lacking (Tavelli et al., 2022). While *Vibrio* have been found to be a major community member on marine MPs, *Vibrio* concentrations are lower on these surfaces compared to natural marine particles (Bryant et al., 2016; Curren & Leong, 2019; Amaral-Zettler, Zettler & Mincer, 2020). In the context of climate change and public health, warming waters will likely contribute to higher bacterial contamination of seafood, which in turn will increase *Vibrio* exposure risks to humans through ingestion of contaminated seafood products. As *Vibrio* have been found to colonize and live on plastics, the development of specific adaptive mechanisms of *Vibrio* to the toxicity and low bioavailability of these plastic substrates could contribute to the modifications of its cell surface hydrophobicity to permit direct hydrophobic-hydrophobic interactions with these plastic substrates in initial colonization (Krasowska & Sigler, 2014). This could lead to potential priming of the colonization of the host as it has been reported that adequate hydrophobic/hydrophilic properties of bacteria can contribute to colonization of the mucosal membranes in the small intestine and lead to human infection (Qin et al., 2008; Krasowska & Sigler, 2014; de Wouters et al., 2015).

This could explain the rapid colonization of microplates from dispersed *Vibrio* cells from MPs, especially at elevated temperature. This rapid microplate colonization can also be explained by dispersal cells having short term increased motility and adherence phenotypes compared to their biofilm and planktonic counterparts (Chua et al., 2014; Uppuluri et al., 2018; Rumbaugh & Sauer, 2020).

Cell colonization and dispersal depend on microbiological, surface physiochemical and environmental factors (Alotaibi & Bukhari, 2021). The *Vibrio* species and strains' cells in this study have been found to have hydrophobic properties from a previous study, which plays a role in their attachment and biofilm formation on hydrophobic surfaces like plastics (Leighton et al., 2023). Factors such as nutrient levels, pH, temperature and liquid composition have been shown to influence both cell attachment and biofilm dispersal from a variety of species (Karatan & Watnick, 2009; McDougald et al., 2012; Pagán & García-Gonzalo, 2015; Toyofuku et al., 2016). Cell colonization can be increased with increasing flow, temperature or nutrient concentrations (Prakash, Veeregowda & Krishnappa, 2003; Alotaibi & Bukhari, 2021). Conditions likely to be encountered by *V. parahaemolyticus* and *V. vulnificus* biofilms on MPs as they transition to the human intestinal environment by ingestion include increases in temperature, decreases in pH and nutrient availability, changes in fluid composition.

Vibrio must detect and respond to changes in their environment to successfully survive and colonize their host (Gode-Potratz et al., 2011; Billaud et al., 2022). Our study supports this as both species rapidly responded to changes in temperature, pH, nutrient availability, and fluid composition as evident by changes in their biofilm biomass and cell dispersal from MPs and subsequent microplate surface colonization. Several studies have

shown that sudden changes in nutrient availability can induce biofilm dispersal (Hunt et al., 2004; Sauer et al., 2004; Petrova & Sauer, 2016). Our study further suggests this as adding or removing the carbon and nitrogen sources (here, peptone and yeast extract) resulted in specific biofilm dispersal responses, which is also in accordance with Singh et al., 2017 who found a similar response in *V. cholerae*. In our study, *V. vulnificus* was more sensitive to nutrient starvation when compared to *V. parahaemolyticus*. A strong dispersal response occurred in *V. vulnificus* as determined by changes in its overall biofilm biomass, and specific biofilm biomasses on LDPE and PP when exposed to nutrient starved conditions. *V. parahaemolyticus* biofilms only showed a strong dispersal response from LDPE surfaces following nutrient starvation conditions. These dispersal responses likely occur as cells embedded in the biofilm detach to find other suitable surfaces to colonize to repeat their lifecycle, or to escape stressful nutrient scarce conditions (Kaplan, 2010; Barraud, Kjelleberg & Rice Scott, 2015).

Biofilm biomass, biofilm cell viability and cell dispersal of both *V. parahaemolyticus* and *V. vulnificus* decreased at lower pHs (pH 3, 4) on MPs. This is in accordance with Koo, DePaola & Marshall, 2000 and Wang et al., 2019 as they also found pH levels < 4 led to a decrease in cell viability in both *V. parahaemolyticus* and *V. vulnificus*. While *V. parahaemolyticus* did have decreased biofilm cell viability and cell dispersal at acidic (pH = 4) conditions compared to higher pHs, it was still able to tolerate this acidic pH for >2 hours, which was consistent with results of Wang et al., 2019 and Wang et al., 2020. There was also a decrease in biofilm cell viability and cell dispersal of both species after exposure to SGF, which more closely resembles the gastric liquid composition in the stomach's environment. This suggests that acidic pH's, which

resemble the stomach environment, are effective in eradicating active viable potential pathogenic *Vibrio* on MPs. While the acidic conditions resembling the human digestive system, especially those found in the stomach, seem to do an effective job in killing viable *Vibrio* cells, it is important to note that *Vibrio* are likely co-ingested with contaminated seafood, which alters the environmental conditions during digestion.

Vibrio biofilms on MPs are likely to be co-ingested with seafood, and since seafood consumption temporarily and significantly increases the pH level of gastric fluid in the stomach, this consequently can provide a protective effect and enable *V. parahaemolyticus* and *V. vulnificus* to survive exposure to these harsh digestion conditions (Conway, Gorbach & Goldin, 1987; Koo, DePaola & Marshall, 2000; Wang et al., 2019; Çam & Brinkmeyer, 2020). As conditions become more favorable in the small intestine and provide an optimal growth environment for both species, *Vibrio* may potentially leave their protective biofilm bunker on MPs and disperse and subsequently colonize the human intestinal tract (Tang et al., 2015). Our study supports this as higher pHs like those found in the small intestine led to higher cell dispersal from MPs and subsequent microplate colonization of both species, signifying that potentially ingested *Vibrio* on MPs can adequately disperse and potentially colonize the surfaces of the intestinal tract. This is further supported by an increase in biofilm cell viability and cell dispersal of both species after exposure to SIF, which closely resembles the intestinal fluid composition found in the intestinal environment. While environmental exposure time was capped after 2 hours to better reflect human digestion processes and to target dispersed rather than planktonic cells, the exposure time to these environmental factors likely had major impact on biofilm dispersal, and longer or shorter exposure times to the

same or different environmental conditions tested may lead to different biofilm responses (Marks et al., 2013; Barraud et al., 2014; Singh et al., 2017; Nair et al., 2021). Temperature was found to not be a major factor in influencing biofilm biomass in comparing MSYE and MS. This likely is due to the short exposure time of 2 hours and the media was not prewarmed at 37°C prior to exposure. There were also little significant differences in cell concentrations, cell colonization and cell dispersal on and from plastics when exposed to SGF, SIF and HPLM compared to MSYE with similar pHs. This could mean exposure to pH, rather than the media composition, is more of a major determining factor of these biofilm processes on these surfaces.

In our study, *V. parahaemolyticus* was previously isolated from the human enteric system, so this strain has likely adapted to survive and colonize the intestinal tract. Our study supports this as it did show resistance to conditions that resemble the human gastrointestinal environment such as in SGF and SIF at 37°C. Interestingly, it also showed greater resistance to these conditions compared to *V. vulnificus*, which was isolated from blood. This confirms that strain isolation source matters and is crucial when examining specific responses in human exposure studies. This is further supported by the resazurin metabolic assay which revealed that *V. parahaemolyticus* biofilm cells were able to survive exposure to media with low pH (3) and in SGF which had a pH of 1.5 for 2 hours, but *V. vulnificus* did not recover as well or survive. However, this survival could be due to the presence of persister cells, as these cells were able to survive the stressors, and once the stressor was removed, were able to become metabolically active again and the biofilms recover in growth and development (Xiong et al., 2022). *V. parahaemolyticus*, while not being isolated from blood, still had high amounts of biofilm

biomass, biofilm cell concentrations, cell colonization and dispersal in HPLM at 25°C and 37°C. HPLM contains all the amino acids, vitamins, salts, sugars, and acids found in actual human blood, but without the immune response cells. Our study confirms HPLM might be a better alternative in human exposure studies and models compared to conventionally used media.

Also to be noted is that in our study, one of our *V. vulnificus* isolates, that was from human blood, has likely adapted to colonize wounds and blood serum (Çam & Brinkmeyer, 2020). Our study supports this as exposure to HPLM increased biofilm biomass and cell viability, especially at human body temperature (37°C). This further confirms that HPLM represents a favorable media for growth and exposure studies with human bloodborne pathogens compared to conventional media currently used to resemble pathogen responses in human systems. *V. vulnificus* at 37°C produced more biofilm, had greater concentrations of biofilm cells, greater colonization, and cell dispersal concentrations on and from every plastic type in HPLM in almost every exposure scenario compared to *V. parahaemolyticus,* which was isolated from the human enteric system. This further confirms that strain isolation source matters and is crucial when examining specific human exposure responses. In some cases, rapid changes in temperature from 25°C to 37°C also contributed to increases in biofilm biomass and cell colonization by *V. vulnificus* on LDPE, PP and PS in simulated human media. This suggests that *V. vulnificus* may produce greater amounts of biofilm on MPs as a survival mechanism in response to higher temperatures in the human environment.

C-di-GMP signaling and concentration levels within cells can fluctuate in response to environmental cues, specifically those related to human host stressors

(Koestler & Waters, 2014; Chua et al., 2015; Khan et al., 2016). C-di-GMP concentration levels dictate different mechanistic actions, as high concentrations lead to biofilm formation and low concentrations lead to dispersion (Valentini & Filloux, 2016; Andersen et al., 2021). Our study supports both the environment and cell state having impacts on c-di-GMP production, as both *V. parahaemolyticus* and *V. vulnificus* had higher levels of c-di-GMP in the biofilm state compared to dispersal state after MSYE and HPLM exposure at 37°C. Both species had high viability and biofilm biomass and cell concentrations in these medias, and coincidently lower c-di-GMP levels compared to SIF. Both species produced significantly more c-di-GMP in SIF in the biofilm state compared to HPLM and MSYE. Both species also had high levels of c-di-GMP in the dispersal state after exposure to SIF, potentially signifying a stress response in both biofilm and dispersal states. Compared to MSYE and HPLM, SIF contains bile salts, which have been found to induce stress and increase c-di-GMP concentrations in *V. cholerae*, another intestinal pathogen of the same genus (Koestler & Waters, 2014). Our study supports this notion that stressors related to digestion (i.e. bile salts) may impact and increase intracellular c-di-GMP concentrations in *Vibrio*. Intestinal pathogens like *V. parahaemolyticus* and *V. vulnificus* may also experience changes in temperature and nutrient starvation in the digestive system as they transition environments by ingestion (Hooper, Midtvedt & Gordon, 2002; Purcell et al., 2017). Temperature and nutrient starvation have been found and speculated to impact intracellular c-di-GMP levels concentrations in these species, and further studies are needed to confirm this after exposure to elevated temperature under these conditions (Gjermansen et al., 2010;

Bharati et al., 2012; Townsley & Yildiz, 2015; Song et al., 2017; Chodur Daniel et al., 2018).

Finally, these results indicate that human pathogenic strains of *V. parahaemolyticus* and *V. vulnificus* can rapidly respond to different marine and simulated human environmental conditions by dispersing high viable cell concentrations from biofilms on different MP material types *in vitro*. However, this dispersal process is highly variable, and while natural variability exists in nature from species to species, strain to strain, and even cell to cell, the variability observed in this study also depended on plastic type and environmental exposures like pH, temperature, nutrient availability, and media composition. Further studies are needed to compare these human isolated *Vibrio* strains biofilm processes to marine animal and environmentally isolated strains. Studies are also needed to compare these *Vibrio in vitro* plastic dispersal processes under simulated human conditions to those found more closely in the natural human environment, which a continuous model system would provide with consecutive exposures to different elements of the human digestive environment (Wang et al., 2019). More studies are needed to examine the environmental signals that regulate c-di-GMP levels and biofilm formation in response to these changing environmental conditions. The present results highlight the ability of *Vibrio* species to disperse from MPs under simulated human conditions and may need to be incorporated into simulated human models to better predict potential bacterial interactions with human hosts. However, further studies are needed to examine bacterial response on MPs in consumed seafood to better predict exposure risk. Also, as *Vibrio* are in close proximity to each other on MPs, there is a high chance of horizontal gene transfer, which could transfer antibiotic resistance and virulence genes, so

examining transcriptomic profiles of these bacteria attached to MPs after exposure to human environmental cues will provide more information on potential virulence and antibiotic resistance gene regulation (Hu, Zhao & Xu, 2022). Finally, further studies are needed to examine the interactions of *Vibrio* on MPs with the human intestinal environment and surface, as it has been shown that the presence of MPs and pathogens both separately and together in marine animal intestinal systems can change and damage gut microbiota and intestinal mucosa (Kamada et al., 2013; Yan et al., 2021; Hu, Zhao & Xu, 2022).

2.6 References

Abdallah, M., C. Benoliel, D. Drider, P. Dhulster and N.-E. Chihib (2014). "Biofilm formation and persistence on abiotic surfaces in the context of food and medical environments." Archives of Microbiology **196**(7): 453-472.

Alotaibi, G. F. and M. A. Bukhari (2021). "Factors influencing bacterial biofilm formation and development." American Journal of Biomedical Science and Research **12**(6): 617-626.

Amaral-Zettler, L. A., E. R. Zettler and T. J. Mincer (2020). "Ecology of the plastisphere." Nature Reviews Microbiology **18**(3): 139-151.

Andersen, J. B., L. D. Hultqvist, C. U. Jansen, T. H. Jakobsen, M. Nilsson, M. Rybtke, J. Uhd, B. G. Fritz, R. Seifert, J. Berthelsen, T. E. Nielsen, K. Qvortrup, M. Givskov and T. Tolker-Nielsen (2021). "Identification of small molecules that interfere with c-di-GMP signaling and induce dispersal of *Pseudomonas aeruginosa* biofilms." npj Biofilms and Microbiomes **7**(1): 59.

Austin, B. (2010). "*Vibrios* as causal agents of zoonoses." Veterinary Microbiology **140**(3): 310-317.

Barraud, N., S. Kjelleberg and A. Rice Scott (2015). "Dispersal from Microbial Biofilms." Microbiology Spectrum **3**(6): 3.6.05.

Barraud, N., J. A. Moscoso, J.-M. Ghigo and A. Filloux (2014). Methods for studying biofilm dispersal in *Pseudomonas aeruginosa*. *Pseudomonas* methods and protocols, Springer**:** 643-651.

Bharati, B. K., I. M. Sharma, S. Kasetty, M. Kumar, R. Mukherjee and D. Chatterji (2012). "A full-length bifunctional protein involved in c-di-GMP turnover is required for long-term survival under nutrient starvation in *Mycobacterium smegmatis*." Microbiology **158**(6): 1415-1427.

Billaud, M., F. Seneca, E. Tambutté and D. Czerucka (2022). "An Increase of Seawater Temperature Upregulates the Expression of *Vibrio parahaemolyticus* Virulence Factors Implicated in Adhesion and Biofilm Formation." Frontiers in Microbiology **13**.

Bjerkan, G., E. Witsø and K. Bergh (2009). "Sonication is superior to scraping for retrieval of bacteria in biofilm on titanium and steel surfaces in vitro." Acta Orthopaedica **80**(2): 245-250.

Bonnet, M., J. C. Lagier, D. Raoult and S. Khelaifia (2019). "Bacterial culture through selective and non-selective conditions: the evolution of culture media in clinical microbiology." New Microbes and New Infections **34**: 100622-100622.

Bowley, J., C. Baker-Austin, A. Porter, R. Hartnell and C. Lewis (2021). "Oceanic Hitchhikers – Assessing Pathogen Risks from Marine Microplastic." Trends in Microbiology **29**(2): 107-116.

Broberg, C. A., T. J. Calder and K. Orth (2011). "*Vibrio parahaemolyticus* cell biology and pathogenicity determinants." Microbes and infection **13**(12-13): 992-1001.

Bryant, J. A., T. M. Clemente, D. A. Viviani, A. A. Fong, K. A. Thomas, P. Kemp, D. M. Karl, A. E. White, E. F. DeLong and J. K. Jansson (2016). "Diversity and Activity of Communities Inhabiting Plastic Debris in the North Pacific Gyre." mSystems **1**(3): e00024-00016.

Çam, S. and R. Brinkmeyer (2020). "The effects of temperature, pH, and iron on biofilm formation by clinical versus environmental strains of *Vibrio vulnificus.*" Folia Microbiologica **65**(3): 557-566.

Centers for Disease Control and Prevention (2019). *Vibrio* species causing Vibriosis.

Chodur Daniel, M., P. Coulter, J. Isaacs, M. Pu, N. Fernandez, M. Waters Chris and A. Rowe-Magnus Dean (2018). "Environmental Calcium Initiates a Feed-Forward Signaling Circuit That Regulates Biofilm Formation and Rugosity in *Vibrio* vulnificus." mBio **9**(4): e01377-01318.

Chua, S. L., Y. Liu, J. K. Yam, Y. Chen, R. M. Vejborg, B. G. Tan, S. Kjelleberg, T. Tolker-Nielsen, M. Givskov and L. Yang (2014). "Dispersed cells represent a distinct stage in the transition from bacterial biofilm to planktonic lifestyles." Nature Communications **5**: 4462.

Chua, S. L., K. Sivakumar, M. Rybtke, M. Yuan, J. B. Andersen, T. E. Nielsen, M. Givskov, T. Tolker-Nielsen, B. Cao, S. Kjelleberg and L. Yang (2015). "C-di-

GMP regulates *Pseudomonas aeruginosa* stress response to tellurite during both planktonic and biofilm modes of growth." Scientific Reports **5**(1): 10052.

Collins, C. H. (1967). "Microbiological methods." Microbiological Methods.(2nd Edition).

Conway, P. L., S. L. Gorbach and B. R. Goldin (1987). "Survival of lactic acid bacteria in the human stomach and adhesion to intestinal cells." Journal of Dairy Science **70**(1): 1-12.

Curren, E., C. P. Leaw, P. T. Lim and S. C. Y. Leong (2020). "Evidence of Marine Microplastics in Commercially Harvested Seafood." Frontiers in Bioengineering and Biotechnology **8**: 562760-562760.

Curren, E. and S. C. Y. Leong (2019). "Profiles of bacterial assemblages from microplastics of tropical coastal environments." Science of The Total Environment **655**: 313-320.

Cverenkárová, K., M. Valachovičová, T. Mackuľak, L. Žemlička and L. Bírošová (2021). "Microplastics in the food chain." Life **11**(12): 1349.

Dang, H. and C. R. Lovell (2016). "Microbial Surface Colonization and Biofilm Development in Marine Environments." Microbiology and Molecular Biology Reviews **80**(1): 91-138.

Davidson, K. and S. E. Dudas (2016). "Microplastic Ingestion by Wild and Cultured Manila Clams (*Venerupis philippinarum*) from Baynes Sound, British Columbia." Archives Environmental Contamination Toxicology **71**(2): 147-156.

Davies, D. (2003). "Understanding biofilm resistance to antibacterial agents." Nature Reviews Drug discovery **2**(2): 114-122.

Davis, B., R. Dulbecco, H. Eiser and H. Ginsberg (1980). "Microbiology: Including immunology and Molecular genetics, Harper and Row." Hagerstown, Md **19802**.

de Carvalho, C. C. C. R. (2018). "Marine Biofilms: A Successful Microbial Strategy With Economic Implications." Frontiers in Marine Science **5**(126).

De Tender, C. A., L. I. Devriese, A. Haegeman, S. Maes, T. Ruttink and P. Dawyndt (2015). "Bacterial Community Profiling of Plastic Litter in the Belgian Part of the North Sea." Environmental Science & Technology **49**(16): 9629-9638.

de Wouters, T., C. Jans, T. Niederberger, P. Fischer and P. A. Rühs (2015). "Adhesion Potential of Intestinal Microbes Predicted by Physico-Chemical Characterization Methods." PLOS ONE **10**(8): e0136437.

Egwuatu, T. O., Ogunsola, F. T., Okodugha, I. M., Jide, B., Arewa, D. G., & Osinupebi, O. A. (2014). Effect of blood agar from different animal blood on growth rates and morphology of common pathogenic bacteria. Advances in Microbiology, 4(16), 1237.

Elmahdi, S., S. Parveen, S. Ossai, L. V. DaSilva, M. Jahncke, J. Bowers and J. Jacobs (2018). "*Vibrio parahaemolyticus* and *Vibrio vulnificus* Recovered from Oysters during an Oyster Relay Study." Applied and Environmental Microbiology **84**(3): e01790-01717.

Fabra, M., L. Williams, J. E. M. Watts, M. S. Hale, F. Couceiro and J. Preston (2021). "The plastic Trojan horse: Biofilms increase microplastic uptake in marine filter feeders impacting microbial transfer and organism health." Science of The Total Environment **797**: 149217.

Flemming, H.-C., T. R. Neu and D. J. Wozniak (2007). "The EPS matrix: the “house of biofilm cells”." Journal of Bacteriology **189**(22): 7945-7947.

Food and Drug Administration. (2010). Quantitative risk assessment on the public health impact of pathogenic *Vibrio parahaemolyticus* in raw oysters. U.S. Food and Drug Administration, Washington, D.C

Food and Drug Administration. (2012) Bad Bug Book, Foodborne Pathogenic Microorganisms and Natural Toxins. Second Edition. 27, 47.

Froelich, B. A. and D. A. Daines (2020). "In hot water: effects of climate change on *Vibrio*–human interactions." Environmental Microbiology **22**(10): 4101-4111.

Galperin, M. Y. (2004). "Bacterial signal transduction network in a genomic perspective." Environmental Microbiology **6**(6): 552-567.

Gaylarde, C. C., M. P. de Almeida, C. V. Neves, J. A. Neto and E. M. da Fonseca (2023) "The Importance of Biofilms on Microplastic Particles in Their Sinking Behavior and the Transfer of Invasive Organisms between Ecosystems." Micro **3**, 320-337 DOI: 10.3390/micro3010022.

Gjermansen, M., M. Nilsson, L. Yang and T. Tolker-Nielsen (2010). "Characterization of starvation-induced dispersion in *Pseudomonas putida* biofilms: genetic elements and molecular mechanisms." Molecular Microbiology **75**(4): 815-826.

Gjermansen, M., P. Ragas, C. Sternberg, S. Molin and T. Tolker-Nielsen (2005). "Characterization of starvation-induced dispersion in *Pseudomonas putida* biofilms." Environmental Microbiology **7**(6): 894-906.

Gode-Potratz, C. J., R. J. Kustusch, P. J. Breheny, D. S. Weiss and L. L. McCarter (2011). "Surface sensing in *Vibrio parahaemolyticus* triggers a programme of

gene expression that promotes colonization and virulence." Molecular Microbiology **79**(1): 240-263.

Greenfield, D., J. Gooch Moore, J. Stewart, E. Hilborn, B. George, Q. Li, J. Dickerson, C. Keppler and P. Sandifer (2017). "Temporal and environmental factors driving *Vibrio vulnificus* and *V. parahaemolyticus* populations and their associations with harmful algal blooms in South Carolina detention ponds and receiving tidal creeks." GeoHealth **1**(9): 306-317.

Guilhen, C., C. Forestier and D. Balestrino (2017). "Biofilm dispersal: multiple elaborate strategies for dissemination of bacteria with unique properties." Molecular Microbiology **105**(2): 188-210.

Hamanaka, D., M. Onishi, T. Genkawa, F. Tanaka and T. Uchino (2012). "Effects of temperature and nutrient concentration on the structural characteristics and removal of vegetable-associated *Pseudomonas* biofilm." Food Control **24**(1): 165-170.

Hengge, R. (2009). "Principles of c-di-GMP signalling in bacteria." Nature Reviews Microbiology **7**(4): 263-273.

Hernández-Cabanyero, C., C. T. Lee, V. Tolosa-Enguis, E. Sanjuán, D. Pajuelo, F. Reyes-López, L. Tort and C. Amaro (2019). "Adaptation to host in *Vibrio vulnificus*, a zoonotic pathogen that causes septicemia in fish and humans." Environmental Microbiology **21**(8): 3118-3139.

Honda, T. and T. Iida (1993). "The pathogenicity of *Vibrio parahaemolyticus* and the role of the thermostable direct haemolysin and related haemolysins." Reviews in Medical Microbiology **4**(2): 106-113.

Hooper, L. V., T. Midtvedt and J. I. Gordon (2002). "How host-microbial interactions shape the nutrient environment of the mammalian intestine." Annual Review of Nutrition **22**(1): 283-307.

Hu, L., Y. Zhao and H. Xu (2022). "Trojan horse in the intestine: A review on the biotoxicity of microplastics combined environmental contaminants." Journal of Hazardous Materials **439**: 129652.

Hunt, S. M., E. M. Werner, B. Huang, M. A. Hamilton and P. S. Stewart (2004). "Hypothesis for the role of nutrient starvation in biofilm detachment." Applied and Environmental Microbiology **70**(12): 7418-7425.

Jamal, M., W. Ahmad, S. Andleeb, F. Jalil, M. Imran, M. A. Nawaz, T. Hussain, M. Ali, M. Rafiq and M. A. Kamil (2018). "Bacterial biofilm and associated infections." Journal of the Chinese Medical Association **81**(1): 7-11.

Jones, M. K. and J. D. Oliver (2009). "*Vibrio vulnificus*: disease and pathogenesis." Infection and Immunity **77**(5): 1723-1733.

Kamada, N., G. Y. Chen, N. Inohara and G. Núñez (2013). "Control of pathogens and pathobionts by the gut microbiota." Nature Immunology **14**(7): 685-690.

Kaplan, J. B. (2010). "Biofilm dispersal: mechanisms, clinical implications, and potential therapeutic uses." Journal of Dental Research **89**(3): 205-218.

Karatan, E. and P. Watnick (2009). "Signals, Regulatory Networks, and Materials That Build and Break Bacterial Biofilms." Microbiology and Molecular Biology Reviews **73**(2): 310-347.

Kaysner, C. A., A. DePaola and J. Jones (2004). "Bacteriological analytical manual chapter 9: *Vibrio*." Food and Drug Administration, Maryland.[https://www. fda.

gov/food/laboratory-methods-food/bam-chapter-9-*Vibrio*]. Reviewed: December **19**: 2019.

Keswani, A., D. M. Oliver, T. Gutierrez and R. S. Quilliam (2016). "Microbial hitchhikers on marine plastic debris: Human exposure risks at bathing waters and beach environments." Marine Environmental Research **118**: 10-19.

Kesy, K., M. Labrenz, B. S. Scales, B. Kreikemeyer and S. Oberbeckmann (2021). "*Vibrio* Colonization Is Highly Dynamic in Early Microplastic-Associated Biofilms as Well as on Field-Collected Microplastics." Microorganisms **9**(1): 76.

Khan, M., S. Harms Jerome, M. Marim Fernanda, L. Armon, L. Hall Cherisse, Y.-P. Liu, M. Banai, C. Oliveira Sergio, A. Splitter Gary and A. Smith Judith (2016). "The Bacterial Second Messenger Cyclic di-GMP Regulates Brucella Pathogenesis and Leads to Altered Host Immune Response." Infection and Immunity **84**(12): 3458-3470.

Kirstein, I. V., S. Kirmizi, A. Wichels, A. Garin-Fernandez, R. Erler, M. Löder and G. Gerdts (2016). "Dangerous hitchhikers? Evidence for potentially pathogenic *Vibrio* spp. on microplastic particles." Marine Environmental Research **120**: 1-8.

Koelmans, A. A., T. Gouin, R. Thompson, N. Wallace and C. Arthur (2014). "Plastics in the marine environment." Environmental Toxicology and Chemistry **33**(1): 5-10.

Koestler, B. J. and C. M. Waters (2014). "Bile acids and bicarbonate inversely regulate intracellular cyclic di-GMP in *Vibrio cholerae*." Infection Immunity **82**(7): 3002-3014.

Koo, J., A. DePaola and D. L. Marshall (2000). "Effect of Simulated Gastric Fluid and Bile on Survival of *Vibrio vulnificus* and *Vibrio vulnificus* Phage†." Journal of Food Protection **63**(12): 1665-1669.

Krasowska, A. and K. Sigler (2014). "How microorganisms use hydrophobicity and what does this mean for human needs?" Frontiers Cell Infection Microbiology **4**: 112.

Lage, O. M., & Graça, A. P. (2016). Biofilms: an extra coat on macroalgae. In Algae-Organisms for Imminent Biotechnology. IntechOpen.

Lambert, S., C. Sinclair and A. Boxall (2014). Occurrence, degradation, and effect of polymer-based materials in the environment. Reviews of Environmental Contamination and Toxicology, 227, 1-53.

Leighton, R. E., K. E. Correa Vélez, L. Xiong, A. G. Creech, K. P. Amirichetty, G. K. Anderson, G. Cai, R. S. Norman and A. W. Decho (2023). "*Vibrio parahaemolyticus* and *Vibrio vulnificus in vitro* colonization on plastics influenced by temperature and strain variability." Frontiers in Microbiology **13**.

Maquart, P.-O., Y. Froehlich and S. Boyer (2022). "Plastic pollution and infectious diseases." The Lancet Planetary Health **6**(10): e842-e845.

Marks, L. R., B. A. Davidson, P. R. Knight and A. P. Hakansson (2013). "Interkingdom signaling induces *Streptococcus pneumoniae* biofilm dispersion and transition from asymptomatic colonization to disease." mBio **4**(4): e00438-00413.

Marx, J., R. Hockberger and R. Walls (2013). Rosen's Emergency Medicine-Concepts and Clinical Practice E-Book: 2-Volume Set, Elsevier Health Sciences.

McDougald, D., S. A. Rice, N. Barraud, P. D. Steinberg and S. Kjelleberg (2012). "Should we stay or should we go: mechanisms and ecological consequences for biofilm dispersal." Nature Reviews Microbiology **10**(1): 39-50.

Mead, P. S., L. Slutsker, V. Dietz, L. F. McCaig, J. S. Bresee, C. Shapiro, P. M. Griffin and R. V. Tauxe (1999). "Food-related illness and death in the United States." Emerging Infectious Diseases **5**(5): 607-625.

Motta, J.-P., J. L. Wallace, A. G. Buret, C. Deraison and N. Vergnolle (2021). "Gastrointestinal biofilms in health and disease." Nature Reviews Gastroenterology & Hepatology **18**(5): 314-334.

Nair, H. A. S., S. Subramoni, W. H. Poh, N. T. B. Hasnuddin, M. Tay, M. Givskov, T. Tolker-Nielsen, S. Kjelleberg, D. McDougald and S. A. Rice (2021). "Carbon starvation of *Pseudomonas aeruginosa* biofilms selects for dispersal insensitive mutants." BMC Microbiology **21**(1): 255.

O'Neil, J. M., T. W. Davis, M. A. Burford and C. J. Gobler (2012). "The rise of harmful cyanobacteria blooms: the potential roles of eutrophication and climate change." Harmful algae **14**: 313-334.

O'Toole, G., H. B. Kaplan and R. Kolter (2000). "Biofilm formation as microbial development." Annual Review of Microbiology **54**: 49.

O'Toole, G. A. (2011). "Microtiter dish biofilm formation assay." Journal of Visualized Experiments : JoVE(47): 2437.

Oberbeckmann, S., Löder, M. G., & Labrenz, M. (2015). Marine microplastic-associated biofilms–a review. Environmental chemistry, *12*(5), 551-562.

Oliver, J. D. (2015). "The biology of *Vibrio vulnificus*." Microbiology spectrum **3**(3): 3.3. 01.

Oliver, J. D. and R. R. Colwell (1973). "Extractable lipids of Gram-negative marine bacteria: phospholipid composition." Journal of Bacteriology **114**(3): 897-908.

Oliver, J. D., C. Pruzzo, L. Vezzulli and J. B. Kaper (2012). *Vibrio* Species. Food Microbiology**:** 401-439.

Pagán, R. and D. García-Gonzalo (2015). "Influence of environmental factors on bacterial biofilm formation in the food industry: a review." Postdoc j.(ART-2015-95845).

Petrova, O. E. and K. Sauer (2016). "Escaping the biofilm in more than one way: desorption, detachment or dispersion." Current Opinions in Microbiology **30**: 67-78.

Portillo, M. E., M. Salvadó, A. Trampuz, V. Plasencia, M. Rodriguez-Villasante, L. Sorli, L. Puig and J. P. Horcajada (2013). "Sonication versus vortexing of implants for diagnosis of prosthetic joint infection." Journal of Clinical Microbiology **51**(2): 591-594.

Prakash, B., B. M. Veeregowda and G. Krishnappa (2003). "Biofilms: A survival strategy of bacteria." Current Science **85**(9): 1299-1307.

Purcell, E. B., R. W. McKee, D. S. Courson, E. M. Garrett, S. M. McBride, R. E. Cheney and R. Tamayo (2017). "A Nutrient-Regulated Cyclic Diguanylate Phosphodiesterase Controls *Clostridium difficile* Biofilm and Toxin Production during Stationary Phase." Infection and Immunity **85**(9): e00347-00317.

Purevdorj-Gage, B., W. Costerton and P. Stoodley (2005). "Phenotypic differentiation and seeding dispersal in non-mucoid and mucoid *Pseudomonas aeruginosa* biofilms." Microbiology **151**(5): 1569-1576.

Qin, X., F. J. Caputo, D. Z. Xu and E. A. Deitch (2008). "Hydrophobicity of mucosal surface and its relationship to gut barrier function." Shock **29**(3): 372-376.

Reidl, J. and K. E. Klose (2002). "*Vibrio cholerae* and cholera: out of the water and into the host." FEMS Microbiology Reviews **26**(2): 125-139.

Riss, T. L., R. A. Moravec, A. L. Niles, S. Duellman, H. A. Benink, T. J. Worzella and L. Minor (2004). Cell Viability Assays. Assay Guidance Manual. S. Markossian, G. S. Sittampalam, A. Grossman et al. Bethesda (MD), Eli Lilly & Company and the National Center for Advancing Translational Sciences.

Römling, U., M. Y. Galperin and M. Gomelsky (2013). "Cyclic di-GMP: the first 25 years of a universal bacterial second messenger." Microbiology and Molecular Biology Reviews **77**(1): 1-52.

Rumbaugh, K. P. and K. Sauer (2020). "Biofilm dispersion." Nature Reviews Microbiology **18**(10): 571-586.

Sauer, K., M. Cullen, A. Rickard, L. Zeef, D. G. Davies and P. Gilbert (2004). "Characterization of nutrient-induced dispersion in *Pseudomonas aeruginosa* PAO1 biofilm." Journal of Bacteriology **186**(21): 7312-7326.

Sauer, K., P. Stoodley, D. M. Goeres, L. Hall-Stoodley, M. Burmølle, P. S. Stewart and T. Bjarnsholt (2022). "The biofilm life cycle: expanding the conceptual model of biofilm formation." Nature Reviews Microbiology **20**(10): 608-620.

Singh, P. K., S. Bartalomej, R. Hartmann, H. Jeckel, L. Vidakovic, C. D. Nadell and K. Drescher (2017). "*Vibrio cholerae* Combines Individual and Collective Sensing to Trigger Biofilm Dispersal." Current Biology **27**(21): 3359-3366.e3357.

Song, X., Y. Ma, J. Fu, A. Zhao, Z. Guo, P. K. Malakar, Y. Pan and Y. Zhao (2017). "Effect of temperature on pathogenic and non-pathogenic *Vibrio parahaemolyticus* biofilm formation." Food Control **73**: 485-491.

Tang, X., Y. Zhao, X. Sun, J. Xie, Y. Pan and P. K. Malakar (2015). "Predictive model of *Vibrio parahaemolyticus* O3: K6 growth on cooked Litopenaeus vannamei." Annals of Microbiology **65**(1): 487-493.

Tavelli, R., M. Callens, C. Grootaert, M. F. Abdallah and A. Rajkovic (2022). "Foodborne pathogens in the plastisphere: Can microplastics in the food chain threaten microbial food safety?" Trends in Food Science & Technology **129**: 1-10.

Tischler, A. H., L. Lie, C. M. Thompson and K. L. Visick (2018). "Discovery of Calcium as a Biofilm-Promoting Signal for *Vibrio* fischeri Reveals New Phenotypes and Underlying Regulatory Complexity." Journal of Bacteriology **200**(15): e00016-00018.

Townsley, L. and F. H. Yildiz (2015). "Temperature affects c-di-GMP signalling and biofilm formation in *Vibrio cholerae*." Environmental Microbiology **17**(11): 4290-4305.

Toyofuku, M., T. Inaba, T. Kiyokawa, N. Obana, Y. Yawata and N. Nomura (2016). "Environmental factors that shape biofilm formation." Bioscience, Biotechnology, and Biochemistry **80**(1): 7-12.

Uppuluri, P., M. Acosta Zaldívar, M. Z. Anderson, M. J. Dunn, J. Berman, J. L. Lopez Ribot and J. R. Köhler (2018). "*Candida albicans* dispersed cells are developmentally distinct from biofilm and planktonic cells." mBio **9**(4): e01338-01318.

Valentini, M. and A. Filloux (2016). "Biofilms and Cyclic di-GMP (c-di-GMP) Signaling: Lessons from *Pseudomonas aeruginosa* and Other Bacteria." Journal of Biological Chemistry **291**(24): 12547-12555.

Valquier-Flynn, H., C. L. Wilson, A. E. Holmes and C. D. Wentworth (2017). "Growth Rate of *Pseudomonas aeruginosa* Biofilms on Slippery Butyl Methacrylate-Co-Ethylene Dimethacrylate (BMA-EDMA), Glass and Polycarbonate Surfaces." Journal of Biotechnology & Biomaterials **7**(4): 274.

Visser, P. M., J. M. Verspagen, G. Sandrini, L. J. Stal, H. C. Matthijs, T. W. Davis, H. W. Paerl and J. Huisman (2016). "How rising CO2 and global warming may stimulate harmful cyanobacterial blooms." Harmful Algae **54**: 145-159.

Waite, H. R., M. J. Donnelly and L. J. Walters (2018). "Quantity and types of microplastics in the organic tissues of the eastern oyster Crassostrea virginica and Atlantic mud crab Panopeus herbstii from a Florida estuary." Marine Pollution Bulletin **129**(1): 179-185.

Wang, R., B. A. Khan, G. Y. Cheung, T.-H. L. Bach, M. Jameson-Lee, K.-F. Kong, S. Y. Queck and M. Otto (2011). "*Staphylococcus epidermidis* surfactant peptides promote biofilm maturation and dissemination of biofilm-associated infection in mice." The Journal of Clinical Investigation **121**(1): 238-248.

Wang, S., Z. Zhang, P. K. Malakar, Y. Pan and Y. Zhao (2019). "The Fate of Bacteria in Human Digestive Fluids: A New Perspective Into the Pathogenesis of *Vibrio parahaemolyticus*." Frontiers in Microbiology **10**.

Wang, Y., Y. Zhao, Y. Pan and H. Liu (2020). "Comparison on the Growth Variability of *Vibrio parahaemolyticus* Coupled With Strain Sources and Genotypes Analyses in Simulated Gastric Digestion Fluids." Frontiers in Microbiology **11**(212).

Ward, J. E. and D. J. Kach (2009). "Marine aggregates facilitate ingestion of nanoparticles by suspension-feeding bivalves." Marine Environmental Research **68**(3): 137-142.

Wong, K. K. and P. M. Griffin (2018). 159 - Other *Vibrio* Species. Principles and Practice of Pediatric Infectious Diseases (Fifth Edition). S. S. Long, C. G. Prober and M. Fischer, Elsevier**:** 879-881.e871.

World Health Organization. (2005). Risk assessment of *Vibrio vulnificus* in raw oysters: interpretative summary and technical report" (Vol. 8). World Health Organization.

Wright, S. L., R. C. Thompson and T. S. Galloway (2013). "The physical impacts of microplastics on marine organisms: a review." Environmental Pollution **178**: 483-492.

Xiong, X., J. Kong, D. Qi, X. Xiong, Y. Liu and X. Cui (2022). "Presence, formation, and elimination of foodborne pathogen persisters." JSFA Reports **2**(1): 4-16.

Yan, M., W. Li, X. Chen, Y. He, X. Zhang and H. Gong (2021). "A preliminary study of the association between colonization of microorganism on microplastics and

intestinal microbiota in shrimp under natural conditions." Journal of Hazardous Materials **408**: 124882.

Yang, Y., W. Liu, Z. Zhang, H.-P. Grossart and G. M. Gadd (2020). "Microplastics provide new microbial niches in aquatic environments." Applied Microbiology and Biotechnology **104**(15): 6501-6511.

Yildiz, F. H. (2008). "Cyclic dimeric GMP signaling and regulation of surface-associated developmental programs." Journal of Bacteriology **190**(3): 781-783.

Zettler, E., T. Mincer and L. Amaral-Zettler (2013). "Life in the "Plastisphere": Microbial Communities on Plastic Marine Debris." Environmental Science & Technology **47**.

Table 2.1 *Vibrio* strains used in this study.

Species	**Isolation Source**	**Strain ID**	**Isolate Origin**	**Characteristics**	**Estimated Human[1] Threshold ID_{50}**
V. parahaemolyticus	ATCC	ATCC17802	Human (enteric)	*tlh / trh*	10^5 - 10^8 CFUs[2,3,4]
V. vulnificus	ATCC	ATCC27562	Human (blood)	16S Type B	10^3 CFUs[4,5]

[1]Susceptible, usually with pre-existing, underlying health conditions
[2]Marx, Hockberger & Walls (2013).
[3]Food and Drug Administration (2010).
[4]Food and Drug Administration (2012).
[5]World Health Organization (2005).

Table 2.2. Environmental conditions used in this study.

Media Type	pH	Temperature (°C)	Exposure Time (hours)	Shaking Speed (rpm)
Modified Seawater Yeast Extract (MSYE)	3, 4, 5, 6, 7, 7.4, 8.1	25, 37	2	125
Modified Seawater (MS)	3, 4, 5, 6, 7, 7.4, 8.1	25, 37	2	125
Simulated Gastric Fluid w/ pepsin (SGF)	1.5	25, 37	2	125
Simulated Intestinal Fluid w/ trypsin and pancreatin (SIF)	6.8	25, 37	2	125
Human Plasma-Like Media (HPLM)	7.4	25, 37	2	125

Table 2.3. Coupon types and characteristics used in this study.

Coupon Type	Chemical Formula	Density	Length/Thickness	Surface Area	Usage
Low-Density Polyethylene	$(C_2H_4)_n$	0.96g/cm³	4mm/1.6mm	24mm^2	Plastic bags, six-pack rings, packaging film, bottles, netting
Polypropylene	$(C_3H_6)_n$	0.93g/cm³	4mm/1.6mm	24mm^2	Rope, bottle caps, packaging

						film, netting
	Polystyrene	$(C_8H_8)_n$	1.6g/cm³	4mm/0.6mm	14mm²	Plastic utensils, food containers

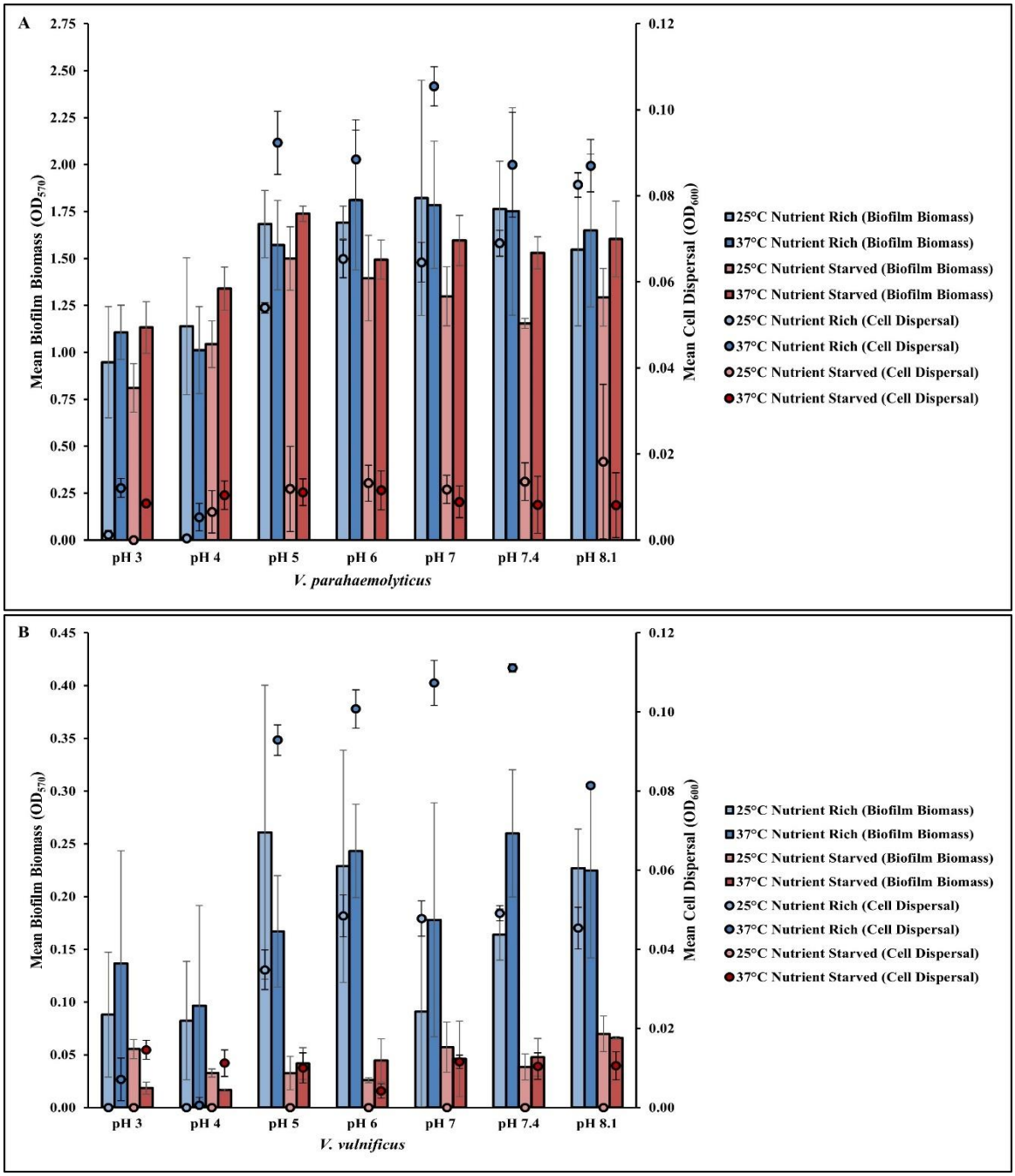

Figure 2.1. Exposure to elevated temperature, changes in pH, and nutrient starvation

influences overall *V. parahaemolyticus* and *V. vulnificus* biofilm biomass and cell dispersal in microplates. Comparison of overall biofilm biomass and cell dispersal (values represent X ± SD, n = 3 replicate samples from three independent experiments) of *V. parahaemolyticus* (A) and *V. vulnificus* (B) between different pH, temperature, and nutrient availability (means of all biological triplicates and three independent experiments after 2-hour exposure.

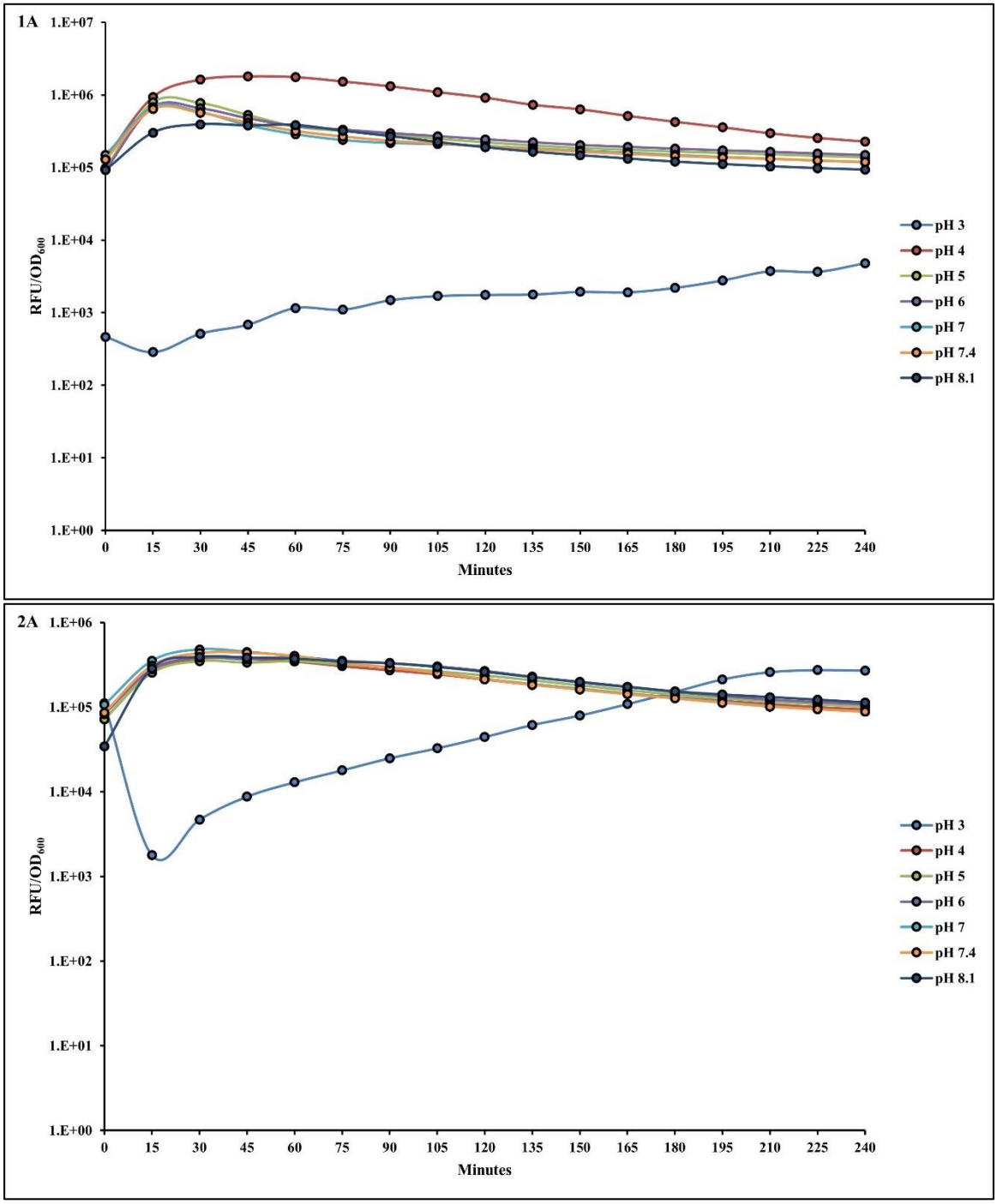

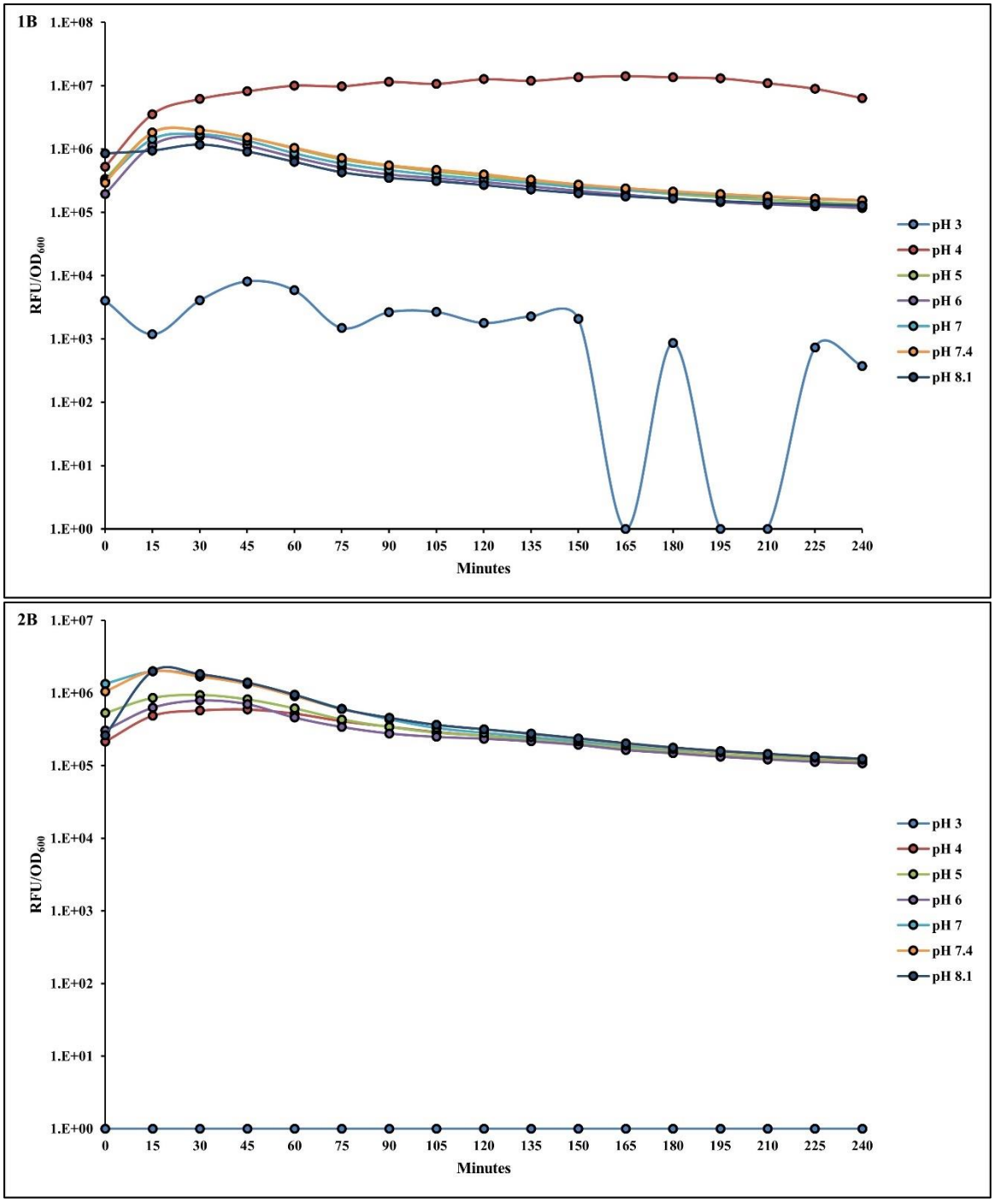

Figure 2.2. Exposure to nutrient starvation and changes in pH influences overall *V. parahaemolyticus* and *V. vulnificus* biofilm viability in microplates. Comparison of biofilm viability (RFU/OD_{600}) of *V. parahaemolyticus* after 2-hour exposure to nutrient rich (1A) and nutrient starved (2A) conditions and *V. vulnificus* after 2-hour exposure to nutrient rich (1B) and nutrient starved (2B) conditions at different pH at 37°C.

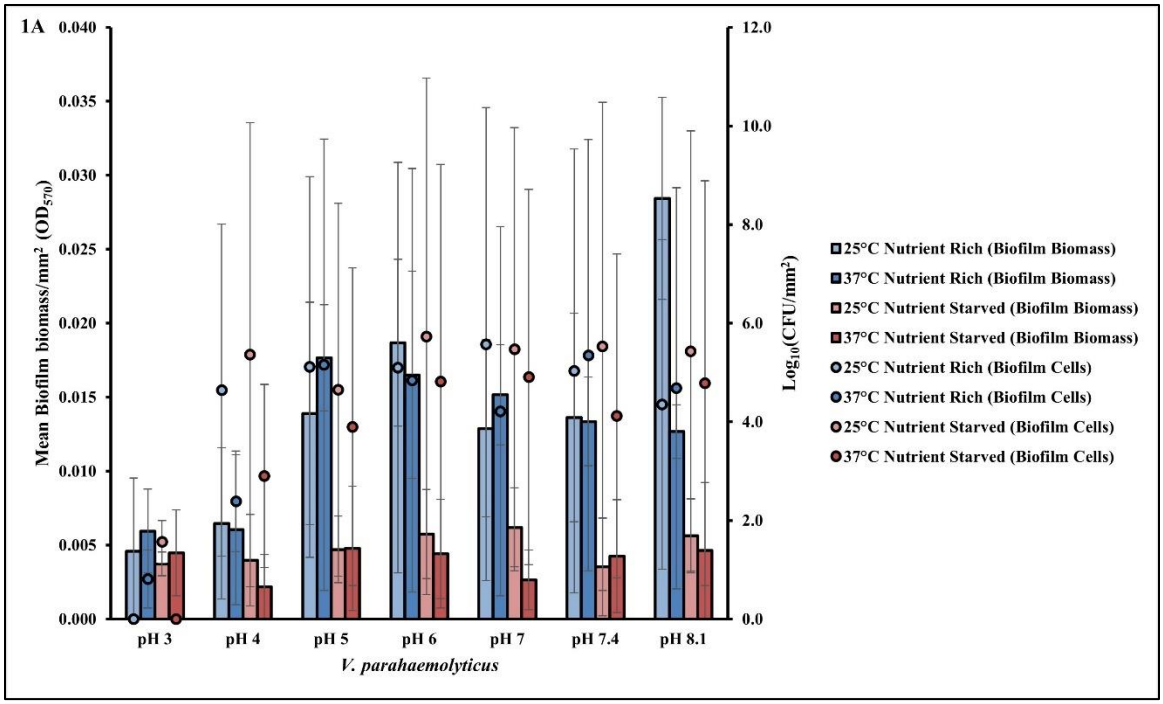
1A
Mean Biofilm biomass/mm² (OD570)
Log10(CFU/mm²)
0.040
0.035
0.030
0.025
0.020
0.015
0.010
0.005
0.000
12.0
10.0
8.0
6.0
4.0
2.0
0.0
pH 3
pH 4
pH 5
pH 6
pH 7
pH 7.4
pH 8.1
V. parahaemolyticus
25°C Nutrient Rich (Biofilm Biomass)
37°C Nutrient Rich (Biofilm Biomass)
25°C Nutrient Starved (Biofilm Biomass)
37°C Nutrient Starved (Biofilm Biomass)
25°C Nutrient Rich (Biofilm Cells)
37°C Nutrient Rich (Biofilm Cells)
25°C Nutrient Starved (Biofilm Cells)
37°C Nutrient Starved (Biofilm Cells)

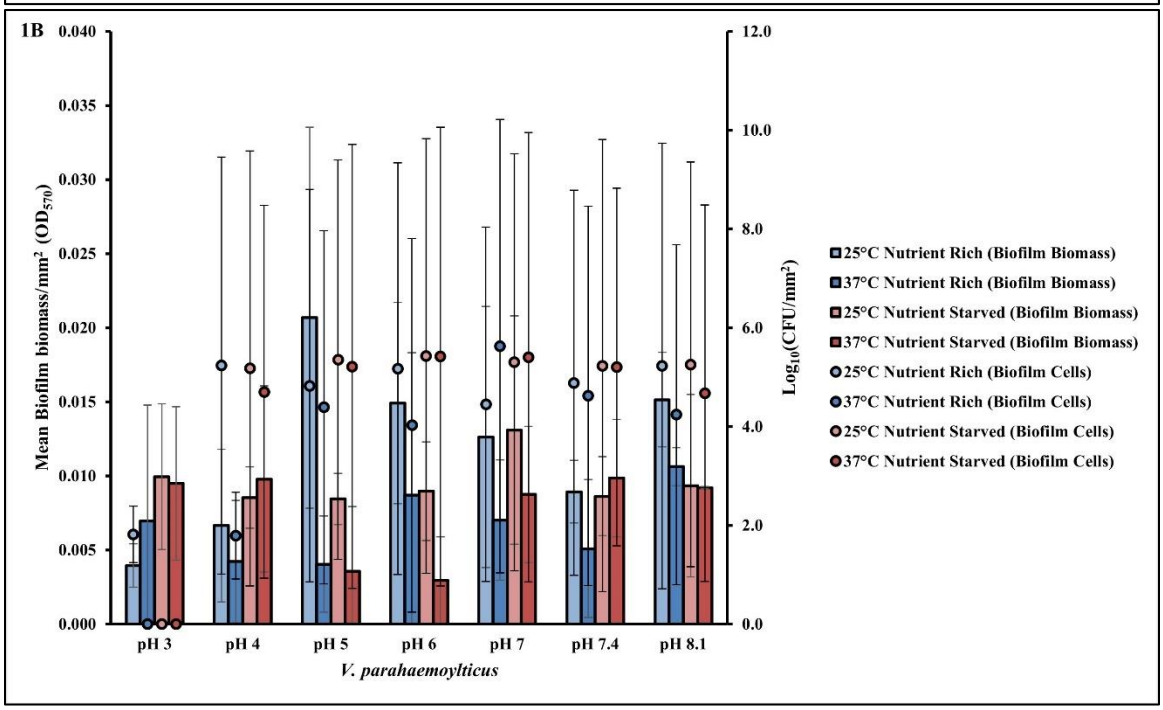
1B
Mean Biofilm biomass/mm² (OD570)
Log10(CFU/mm²)
0.040
0.035
0.030
0.025
0.020
0.015
0.010
0.005
0.000
12.0
10.0
8.0
6.0
4.0
2.0
0.0
pH 3
pH 4
pH 5
pH 6
pH 7
pH 7.4
pH 8.1
V. parahaemoylticus
25°C Nutrient Rich (Biofilm Biomass)
37°C Nutrient Rich (Biofilm Biomass)
25°C Nutrient Starved (Biofilm Biomass)
37°C Nutrient Starved (Biofilm Biomass)
25°C Nutrient Rich (Biofilm Cells)
37°C Nutrient Rich (Biofilm Cells)
25°C Nutrient Starved (Biofilm Cells)
37°C Nutrient Starved (Biofilm Cells)

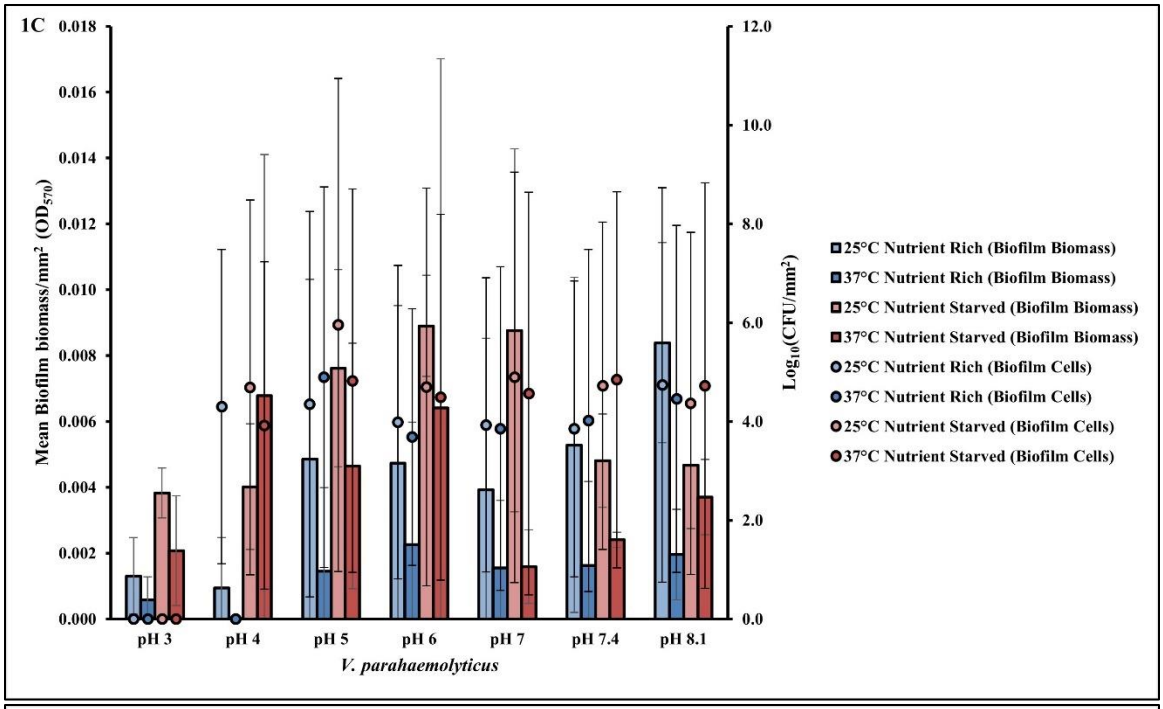
1C
Mean Biofilm biomass/mm² (OD570)
Log10(CFU/mm²)
0.018
0.016
0.014
0.012
0.010
0.008
0.006
0.004
0.002
0.000
12.0
10.0
8.0
6.0
4.0
2.0
0.0
pH 3
pH 4
pH 5
pH 6
pH 7
pH 7.4
pH 8.1
V. parahaemolyticus
25°C Nutrient Rich (Biofilm Biomass)
37°C Nutrient Rich (Biofilm Biomass)
25°C Nutrient Starved (Biofilm Biomass)
37°C Nutrient Starved (Biofilm Biomass)
25°C Nutrient Rich (Biofilm Cells)
37°C Nutrient Rich (Biofilm Cells)
25°C Nutrient Starved (Biofilm Cells)
37°C Nutrient Starved (Biofilm Cells)

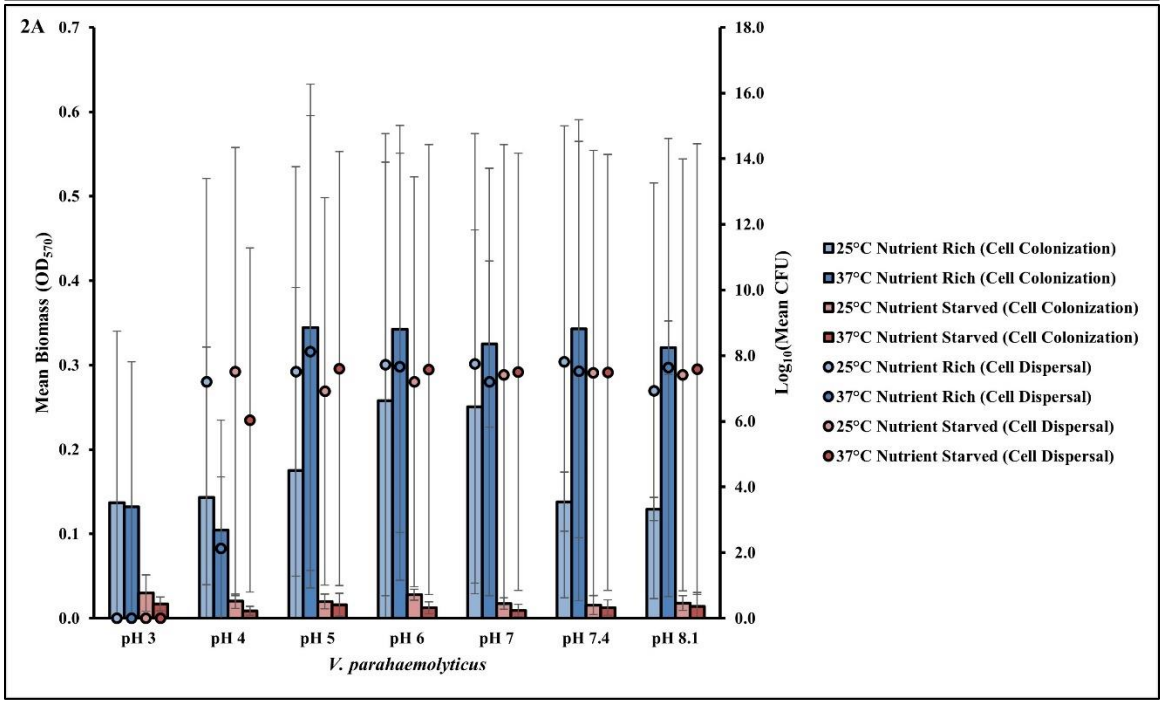
2A
Mean Biomass (OD570)
Log10(Mean CFU)
0.7
0.6
0.5
0.4
0.3
0.2
0.1
0.0
18.0
16.0
14.0
12.0
10.0
8.0
6.0
4.0
2.0
0.0
pH 3
pH 4
pH 5
pH 6
pH 7
pH 7.4
pH 8.1
V. parahaemolyticus
25°C Nutrient Rich (Cell Colonization)
37°C Nutrient Rich (Cell Colonization)
25°C Nutrient Starved (Cell Colonization)
37°C Nutrient Starved (Cell Colonization)
25°C Nutrient Rich (Cell Dispersal)
37°C Nutrient Rich (Cell Dispersal)
25°C Nutrient Starved (Cell Dispersal)
37°C Nutrient Starved (Cell Dispersal)

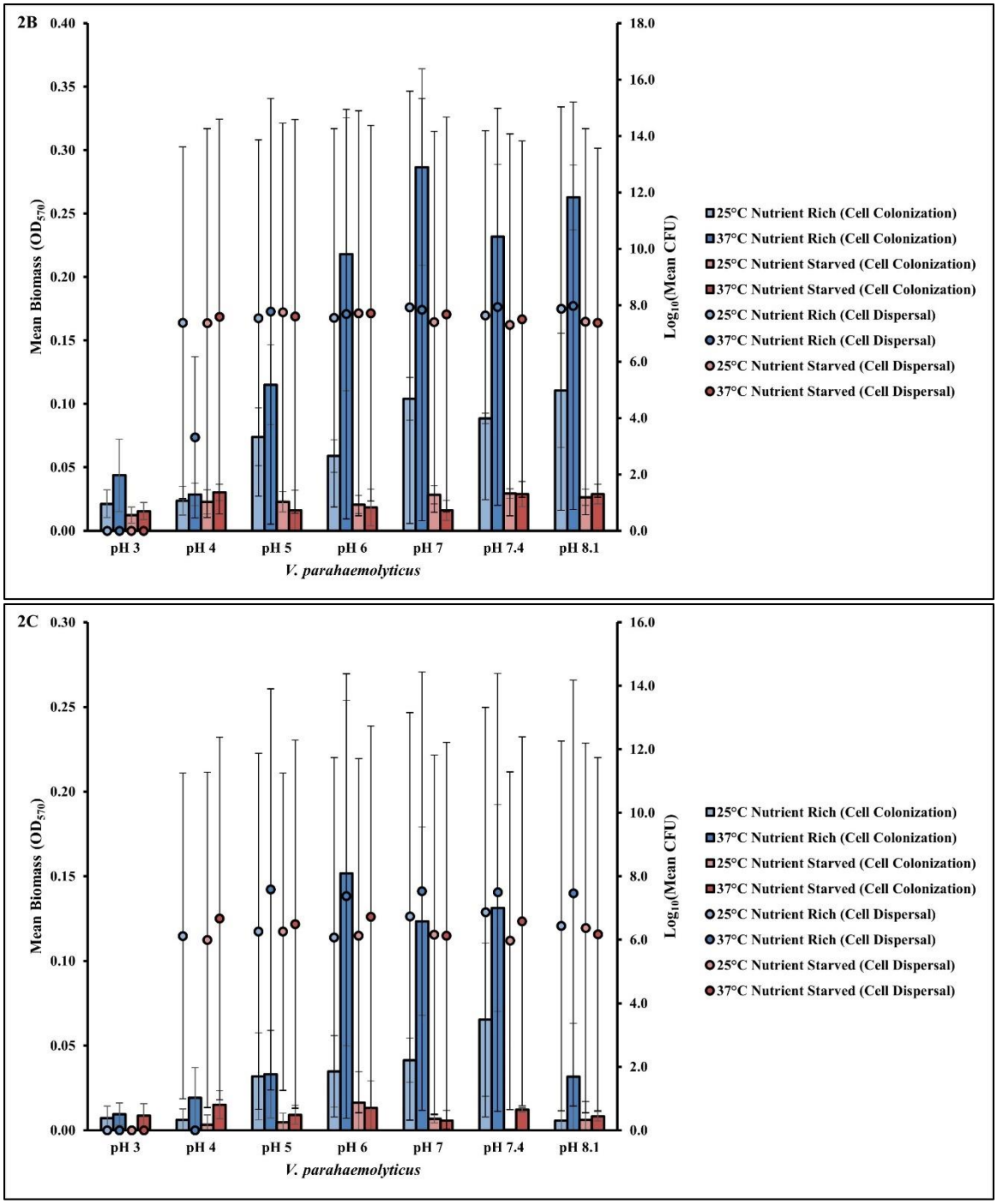

Figure 2.3. Exposure to elevated temperature, changes in pH, and nutrient starvation influences *V. parahaemolyticus* biofilm processes on and from LDPE, PP, and PS MPs. Comparison of biofilm biomass and CFUs (values represent X ± SD, n=3 replicate samples from three independent experiments) on LDPE (1A), PP (1B), and PS (1C) and subsequent biofilm cell dispersal CFUs and microplate colonization biofilm biomass (values represent X ± SD, n = 3 replicate samples from three independent experiments) from LDPE (2A), PP (2B), and PS (2C) after 2-hour exposure to different pH, temperature and nutrient availability.

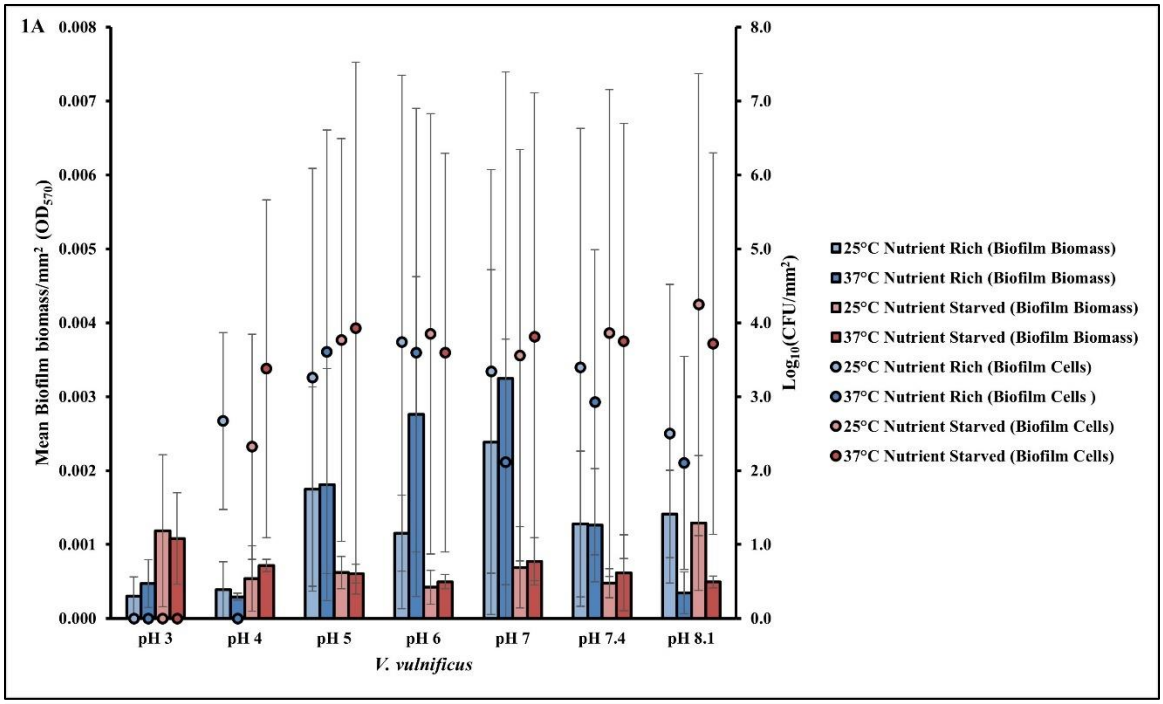
1A
Mean Biofilm biomass/mm² (OD570)
Log10(CFU/mm²)
0.000
0.001
0.002
0.003
0.004
0.005
0.006
0.007
0.008
0.0
1.0
2.0
3.0
4.0
5.0
6.0
7.0
8.0
pH 3
pH 4
pH 5
pH 6
pH 7
pH 7.4
pH 8.1
V. vulnificus
25°C Nutrient Rich (Biofilm Biomass)
37°C Nutrient Rich (Biofilm Biomass)
25°C Nutrient Starved (Biofilm Biomass)
37°C Nutrient Starved (Biofilm Biomass)
25°C Nutrient Rich (Biofilm Cells)
37°C Nutrient Rich (Biofilm Cells)
25°C Nutrient Starved (Biofilm Cells)
37°C Nutrient Starved (Biofilm Cells)

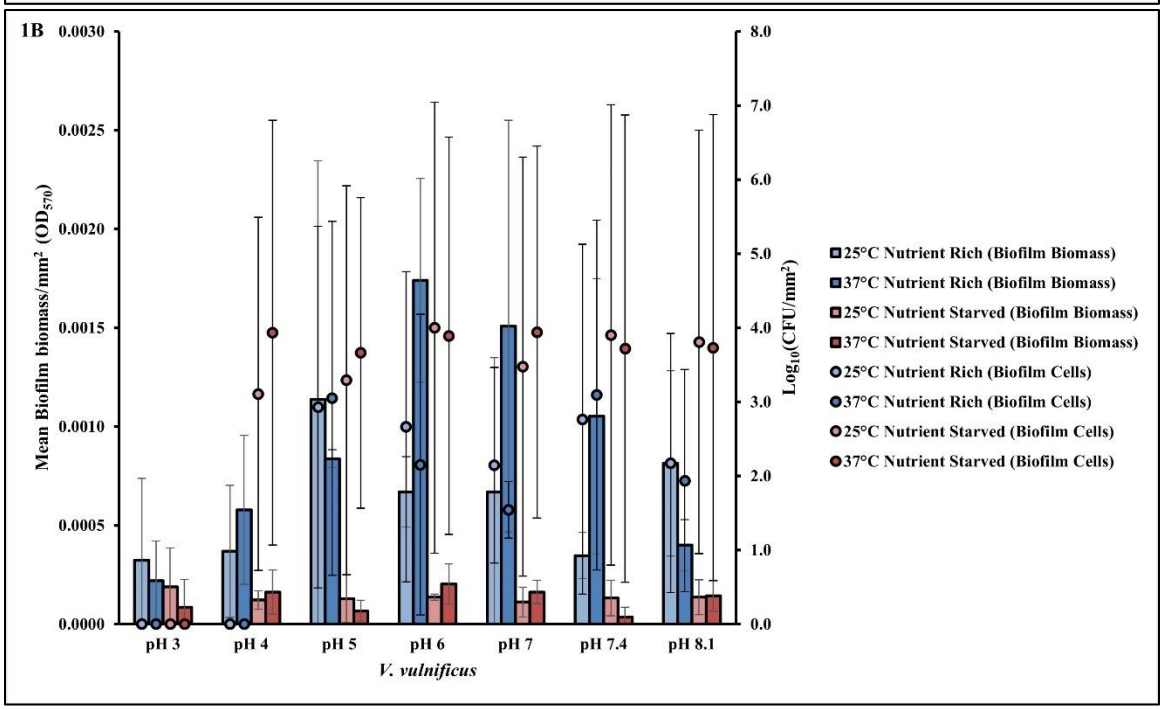
1B
Mean Biofilm biomass/mm² (OD570)
Log10(CFU/mm²)
0.0000
0.0005
0.0010
0.0015
0.0020
0.0025
0.0030
0.0
1.0
2.0
3.0
4.0
5.0
6.0
7.0
8.0
pH 3
pH 4
pH 5
pH 6
pH 7
pH 7.4
pH 8.1
V. vulnificus
25°C Nutrient Rich (Biofilm Biomass)
37°C Nutrient Rich (Biofilm Biomass)
25°C Nutrient Starved (Biofilm Biomass)
37°C Nutrient Starved (Biofilm Biomass)
25°C Nutrient Rich (Biofilm Cells)
37°C Nutrient Rich (Biofilm Cells)
25°C Nutrient Starved (Biofilm Cells)
37°C Nutrient Starved (Biofilm Cells)

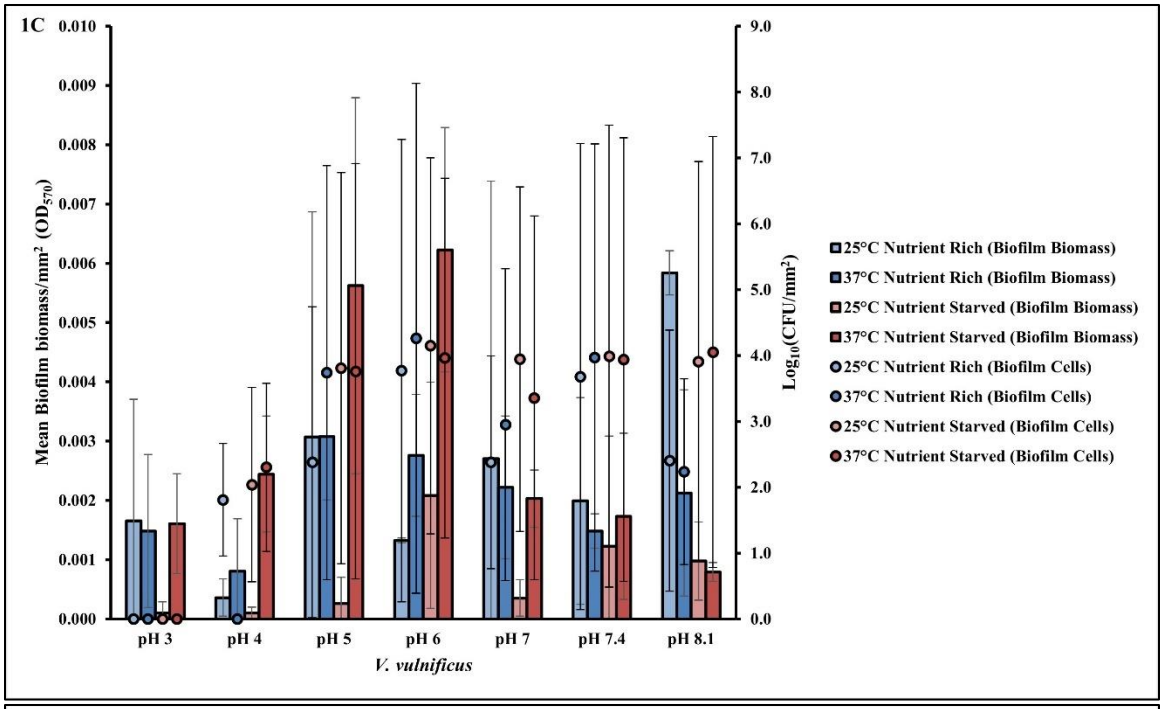
1C
Mean Biofilm biomass/mm² (OD570)
Log10(CFU/mm²)
0.010
0.009
0.008
0.007
0.006
0.005
0.004
0.003
0.002
0.001
0.000
9.0
8.0
7.0
6.0
5.0
4.0
3.0
2.0
1.0
0.0
pH 3
pH 4
pH 5
pH 6
pH 7
pH 7.4
pH 8.1
V. vulnificus
25°C Nutrient Rich (Biofilm Biomass)
37°C Nutrient Rich (Biofilm Biomass)
25°C Nutrient Starved (Biofilm Biomass)
37°C Nutrient Starved (Biofilm Biomass)
25°C Nutrient Rich (Biofilm Cells)
37°C Nutrient Rich (Biofilm Cells)
25°C Nutrient Starved (Biofilm Cells)
37°C Nutrient Starved (Biofilm Cells)

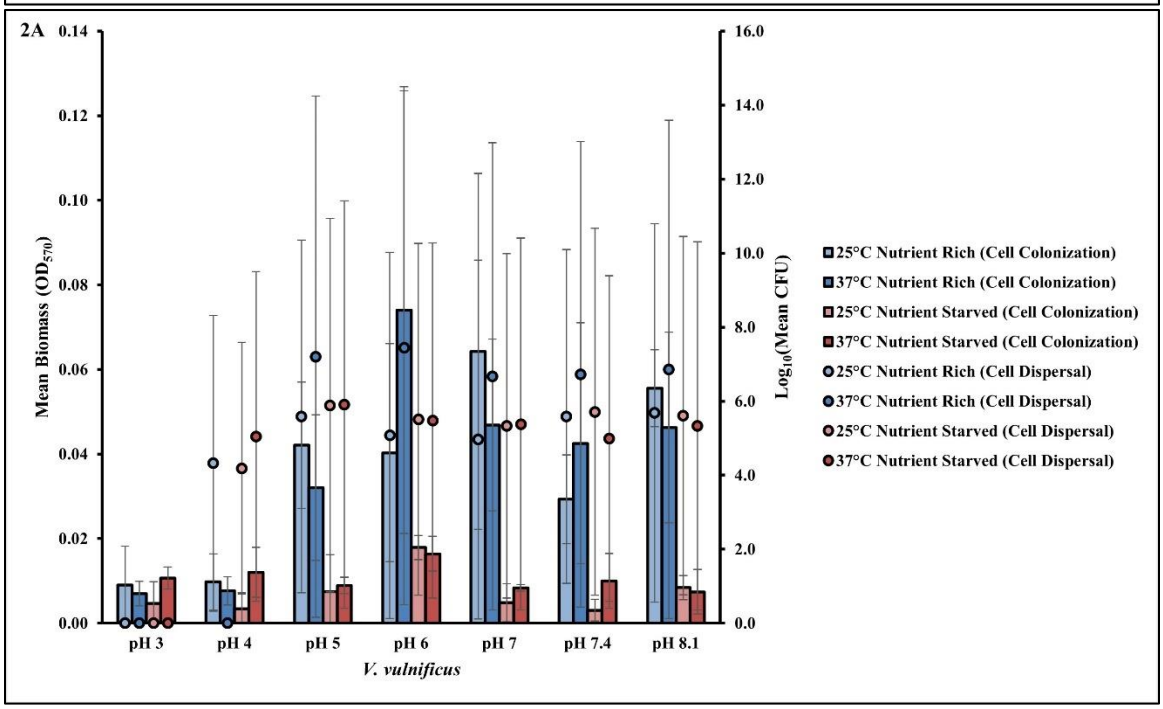
2A
Mean Biomass (OD570)
Log10(Mean CFU)
0.14
0.12
0.10
0.08
0.06
0.04
0.02
0.00
16.0
14.0
12.0
10.0
8.0
6.0
4.0
2.0
0.0
pH 3
pH 4
pH 5
pH 6
pH 7
pH 7.4
pH 8.1
V. vulnificus
25°C Nutrient Rich (Cell Colonization)
37°C Nutrient Rich (Cell Colonization)
25°C Nutrient Starved (Cell Colonization)
37°C Nutrient Starved (Cell Colonization)
25°C Nutrient Rich (Cell Dispersal)
37°C Nutrient Rich (Cell Dispersal)
25°C Nutrient Starved (Cell Dispersal)
37°C Nutrient Starved (Cell Dispersal)

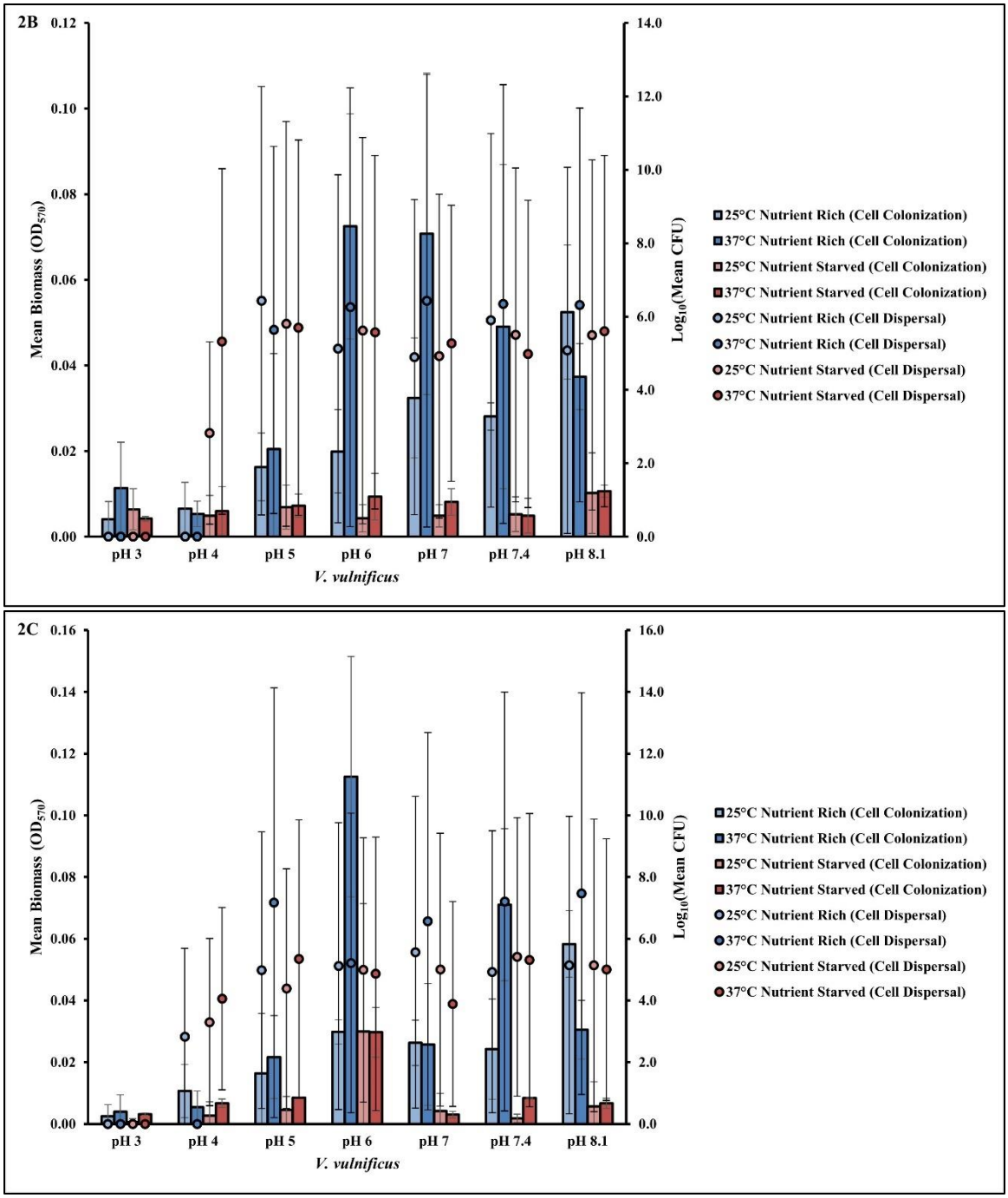

Figure 2.4. Exposure to elevated temperature, changes in pH and nutrient starvation influences *V. vulnificus* biofilm processes on and from LDPE, PP, and PS MPs. Comparison of biofilm biomass and CFUs (values represent X ± SD, n = 3 replicate samples from three independent experiments) on LDPE (1A), PP (1B), and PS (1C) and subsequent biofilm cell dispersal CFUs and microplate colonization biofilm biomass (values represent X ± SD, n = 3 replicate samples from three independent experiments) from LDPE (2A), PP (2B), and PS (2C) after 2-hour exposure to different pH, temperature and nutrient availability.

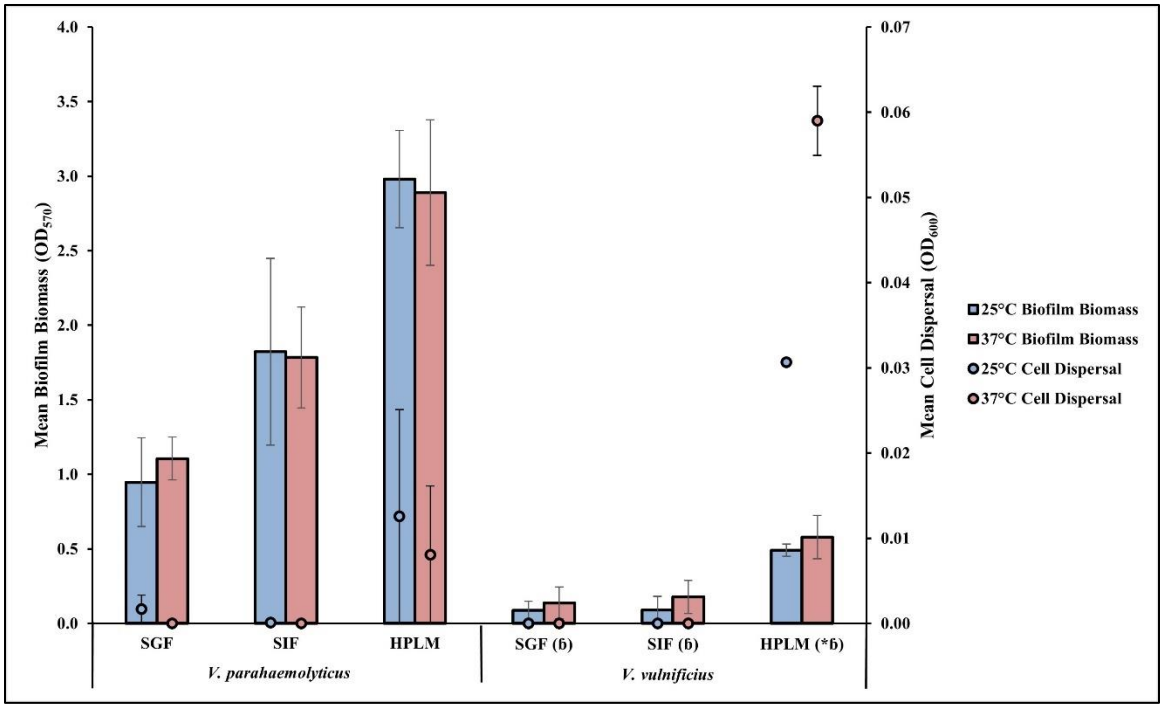

Figure 2.5. Exposure to different simulated human medias influences overall *V. parahaemolyticus* and *V. vulnificus* biofilm biomass and cell dispersal in microplates. Comparison of overall biofilm biomass and cell dispersal (values represent X ± SD, n = 3 replicate samples from three independent experiments) between different simulated human medias at different temperatures after 2-hour exposure). * = significantly greater biofilm biomass compared to similar pH MSYE, ϐ = significantly less biofilm biomass compared to *V. parahaemolyticus* in same type of media.

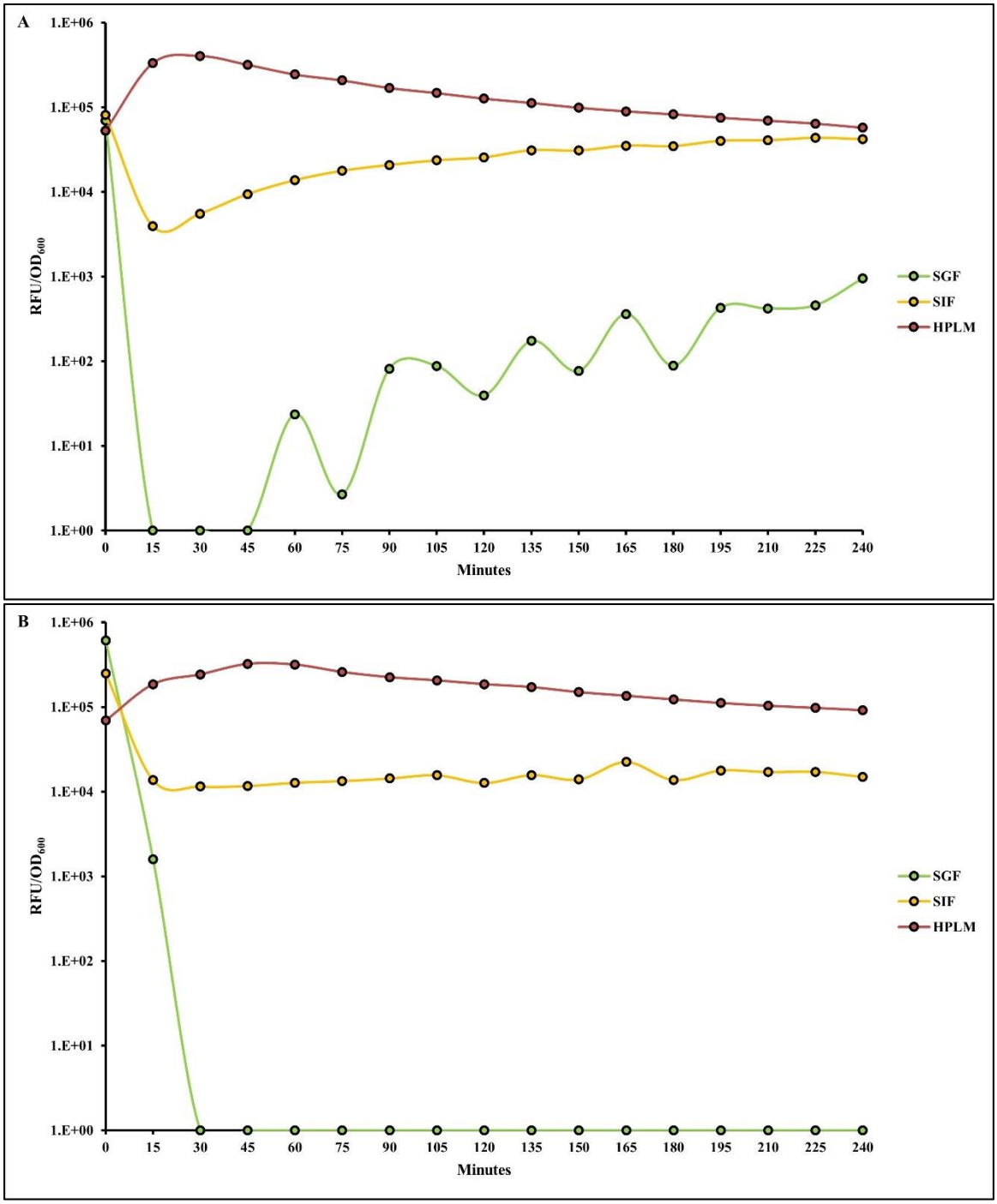

Figure 2.6. Exposure to different simulated human medias influences overall *V. parahaemolyticus* and *V. vulnificus* biofilm viability in microplates. Comparison of biofilm viability (RFU/OD_{600}) of *V. parahaemolyticus* (A) and *V. vulnificus* (B) after 2-hour exposure to simulated human medias at 37°C.

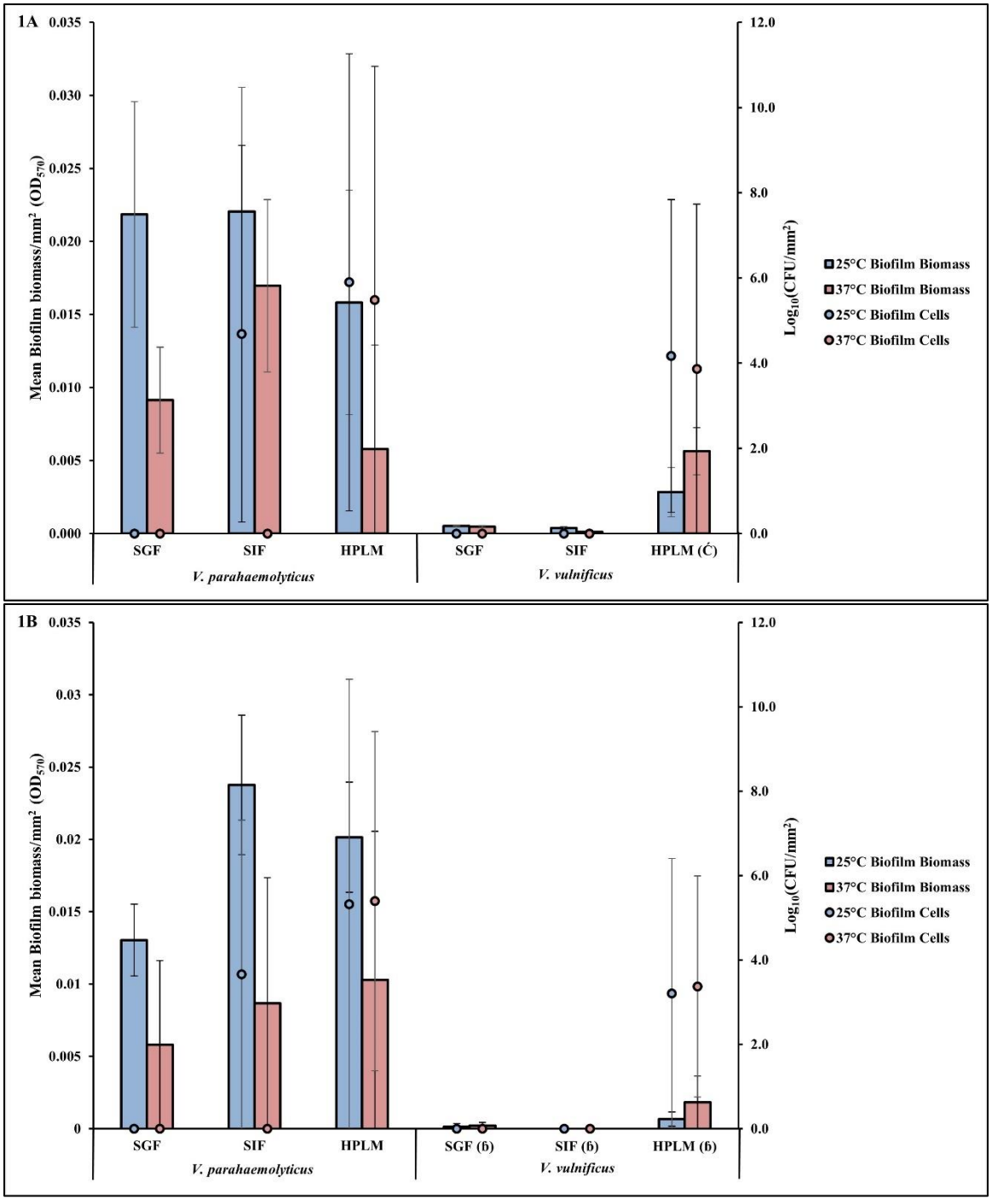
1A
Mean Biofilm biomass/mm² (OD570)
Log10(CFU/mm²)
0.035
0.030
0.025
0.020
0.015
0.010
0.005
0.000
12.0
10.0
8.0
6.0
4.0
2.0
0.0
SGF
SIF
HPLM
SGF
SIF
HPLM (Ć)
V. parahaemolyticus
V. vulnificus
25°C Biofilm Biomass
37°C Biofilm Biomass
25°C Biofilm Cells
37°C Biofilm Cells
1B
Mean Biofilm biomass/mm² (OD570)
Log10(CFU/mm²)
0.035
0.03
0.025
0.02
0.015
0.01
0.005
0
12.0
10.0
8.0
6.0
4.0
2.0
0.0
SGF
SIF
HPLM
SGF (б)
SIF (б)
HPLM (б)
V. parahaemolyticus
V. vulnificus
25°C Biofilm Biomass
37°C Biofilm Biomass
25°C Biofilm Cells
37°C Biofilm Cells

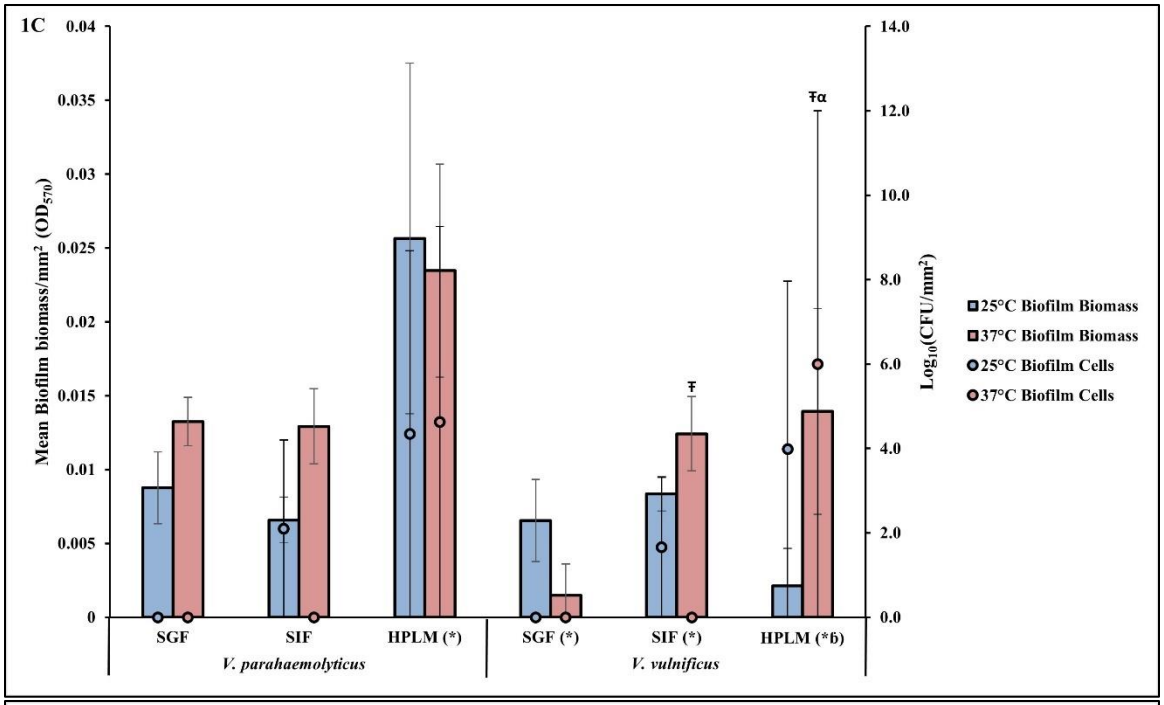
1C
Mean Biofilm biomass/mm² (OD570)
Log10(CFU/mm²)
0.04
0.035
0.03
0.025
0.02
0.015
0.01
0.005
0
14.0
12.0
10.0
8.0
6.0
4.0
2.0
0.0
Ŧα
Ŧ
25°C Biofilm Biomass
37°C Biofilm Biomass
25°C Biofilm Cells
37°C Biofilm Cells
SGF
SIF
HPLM (*)
SGF (*)
SIF (*)
HPLM (*ƃ)
V. parahaemolyticus
V. vulnificus

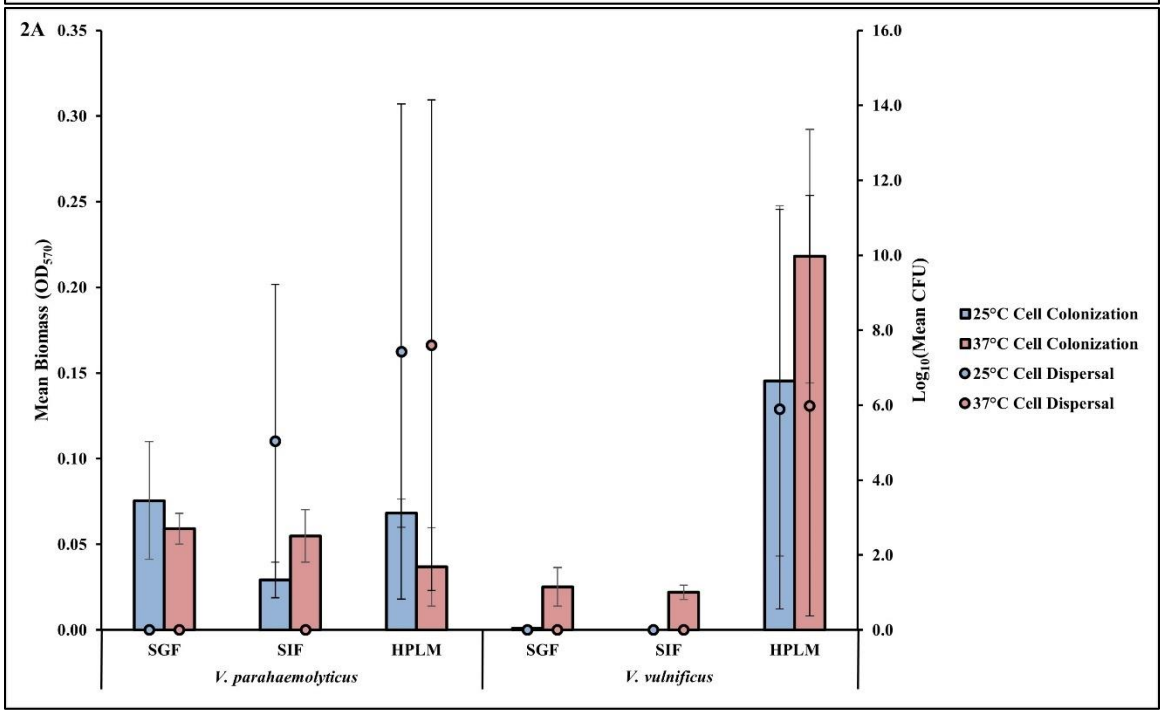
2A
Mean Biomass (OD570)
Log10(Mean CFU)
0.35
0.30
0.25
0.20
0.15
0.10
0.05
0.00
16.0
14.0
12.0
10.0
8.0
6.0
4.0
2.0
0.0
25°C Cell Colonization
37°C Cell Colonization
25°C Cell Dispersal
37°C Cell Dispersal
SGF
SIF
HPLM
SGF
SIF
HPLM
V. parahaemolyticus
V. vulnificus

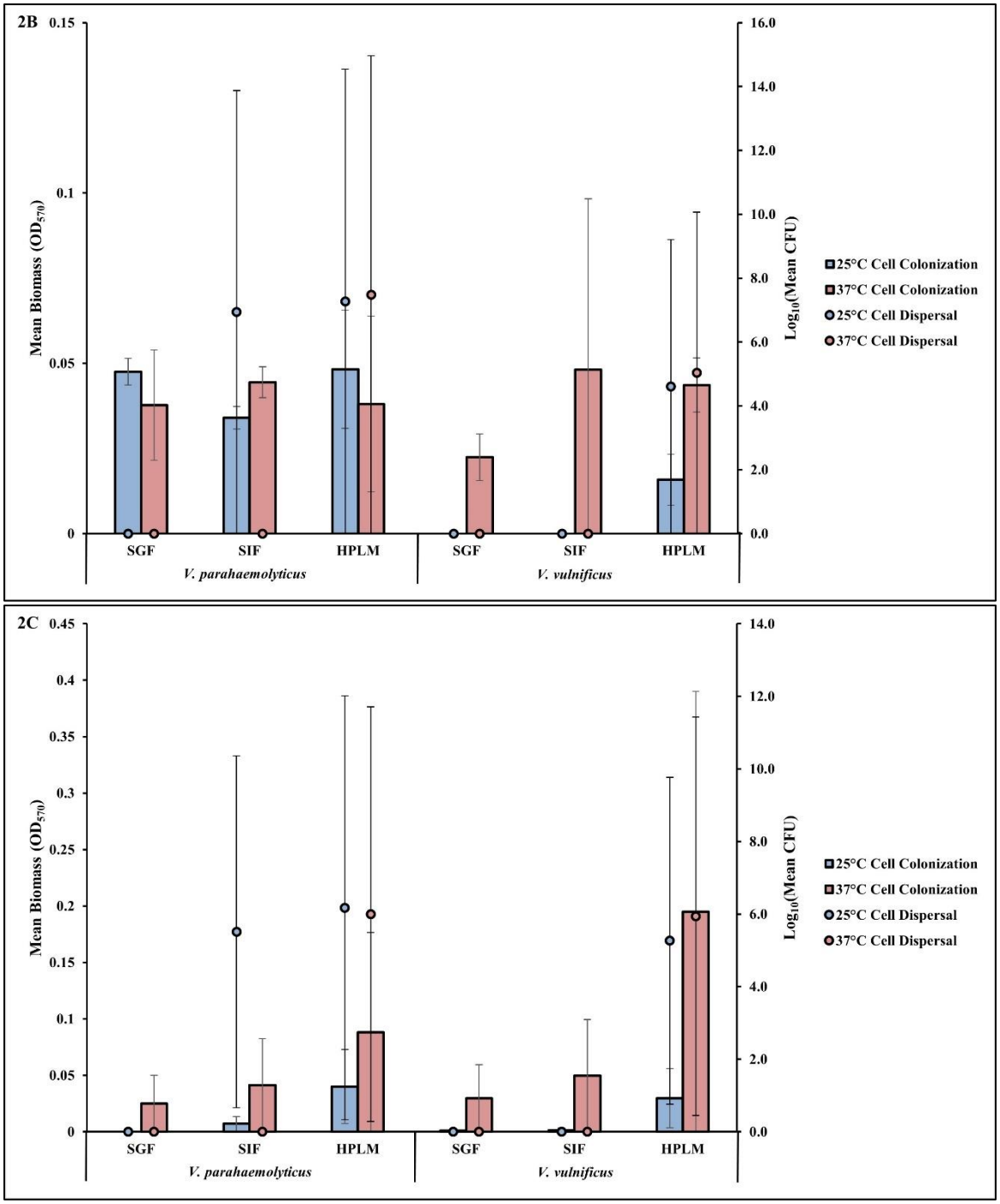

Figure 2.7. Exposure to different simulated human medias influences *V. parahaemolyticus* and *V. vulnificus* biofilm processes on and from LDPE, PP and PS MPs. Comparison of biofilm biomass and CFUs (values represent X ± SD, n = 3 replicate samples from three independent experiments) on LDPE (1A), PP (1B), and PS (1C) and subsequent biofilm cell dispersal CFUs and microplate colonization biofilm biomass (values represent X ± SD, n = 3 replicate samples from three independent experiments) from LDPE (2A), PP (2B), and PS (2C) after 2-hour exposure to different simulated human medias at different temperatures. * = significantly greater biofilm biomass compared to similar pH MSYE, Ć = significantly greater biofilm cell density compared to

similar pH MSYE, ϐ = significantly less biofilm biomass compared to *V. parahaemolyticus* in same type of media, Ŧ = significantly greater biofilm biomass compared to 25°C, α = significantly greater biofilm cell density compared to 25°C.

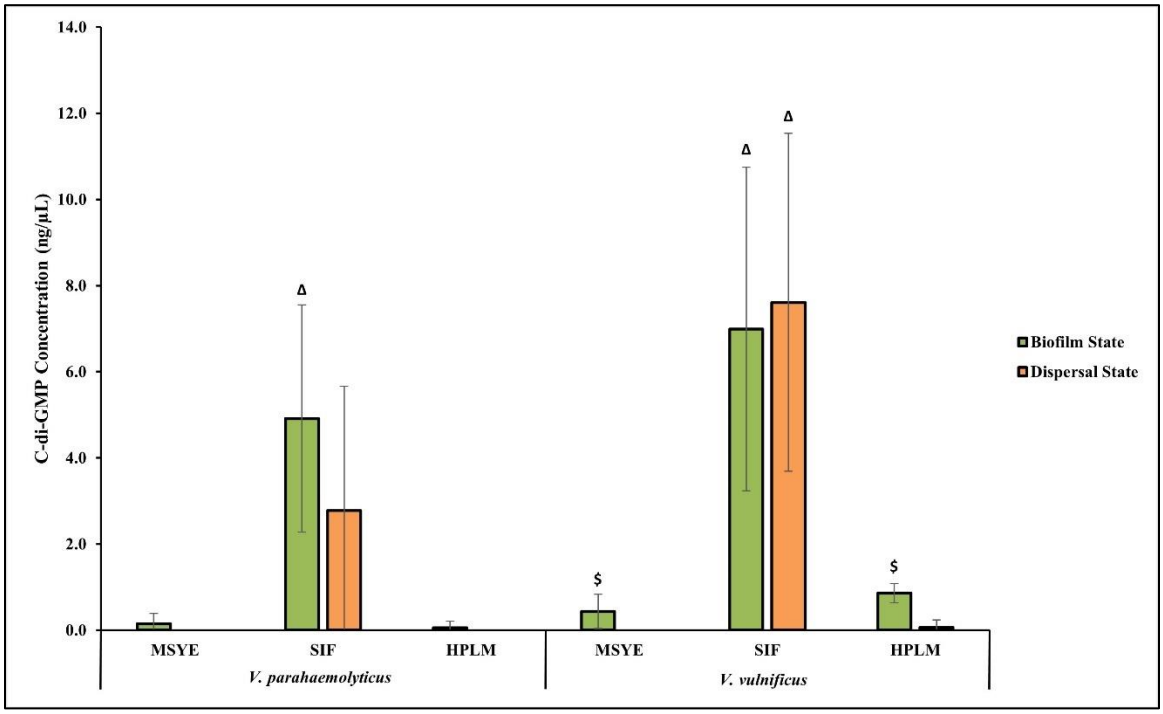

Figure 2.8. Exposure to different media compositions and cell states influences *V. parahaemolyticus* and *V. vulnificus* c-di-GMP concentrations. Comparison of estimated c-di-GMP concentrations (values represent X ± SD, n = 3 replicate samples from three independent experiments) produced by *V. parahaemolyticus* and *V. vulnificus* biofilm and dispersed cells after 2-hour exposure to MSYE, SIF, and HPLM at 37°C. Δ = significantly greater c-di-GMP concentration compared to MSYE and HPLM, $ = significantly greater c-di-GMP concentration compared to dispersal state in same media.

CONCLUSION

Plastic pollution in the marine environment remains a global concern, and their role as substrates for microbial habitats and subsequently vectors for the dispersion of pathogenic or non-pathogenic bacteria must be further evaluated, especially under evolving climate change scenarios (Zettler, Mincer & Amaral-Zettler, 2013; Kirstein et al., 2016). *V. parahaemolyticus* and *V. vulnificus* are potential pathogenic bacteria that can infect both marine animals and humans (Johnson et al., 2012). In past decades, *Vibrio* habitat range has increased and coincided with an increase in plastic production and growth (Laverty et al., 2020). This expansion of *Vibrio* coupled with their potential to colonize and live on numerous plastic types will increase the potential risk of both marine animal and human exposure to *Vibrio* species (Pedrotti et al., 2022). To better understand the emerging environmental and public health risks associated with bacterial colonization of plastic particles, studies are needed to determine how these cell processes are affected by different marine and human environmental conditions, especially on different plastic types.

Temperature and pH are primary environmental variables that influence *Vibrio* planktonic and biofilm lifecycles, and contribute greatly to growth and habitat range (Gilbert et al., 2012; Tiruvayipati & Bhassu, 2016; Ward et al., 2017; Hernández-Cabanyero et al., 2020). Most cases of vibriosis occur during summer months due to warmer sea surface temperatures in which the bacteria thrive. However, *V.*

parahaemolyticus and *V. vulnificus* infections are increasing in prevalence due to climate change contributing to rising seawater temperatures and extending the length of time of warm sea surface temperatures (Parry et al., 2007; Whitehead et al., 2009; Baker-Austin et al., 2013; Baker-Austin et al., 2016; Vezzulli et al., 2016; Deeb et al., 2018; Control & Prevention, 2019). At the same time, increased nutrient pollution and elevated dissolved CO_2 concentrations have led to increased prevalence of cyanobacterial harmful algal blooms (HABs) (O'Neil et al., 2012; Visser et al., 2016). HAB metabolism can rapidly change pH in marine environments ranging from acidic (pH < 6) to alkaline levels (pH > 9) (Raven, Gobler & Hansen, 2020). HAB outbreaks have also been suggested to enhance *V. parahaemolyticus* and *V. vulnificus* growth (Greenfield et al., 2017). Since these two *Vibrio* species are known to form biofilms and have been shown to be early colonizers of plastic surfaces, this presents a possibility that bacterial cells enclosed in the biofilm matrix on plastic surfaces may be responding to these environmental changes by exhibiting different growth and activity patterns compared to their planktonic counterparts (Guzmán-Soto et al., 2021; Kesy et al., 2021; Tavelli et al., 2022). These environmental changes could be contributing to higher *Vibrio* concentrations in contaminated seafood via plastics, ultimately leading to increased levels of *Vibrio* exposure to humans if consumed raw (Keswani et al., 2016; Kesy et al., 2021).

Recent studies conducted in marine environments have found microbial communities associate and live on plastic surfaces. These plastic-associated communities have been termed the "Plastisphere," and has raised serious implications for both marine life and human health (Ward & Kach, 2009; Zettler, Mincer & Amaral-Zettler, 2013). *Vibrio* have been found to be a major community member on marine plastics, but *Vibrio*

concentrations on plastic surfaces have appeared lower compared to natural marine particles (Bryant et al., 2016; Amaral-Zettler, Zettler & Mincer, 2020; Curren et al., 2020). However, since *Vibrio* biofilms have still been found on numerous macro and microplastic substate surface types in several marine surface waters, this implies that plastic particles could act as transport vectors of potentially pathogenic *Vibrio* to new areas outside of their native range and to marine animals that may accidently or selectively ingest the biofilm-associated plastic particles coincidently with food particles (Goldstein, Carson & Eriksen, 2014; Reisser et al., 2014; Kirstein et al., 2016; Viršek et al., 2017; Bowley et al., 2021). In addition, since these bacteria are in close proximity to each other in biofilms on plastics, there is high potential for horizontal transfer of antibiotic-resistance genes, compounding the exposure risk to both marine and human health (Arias-Andres et al., 2018; Laverty et al., 2020).

Due to expansion and intensification of aquaculture to keep up with global demand, there has consequently been an increase in infections and diseases affecting numerous aquaculture species, including *V. parahaemolyticus* and *V. vulnificus* (Karunasagar et al., 1994; Austin & Zhang, 2006; Chiu et al., 2007; Gillett, 2008; Moffitt & Cajas-Cano, 2014). The overuse of antibiotics in aquaculture to try to combat these pathogens and maintain aquaculture health is associated with increased bacterial antibiotic resistance (Matyar, 2012). This makes screening, treatment, and control of pathogens in these stocks more difficult as planktonic *V. parahaemolyticus* and *V. vulnificus* cells can be more easily controlled by antibiotics compared to cells in the biofilm state (Costerton, Stewart & Greenberg, 1999; Stewart & William Costerton, 2001). As aquacultural systems have rapidly changed as demand has increased, the

technologies and materials to support aquaculture facilities have also advanced. The materials that have been used to build and maintain the aquaculture systems have coincided with the development of synthetic organic polymers, plastics. There are several types of plastic, which include polyethylene (PE), polypropylene (PP), polystyrene (PS), poly(ethylene terephthalate) (PET), and poly(vinyl chloride) (PVC) (Andrady, 2003). Due to their usage and production, these types are more likely to end up in aquaculture, especially the more degradable, buoyant plastics like PE (high and low density), PP and PS (Brien, 2007; Andrady, 2011). Environmental processes and conditions can degrade macroplastics into smaller pieces, and those small enough (being less than 5 millimeters in size) have been classified as microplastics (MPs) (Gregory & Andrady, 2003; Betts, 2008; Arthur, Baker & Bamford, 2009). *V. parahaemolyticus* and *V. vulnificus*' ability to attain a biofilm state on both macro and MPs can present a significant problem for marine animal health due to potentially increasing the risk of physical contact with these pathogens, which consequently can increase the exposure risk to humans by consumption of raw seafood.

The expansion of *Vibrio* coupled with their potential to colonize, live, and disperse from numerous plastic types will increase the potential infection risk of human exposure, especially by ingestion of contaminated seafood (Keswani et al., 2016; Bowley et al., 2021; Cverenkárová et al., 2021). Biofilm formation plays a key role in the ability of pathogenic bacteria like *Vibrio* to colonize most environmental niches like MPs, and biofilm dispersal enables the bacteria embedded in the biofilm to be translocated to their human hosts (Austin, 2010; Kaplan, 2010; Yang et al., 2020). MPs' role as substrates for microbial habitats and subsequently vectors of pathogenic *Vibrio* to humans must be

further evaluated, especially during human ingestion scenarios (Zettler, Mincer & Amaral-Zettler, 2013; Kirstein et al., 2016). Biofilms contribute to most microbial infections, accounting for over 75% of human microbial infections (Davies, 2003; Guilhen, Forestier & Balestrino, 2017). One of these mechanisms of biofilm related infections can be influenced by the environment, called active environmentally induced biofilm dispersion, which triggers the release of bacteria from biofilms into the hosts' body environment (Flemming, Neu & Wozniak, 2007; Wang et al., 2011; Marks et al., 2013 Jamal et al., 2018; Rumbaugh & Sauer, 2020). Active seeding dispersal of cells from biofilms can occur in response to detecting changes in environmental conditions such as sudden changes in temperature, pH and nutrient conditions, as the bacteria leave the biofilm to find a more stable environment to colonize (McDougald et al., 2012). Biofilm dispersal can be a major mechanism of foodborne and waterborne *Vibrio* infections in humans by ingestion (Abdallah et al., 2014). Symptoms of both *V. parahaemolyticus* and *V. vulnificus* bacterial infections can include cramps, nausea, fever, and bloody diarrhea. *V. vulnificus* infections can be more severe and cause deadly skin infections if an open wound encounters salt or brackish water in the environment (Control & Prevention, 2019). Mitigating the severity of *Vibrio* infections has become more difficult due to widespread antibiotic resistance, so potential alternatives are being explored to better combat these pathogens like quorum sensing exploitation.

Microbiological factors like quorum sensing (QS) greatly contribute to changes in bacteria growth, survivability, and virulence (Rutherford & Bassler, 2012). In using QS, bacteria produce, detect, and respond to extracellular signaling chemicals classified as autoinducers (AI), which allows the bacteria to monitor cell population density and

collectively change gene expression (Rutherford & Bassler, 2012). QS and its exploitation by quorum sensing inhibiors (QSIs) is being explored as alternatives in pathogen treatment (LaSarre & Federle, 2013). QSIs function by shutting down signal synthesis, directly degrading the signal molecule, inhibiting the signal molecule by preventing binding to its receptor, or inhibiting the signal transduction cascade (Brackman & Coenye, 2015). Since these QSIs can disrupt QS signaling systems, and potentially disrupt pathogenicity, there is an increasing interest in developing new types of these compounds to combat pathogens. This means that QSIs in combination with antibiotics could prove to have a synergistic effect than antibiotic treatment alone on influencing *V. parahaemolyticus* and *V. vulnificus* biofilm dispersal and eradication, which could lead to therapeutic uses in alternative contamination or infection treatment (Zeng et al., 2008; Kalia, 2013).

Future studies are needed to assess simulated climate change and human environmental conditions and how these stressors may influence *Vibrio* pathogenicity and their biofilm processes on microplastics, which may ultimately lead to alternatives for plastic usage and infection controls. *Vibrio* biofilm processes on different types of surfaces like plastics remains largely unexplored but is key to understanding their survival and persistence in marine and human environmental conditions. The knowledge gap regarding the responses of these bacteria to changing environmental factors, which may alter growth, viability, chemical communication, and pathogenicity is important to address in developing better models to protect both marine and human health. Studies are needed to examine how seasonality may affect *Vibrio* biofilm growth on MPs, as *Vibrio* may be hiding out in biofilms on different surfaces such as MPs during fall and winter,

but when conditions become more favorable and warmer, they disperse from the biofilm, which may contribute to the increased planktonic cell concentrations observed during the summer. Further studies are needed to compare different strains and species of *Vibrio in vitro* biofilm processes and responses to those found *in vivo* in marine and human environments, including the use of molecular methods for pathogenic gene screening, identification, and examining transcriptomic profiles for potential virulence and antibiotic resistance gene regulation. Studies are also needed to examine interactions between *Vibrio* and different bacteria and algal species on MPs, as these interactions have been found to occur in the natural marine environment. Additional screening for MPs in seafood must also be considered as humans are likely being frequently exposed to MPs, and the bacterial response on MPs in consumed seafood needs to be further studied to better predict exposure risk. Understanding the processes in which *Vibrio* respond to marine and human environmental cues (especially on MPs) will provide more data to be used in the assessment of other zoonotic pathogens. Further research may lead to the development and implementation of plastic and antibiotic alternatives like QSIs, which may ultimately lead to increased seafood quality and policy changes for better protection of One Health.

Our studies focused on how different bacterial strains from distinct isolation sources of both *V. parahaemolyticus* and *V. vulnificus* planktonic, biofilm and dispersal states are affected by exposure to different marine and human environmental conditions such as temperature, pH, nutrients, and media composition. Our results suggest that different strain types of *V. parahaemolyticus* and *V. vulnificus* can adapt to temperature and pH changes that resemble those under climate change scenarios in coastal

environments by switching between planktonic and biofilm state, ultimately increasing their potential to survive under these stressful, changing environmental conditions. These results also suggest that temperature can affect different strain types of *V. parahaemolyticus* and *V. vulnificus* in their ability to colonize and form biofilms on different plastic types *in vitro*. Lastly, our results indicate that human pathogenic strains of *V. parahaemolyticus* and *V. vulnificus* can rapidly respond to different environmental conditions that resemble the human gastrointestinal environment by dispersing from biofilms on different MP material types *in vitro*. While our studies mainly focused on bacterial interaction with plastics, they did not focus on the plastics themselves, or the surrounding environment's effect on the plastics.

The main limitations of these studies are the different plastic types themselves were not examined in how their own characteristics (including toxicity) contributed to colonization, and how these characteristics (like hydrophobicity or surface topography) changed after bacterial colonization. However, there are other studies that have addressed these specific limitations. Studies have found that increases in surface roughness contribute to increased colonization, and this colonization can lead to decreased hydrophobicity of the plastics themselves (Michels et al., 2018; Ganesan et al., 2022). The environment's interaction with the plastics was also not examined, as conditioning films, which are formed by absorption of available biomolecules in the surrounding environment, can greatly contribute to bacterial colonization. This has also been addressed by other studies that examined marine conditioning films on plastics preceding bacterial attachment by microscopy and mass spectrometry (Bhagwat et al., 2021; Rummel et al., 2021). Plastics themselves were not examined in how they contributed to

potential stress to the bacteria, as plastics are known to potentially contain many harmful chemicals and additives and may also leach these chemicals into the surrounding environment (Bolgar et al., 2015; Groh & Muncke, 2017). However, other studies have examined this by measuring potential toxicity of organic and inorganic plastic additives to bacteria, including *Vibrio* species (Zimmermann et al., 2019; Tetu, Sarker & Moore, 2020). Further studies will need to address these specific issues on how the characteristics of different types of plastics affect *Vibrio* colonization, biofilm maturation, cell viability and dispersal. Regardless of the limitations in our studies, we still addressed some of the mentioned knowledge gaps by examining *V. parahaemolyticus* and *V. vulnificus* responses, especially on plastics, to changing environmental conditions.

Taken together, we have gained an improved understanding how different strain types of *V. parahaemolyticus* and *V. vulnificus* can rapidly grow and respond to different changes in marine and human environmental conditions such as temperature, pH, nutrient availability and simulated human medias *in vitro*, especially on different plastic material types. However, these growth, colonization and dispersal processes are highly variable and depends on species, strain and plastic type, especially under different environmental exposures. While further studies are needed to examine and compare these *Vibrio* responses found *in vitro* to those found *in vivo*, these data can still be used for further examining other marine animal and human pathogenic species in their phenotype and genotype responses, and modeling *Vibrio* exposure risk to both marine animals and humans. By better understanding the interactions between *Vibrio* and plastics in various environmental conditions, this may ultimately lead to better protection of One Health by development of more accurate exposure risk models, new pathogen treatments and policy

changes aimed at both limiting plastics and implementation of potential plastic alternatives.

BIBLIOGRAPHY

Abdallah, M., C. Benoliel, D. Drider, P. Dhulster and N.-E. Chihib (2014). "Biofilm formation and persistence on abiotic surfaces in the context of food and medical environments." Archives of Microbiology **196**(7): 453-472.

Amaral-Zettler, L. A., E. R. Zettler and T. J. Mincer (2020). "Ecology of the plastisphere." Nature Reviews Microbiology **18**(3): 139-151.

Alotaibi, G. F. and M. A. Bukhari (2021). "Factors influencing bacterial biofilm formation and development." Am. J. Biomed. Sci. Res **12**(6): 617-626.

Amaro, C. (1992). "Comparative study of phenotypic and virulence properties in *Vibrio vulnificus* biotype 1 and 2 obtained from a European eel farm experiencing mortalities." Diseases of Aquatic Organisms **13**: 29-35.

Amaro, C. and E. G. Biosca (1996). "*Vibrio vulnificus* biotype 2, pathogenic for eels, is also an opportunistic pathogen for humans." Applied and Environmental Microbiology **62**(4): 1454-1457.

Andersen, J. B., L. D. Hultqvist, C. U. Jansen, T. H. Jakobsen, M. Nilsson, M. Rybtke, J. Uhd, B. G. Fritz, R. Seifert, J. Berthelsen, T. E. Nielsen, K. Qvortrup, M. Givskov and T. Tolker-Nielsen (2021). "Identification of small molecules that interfere with c-di-GMP signaling and induce dispersal of *Pseudomonas aeruginosa* biofilms." npj Biofilms and Microbiomes **7**(1): 59.

Andrady, A. L. (2003). Plastics and the Environment, John Wiley & Sons.

Andrady, A. L. (2011). "Microplastics in the marine environment." Marine Pollution Bulletin **62**(8): 1596-1605.

Arias-Andres, M., U. Klümper, K. Rojas-Jimenez and H.-P. Grossart (2018). "Microplastic pollution increases gene exchange in aquatic ecosystems." Environmental Pollution **237**: 253-261.

Arthur, C., J. Baker and H. Bamford (2009). Proceedings of the International Research Workshop on the Occurrence, Effects, and Fate of Microplastic Marine Debris, September 9-11, 2008.

Austin, B. (2010). "Vibrios as causal agents of zoonoses." Veterinary Microbiology **140**(3): 310-317.

Austin, B. and X.-H. Zhang (2006). "Vibrio harveyi: a significant pathogen of marine vertebrates and invertebrates." Letters in Applied Microbiology **43**(2): 119-124.

Baker-Austin, C., J. D. Oliver, M. Alam, A. Ali, M. K. Waldor, F. Qadri and J. Martinez-Urtaza (2018). "*Vibrio* spp. infections." Nature Reviews Disease Primers **4**(1): 1-19.

Baker-Austin, C., L. Stockley, R. Rangdale and J. Martinez-Urtaza (2010). "Environmental occurrence and clinical impact of *Vibrio vulnificus* and *Vibrio parahaemolyticus*: a European perspective." Environmental Microbiology Reports **2**(1): 7-18.

Baker-Austin, C., J. A. Trinanes, S. Salmenlinna, M. Löfdahl, A. Siitonen, N. G. Taylor and J. Martinez-Urtaza (2016). "Heat wave–associated vibriosis, Sweden and Finland, 2014." Emerging Infectious Diseases **22**(7): 1216.

Baker-Austin, C., J. A. Trinanes, N. G. Taylor, R. Hartnell, A. Siitonen and J. Martinez-Urtaza (2013). "Emerging *Vibrio* risk at high latitudes in response to ocean warming." Nature Climate Change **3**(1): 73-77.

Barraud, N., S. Kjelleberg and A. Rice Scott (2015). "Dispersal from Microbial Biofilms." Microbiology Spectrum **3**(6): 3.6.05.

Barraud, N., J. A. Moscoso, J.-M. Ghigo and A. Filloux (2014). Methods for studying biofilm dispersal in *Pseudomonas aeruginosa*. *Pseudomonas* methods and protocols, Springer**:** 643-651.

Bell, A. and M. Bott (2021). "Vibriosis:: What You and Your Patients Need To Know." Delaware Journal of Public Health **7**(1): 14-21.

Betts, K. (2008). Why small plastic particles may pose a big problem in the oceans, ACS Publications.

Bharati, B. K., I. M. Sharma, S. Kasetty, M. Kumar, R. Mukherjee and D. Chatterji (2012). "A full-length bifunctional protein involved in c-di-GMP turnover is required for long-term survival under nutrient starvation in *Mycobacterium smegmatis*." Microbiology **158**(6): 1415-1427.

Billaud, M., F. Seneca, E. Tambutté and D. Czerucka (2022). "An Increase of Seawater Temperature Upregulates the Expression of *Vibrio parahaemolyticus* Virulence Factors Implicated in Adhesion and Biofilm Formation." Frontiers in Microbiology **13**.

Bjerkan, G., E. Witsø and K. Bergh (2009). "Sonication is superior to scraping for retrieval of bacteria in biofilm on titanium and steel surfaces in vitro." Acta orthopaedica **80**(2): 245-250.

Bonnet, M., J. C. Lagier, D. Raoult and S. Khelaifia (2019). "Bacterial culture through selective and non-selective conditions: the evolution of culture media in clinical microbiology." New Microbes and New Infections **34**: 100622-100622.

Bowley, J., C. Baker-Austin, A. Porter, R. Hartnell and C. Lewis (2021). "Oceanic Hitchhikers – Assessing Pathogen Risks from Marine Microplastic." Trends in Microbiology **29**(2): 107-116.

Brackman, G. and T. Coenye (2015). "Quorum sensing inhibitors as anti-biofilm agents." Currrent Pharmaceutical Design **21**(1): 5-11.

Bramhachari, P., P. K. Kishor, R. Ramadevi, B. R. Rao and S. K. Dubey (2007). "Isolation and characterization of mucous exopolysaccharide (EPS) produced by *Vibrio furnissii* strain VB0S3." Journal of Microbiology and Technology **17**(1): 44-51.

Brien, S. (2007). Vinyls Industry Update. Presentation at the World Vinyl Forum 2007.

Broberg, C. A., T. J. Calder and K. Orth (2011). "*Vibrio parahaemolyticus* cell biology and pathogenicity determinants." Microbes and infection **13**(12-13): 992-1001.

Bryant, J. A., T. M. Clemente, D. A. Viviani, A. A. Fong, K. A. Thomas, P. Kemp, D. M. Karl, A. E. White, E. F. DeLong and J. K. Jansson (2016). "Diversity and Activity of Communities Inhabiting Plastic Debris in the North Pacific Gyre." mSystems **1**(3): e00024-00016.

Çam, S. and R. Brinkmeyer (2020). "The effects of temperature, pH, and iron on biofilm formation by clinical versus environmental strains of *Vibrio vulnificus*." Folia Microbiologica **65**(3): 557-566.

Çam, S., R. Brinkmeyer and J. R. Schwarz (2019). "Quantitative PCR enumeration of vcgC and 16S rRNA type A and B genes as virulence indicators for environmental and clinical strains of *Vibrio vulnificus* in Galveston Bay oysters." Canadian Journal of Microbiology **65**(8): 613-621.

Chiu, C.-H., Y.-K. Guu, C.-H. Liu, T.-M. Pan and W. Cheng (2007). "Immune responses and gene expression in white shrimp, Litopenaeus vannamei, induced by Lactobacillus plantarum." Fish & Shellfish Immunology **23**(2): 364-377.

Chodur Daniel, M., P. Coulter, J. Isaacs, M. Pu, N. Fernandez, M. Waters Chris and A. Rowe-Magnus Dean (2018). "Environmental Calcium Initiates a Feed-Forward Signaling Circuit That Regulates Biofilm Formation and Rugosity in *Vibrio* vulnificus." mBio **9**(4): e01377-01318.

Chua, S. L., Y. Liu, J. K. Yam, Y. Chen, R. M. Vejborg, B. G. Tan, S. Kjelleberg, T. Tolker-Nielsen, M. Givskov and L. Yang (2014). "Dispersed cells represent a distinct stage in the transition from bacterial biofilm to planktonic lifestyles." Nature Communications **5**: 4462.

Chua, S. L., K. Sivakumar, M. Rybtke, M. Yuan, J. B. Andersen, T. E. Nielsen, M. Givskov, T. Tolker-Nielsen, B. Cao, S. Kjelleberg and L. Yang (2015). "C-di-GMP regulates *Pseudomonas aeruginosa* stress response to tellurite during both planktonic and biofilm modes of growth." Scientific Reports **5**(1): 10052.

Collins, C. H. (1967). "Microbiological methods." Microbiological Methods.(2nd Edition).

Control, C. f. D. and Prevention (2019). *Vibrio* species causing vibriosis.

Conway, P. L., S. L. Gorbach and B. R. Goldin (1987). "Survival of lactic acid bacteria in the human stomach and adhesion to intestinal cells." Journal of Dairy Science **70**(1): 1-12.

Costerton, J. W., P. S. Stewart and E. P. Greenberg (1999). "Bacterial Biofilms: A Common Cause of Persistent Infections." Science **284**(5418): 1318-1322.

Cózar, A., F. Echevarría, J. I. González-Gordillo, X. Irigoien, B. Úbeda, S. Hernández-León, Á. T. Palma, S. Navarro, J. García-de-Lomas and A. Ruiz (2014). "Plastic debris in the open ocean." Proceedings of the National Academy of Sciences **111**(28): 10239-10244.

Curren, E., C. P. Leaw, P. T. Lim and S. C. Y. Leong (2020). "Evidence of Marine Microplastics in Commercially Harvested Seafood." Frontiers in Bioengineering and Biotechnology **8**: 562760-562760.

Curren, E. and S. C. Y. Leong (2019). "Profiles of bacterial assemblages from microplastics of tropical coastal environments." Science of The Total Environment **655**: 313-320.

Cverenkárová, K., M. Valachovičová, T. Mackuľak, L. Žemlička and L. Bírošová (2021). "Microplastics in the food chain." Life **11**(12): 1349.

Dang, H. and C. R. Lovell (2016). "Microbial Surface Colonization and Biofilm Development in Marine Environments." Microbiology and Molecular Biology Reviews **80**(1): 91-138.

Davidson, K. and S. E. Dudas (2016). "Microplastic Ingestion by Wild and Cultured Manila Clams (*Venerupis philippinarum*) from Baynes Sound, British Columbia." Archives of Environmental Contamination Toxicology **71**(2): 147-156.

Davies, D. (2003). "Understanding biofilm resistance to antibacterial agents." Nature Reviews Drug discovery **2**(2): 114-122.

Davis, B., R. Dulbecco, H. Eiser and H. Ginsberg (1980). "Microbiology: Including immunology and Molecular genetics, Harper and Row." Hagerstown, Md **19802**.

de Carvalho, C. C. C. R. (2018). "Marine Biofilms: A Successful Microbial Strategy With Economic Implications." Frontiers in Marine Science **5**(126).

De Kievit, T. R., R. Gillis, S. Marx, C. Brown and B. H. Iglewski (2001). "Quorum-Sensing Genes in *Pseudomonas aeruginosa* Biofilms: Their Role and Expression Patterns." Applied and Environmental Microbiology **67**(4): 1865.

De Tender, C. A., L. I. Devriese, A. Haegeman, S. Maes, T. Ruttink and P. Dawyndt (2015). "Bacterial Community Profiling of Plastic Litter in the Belgian Part of the North Sea." Environmental Science & Technology **49**(16): 9629-9638.

de Wouters, T., C. Jans, T. Niederberger, P. Fischer and P. A. Rühs (2015). "Adhesion Potential of Intestinal Microbes Predicted by Physico-Chemical Characterization Methods." PLOS ONE **10**(8): e0136437.

Debroas, D., A. Mone and A. Ter Halle (2017). "Plastics in the North Atlantic garbage patch: A boat-microbe for hitchhikers and plastic degraders." Science of The Total Environment **599-600**: 1222-1232.

Decho, A. W. and T. Gutierrez (2017). "Microbial Extracellular Polymeric Substances (EPSs) in Ocean Systems." Frontiers in Microbiology **8**(922).

Deeb, R., D. Tufford, G. I. Scott, J. G. Moore and K. Dow (2018). "Impact of Climate Change on *Vibrio vulnificus* Abundance and Exposure Risk." Estuaries and coasts : Journal of the Estuarine Research Federation **41**(8): 2289-2303.

Delacuvellerie, A., A. Géron, S. Gobert and R. Wattiez (2022). "New insights into the functioning and structure of the PE and PP plastispheres from the Mediterranean Sea." Environmental Pollution **295**: 118678.

Donlan, R. M. (2002). "Biofilms: microbial life on surfaces." Emerging Infectious Diseases **8**(9): 881-890.

Dragoš, A. and Á. T. Kovács (2017). "The peculiar functions of the bacterial extracellular matrix." Trends in Microbiology **25**(4): 257-266.

Drake, S. L., A. DePaola and L.-A. Jaykus (2007). "An Overview of *Vibrio vulnificus* and *Vibrio parahaemolyticus*." Comprehensive Reviews in Food Science and Food Safety **6**(4): 120-144.

Dubois, M., K. Gilles, J. Hamilton, P. Rebers and F. Smith (1951). "A colorimetric method for the determination of sugars." Nature **168**(4265): 167-167.

Egwuatu, T. O., Ogunsola, F. T., Okodugha, I. M., Jide, B., Arewa, D. G., & Osinupebi, O. A. (2014). Effect of blood agar from different animal blood on growth rates and morphology of common pathogenic bacteria. Advances in Microbiology, **4**(16), 1237.

Elmahdi, S., S. Parveen, S. Ossai, L. V. DaSilva, M. Jahncke, J. Bowers and J. Jacobs (2018). "*Vibrio parahaemolyticus* and *Vibrio vulnificus* Recovered from Oysters during an Oyster Relay Study." Applied and Environmental Microbiology **84**(3): e01790-01717.

Eriksen, M., L. Lebreton, H. Carson, M. Thiel, C. Moore, J. Borerro, F. Glagani, P. Ryan and J. Reisser (2014). "Plastic pollution in the world's oceans." PLOS ONE **9**.

Fabra, M., L. Williams, J. E. M. Watts, M. S. Hale, F. Couceiro and J. Preston (2021). "The plastic Trojan horse: Biofilms increase microplastic uptake in marine filter feeders impacting microbial transfer and organism health." Science of The Total Environment **797**: 149217.

Ferchichi, H., A. St-Hilaire, T. B. M. J. Ouarda and B. Lévesque (2021). "Impact of the future coastal water temperature scenarios on the risk of potential growth of pathogenic *Vibrio* marine bacteria." Estuarine, Coastal and Shelf Science **250**: 107094.

Flemming, H.-C., T. R. Neu and D. J. Wozniak (2007). "The EPS matrix: the "house of biofilm cells"." Journal of Bacteriology **189**(22): 7945-7947.

Flemming, H.-C. (2016). "EPS—then and now." Microorganisms **4**(4): 41.

Froelich, B. A. and D. A. Daines (2020). "In hot water: effects of climate change on *Vibrio*–human interactions." Environmental Microbiology **22**(10): 4101-4111.

Froelich, B. A. and R. T. Noble (2016). "*Vibrio* bacteria in raw oysters: managing risks to human health." Philosophical Transactions Royal Society London B Biological Sciences **371**(1689).

Galperin, M. Y. (2004). "Bacterial signal transduction network in a genomic perspective." Environmental Microbiology **6**(6): 552-567.

Gaylarde, C. C., M. P. de Almeida, C. V. Neves, J. A. Neto and E. M. da Fonseca (2023) "The Importance of Biofilms on Microplastic Particles in Their Sinking Behavior and the Transfer of Invasive Organisms between Ecosystems." Micro **3**, 320-337 DOI: 10.3390/micro3010022.

Ghenem, L., N. Elhadi, F. Alzahrani and M. Nishibuchi (2017). "*Vibrio parahaemolyticus*: A Review on Distribution, Pathogenesis, Virulence Determinants and Epidemiology." Saudi Journal of Medicine & Medical sSiences **5**(2): 93-103.

Giaouris, E., M.-P. Chapot-Chartier and R. Briandet (2009). "Surface physicochemical analysis of natural *Lactococcus lactis* strains reveals the existence of hydrophobic and low charged strains with altered adhesive properties." International Journal of Food Microbiology **131**(1): 2-9.

Gilbert, J. A., J. A. Steele, J. G. Caporaso, L. Steinbrück, J. Reeder, B. Temperton, S. Huse, A. C. McHardy, R. Knight and I. Joint (2012). "Defining seasonal marine microbial community dynamics." The ISME journal **6**(2): 298-308.

Gillett, R. (2008). Global study of shrimp fisheries, Food and Agriculture Organization of the United Nations Rome.

Gjermansen, M., M. Nilsson, L. Yang and T. Tolker-Nielsen (2010). "Characterization of starvation-induced dispersion in *Pseudomonas putida* biofilms: genetic elements and molecular mechanisms." Molecular Microbiology **75**(4): 815-826.

Gjermansen, M., P. Ragas, C. Sternberg, S. Molin and T. Tolker-Nielsen (2005). "Characterization of starvation-induced dispersion in *Pseudomonas putida* biofilms." Environmental Microbiology **7**(6): 894-906.

Gode-Potratz, C. J., R. J. Kustusch, P. J. Breheny, D. S. Weiss and L. L. McCarter (2011). "Surface sensing in *Vibrio parahaemolyticus* triggers a programme of gene expression that promotes colonization and virulence." Molecular Microbiology **79**(1): 240-263.

Goldstein, M. C., H. S. Carson and M. Eriksen (2014). "Relationship of diversity and habitat area in North Pacific plastic-associated rafting communities." Marine Biology **161**(6): 1441-1453.

Grande, R., M. C. Di Marcantonio, I. Robuffo, A. Pompilio, C. Celia, L. Di Marzio, D. Paolino, M. Codagnone, R. Muraro, P. Stoodley, L. Hall-Stoodley and G. Mincione (2015). "*Helicobacter pylori* ATCC 43629/NCTC 11639 Outer Membrane Vesicles (OMVs) from Biofilm and Planktonic Phase Associated with Extracellular DNA (eDNA)." Frontiers in Microbiology **6**(1369).

Grau, B. L., M. C. Henk, K. L. Garrison, B. J. Olivier, R. M. Schulz, K. L. O'Reilly and G. S. Pettis (2008). "Further characterization of *Vibrio vulnificus* rugose variants and identification of a capsular and rugose exopolysaccharide gene cluster." Infection and immunity **76**(4): 1485-1497.

Greenfield, D., J. Gooch Moore, J. Stewart, E. Hilborn, B. George, Q. Li, J. Dickerson, C. Keppler and P. Sandifer (2017). "Temporal and environmental factors driving *Vibrio vulnificus* and *V. parahaemolyticus* populations and their associations with harmful algal blooms in South Carolina detention ponds and receiving tidal creeks." GeoHealth **1**(9): 306-317.

Gregory, M. R. (2009). "Environmental implications of plastic debris in marine settings--entanglement, ingestion, smothering, hangers-on, hitch-hiking and alien invasions." Philosophical transactions of the Royal Society of London. Series B, Biological Sciences **364**(1526): 2013-2025.

Gregory, M. R. and A. L. Andrady (2003). "Plastics in the marine environment." Plastics and the Environment **379**: 389-390.

Guilhen, C., C. Forestier and D. Balestrino (2017). "Biofilm dispersal: multiple elaborate strategies for dissemination of bacteria with unique properties." Molecular Microbiology **105**(2): 188-210.

Guzmán-Soto, I., C. McTiernan, M. Gonzalez-Gomez, A. Ross, K. Gupta, E. J. Suuronen, T.-F. Mah, M. Griffith and E. I. Alarcon (2021). "Mimicking biofilm formation and development: Recent progress in in vitro and in vivo biofilm models." iScience **24**(5): 102443.

Hamanaka, D., M. Onishi, T. Genkawa, F. Tanaka and T. Uchino (2012). "Effects of temperature and nutrient concentration on the structural characteristics and removal of vegetable-associated *Pseudomonas* biofilm." Food Control **24**(1): 165-170.

Han, N., M. Mizan, I. Jahid and S.-D. Ha (2016). "Biofilm formation by *Vibrio parahaemolyticus* on food and food contact surfaces increases with rise in temperature." Food Control **70**: 161-166.

Harrison, J. P., M. Schratzberger, M. Sapp and A. M. Osborn (2014). "Rapid bacterial colonization of low-density polyethylene microplastics in coastal sediment microcosms." BMC Microbiology **14**(1): 232.

Heipieper, H. J., S. Cornelissen and M. Pepi (2010). Surface Properties and Cellular Energetics of Bacteria in Response to the Presence of Hydrocarbons. Handbook of Hydrocarbon and Lipid Microbiology. K. N. Timmis. Berlin, Heidelberg, Springer Berlin Heidelberg**:** 1615-1624.

Hengge, R. (2009). "Principles of c-di-GMP signalling in bacteria." Nature Reviews Microbiology **7**(4): 263-273.

Hernández-Cabanyero, C. and C. Amaro (2020). "Phylogeny and life cycle of the zoonotic pathogen *Vibrio vulnificus*." Environmental Microbiology **22**(10): 4133-4148.

Hernández-Cabanyero, C., E. Sanjuán, B. Fouz, D. Pajuelo, E. Vallejos-Vidal, F. E. Reyes-López and C. Amaro (2020). "The Effect of the Environmental Temperature on the Adaptation to Host in the Zoonotic Pathogen *Vibrio vulnificus*." Frontiers in microbiology **11**: 489-489.

Hernández-Cabanyero, C., C. T. Lee, V. Tolosa-Enguis, E. Sanjuán, D. Pajuelo, F. Reyes-López, L. Tort and C. Amaro (2019). "Adaptation to host in *Vibrio vulnificus*, a zoonotic pathogen that causes septicemia in fish and humans." Environmental microbiology **21**(8): 3118-3139.

Honda, T. and T. Iida (1993). "The pathogenicity of *Vibrio parahaemolyticus* and the role of the thermostable direct haemolysin and related haemolysins." Reviews in Medical Microbiology **4**(2): 106-113.

Hooper, L. V., T. Midtvedt and J. I. Gordon (2002). "How host-microbial interactions shape the nutrient environment of the mammalian intestine." Annual Review of Nutrition **22**(1): 283-307.

Hu, L., Y. Zhao and H. Xu (2022). "Trojan horse in the intestine: A review on the biotoxicity of microplastics combined environmental contaminants." Journal of Hazardous Materials **439**: 129652.

Hunt, S. M., E. M. Werner, B. Huang, M. A. Hamilton and P. S. Stewart (2004). "Hypothesis for the role of nutrient starvation in biofilm detachment." Applied and Environmental Microbiology **70**(12): 7418-7425.

Jacobs, J. M., M. Rhodes, C. W. Brown, R. R. Hood, A. Leight, W. Long and R. Wood (2014). "Modeling and forecasting the distribution of *Vibrio vulnificus* in Chesapeake Bay." Journal of Applied Microbiology **117**(5): 1312-1327.

Jamal, M., W. Ahmad, S. Andleeb, F. Jalil, M. Imran, M. A. Nawaz, T. Hussain, M. Ali, M. Rafiq and M. A. Kamil (2018). "Bacterial biofilm and associated infections." Journal of the Chinese Medical Association **81**(1): 7-11.

Jeong, H.-G. and K. J. F. Satchell (2012). "Additive Function of *Vibrio vulnificus* MARTXVv and VvhA Cytolysins Promotes Rapid Growth and Epithelial Tissue Necrosis During Intestinal Infection." PLOS Pathogens **8**(3): e1002581.

Jiao, Y., G. D. Cody, A. K. Harding, P. Wilmes, M. Schrenk, K. E. Wheeler, J. F. Banfield and M. P. Thelen (2010). "Characterization of extracellular polymeric substances from acidophilic microbial biofilms." Applied and Environmental Microbiology **76**(9): 2916-2922.

Johnson, C. N., J. C. Bowers, K. J. Griffitt, V. Molina, R. W. Clostio, S. Pei, E. Laws, R. N. Paranjpye, M. S. Strom, A. Chen, N. A. Hasan, A. Huq, N. F. Noriea, 3rd, D. J. Grimes and R. R. Colwell (2012). "Ecology of Vibrio parahaemolyticus and Vibrio vulnificus in the coastal and estuarine waters of Louisiana, Maryland, Mississippi, and Washington (United States)." Applied Environmental Microbiology **78**(20): 7249-7257.

Jones, M. K. and J. D. Oliver (2009). "*Vibrio vulnificus*: Disease and Pathogenesis." Infection and Immunity **77**(5): 1723-1733.

Joseph, L. A. and A. C. Wright (2004). "Expression of *Vibrio vulnificus* capsular polysaccharide inhibits biofilm formation." Journal of Bacteriology **186**(3): 889-893.

Kalia, V. C. (2013). "Quorum sensing inhibitors: An overview." Biotechnology Advances **31**(2): 224-245.

Kamada, N., G. Y. Chen, N. Inohara and G. Núñez (2013). "Control of pathogens and pathobionts by the gut microbiota." Nature Immunology **14**(7): 685-690.

Kamp, H. D., B. Patimalla-Dipali, D. W. Lazinski, F. Wallace-Gadsden and A. Camilli (2013). "Gene fitness landscapes of *Vibrio cholerae* at important stages of its life cycle." PLOS Pathogons **9**(12): e1003800.

Kaplan, J. B. (2010). "Biofilm dispersal: mechanisms, clinical implications, and potential therapeutic uses." Journal of Dental Research **89**(3): 205-218.

Karatan, E. and P. Watnick (2009). "Signals, Regulatory Networks, and Materials That Build and Break Bacterial Biofilms." Microbiology and Molecular Biology Reviews **73**(2): 310-347.

Karunasagar, I., R. Pai, G. R. Malathi and I. Karunasagar (1994). "Mass mortality of Penaeus monodon larvae due to antibiotic-resistant Vibrio harveyi infection." Aquaculture **128**(3): 203-209.

Kavita, K., A. Mishra and B. Jha (2013). "Extracellular polymeric substances from two biofilm forming *Vibrio* species: characterization and applications." Carbohydrate Polymers **94**(2): 882-888.

Kaysner, C. A., A. DePaola and J. Jones (2004). "Bacteriological analytical manual chapter 9: *Vibrio*." Food and Drug Administration, Maryland.[https://www. fda.

gov/food/laboratory-methods-food/bam-chapter-9-*Vibrio*]. Reviewed: December **19**: 2019.

Keswani, A., D. M. Oliver, T. Gutierrez and R. S. Quilliam (2016). "Microbial hitchhikers on marine plastic debris: Human exposure risks at bathing waters and beach environments." Marine Environmental Research **118**: 10-19.

Kesy, K., M. Labrenz, B. S. Scales, B. Kreikemeyer and S. Oberbeckmann (2021). "*Vibrio* Colonization Is Highly Dynamic in Early Microplastic-Associated Biofilms as Well as on Field-Collected Microplastics." Microorganisms **9**(1): 76.

Kesy, K., S. Oberbeckmann, B. Kreikemeyer and M. Labrenz (2019). "Spatial Environmental Heterogeneity Determines Young Biofilm Assemblages on Microplastics in Baltic Sea Mesocosms." Frontiers in Microbiology **10**(1665).

Khan, M., S. Harms Jerome, M. Marim Fernanda, L. Armon, L. Hall Cherisse, Y.-P. Liu, M. Banai, C. Oliveira Sergio, A. Splitter Gary and A. Smith Judith (2016). "The Bacterial Second Messenger Cyclic di-GMP Regulates Brucella Pathogenesis and Leads to Altered Host Immune Response." Infection and Immunity **84**(12): 3458-3470.

Kim, H.-J., J.-O. Ryu, S.-Y. Lee, E.-S. Kim and H.-Y. Kim (2015). "Multiplex PCR for detection of the *Vibrio* genus and five pathogenic *Vibrio* species with primer sets designed using comparative genomics." BMC microbiology **15**: 239-239.

Kim, M., J.-M. Park, H.-J. Um, K.-H. Lee, H. Kim, J. Min and Y.-H. Kim (2011). "The antifouling potentiality of galactosamine characterized from *Vibrio vulnificus* exopolysaccharide." Biofouling **27**(8): 851-857.

Kirstein, I. V., S. Kirmizi, A. Wichels, A. Garin-Fernandez, R. Erler, M. Löder and G. Gerdts (2016). "Dangerous hitchhikers? Evidence for potentially pathogenic *Vibrio* spp. on microplastic particles." Marine Environmental Research **120**: 1-8.

Kochkodan, V., S. Tsarenko, N. Potapchenko, V. Kosinova and V. Goncharuk (2008). "Adhesion of microorganisms to polymer membranes: a photobactericidal effect of surface treatment with TiO2." Desalination **220**(1): 380-385.

Koelmans, A. A., T. Gouin, R. Thompson, N. Wallace and C. Arthur (2014). "Plastics in the marine environment." Environmental Toxicology and Chemistry **33**(1): 5-10.

Koestler, B. J. and C. M. Waters (2014). "Bile acids and bicarbonate inversely regulate intracellular cyclic di-GMP in *Vibrio cholerae*." Infection Immunity **82**(7): 3002-3014.

Koo, J., A. DePaola and D. L. Marshall (2000). "Effect of Simulated Gastric Fluid and Bile on Survival of *Vibrio vulnificus* and *Vibrio vulnificus* Phage†." Journal of Food Protection **63**(12): 1665-1669.

Krasowska, A. and K. Sigler (2014). "How microorganisms use hydrophobicity and what does this mean for human needs?" Frontiers Cell Infection Microbiology **4**: 112.

Kwaszewska, A. K., A. Brewczynska and E. M. Szewczyk (2006). "Hydrophobicity and biofilm formation of lipophilic skin corynebacteria." Polish Journal of Microbiology **55**(3): 189-193.

Lage, O. M., & Graça, A. P. (2016). Biofilms: an extra coat on macroalgae. In Algae-Organisms for Imminent Biotechnology. IntechOpen.

Lambert, S., C. Sinclair and A. Boxall (2014). Occurrence, degradation, and effect of polymer-based materials in the environment. Reviews of Environmental Contamination and Toxicology, 227, 1-53.

Lami, R. (2019). Chapter 3 - Quorum Sensing in Marine Biofilms and Environments. Quorum Sensing. G. Tommonaro, Academic Press**:** 55-96.

LaSarre, B. and M. J. Federle (2013). "Exploiting quorum sensing to confuse bacterial pathogens." Microbiology and molecular biology reviews : MMBR **77**(1): 73-111.

Laverty, A. L., S. Primpke, C. Lorenz, G. Gerdts and F. C. Dobbs (2020). "Bacterial biofilms colonizing plastics in estuarine waters, with an emphasis on *Vibrio* spp. and their antibacterial resistance." PLOS ONE **15**(8): e0237704.

Lee, K.-J., J.-A. Kim, W. Hwang, S.-J. Park and K.-H. Lee (2013). "Role of capsular polysaccharide (CPS) in biofilm formation and regulation of CPS production by quorum-sensing in *Vibrio vulnificus*." Molecular Microbiology **90**(4): 841-857.

Leighton, R. E., K. E. Correa Vélez, L. Xiong, A. G. Creech, K. P. Amirichetty, G. K. Anderson, G. Cai, R. S. Norman and A. W. Decho (2023). "*Vibrio parahaemolyticus* and *Vibrio vulnificus in vitro* colonization on plastics influenced by temperature and strain variability." Frontiers in Microbiology **13**.

Li, W., J. J. Wang, H. Qian, L. Tan, Z. Zhang, H. Liu, Y. Pan and Y. Zhao (2020). "Insights Into the Role of Extracellular DNA and Extracellular Proteins in Biofilm Formation of *Vibrio parahaemolyticus*." Frontiers in Microbiology **11**(813).

Maquart, P.-O., Y. Froehlich and S. Boyer (2022). "Plastic pollution and infectious diseases." The Lancet Planetary Health **6**(10): e842-e845.

Marks, L. R., B. A. Davidson, P. R. Knight and A. P. Hakansson (2013). "Interkingdom signaling induces *Streptococcus pneumoniae* biofilm dispersion and transition from asymptomatic colonization to disease." mBio **4**(4): e00438-00413.

Marx, J., R. Hockberger and R. Walls (2013). Rosen's Emergency Medicine-Concepts and Clinical Practice E-Book: 2-Volume Set, Elsevier Health Sciences.

Matyar, F. (2012). "Antibiotic and Heavy Metal Resistance in Bacteria Isolated from the Eastern Mediterranean Sea Coast." Bulletin of Environmental Contamination and Toxicology **89**(3): 551-556.

McDougald, D., S. A. Rice, N. Barraud, P. D. Steinberg and S. Kjelleberg (2012). "Should we stay or should we go: mechanisms and ecological consequences for biofilm dispersal." Nature Reviews Microbiology **10**(1): 39-50.

Mead, P. S., L. Slutsker, V. Dietz, L. F. McCaig, J. S. Bresee, C. Shapiro, P. M. Griffin and R. V. Tauxe (1999). "Food-related illness and death in the United States." Emerging Infectious Diseases **5**(5): 607-625.

Mizan, M. F. R., I. K. Jahid, M. Kim, K.-H. Lee, T. J. Kim and S.-D. Ha (2016). "Variability in biofilm formation correlates with hydrophobicity and quorum sensing among *Vibrio parahaemolyticus* isolates from food contact surfaces and the distribution of the genes involved in biofilm formation." Biofouling **32**(4): 497-509.

Moffitt, C. M. and L. Cajas-Cano (2014). "Blue growth: the 2014 FAO state of world fisheries and aquaculture." Fisheries (Bethesda) **39**(11): 552-553.

Motes, M., A. DePaola, D. Cook, J. Veazey, J. Hunsucker, W. Garthright, R. Blodgett and S. Chirtel (1998). "Influence of water temperature and salinity on *Vibrio*

vulnificus in northern gulf and atlantic coast oysters (Crassostrea virginica)." Applied Environmental Microbiology **64**(4): 1459-1465.

Motta, J.-P., J. L. Wallace, A. G. Buret, C. Deraison and N. Vergnolle (2021). "Gastrointestinal biofilms in health and disease." Nature Reviews Gastroenterology & Hepatology **18**(5): 314-334.

Nair, H. A. S., S. Subramoni, W. H. Poh, N. T. B. Hasnuddin, M. Tay, M. Givskov, T. Tolker-Nielsen, S. Kjelleberg, D. McDougald and S. A. Rice (2021). "Carbon starvation of *Pseudomonas aeruginosa* biofilms selects for dispersal insensitive mutants." BMC Microbiology **21**(1): 255.

Nakanishi, E. Y., J. H. Palacios, S. Godbout and S. Fournel (2021). "Interaction between Biofilm Formation, Surface Material and Cleanability Considering Different Materials Used in Pig Facilities—An Overview." Sustainability **13**(11): 5836.

Nicole, W. (2021). "Microplastics in Seafood: How Much Are People Eating?" Environmental Health Perspectives **129**(3): 034001.

Nilsson, W. B., R. N. Paranjype, A. DePaola and M. S. Strom (2003). "Sequence polymorphism of the 16S rRNA gene of *Vibrio vulnificus* is a possible indicator of strain virulence." Journal of Clinical Microbiology **41**(1): 442-446.

Nwanyanwu, C., C. Alisi, C. Nweke and J. Orji (2012). "Cell surface properties of phenol-utilizing bacteria isolated from petroleum refinery wastewater." Journal of Research in Biology **2**: 383-391.

O'Neil, J. M., T. W. Davis, M. A. Burford and C. J. Gobler (2012). "The rise of harmful cyanobacteria blooms: the potential roles of eutrophication and climate change." Harmful Algae **14**: 313-334.

O'Toole, G. A. (2011). "Microtiter dish biofilm formation assay." Journal of Visualized Experiments : JoVE(47): 2437.

O'Toole, G., H. B. Kaplan and R. Kolter (2000). "Biofilm formation as microbial development." Annual Review of Microbiology **54**: 49.

Oberbeckmann, S., M. G. J. Lder and M. Labrenz (2015). "Marine microplastic-associated biofilms a review." Environmental Chemistry 12(5): 551-562.

Obuekwe, C. O., Z. K. Al-Jadi and E. S. Al-Saleh (2009). "Hydrocarbon degradation in relation to cell-surface hydrophobicity among bacterial hydrocarbon degraders from petroleum-contaminated Kuwait desert environment." International Biodeterioration & Biodegradation **63**(3): 273-279.

Odeyemi, O. A. and A. Ahmad (2017). "Population dynamics, antibiotics resistance and biofilm formation of Aeromonas and *Vibrio* species isolated from aquatic sources in Northern Malaysia." Microbial Pathogenesis **103**: 178-185.

Oliver, J. D. (2015). "The biology of *Vibrio vulnificus*." Microbiology spectrum **3**(3): 3.3. 01.

Oliver, J. D. and R. R. Colwell (1973). "Extractable lipids of gram-negative marine bacteria: phospholipid composition." Journal of Bacteriology **114**(3): 897-908.

Oliver, J. D., C. Pruzzo, L. Vezzulli and J. B. Kaper (2012). *Vibrio* Species. Food Microbiology**:** 401-439.

Pagán, R. and D. García-Gonzalo (2015). "Influence of environmental factors on bacterial biofilm formation in the food industry: a review." Postdoc j.(ART-2015-95845).

Parry, M. L., O. F. Canziani, J. P. Palutikof, P. J. Van Der Linden and C. E. Hanson (2007). "IPCC, 2007: climate change 2007: impacts, adaptation and vulnerability. Contribution of working group II to the fourth assessment report of the intergovernmental panel on climate change." Cambridge University Press, Cambridge, UK.

Pedrotti, M. L., A. L. de Figueiredo Lacerda, S. Petit, J. F. Ghiglione and G. Gorsky (2022). "Vibrio spp and other potential pathogenic bacteria associated to microfibers in the North-Western Mediterranean Sea." PLOS ONE **17**(11): e0275284.

Petrova, O. E. and K. Sauer (2016). "Escaping the biofilm in more than one way: desorption, detachment or dispersion." Current Opinions in Microbiology **30**: 67-78.

Portillo, M. E., M. Salvadó, A. Trampuz, V. Plasencia, M. Rodriguez-Villasante, L. Sorli, L. Puig and J. P. Horcajada (2013). "Sonication versus vortexing of implants for diagnosis of prosthetic joint infection." Journal of Clinical Microbiology **51**(2): 591-594.

Prakash, B., B. M. Veeregowda and G. Krishnappa (2003). "Biofilms: A survival strategy of bacteria." Current Science **85**(9): 1299-1307.

Purcell, E. B., R. W. McKee, D. S. Courson, E. M. Garrett, S. M. McBride, R. E. Cheney and R. Tamayo (2017). "A Nutrient-Regulated Cyclic Diguanylate Phosphodiesterase Controls *Clostridium difficile* Biofilm and Toxin Production during Stationary Phase." Infection and Immunity **85**(9): e00347-00317.

Purevdorj-Gage, B., W. Costerton and P. Stoodley (2005). "Phenotypic differentiation and seeding dispersal in non-mucoid and mucoid *Pseudomonas aeruginosa* biofilms." Microbiology **151**(5): 1569-1576.

Qin, X., F. J. Caputo, D. Z. Xu and E. A. Deitch (2008). "Hydrophobicity of mucosal surface and its relationship to gut barrier function." Shock **29**(3): 372-376.

Raghul, S., S. Bhat, M. Chandrasekaran, V. Francis and E. Thachil (2014). "Biodegradation of polyvinyl alcohol-low linear density polyethylene-blended plastic film by consortium of marine benthic *Vibrio*s." International Journal of Environmental Science and Technology **11**(7): 1827-1834.

Raven, J. A., C. J. Gobler and P. J. Hansen (2020). "Dynamic CO2 and pH levels in coastal, estuarine, and inland waters: Theoretical and observed effects on harmful algal blooms." Harmful Algae **91**: 101594.

Reidl, J. and K. E. Klose (2002). "*Vibrio cholerae* and cholera: out of the water and into the host." FEMS Microbiology Reviews **26**(2): 125-139.

Reifsteck, F., S. Wee and B. Wilkinson (1987). "Hydrophobicity—hydrophilicity of staphylococci." Journal of Medical Microbiology **24**(1): 65-73.

Reisser, J., J. Shaw, G. Hallegraeff, M. Proietti, D. K. A. Barnes, M. Thums, C. Wilcox, B. D. Hardesty and C. Pattiaratchi (2014). "Millimeter-sized marine plastics: a new pelagic habitat for microorganisms and invertebrates." PLOS ONE **9**(6): e100289-e100289.

Riss, T. L., R. A. Moravec, A. L. Niles, S. Duellman, H. A. Benink, T. J. Worzella and L. Minor (2004). Cell Viability Assays. Assay Guidance Manual. S. Markossian, G.

S. Sittampalam, A. Grossman et al. Bethesda (MD), Eli Lilly & Company and the National Center for Advancing Translational Sciences.

Römling, U., M. Y. Galperin and M. Gomelsky (2013). "Cyclic di-GMP: the first 25 years of a universal bacterial second messenger." Microbiology and Molecular Biology Reviews **77**(1): 1-52.

Rosenberg, M. (1984). "Bacterial adherence to hydrocarbons: a useful technique for studying cell surface hydrophobicity." FEMS Microbiology Letters **22**(3): 289-295.

Rumbaugh, K. P. and K. Sauer (2020). "Biofilm dispersion." Nature Reviews Microbiology **18**(10): 571-586.

Rutherford, S. T. and B. L. Bassler (2012). "Bacterial quorum sensing: its role in virulence and possibilities for its control." Cold Spring Harbor Perspectives in Medicine **2**(11): a012427.

Sauer, K., M. Cullen, A. Rickard, L. Zeef, D. G. Davies and P. Gilbert (2004). "Characterization of nutrient-induced dispersion in *Pseudomonas aeruginosa* PAO1 biofilm." Journal of Bacteriology **186**(21): 7312-7326.

Sauer, K., P. Stoodley, D. M. Goeres, L. Hall-Stoodley, M. Burmølle, P. S. Stewart and T. Bjarnsholt (2022). "The biofilm life cycle: expanding the conceptual model of biofilm formation." Nature Reviews Microbiology **20**(10): 608-620.

Schroeder, M., B. D. Brooks and A. E. Brooks (2017). "The Complex Relationship between Virulence and Antibiotic Resistance." Genes **8**(1): 39.

Sheikh, H. I., M. Najiah, A. Fadhlina, A. A. Laith, M. M. Nor, K. C. A. Jalal and N. A. Kasan (2022). "Temperature Upshift Mostly but not Always Enhances the Growth of *Vibrio* Species: A Systematic Review." Frontiers in Marine Science **9**.

Singh, P. K., S. Bartalomej, R. Hartmann, H. Jeckel, L. Vidakovic, C. D. Nadell and K. Drescher (2017). "*Vibrio cholerae* Combines Individual and Collective Sensing to Trigger Biofilm Dispersal." Current Biology **27**(21): 3359-3366.e3357.

Song, X., Y. Ma, J. Fu, A. Zhao, Z. Guo, P. K. Malakar, Y. Pan and Y. Zhao (2017). "Effect of temperature on pathogenic and non-pathogenic *Vibrio parahaemolyticus* biofilm formation." Food Control **73**: 485-491.

Stewart, P. S. and J. William Costerton (2001). "Antibiotic resistance of bacteria in biofilms." The Lancet **358**(9276): 135-138.

Strom, M. S. and R. N. Paranjpye (2000). "Epidemiology and pathogenesis of *Vibrio vulnificus*." Microbes and Infection **2**(2): 177-188.

Sullivan, T. J. and J. E. Neigel (2018). "Effects of temperature and salinity on prevalence and intensity of infection of blue crabs, Callinectes sapidus, by *Vibrio cholerae*, *V. parahaemolyticus*, and *V. vulnificus* in Louisiana." Journal of Invertebrate Pathology **151**: 82-90.

Takemura, A. F., D. M. Chien and M. F. Polz (2014). "Associations and dynamics of *Vibrionaceae* in the environment, from the genus to the population level." Frontiers in Microbiology **5**: 38.

Tang, X., Y. Zhao, X. Sun, J. Xie, Y. Pan and P. K. Malakar (2015). "Predictive model of *Vibrio parahaemolyticus* O3: K6 growth on cooked Litopenaeus vannamei." Annals of Microbiology **65**(1): 487-493.

Tavelli, R., M. Callens, C. Grootaert, M. F. Abdallah and A. Rajkovic (2022). "Foodborne pathogens in the plastisphere: Can microplastics in the food chain threaten microbial food safety?" Trends in Food Science & Technology **129**: 1-10.

Tiruvayipati, S. and S. Bhassu (2016). "Host, pathogen and the environment: the case of Macrobrachium rosenbergii, *Vibrio parahaemolyticus* and magnesium." Gut Pathogens **8**(1): 15.

Tischler, A. H., L. Lie, C. M. Thompson and K. L. Visick (2018). "Discovery of Calcium as a Biofilm-Promoting Signal for *Vibrio fischeri* Reveals New Phenotypes and Underlying Regulatory Complexity." Journal of Bacteriology **200**(15): e00016-00018.

Townsley, L. and F. H. Yildiz (2015). "Temperature affects c-di-GMP signalling and biofilm formation in *Vibrio cholerae*." Environmental Microbiology **17**(11): 4290-4305.

Toyofuku, M., T. Inaba, T. Kiyokawa, N. Obana, Y. Yawata and N. Nomura (2016). "Environmental factors that shape biofilm formation." Bioscience, Biotechnology, and Biochemistry **80**(1): 7-12

Uppuluri, P., M. Acosta Zaldívar, M. Z. Anderson, M. J. Dunn, J. Berman, J. L. Lopez Ribot and J. R. Köhler (2018). "*Candida albicans* dispersed cells are developmentally distinct from biofilm and planktonic cells." mBio **9**(4): e01338-01318.

Valentini, M. and A. Filloux (2016). "Biofilms and Cyclic di-GMP (c-di-GMP) Signaling: Lessons from *Pseudomonas aeruginosa* and Other Bacteria." Journal of Biological Chemistry **291**(24): 12547-12555.

Valquier-Flynn, H., C. L. Wilson, A. E. Holmes and C. D. Wentworth (2017). "Growth Rate of *Pseudomonas aeruginosa* Biofilms on Slippery Butyl Methacrylate-Co-Ethylene Dimethacrylate (BMA-EDMA), Glass and Polycarbonate Surfaces." Journal of Biotechnology & Biomaterials **7**(4): 274.

Van Sebille, E., C. Wilcox, L. Lebreton, N. Maximenko, B. D. Hardesty, J. A. Van Franeker, M. Eriksen, D. Siegel, F. Galgani and K. L. Law (2015). "A global inventory of small floating plastic debris." Environmental Research Letters **10**(12): 124006.

Vezzulli, L., C. Grande, P. C. Reid, P. Hélaouët, M. Edwards, M. G. Höfle, I. Brettar, R. R. Colwell and C. Pruzzo (2016). "Climate influence on *Vibrio* and associated human diseases during the past half-century in the coastal North Atlantic." Proceedings of the National Academy of Sciences **113**(34): E5062-E5071.

Vickery, M. C., W. B. Nilsson, M. S. Strom, J. L. Nordstrom and A. DePaola (2007). "A real-time PCR assay for the rapid determination of 16S rRNA genotype in *Vibrio vulnificus*." Journal of Microbiological Methods **68**(2): 376-384.

Villeneuve, A., A. Bouchez and B. Montuelle (2011). "In situ interactions between the effects of season, current velocity and pollution on a river biofilm." Freshwater Biology **56**(11): 2245-2259.

Viršek, M. K., M. N. Lovšin, Š. Koren, A. Kržan and M. Peterlin (2017). "Microplastics as a vector for the transport of the bacterial fish pathogen species Aeromonas salmonicida." Marine Pollution Bulletin **125**(1): 301-309.

Visser, P. M., J. M. Verspagen, G. Sandrini, L. J. Stal, H. C. Matthijs, T. W. Davis, H. W. Paerl and J. Huisman (2016). "How rising CO2 and global warming may stimulate harmful cyanobacterial blooms." Harmful Algae **54**: 145-159.

Vu, B., M. Chen, R. J. Crawford and E. P. Ivanova (2009). "Bacterial extracellular polysaccharides involved in biofilm formation." Molecules **14**(7): 2535-2554.

Wagner, M., N. P. Ivleva, C. Haisch, R. Niessner and H. Horn (2009). "Combined use of confocal laser scanning microscopy (CLSM) and Raman microscopy (RM): Investigations on EPS–Matrix." Water Research **43**(1): 63-76.

Waite, H. R., M. J. Donnelly and L. J. Walters (2018). "Quantity and types of microplastics in the organic tissues of the eastern oyster *Crassostrea virginica* and Atlantic mud crab *Panopeus herbstii* from a Florida estuary." Marine Pollution Bulletin **129**(1): 179-185

Wang, R., B. A. Khan, G. Y. Cheung, T.-H. L. Bach, M. Jameson-Lee, K.-F. Kong, S. Y. Queck and M. Otto (2011). "*Staphylococcus epidermidis* surfactant peptides promote biofilm maturation and dissemination of biofilm-associated infection in mice." The Journal of Clinical Investigation **121**(1): 238-248.

Wang, S., Z. Zhang, P. K. Malakar, Y. Pan and Y. Zhao (2019). "The Fate of Bacteria in Human Digestive Fluids: A New Perspective Into the Pathogenesis of *Vibrio parahaemolyticus*." Frontiers in Microbiology **10**.

Wang, Y., Y. Zhao, Y. Pan and H. Liu (2020). "Comparison on the Growth Variability of *Vibrio parahaemolyticus* Coupled With Strain Sources and Genotypes Analyses in Simulated Gastric Digestion Fluids." Frontiers in Microbiology **11**(212).

Ward, C. S., C.-M. Yung, K. M. Davis, S. K. Blinebry, T. C. Williams, Z. I. Johnson and D. E. Hunt (2017). "Annual community patterns are driven by seasonal switching between closely related marine bacteria." The ISME Journal **11**(6): 1412-1422.

Ward, J. E. and D. J. Kach (2009). "Marine aggregates facilitate ingestion of nanoparticles by suspension-feeding bivalves." Marine Environmental Research **68**(3): 137-142.

Westrich, J. R., A. M. Ebling, W. M. Landing, J. L. Joyner, K. M. Kemp, D. W. Griffin and E. K. Lipp (2016). "Saharan dust nutrients promote *Vibrio* bloom formation in marine surface waters." Proceedings of the National Academy of Sciences **113**(21): 5964-5969.

Whitehead, P. G., R. L. Wilby, R. W. Battarbee, M. Kernan and A. J. Wade (2009). "A review of the potential impacts of climate change on surface water quality." Hydrological Sciences Journal **54**(1): 101-123.

Whiting, R. C. and M. H. Golden (2002). "Variation among *Escherichia coli* O157:H7 strains relative to their growth, survival, thermal inactivation, and toxin production in broth." International Journal of Food Microbiology **75**(1): 127-133.

Wong, H.-C. and C.-N. Chang (2005). "Hydrophobicity, Cell Adherence, Cytotoxicity, and Enterotoxigenicity of Starved *Vibrio parahaemolyticus*." Journal of Food Protection **68**(1): 154-156.

Wong, K. K. and P. M. Griffin (2018). 159 - Other *Vibrio* Species. Principles and Practice of Pediatric Infectious Diseases (Fifth Edition). S. S. Long, C. G. Prober and M. Fischer, Elsevier**:** 879-881.e871.

Wright, S. L., R. C. Thompson and T. S. Galloway (2013). "The physical impacts of microplastics on marine organisms: a review." Environmental Pollution **178**: 483-492.

Wu, W., Z. Jing, X. Yu, Q. Yang, J. Sun, C. Liu, W. Zhang, L. Zeng and H. He (2019). "Recent advances in screening aquatic products for *Vibrio* spp." TrAC Trends in Analytical Chemistry **111**: 239-251.

Wu, Z., Y. Wu, H. Gao, X. He, Q. Yao, Z. Yang, J. Zhou, L. Ji, J. Gao, X. Jia, Y. Dou, X. Wang and P. Shao (2022). "Identification and whole-genome sequencing analysis of *Vibrio vulnificus* strains causing pearl gentian grouper disease in China." BMC Microbiology **22**(1): 200.

Xiong, X., J. Kong, D. Qi, X. Xiong, Y. Liu and X. Cui (2022). "Presence, formation, and elimination of foodborne pathogen persisters." JSFA Reports **2**(1): 4-16.

Yan, M., W. Li, X. Chen, Y. He, X. Zhang and H. Gong (2021). "A preliminary study of the association between colonization of microorganism on microplastics and intestinal microbiota in shrimp under natural conditions." Journal of Hazardous Materials **408**: 124882.

Yang, Y., W. Liu, Z. Zhang, H.-P. Grossart and G. M. Gadd (2020). "Microplastics provide new microbial niches in aquatic environments." Applied Microbiology and Biotechnology **104**(15): 6501-6511.

Yildiz, F. H. (2008). "Cyclic dimeric GMP signaling and regulation of surface-associated developmental programs." Journal of Bacteriology **190**(3): 781-783.

Zeng, Z., L. Qian, L. Cao, H. Tan, Y. Huang, X. Xue, Y. Shen and S. Zhou (2008). "Virtual screening for novel quorum sensing inhibitors to eradicate biofilm formation of *Pseudomonas aeruginosa*." Applied Microbiology and Biotechnology **79**(1): 119-126

Zettler, E., T. Mincer and L. Amaral-Zettler (2013). "Life in the "Plastisphere": Microbial Communities on Plastic Marine Debris." Environmental Science & Technology **47**.

APPENDIX A:

CHAPTER 1 SUPPLEMENTARY MATERIAL

Permission to Reprint:

Supplementary Data

Bacterial Isolation and Identification

V. vulnificus strain vv155 was isolated from seawater samples from a past study and was provided as a gift from NOAA to be used as the *V. vulnificus* environmental strain in this study. Seawater samples were collected in 1L sterile, polypropylene containers and diluted and filtered through 0.22µm nitrocellulose membrane filter. Filters were then placed on two types of selective media, CPC+ and CHROMagar™ *Vibrio*. Presumptive *V. vulnificus* strains were then identified by species using a TaqMan based real-time PCR targeting the hemolysin *A* gene (vvhA). The characterization of each isolate as type A (environmental), Type B (clinical) or Type AB was performed using qPCR according to a protocol developed by Vickery et al., 2007. Dr. Joanna Mort (James Madison University), Dr. Jerold Dickerson (James Madison University) and Dr. Janet Moore (NOAA) all contributed to this past isolation and characterization study.

V. parahaemolyticus strain vpC12 was isolated from seawater samples to be used as the *V. parahaemolyticus* environmental strain for this study. Water samples (800 mL) were collected using an ISCO 6700 autosampler (ISCO, Lincoln, NE, USA) for 24 hours during low and high tides at the Oyster Landing Dock at the Baruch Marine Research Laboratory, Georgetown, SC (33°20'58" N 79°11'20" W). Water samples from each tidal period were combined and homogenized. One liter of the combined sample was filtered through a 0.22µm polyethersulfone (PES) membrane filter (Thermo Sci., Waltham, MA,

USA) to concentrate the microbial community in the 0.22µm filter. The microbial community collected in the filter was reconstituted in 20 mL of the unfiltered combined samples. The reconstituted sample was diluted using serial dilutions. From each dilution, 550µL of the sample was grown in selective and differential media, thiosulfate citrate bile sucrose (TCBS, Sigma-Aldrich, St. Louis, MO, USA), and CHROMagar™ *Vibrio* (Kanto Chemical, Chuo-Ku, Tokyo, Japan). The green colonies in TCBS and the purple/mauve colonies in CHROMagar™ *Vibrio* were identified as presumptive *Vibrio*. All presumptive *Vibrio* strains then were identified by species using multiplex polymerase chain reaction (PCR) using primers developed by Kim et al., 2015 to identify the *tlh* species marker gene. [Accession number: OP912877]

Table A.1 Effect of temperature on mean biofilm production[1] per mm^2 on different plastic surface types[2] by *V. parahaemolyticus* and *V. vulnificus* individual strains compared to glass and 25°C.

Species	**Strain**	**Surface Type**	**25°C (± SD)**	**30°C (± SD)**	**35°C (± SD)**	**Surface *p*-value**
V. parahaemolyticus	ATCC17802	GL	3.35E-04 (1.58E-04)	6.84E-04 (2.35E-04)	1.32E-03 (6.67E-04)	
		LDPE	2.56E-03* (1.95E-03)	5.98E-03*$ (1.36E-03)	5.75E-03*$ (7.23E-04)	≤0.01
		PP	1.87E-03* (1.84E-03)	6.04E-03*$ (8.07E-04)	5.83E-03*$ (4.71E-04)	≤0.01

		PS	7.27E-04* (6.91E-04)	2.02E-03*$ (3.14E-04)	1.15E-03*$ (3.86E-04)	≤0.05
Temperature *p*-value				≤0.01	≤0.01	
V. parahaemolyticus	ATCC43996	GL	4.08E-04 (2.89E-04)	2.61E-04 (1.60E-04)	2.05E-04 (1.27E-04)	
		LDPE	1.31E-03* (1.53E-04)	7.24E-04*x (3.79E-04)	6.87E-04*x (4.77E-04)	≤0.01
		PP	8.91E-04* (8.00E-04)	3.40E-04*x (1.44E-04)	3.75E-04*x (1.42E-04)	≤0.01
		PS	1.01E-03* (9.21E-04)	8.46E-04*x (2.07E-04)	6.84E-04*x (2.84E-04)	≤0.01
Temperature *p*-value				≤0.01	≤0.01	
V. parahaemolyticus	vpC12	GL	3.09E-04 (2.08E-04)	3.06E-04 (1.46E-04)	6.99E-04 (3.06E-04)	
		LDPE	8.06E-04 (3.92E-04)	1.58E-04x (5.97E-05)	6.40E-04 (1.37E-04)	0.86
		PP	5.65E-04 (3.66E-04)	7.88E-05x (6.34E-05)	5.37E-04 (8.90E-05)	0.42
		PS	9.02E-04 (2.63E-04)	4.34E-04x (2.63E-04)	7.00E-04 (2.95E-05)	0.28
Temperature *p*-value				≤0.05	0.84	

V. vulnificus	ATCC27562	GL	2.31E-03 (5.94E-04)	1.37E-03 (8.01E-04)	6.41E-04 (2.23E-04)	
		LDPE	2.08E-03 (2.05E-03)	8.49E-04x (6.25E-04)	1.38E-03x (6.46E-04)	0.99
		PP	1.93E-03 (1.52E-03)	4.23E-04x (2.13E-04)	5.24E-04x (3.12E-04)	0.46
		PS	3.67E-03 (1.09E-03)	2.18E-03x (6.19E-04)	1.53E-03x (1.94E-04)	0.31
Temperature *p*-value				≤0.05	≤0.05	
V. vulnificus	ATCC33147	GL	1.96E-03 (5.28E-04)	4.02E-04 (1.30E-04)	2.59E-04 (8.0E-05)	
		LDPE	2.01E-03 (1.63E-03)	1.20E-03x (5.12E-04)	1.24E-03x (3.13E-04)	0.09
		PP	1.18E-03 (8.50E-04)	7.34E-04x (4.99E-04)	3.49E-04x (2.81E-04)	0.99
		PS	4.00E-03* (1.31E-03)	1.59E-03*x (3.53E-04)	1.08E-03*x (4.40E-04)	≤0.05
Temperature *p*-value				≤0.05	≤0.01	
V. vulnificus	vv155	GL	2.90E-03 (3.80E-04)	1.18E-03 (4.33E-04)	1.95E-03 (3.33E-04)	
		LDPE	4.66E-03 (1.68E-03)	3.25E-03 (5.19E-04)	4.31E-03 (7.55E-04)	0.06

	PP	2.27E-03 (1.17E-03)	2.75E-03 (1.60E-03)	2.35E-03 (1.75E-04)	0.99
	PS	5.09E-03* (1.62E-03)	4.54E-03* (1.14E-03)	3.15E-03* (2.43E-04)	≤0.05
Temperature *p*-value			0.34	0.54	

[1]Optical density at 570 nm
[2]Biomass values divided by total coupon surface area (405 mm^2)
(± SD) Standard deviation
(*) Significant increase of biofilm production on plastic surface type compared to glass
($) Significant increase of biofilm production on surface at this temperature compared to 25°C
(x) Significant decrease of biofilm production on surface at this temperature compared to 25°C

Table A.2 Statistical comparison of *V. parahaemolyticus* and *V. vulnificus* animal and seawater isolates' biofilm production compared to human isolated strains

Species	**Isolation Source**	**Strain**	**Coefficient**	***p***
V. parahaemolyticus	Animal	ATCC43996	-0.89*	≤0.001
	Seawater	vpC12	-0.94*	≤0.001
V. vulnificus	Animal	ATCC33147	-0.09	0.99
	Seawater	vv155	0.65*	≤0.001

*Significant increase (+) /decrease (-) in biofilm production

Table A.3 Statistical comparison of *V. parahaemolyticus* biofilm production on different surface types compared to glass.

Species	Surface Type	Coefficient	*p*
V. parahaemolyticus	LDPE	0.63	0.29
	PP	0.53	0.72
	PS	0.17	0.99

*Significant increase (+) /decrease (-) in biofilm production

Table A.4 Statistical comparison of *V. vulnificus* biofilm production on different surface types compared to glass.

Species	Surface Type	Coefficient	*p*
V. vulnificus	LDPE	0.35	0.14
	PP	-0.02	0.99
	PS	0.62*	$\leq$0.001

*Significant increase (+) /decrease (-) in biofilm production

Table A.5 Statistical comparison of *V. parahaemolyticus* and *V. vulnificus* biofilm production at higher temperatures (30, 35°C) compared to lower temperature (25°C).

Species	Temperature	Coefficient	*p*
V. parahaemolyticus	30°C	0.20	0.99
	35°C	0.23	0.99

V. vulnificus	30°C	-0.48*	≤0.01
	35°C	-0.51*	≤0.01

*Significant increase (+) /decrease (-) in biofilm production

Table A.6 Effect of temperature on *V. parahaemolyticus* and *V. vulnificus* individual strain CFUs[1] per mm^2 on different plastic surface types[2] by compared to glass and 25°C.

Species	**Strain**	**Surface Type**	**25°C (± SD)**	**30°C (± SD)**	**35°C (± SD)**	**Surface *p*-value**
V. parahaemolyticus	ATCC17802	GL	2.31 (1.42)	4.23 (1.01)	3.16 (2.41)	
		LDPE	3.81* (2.24)	4.23*$ (3.05)	4.31*$ (3.21)	≤0.001
		PP	3.36* (1.79)	4.18*$ (3.09)	4.31*$ (3.59)	≤0.001
		PS	3.56* (2.15)	3.05*$ (3.35)	3.88*$ (2.87)	≤0.01
Temperature *p*-value				≤0.05	≤0.01	
V. parahaemolyticus	ATCC43996	GL	2.97 (1.85)	3.28 (2.40)	2.60 (1.56)	
		LDPE	3.76 (2.41)	3.39 (2.44)	3.36 (2.06)	0.19
		PP	3.43 (2.72)	2.57 (2.39)	3.26 (2.39)	0.35
		PS	3.73 (3.06)	2.55 (1.48)	2.75 (1.66)	0.99
Temperature *p*-value				0.20	0.12	

V. parahaemolyticus	vpC12	GL	2.54 (1.43)	3.06 (1.50)	3.31 (2.37)	
		LDPE	3.98 (3.40)	2.39 (2.53)	2.97 (2.23)	0.76
		PP	3.65 (2.58)	3.06 (1.51)	2.53 (1.12)	0.99
		PS	3.73 (2.54)	4.23 (1.90)	2.97 (2.23)	0.99
Temperature *p*-value				0.13	0.29	
V. vulnificus	ATCC27562	GL	4.16 (3.22)	3.98 (3.31)	2.78 (1.78)	
		LDPE	3.44 (2.77)	3.59 (2.88)	4.02 (3.42)	0.99
		PP	3.73 (2.82)	3.12 (1.94)	3.95 (3.21)	0.99
		PS	4.19 (3.58)	4.08 (2.63)	3.67 (3.05)	0.99
Temperature *p*-value				0.99	0.96	
V. vulnificus	ATCC33147	GL	3.53 (2.53)	2.27 (1.54)	2.45 (1.64)	
		LDPE	4.71* (3.37)	4.49* (3.93)	3.75* (2.37)	$\leq$0.05
		PP	2.31 (1.03)	2.28 (1.71)	2.78 (1.80)	0.99
		PS	4.56 (3.65)	3.57 (2.56)	3.72 (2.78)	0.06
Temperature *p*-value				0.18	0.18	

V. vulnificus	vv155	GL	3.50 (3.24)	4.34 (3.49)	3.87 (3.55)	
		LDPE	3.42 (3.16)	4.40 (3.32)	4.75 (3.79)	0.99
		PP	4.07 (3.15)	3.71 (2.30)	4.61 (3.67)	0.99
		PS	3.52 (3.63)	4.76 (3.38)	4.57 (4.25)	0.99
Temperature *p*-value				0.13	0.07	

[1]CFU values were log transformed
[2]CFU values divided by total coupon surface area (405 mm^2)
(± SD) Standard deviation
(*) Significant increase of CFUs on plastic surface type compared to glass
($) Significant increase of CFUs on this surface at this temperature compared to 25°C

Table A.7 Statistical comparison of *V. parahaemolyticus* and *V. vulnificus* animal and water isolates' CFUs compared to human isolated strains.

Species	**Isolation Source**	**Strain**	**Coefficient**	***p***
V. parahaemolyticus	Animal	ATCC43996	-2.90E+06*	≤0.01
	Seawater	vpC12	-2.85E+06*	≤0.01
V. vulnificus	Animal	ATCC33147	1.63E+06	0.99
	Seawater	vv155	6.18E+06*	≤0.05

*Significant increase (+) /decrease (-) in CFU concentration

Table A.8 Statistical comparison of *V. parahaemolyticus* CFUs on different surface types compared to glass.

Species	Surface Type	Coefficient	*p*
V. parahaemolyticus	LDPE	2.61E+06	0.14
	PP	1.98E+06	0.13
	PS	1.48E+06	0.42

Table A.9 Statistical comparison of *V. vulnificus* CFUs on different surface types compared to glass.

Species	Surface Type	Coefficient	*p*
V. vulnificus	LDPE	5.78E+06	0.99
	PP	5.96E+05	0.99
	PS	5.16E+06	0.99

Table A.10 Statistical comparison of *V. parahaemolyticus* and *V. vulnificus* CFUs at higher temperatures (30, 35°C) compared to lower temperature (25°C).

Species	Temperature	Coefficient	*p*
V. parahaemolyticus	30°C	3.70E+05	0.99
	35°C	3.97E+05	0.99
V. vulnificus	30°C	7.25E+05	0.99

	35°C	9.55E+05	0.99

Table A.11 *V. parahaemolyticus* and *V. vulnificus* extracellular polymeric substance biochemical concentrations (µg/mL) and corresponding starting EPS weight (µg) from 10 pooled samples.

Species	Strain	Surface Type	Protein	EPS	Carbohydrates	EPS	eDNA	EPS
V. parahaemolyticus	ATCC17802	LDPE	150	200	145	900	0.94	100
		PP	153	200	146	700	1.25	100
		PS	151	200	18	100	0.36	100
V. vulnificus	vv155	LDPE	80	100	17	100	1.26	100
		PP	83	100	26	300	0.89	100
		PS	140	200	52	200	0.94	100

Table A.12 *V. parahaemolyticus* and *V. vulnificus* individual strain mean adherence to p-xylene (%) at different temperatures.

Species	Strain	25°C (± SD)	30°C (± SD)	35°C (± SD)
V. parahaemolyticus	ATCC17802	55% (5)	49% (4)	49% (6)
	ATCC43996	83% (2)	72% (2)	64% (4)
	vpC12	58% (4)	36% (8)	36% (6)

Correlation between total plastic surface biofilm biomass (*r*)		-0.19	-0.06	-0.04
V. vulnificus	ATCC27562	73% (5)	69% (3)	62% (2)
	ATCC33147	76% (10)	77% (1)	70% (8)
	vv155	71% (1)	66% (4)	66% (2)
Correlation between total plastic surface biofilm biomass (*r*)		-0.47	-0.60	-0.08

(± SD) Standard deviation

Table A.13 *V. parahaemolyticus* and *V. vulnificus* species mean adherence to p-xylene (%) at different temperatures.

Species	**25°C**	**30°C**	**35°C**
V. parahaemolyticus	65%	52%	50%
V. vulnificus	73%	71%	66%

Supplementary Figures and Tables

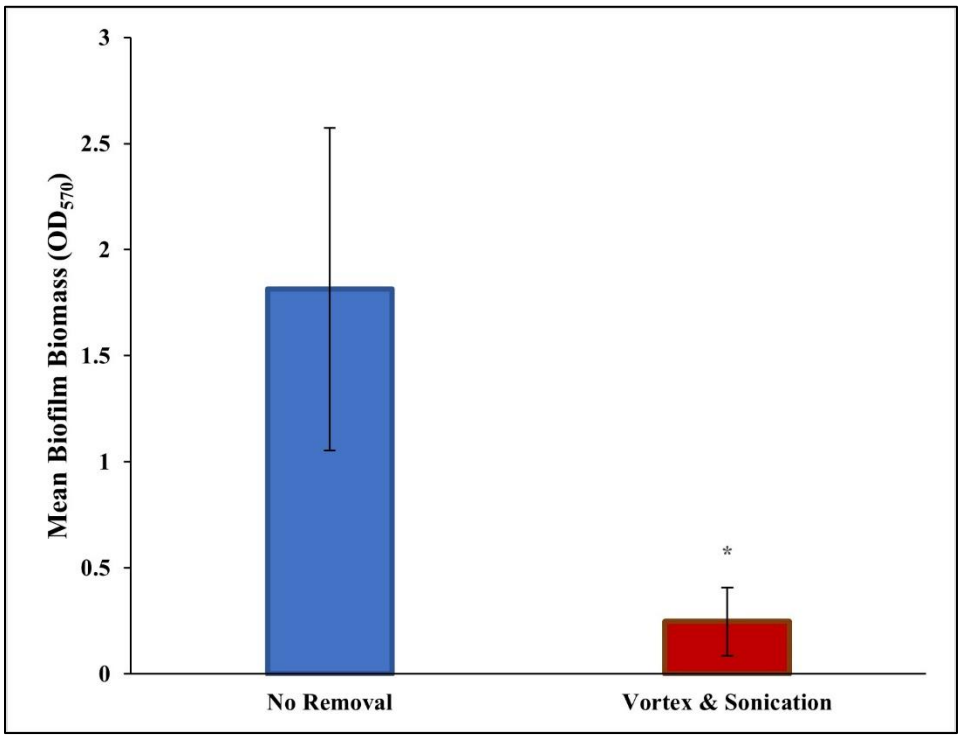

Figure A.1 Assessment of mean *V. vulnificus* (vv155) biofilm biomass removal by vortex & sonication method of combined surface types. * = significant removal of biofilm (α = 0.05) as calculated by t-test.

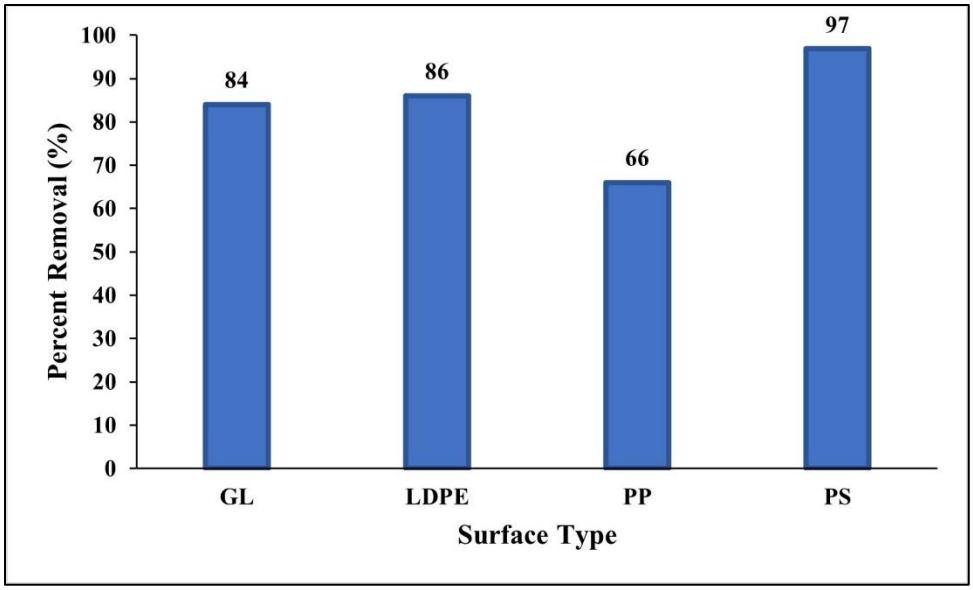

Figure A.2 Assessment of mean *V. vulnificus* (vv155) biofilm biomass removal by vortex and sonication method of individual surface types.

Table A.14 Assessment of vortex and sonication biofilm biomass[1] removal method.

	GL (± SD)	**LDPE** (± SD)	**PP** (± SD)	**PS** (± SD)	**Mean Combined Biofilm Biomass** (± SD)	***p***
Control	1.52 (0.25)	2.74 (0.07)	0.95 (0.2)	2.02 (0.13)	1.81 (0.76)	
Vortex & Sonication	0.24 (0.5)	0.39 (0.04)	0.32 (0.07)	0.02 (0.07)	0.24 (0.16)	≤0.05
Percent Removal	84%	86%	66%	97%	86%	

[1]Optical density at 570 nm
(± SD) Standard deviation

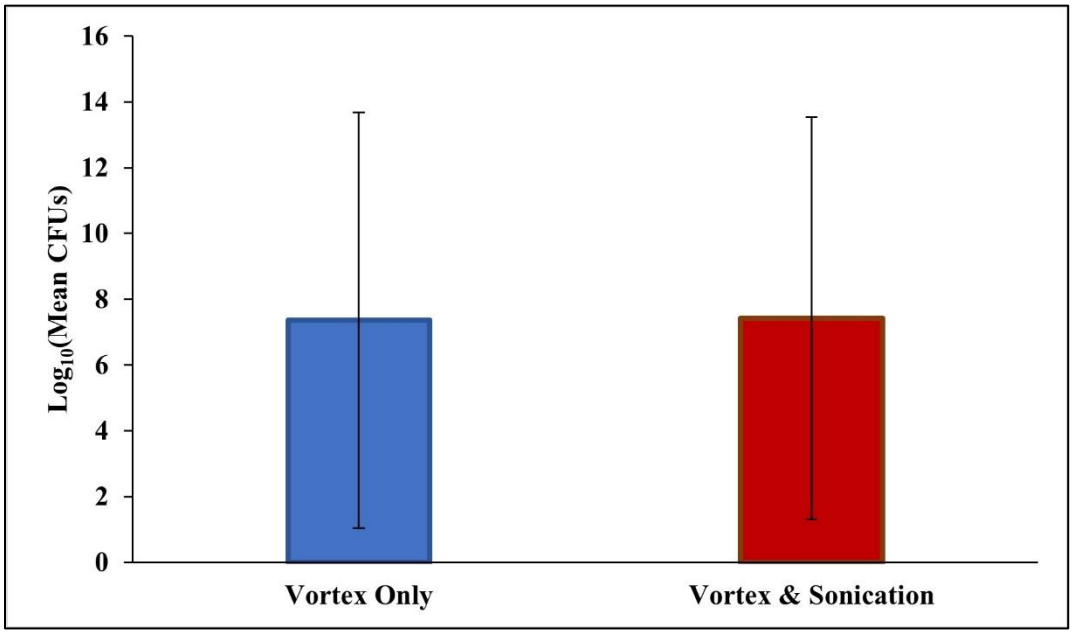

Figure A.3 Assessment of sonication on *V. vulnificus* (vv155) cell viability.

Table A.15 Confirmation that sonication has no significant effect on cell viability.

	Vortex Only (± SD)	Vortex & Sonication (± SD)	*p*
Mean CFUs	2.30E+07 (2.09E+06)	2.62E+07 (1.29E+06)	0.07

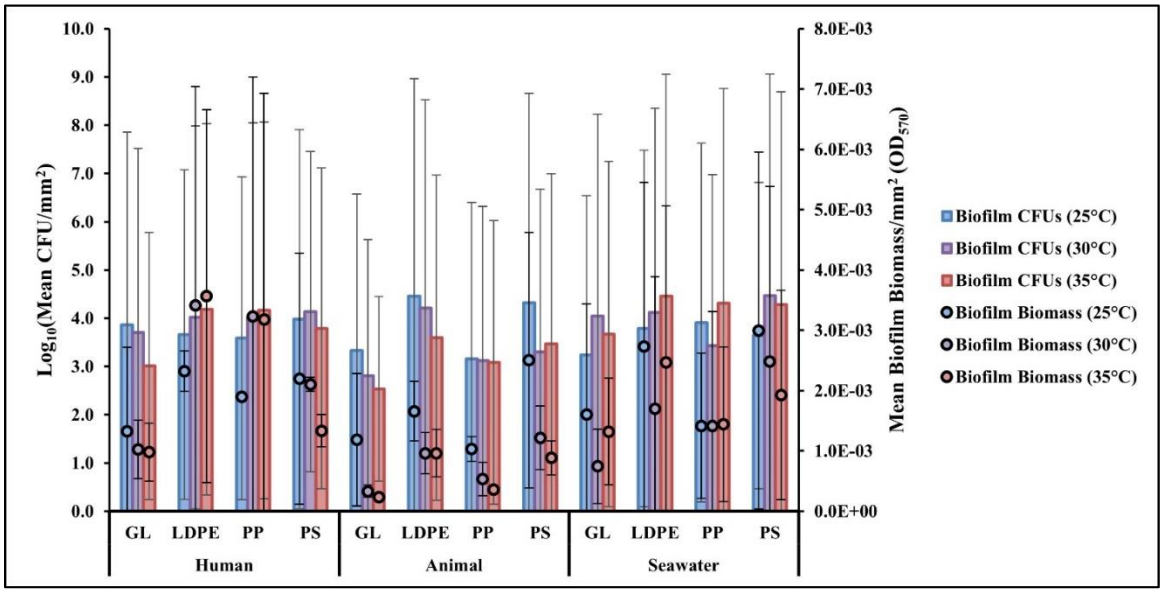

Figure A.4 Comparison of the effect of temperature on biofilm production on different plastic surface types by different *Vibrio* isolation sources.

APPENDIX B:

CHAPTER 2 SUPPLEMENTARY MATERIAL

Supplementary Data

Table B.1. Effect of pH, temperature, and nutrient availability on mean overall biofilm biomass[1] in microplates by *V. parahaemolyticus* and *V. vulnificus*.

Species	pH	Nutrient Rich (25°C) (± SD)	Nutrient Rich (37°C) (± SD)	Nutrient Starved (25°C) (± SD)	Nutrient Starved (37°C) (± SD)
*V. parahaemolyticus**	3	0.95	1.11	0.81	1.13
		0.29	0.14	0.13	0.13
	4	1.14	1.01	1.04	1.34
		0.36	0.23	0.12	0.11
	5	1.68	1.57	1.50	1.74
		0.17	0.23	0.17	0.04
	6	1.69	1.81	1.40	1.49
		0.08	0.37	0.22	0.10
	7	1.82	1.78	1.30	1.60
		0.62	0.33	0.15	0.13
	7.4	1.76	1.75	1.15	1.53
		0.25	0.55	0.02	0.08
	8.1	1.55	1.65	1.29	1.60
		0.40	0.40	0.15	0.20
V. vulnificus	3	0.09	0.14	0.06	0.02
		0.05	0.10	0.00	0.00
	4	0.08	0.10	0.03	0.02
		0.05	0.09	0.00	0.00
	5	0.26	0.17	0.03	0.04
		0.13	0.053	0.01	0.01
	6	0.23	0.24	0.03	0.04
		0.110	0.044	0.002	0.02
	7	0.09	0.18	0.06	0.05
		0.09	0.11	0.02	0.03
	7.4	0.16	0.26	0.04	0.05
		0.02	0.06	0.01	0.01

8.1	0.23	0.22	0.07	0.07
	0.03	0.08	0.01	0.00

[1]Optical density at 570 nm
(± SD) Standard deviation
(*) Significant (+) effect of pH on biofilm biomass

Table B.2. Effect of pH, temperature, and nutrient availability on mean overall final[1] *V. parahaemolyticus* and *V. vulnificus* dispersed cells[2].

Species	**pH**	**Nutrient Rich (25°C) (± SD)**	**Nutrient Rich (37°C) (± SD)**	**Nutrient Starved (25°C) (± SD)**	**Nutrient Starved (37°C) (± SD)**
*V. parahaemolyticus**	3	0.001	0.012	0.000	0.009
		0.001	0.002	0.000	0.001
	4	0.000	0.005	0.007	0.010
		0.001	0.003	0.005	0.003
	5	0.054	0.092	0.012	0.011
		0.001	0.007	0.010	0.003
	6	0.065	0.088	0.013	0.012
		0.004	0.009	0.004	0.005
	7	0.065	0.105	0.012	0.009
		0.005	0.005	0.003	0.004
	7.4	0.069	0.087	0.014	0.008
		0.003	0.012	0.004	0.007
	8.1	0.083	0.087	0.018	0.008
		0.003	0.006	0.018	0.008

V. vulnificus	3	0.000	0.007	0.000	0.015
		0.000	0.005	0.000	0.002
	4	0.000	0.001	0.000	0.011
		0.000	0.002	0.000	0.003
	5	0.035	0.093	0.000	0.010
		0.005	0.004	0.000	0.004
	6	0.048	0.101	0.000	0.004
		0.005	0.005	0.000	0.002
	7	0.048	0.107	0.000	0.012
		0.004	0.006	0.000	0.002
	7.4	0.049	0.111	0.000	0.010
		0.002	0.001	0.000	0.003
	8.1	0.045	0.081	0.000	0.011
		0.005	0.001	0.000	0.004

[1]Original starting values were subtracted from final values after exposure.
[2]Optical density at 600 nm
(± SD) Standard deviation
(*) Significant (+) effect of pH on cell dispersal

Table B.3. Statistical comparison of *V. parahaemolyticus* and *V. vulnificus* overall biofilm biomass[1] and cell dispersal[2] values in nutrient rich media compared to nutrient starved.

		Coefficient	***p***
V. parahaemolyticus	**Biofilm Biomass**	0.13	1.00
	Cell Dispersal	0.04	1.00

V. vulnificus	**Biofilm Biomass**	-0.03	1.00
	Cell Dispersal	0.029	1.00

[1]Optical density at 570 nm
[2]Optical density at 600 nm

Table B.4. Statistical comparison of *V. parahaemolyticus* and *V. vulnificus* biofilm biomass[1] and cell dispersal[2] values at 37°C compared to 25°C.

		Coefficient	***p***
V. parahaemolyticus	**Biofilm Biomass**	-0.01	1.00
	Cell Dispersal	0.01	1.00
V. vulnificus	**Biofilm Biomass**	-0.02	1.00
	Cell Dispersal	-0.02	1.00

[1]Optical density at 570 nm
[2]Optical density at 600 nm

Table B.5. Statistical comparison of effect of pH on *V. parahaemolyticus* and *V. vulnificus* overall biofilm biomass[1] and cell dispersal[2].

		Coefficient	***p***
V. parahaemolyticus	**Biofilm Biomass**	0.14*	$\leq$0.05
	Cell Dispersal	0.02*	$\leq$0.001
V. vulnificus	**Biofilm Biomass**	0.02	0.78
	Cell Dispersal	0.01	0.06

[1]Optical density at 570 nm
[2]Optical density at 600 nm

*Significant increase (+) in biofilm biomass or cell dispersal

Table B.6. Statistical comparison of pH on *V. parahaemolyticus* and *V. vulnificus* overall biofilm biomass[1] and cell dispersal[2] values in nutrient rich media compared to nutrient starved.

		Coefficient	***p***
V. parahaemolyticus	**Biofilm Biomass**	-0.07	1.00
	Cell Dispersal	-0.01	0.051
V. vulnificus	**Biofilm Biomass**	-0.01	1.00
	Cell Dispersal	-0.01	1.00

[1]Optical density at 570 nm
[2]Optical density at 600 nm

Table B.7. Statistical comparison of pH on *V. parahaemolyticus* and *V. vulnificus* overall biofilm biomass[1] and cell dispersal[2] values at 37°C compared to 25°C.

		Coefficient	***p***
V. parahaemolyticus	**Biofilm Biomass**	0.01	1.00
	Cell Dispersal	0.001	1.00
V. vulnificus	**Biofilm Biomass**	0.003	1.00
	Cell Dispersal	0.01	1.00

[1]Optical density at 570 nm
[2]Optical density at 600 nm

Table B.8. Statistical comparison of *V. parahaemolyticus* and *V. vulnificus* biofilm biomass[1] and cell dispersal[2] values at 37°C and nutrient starved media compared to 25°C and nutrient rich media.

		Coefficient	***p***
V. parahaemolyticus	**Biofilm Biomass**	0.23	1.00
	Cell Dispersal	0.003	1.00
V. vulnificus	**Biofilm Biomass**	-0.01	1.00
	Cell Dispersal	0.03	1.00

[1]Optical density at 570 nm
[2]Optical density at 600 nm

Table B.9. Statistical comparison of pH on *V. parahaemolyticus* and *V. vulnificus* overall biofilm biomass and cell dispersal values at 37°C and nutrient starved media compared to 25°C and nutrient rich media.

		Coefficient	***p***
V. parahaemolyticus	**Biofilm Biomass**	0.001	1.00
	Cell Dispersal	-0.004	1.00
V. vulnificus	**Biofilm Biomass**	-0.002	1.00
	Cell Dispersal	-0.01	1.00

[1]Optical density at 570 nm
[2]Optical density at 600 nm

Table B.10. Effect of pH on *V. parahaemolyticus* and *V. vulnificus* overall biofilm metabolic activity[1] in nutrient rich media.

Species	Time (mins)	pH 3	pH 4	pH 5	pH 6	pH 7	pH 7.4	pH 8.1
V. parahaemolyticus	0	465	133352	97380	92458	148801	129109	92084
	15	286	934148	790664	679942	681085	640597	302071
	30	513	1625459	773090	652453	581516	567817	393652
	45	683	1797693	528793	476061	382226	415707	380048
	60	1160	1758139	366432	372790	288373	318948	385735
	75	1102	1532370	318165	333364	239621	267150	320372
	90	1486	1314069	282378	298002	218032	233587	270520
	105	1697	1094049	248619	270474	210938	212931	224025
	120	1757	916987	222512	244677	198093	193906	190045
	135	1778	731128	201113	222818	183718	178245	164855
	150	1937	633560	185672	204646	170719	164692	147410
	165	1909	514445	175203	192433	160585	153515	132661
	180	2203	426426	165771	181720	149078	144249	120382
	195	2789	358051	158575	172595	140166	136787	111248
	210	3735	295963	151483	164874	132528	131289	103847
	225	3664	255637	144267	156076	125214	124564	97966

	240	4814	227748	138078	148832	118265	118960	93398
V. vulnificus	0	4039	525594	336034	195092	318675	293732	851461
	15	1193	3561368	1818971	1151454	1441191	1821863	944692
	30	4071	6194012	1996966	1593665	1714198	1987753	1175000
	45	8179	8175410	1525409	1141948	1356433	1515855	915481
	60	5884	10061465	1016654	742752	860864	1046205	628052
	75	1498	9865254	687005	510502	594934	725676	430376
	90	2665	11538569	537804	397441	466838	553671	351663
	105	2679	10780104	440741	346739	388345	470112	311756
	120	1798	12739924	372688	300674	335688	399467	271323
	135	2272	12045019	307411	257531	292776	327634	230356
	150	2084	13629684	256959	219224	249749	275453	201278
	165	1	14269065	223923	190595	224930	240716	179840
	180	864	13645904	194065	165031	204985	214506	165493
	195	1	13131283	173206	145816	187554	194298	151565
	210	1	11008931	157851	133663	174563	178435	141835
	225	737	8998519	145951	125470	164181	165515	134865
	240	374	6402889	134861	117178	153837	154681	128917

[1]RFU values were divided by corresponding optical density at 600 nm values for normalization.

Table B.11. Effect of pH on *V. parahaemolyticus* and *V. vulnificus* overall biofilm metabolic activity[1] in nutrient starved media.

Species	Time (mins)	pH 3	pH 4	pH 5	pH 6	pH 7	pH 7.4	pH 8.1
V. parahaemolyticus	0	111042	72249	71617	82995	106526	85659	34317
	15	1781	259117	254908	280957	352627	309581	286182
	30	4694	373421	350576	385467	480384	434813	390175
	45	8779	369668	337151	366928	449412	439934	385149
	60	12974	345855	349603	392238	398267	403008	371770
	75	17936	304757	320943	352108	334645	335753	345270
	90	24938	272767	295077	332519	293595	294101	328365
	105	32711	244896	265320	303065	252472	252592	297475
	120	44415	211799	237287	267792	215067	212959	261436
	135	61652	183651	207952	228523	187186	183341	225476
	150	79779	163006	181258	195992	165219	161065	198448
	165	108830	144724	158382	172457	145163	141955	174033
	180	151690	130402	140683	151215	128924	126542	153125

	195	213151	118726	127421	135710	115922	112751	140541
	210	259983	108407	116913	122839	103100	101359	131375
	225	274535	99866	108102	115085	94890	94120	122166
	240	270501	94115	101915	108195	88477	88119	113569
V. vulnificus	0	1	213789	531168	307942	1347714	1055601	262153
	15	1	487114	856258	630045	1991611	2003535	2007300
	30	1	576798	941143	792108	1794634	1696657	1829650
	45	1	594632	818451	706894	1346586	1339767	1405968
	60	1	522266	615717	460869	945798	913211	952219
	75	1	410758	434206	342002	612217	601857	604524
	90	1	344479	342958	278666	435925	457582	457580
	105	1	290315	285935	249795	330647	365094	364821
	120	1	259447	258910	235744	283586	317220	317516
	135	1	230908	229131	216499	247836	272544	276344
	150	1	204545	202038	193509	218007	234392	237808
	165	1	177602	176419	164553	189141	199555	203905
	180	1	156711	157408	148408	169433	174699	177719
	195	1	141464	141739	133096	154635	156296	159311

210	1	129729	132140	122313	141701	143491	145510
225	1	119836	121967	113286	130174	130883	133245
240	1	113545	115870	107821	121816	121755	124107
0	1	213789	531168	307942	1347714	1055601	262153

[1]RFU values were divided by corresponding optical density at 600 nm values for normalization.

Table B.12. Effect of pH, temperature, and nutrient availability on mean biofilm biomass[1] on LDPE[2] by *V. parahaemolyticus* and *V. vulnificus*.

Species	**pH**	**Nutrient Rich (25°C) (± SD)**	**Nutrient Rich (37°C) (± SD)**	**Nutrient Starved (25°C) (± SD)**	**Nutrient Starved (37°C) (± SD)**
*V. parahaemolyticus**	3	0.0046	0.0059	0.0037	0.0045
		0.0050	0.0028	0.0008	0.0029
	4	0.0065	0.0060	0.0040	0.0022
		0.0051	0.0051	0.0031	0.0022
	5	0.0139	0.0177	0.0047	0.0048
		0.0075	0.0036	0.0023	0.0042
	6	0.0187	0.0165	0.0057	0.0044
		0.0056	0.0070	0.0030	0.0037

	7	0.0129	0.0152	0.0062	0.0026
		0.0060	0.0034	0.0027	0.0020
	7.4	0.0136	0.0134	0.0035	0.0043
		0.0070	0.0030	0.0033	0.0038
	8.1	0.0284	0.0127	0.0056	0.0046
		0.0068	0.0018	0.0025	0.0046
V. vulnificus	3	0.0003	0.0005	0.0012	0.0011
		0.0003	0.0003	0.0010	0.0006
	4	0.0004	0.0003	0.0005	0.0007
		0.0004	0.0000	0.0004	0.0001
	5	0.0017	0.0018	0.0006	0.0006
		0.0014	0.0016	0.0002	0.0001
	6	0.0012	0.0028	0.0004	0.0005
		0.0005	0.0019	0.0002	0.0001
	7	0.0024	0.0032	0.0007	0.0008
		0.0023	0.0041	0.0005	0.0003
	7.4	0.0013	0.0013	0.0005	0.0006
		0.0010	0.0008	0.0002	0.0005
	8.1	0.0014	0.0003	0.0013	0.0005
		0.0006	0.0003	0.0009	0.0001

[1]Optical density at 570 nm
[2]Biomass values divided by total microplastic surface area (24 mm^2)
(± SD) Standard deviation
(*) Significant (+) effect of pH on biofilm biomass

Table B.13. Effect of pH, temperature, and nutrient availability on *V. parahaemolyticus* and *V. vulnificus* CFUs[1] on LDPE[2].

Species	pH	Nutrient Rich (25°C) (± SD)	Nutrient Rich (37°C) (± SD)	Nutrient Starved (25°C) (± SD)	Nutrient Starved (37°C) (± SD)
V. parahaemolyticus	3	0.0000	0.8148	1.5659	0.0000
		0.0000	0.5879	0.4331	0.0000
	4	4.6451	2.3882	5.3602	2.8985
		3.3655	1.0206	4.7049	1.8583
	5	5.1112	5.1555	4.6519	3.8985
		3.8583	4.5776	3.7792	3.2218
	6	5.0969	4.8416	5.7315	4.8148
		4.1594	4.2975	5.2358	4.3999
	7	5.5708	4.2145	5.4731	4.9061
		4.7962	3.7442	4.4952	3.8038
	7.4	5.0292	5.3495	5.5283	4.1204
		4.5027	4.3746	4.9526	3.2843
	8.1	4.3522	4.6805	5.4327	4.7861
		3.3434	4.0644	4.4649	4.1048
V. vulnificus	3	0.0000	0.0000	0.0000	0.0000
		0.0000	0.0000	0.0000	0.0000
	4	2.6703	0.0000	2.3216	3.3782
		1.1980	0.0000	1.5240	2.2843
	5	3.2599	3.6051	3.7669	3.9280
		2.8284	3.0005	2.7223	3.5977

6	3.7382	3.5960	3.8485	3.5945
	3.6091	3.3029	2.9796	2.6964
7	3.3413	2.1158	3.5576	3.8111
	2.7303	1.6618	2.7833	3.2974
7.4	3.3955	2.9251	3.8587	3.7523
	3.2345	2.0636	3.2943	2.9427
8.1	2.4987	2.1017	4.2465	3.7167
	2.0178	1.4432	3.1269	2.5819

[1]CFU values were log transformed
[2]CFU values divided by total coupon surface area (24 mm^2)
(± SD) Standard deviation

Table B.14. Effect of pH on mean cell colonization[1] on microplates from LDPE by *V. parahaemolyticus* and *V. vulnificus*.

Species	**pH**	**Nutrient Rich (25°C) (± SD)**	**Nutrient Rich (37°C) (± SD)**	**Nutrient Starved (25°C) (± SD)**	**Nutrient Starved (37°C) (± SD)**
V. parahaemolyticus	3	0.137	0.132	0.030	0.017
		0.203	0.172	0.021	0.008
	4	0.143	0.105	0.020	0.009
		0.178	0.130	0.008	0.005
	5	0.175	0.345	0.020	0.016
		0.217	0.288	0.009	0.014
	6	0.258	0.343	0.028	0.012
		0.282	0.241	0.007	0.007

	7	0.251	0.325	0.018	0.009
		0.209	0.098	0.007	0.007
	7.4	0.138	0.343	0.016	0.013
		0.035	0.248	0.011	0.009
	8.1	0.129	0.320	0.018	0.014
		0.014	0.031	0.009	0.016
*V. vulnificus**	3	0.009	0.007	0.005	0.011
		0.009	0.003	0.005	0.003
	4	0.010	0.008	0.003	0.012
		0.007	0.003	0.004	0.006
	5	0.042	0.032	0.007	0.009
		0.015	0.017	0.009	0.002
	6	0.040	0.074	0.018	0.016
		0.026	0.053	0.003	0.004
	7	0.064	0.047	0.005	0.008
		0.042	0.020	0.004	0.001
	7.4	0.029	0.043	0.003	0.010
		0.011	0.028	0.003	0.006
	8.1	0.056	0.046	0.008	0.007
		0.009	0.023	0.003	0.005

[1]Optical density at 570 nm
(± SD) Standard deviation
(*) Significant (+) effect of pH on biofilm biomass

Table B.15. Effect of pH, temperature and nutrient availability on *V. parahaemolyticus* and *V. vulnificus* CFUs[1] dispersed from LDPE.

Species	pH	Nutrient Rich (25°C) (± SD)	Nutrient Rich (37°C) (± SD)	Nutrient Starved (25°C) (± SD)	Nutrient Starved (37°C) (± SD)
V. parahaemolyticus	3	0.0000 0.0000	0.0000 0.0000	0.0000 0.0000	0.0000 0.0000
	4	7.2050 6.1868	2.1249 2.1840	7.5141 6.8234	6.0374 5.2436
	5	7.5185 6.2386	8.1173 7.1963	6.9138 5.8997	7.6057 6.6065
	6	7.7297 7.0402	7.6659 6.5071	7.2041 6.2386	7.5760 6.8466
	7	7.7533 7.0113	7.1996 6.5129	7.4150 7.0187	7.5051 6.6611
	7.4	7.8084 7.1868	7.5315 6.9934	7.4771 6.7782	7.4914 6.6394
	8.1	6.9294 6.3356	7.6368 6.9755	7.4094 6.5782	7.5873 6.8675
V. vulnificus	3	0.0000 0.0000	0.0000 0.0000	0.0000 0.0000	0.0000 0.0000
	4	4.3243 3.9952	0.0000 0.0000	4.1856 3.4008	5.0427 4.4519
	5	5.5873 4.7614	7.1996 7.0451	5.8865 5.0467	5.9085 5.5024

6	5.0731	7.4430	5.5097	5.4771
	4.9454	6.9397	4.7548	4.7955
7	4.9638	6.6690	5.3358	5.3802
	4.8443	6.3118	4.6541	5.0246
7.4	5.5873	6.7243	5.7132	4.9853
	4.5071	6.2944	4.9578	4.4008
8.1	5.6812	6.8573	5.6092	5.3358
	5.1139	6.7300	4.8466	4.9755

[1]CFU values were log transformed
(± SD) Standard deviation

Table B.16. Effect of pH on mean biofilm biomass[1] on PP[2] by *V. parahaemolyticus* and *V. vulnificus*.

Species	**pH**	**Nutrient Rich (25°C) (± SD)**	**Nutrient Rich (37°C) (± SD)**	**Nutrient Starved (25°C) (± SD)**	**Nutrient Starved (37°C) (± SD)**
V. parahaemolyticus	3	0.0039	0.0070	0.0099	0.0095
		0.0015	0.0078	0.0049	0.0052
	4	0.0067	0.0042	0.0085	0.0098
		0.0052	0.0041	0.0021	0.0063
	5	0.0207	0.0040	0.0084	0.0036
		0.0129	0.0032	0.0017	0.0044
	6	0.0149	0.0087	0.0090	0.0030
		0.0068	0.0096	0.0033	0.0029

	7	0.0126	0.0070	0.0131	0.0087
		0.0088	0.0041	0.0077	0.0046
	7.4	0.0089	0.0051	0.0086	0.0098
		0.0021	0.0047	0.0027	0.0040
	8.1	0.0151	0.0106	0.0093	0.0092
		0.0032	0.0013	0.0062	0.0001
V. vulnificus	3	0.0003	0.0002	0.0002	0.0001
		0.0004	0.0002	0.0002	0.0001
	4	0.0004	0.0006	0.0001	0.0002
		0.0003	0.0004	0.0000	0.0001
	5	0.0011	0.0008	0.0001	0.0001
		0.0012	0.0000	0.0001	0.0001
	6	0.0007	0.0017	0.0001	0.0002
		0.0002	0.0005	0.0000	0.0001
	7	0.0007	0.0015	0.0001	0.0002
		0.0007	0.0010	0.0001	0.0001
	7.4	0.0003	0.0011	0.0001	0.0000
		0.0001	0.0007	0.0001	0.0001
	8.1	0.0008	0.0004	0.0001	0.0001
		0.0005	0.0001	0.0001	0.0001

[1]Optical density at 570 nm
[2]Biomass values divided by total microplastic surface area (24 mm^2)
(± SD) Standard deviation

Table B.17. Effect of pH, temperature, and nutrient availability on *V. parahaemolyticus* and *V. vulnificus* CFUs[1] on PP[2].

Species	pH	Nutrient Rich (25°C) (± SD)	Nutrient Rich (37°C) (± SD)	Nutrient Starved (25°C) (± SD)	Nutrient Starved (37°C) (± SD)
V. parahaemolyticus	3	1.8157	0.0000	0.0000	0.0000
		0.5740	0.0000	0.0000	0.0000
	4	5.2326	1.7901	5.1761	4.7002
		4.2218	0.8810	4.4039	3.7728
	5	4.8248	4.3882	5.3522	5.2145
		3.9694	3.5749	4.0423	4.4952
	6	5.1680	4.0235	5.4237	5.4145
		4.1653	3.7833	4.3999	4.6411
	7	4.4480	5.6255	5.3010	5.4003
		3.5879	4.5879	4.2218	4.5495
	7.4	4.8822	4.6212	5.2290	5.1996
		3.8985	3.8413	4.5776	3.6198
	8.1	5.2255	4.2396	5.2533	4.6741
		4.5101	3.4432	4.0969	3.8102
V. vulnificus	3	0.0000	0.0000	0.0000	0.0000
		0.0000	0.0000	0.0000	0.0000
	4	0.0000	0.0000	3.1065	3.9351
		0.0000	0.0000	2.3812	2.8657
	5	2.9280	3.0474	3.2919	3.6612
		2.4432	2.3878	2.6262	2.0969

6	2.6638	2.1513	4.0000	3.8909
	2.0936	2.0286	3.0423	2.6823
7	2.1427	1.5406	3.4751	3.9406
	1.3216	0.3812	2.8259	2.5101
7.4	2.7638	3.0921	3.9001	3.7179
	2.3620	2.3607	3.1064	3.1523
8.1	2.1721	1.9351	3.8073	3.7304
	1.7478	1.4990	2.8591	3.1438

[1]CFU values were log transformed
[2]CFU values divided by total coupon surface area (24 mm^2)
(± SD) Standard deviation

Table B.18. Effect of pH on mean cell colonization[1] on microplates from PP by *V. parahaemolyticus* and *V. vulnificus*.

Species	pH	Nutrient Rich (25°C) (± SD)	Nutrient Rich (37°C) (± SD)	Nutrient Starved (25°C) (± SD)	Nutrient Starved (37°C) (± SD)
V. parahaemolyticus#	3	0.021	0.044	0.012	0.015
		0.011	0.029	0.006	0.007
	4	0.024	0.029	0.023	0.030
		0.011	0.009	0.010	0.006
	5	0.074	0.115	0.023	0.016
		0.023	0.031	0.008	0.016
	6	0.059	0.218	0.021	0.018
		0.013	0.107	0.007	0.015
	7	0.104	0.287	0.028	0.016
		0.017	0.077	0.007	0.008

	7.4	0.089	0.232	0.029	0.029
		0.004	0.057	0.004	0.010
	8.1	0.111	0.263	0.026	0.029
		0.045	0.026	0.006	0.008
*V. vulnificus**	3	0.004	0.011	0.006	0.004
		0.004	0.011	0.005	0.001
	4	0.007	0.005	0.005	0.006
		0.006	0.003	0.005	0.006
	5	0.016	0.020	0.007	0.007
		0.008	0.022	0.005	0.003
	6	0.020	0.073	0.004	0.009
		0.010	0.026	0.003	0.005
	7	0.032	0.071	0.005	0.008
		0.014	0.038	0.003	0.003
	7.4	0.028	0.049	0.005	0.005
		0.003	0.038	0.004	0.004
	8.1	0.052	0.037	0.010	0.011
		0.016	0.008	0.009	0.001

[1]Optical density at 570 nm
(± SD) Standard deviation
(*) Significant effect of pH on biofilm biomass
(#) Synergistic significant effect of pH, temperature, and nutrient content on biofilm biomass

Table B.19. Effect of pH, temperature, and nutrient availability on *V. parahaemolyticus* and *V. vulnificus* CFUs[1] dispersed from PP.

Species	pH	Nutrient Rich (25°C) (± SD)	Nutrient Rich (37°C) (± SD)	Nutrient Starved (25°C) (± SD)	Nutrient Starved (37°C) (± SD)
V. parahaemolyticus	3	0.0000 0.000	0.0000 0.000	0.0000 0.000	0.0000 0.000
	4	7.3754 6.243	3.3153 2.859	7.3617 6.893	7.5911 7.000
	5	7.5399 6.318	7.7782 7.551	7.7508 6.702	7.5948 6.983
	6	7.5523 6.710	7.6812 7.268	7.7104 7.185	7.7104 6.665
	7	7.9226 7.663	7.8409 7.486	7.4037 6.755	7.6690 7.001
	7.4	7.6402 6.546	7.9412 7.040	7.3010 6.778	7.5006 6.318
	8.1	7.8751 7.149	7.9777 7.221	7.4150 6.845	7.3741 6.184
V. vulnificus	3	0.0000 0.000	0.0000 0.000	0.0000 0.000	0.0000 0.000
	4	0.0000 0.000	0.0000 0.000	2.8239 2.485	5.3188 4.703
	5	6.4276 5.838	5.6368 5.001	5.7993 5.516	5.6990 5.114

6	5.1249	6.2529	5.6163	5.5721
	4.741	5.980	5.259	4.813
7	4.8939	6.4314	4.9226	5.2711
	4.288	6.168	4.411	3.761
7.4	5.8958	6.3424	5.5006	4.9853
	5.091	5.980	4.546	4.184
8.1	5.0792	6.3153	5.4960	5.6021
	4.984	5.363	4.768	4.784

[1]CFU values were log transformed
(± SD) Standard deviation

Table B.20. Effect of pH on mean biofilm biomass[1] on PS[2] by *V. parahaemolyticus* and *V. vulnificus*.

Species	**pH**	**Nutrient Rich (25°C) (± SD)**	**Nutrient Rich (37°C) (± SD)**	**Nutrient Starved (25°C) (± SD)**	**Nutrient Starved (37°C) (± SD)**
V. parahaemolyticus	3	0.0013	0.0006	0.0038	0.0021
		0.0012	0.0007	0.0008	0.0017
	4	0.0009	0.0000	0.0040	0.0068
		0.0015	0.0000	0.0019	0.0073
	5	0.0049	0.0015	0.0076	0.0046
		0.0055	0.0025	0.0030	0.0037
	6	0.0047	0.0023	0.0089	0.0064
		0.0048	0.0037	0.0015	0.0106
	7	0.0039	0.0016	0.0088	0.0016
		0.0046	0.0021	0.0055	0.0011

	7.4	0.0053	0.0016	0.0048	0.0024
		0.0051	0.0026	0.0014	0.0002
	8.1	0.0084	0.0020	0.0047	0.0037
		0.0030	0.0014	0.0019	0.0011
V. vulnificus	3	0.0017	0.0015	0.0001	0.0016
		0.0021	0.0013	0.0002	0.0008
	4	0.0004	0.0008	0.0001	0.0024
		0.0003	0.0009	0.0001	0.0010
	5	0.0031	0.0031	0.0003	0.0056
		0.0038	0.0011	0.0004	0.0032
	6	0.0013	0.0028	0.0021	0.0062
		0.0000	0.0010	0.0019	0.0021
	7	0.0027	0.0022	0.0004	0.0020
		0.0047	0.0012	0.0003	0.0005
	7.4	0.0020	0.0015	0.0012	0.0017
		0.0017	0.0003	0.0019	0.0014
	8.1	0.0058	0.0021	0.0010	0.0008
		0.0004	0.0017	0.0007	0.0002

[1]Optical density at 570 nm
[2]Biomass values divided by total microplastic surface area (14 mm^2)
(± SD) Standard deviation

Table B.21. Effect of pH, temperature, and nutrient availability on *V. parahaemolyticus* and *V. vulnificus* CFUs[1] on PS[2].

Species	pH	Nutrient Rich (25°C) (± SD)	Nutrient Rich (37°C) (± SD)	Nutrient Starved (25°C) (± SD)	Nutrient Starved (37°C) (± SD)
V. parahaemolyticus	3	0.0000 0.0000	0.0000 0.0000	0.0000 0.0000	0.0000 0.0000
	4	4.3021 3.1802	0.0000 0.0000	4.6927 3.7943	3.9208 3.3143
	5	4.3499 3.9012	4.8953 3.8539	5.9531 4.9878	4.8255 3.8830
	6	3.9874 3.1721	3.6842 2.5948	4.6969 4.0254	4.4907 3.7048
	7	3.9306 2.9783	3.8539 3.2764	4.8953 4.1549	4.5643 4.0754
	7.4	3.8495 2.9967	4.0202 3.4604	4.7251 3.3143	4.8466 3.8063
	8.1	4.7385 3.9936	4.4559 3.5150	4.3680 3.4604	4.7251 4.1039
V. vulnificus	3	0.0000 0.0000	0.0000 0.0000	0.0000 0.0000	0.0000 0.0000
	4	1.8081 0.8539	0.0000 0.0000	2.0395 1.4733	2.3010 1.2764
	5	2.3768 2.3610	3.7385 3.1451	3.8081 2.9678	3.7606 3.1551

6	3.7712	4.2593	4.1469	3.9599
	3.5106	3.8719	2.8546	2.7331
7	2.3768	2.9485	3.9450	3.3545
	1.6153	2.3686	2.6153	2.7614
7.4	3.6799	3.9711	3.9895	3.9379
	3.5404	3.2440	3.5080	3.3674
8.1	2.4061	2.2341	3.9082	4.0516
	1.9819	1.4108	3.0379	3.2702

[1]CFU values were log transformed
[2]CFU values divided by total coupon surface area (14 mm^2)
(± SD) Standard deviation

Table B.22. Effect of pH on mean cell colonization[1] on microplates from PS by *V. parahaemolyticus* and *V. vulnificus*.

Species	**pH**	**Nutrient Rich (25°C) (± SD)**	**Nutrient Rich (37°C) (± SD)**	**Nutrient Starved (25°C) (± SD)**	**Nutrient Starved (37°C) (± SD)**
V. parahaemolyticus#	3	0.002 0.007	0.004 0.007	0.001 0.000	0.003 0.007
	4	0.011 0.006	0.005 0.018	0.003 0.006	0.007 0.008
	5	0.016 0.026	0.022 0.026	0.004 0.005	0.008 0.006
	6	0.030 0.021	0.113 0.102	0.030 0.018	0.030 0.016

	7	0.026 0.013	0.026 0.056	0.004 0.002	0.003 0.006
	7.4	0.024 0.045	0.071 0.061	0.002 0.000	0.008 0.001
	8.1	0.058 0.006	0.030 0.032	0.006 0.011	0.007 0.003
V. vulnificus	3	0.007 0.004	0.010 0.005	0.000 0.001	0.009 0.000
	4	0.006 0.009	0.019 0.005	0.003 0.005	0.015 0.001
	5	0.032 0.019	0.033 0.013	0.005 0.004	0.009 0.000
	6	0.035 0.004	0.152 0.039	0.016 0.041	0.013 0.008
	7	0.041 0.007	0.123 0.020	0.007 0.006	0.006 0.001
	7.4	0.065 0.016	0.131 0.025	0.000 0.001	0.012 0.000
	8.1	0.006 0.011	0.032 0.010	0.006 0.008	0.008 0.002

[1]Optical density at 570 nm
(± SD) Standard deviation
(#) Synergistic significant effect of pH, temperature, and nutrient content on biofilm biomass

Table B.23. Effect of pH, temperature, and nutrient availability on *V. parahaemolyticus* and *V. vulnificus* CFUs[1] dispersed from PS.

Species	pH	Nutrient Rich (25°C) (± SD)	Nutrient Rich (37°C) (± SD)	Nutrient Starved (25°C) (± SD)	Nutrient Starved (37°C) (± SD)
V. parahaemolyticus	3	0.0000 0.000	0.0000 0.0000	0.0000 0.0000	0.0000 0.0000
	4	6.1184 5.1338	0.0000 0.0000	5.9927 5.2765	6.6690 5.7103
	5	6.2625 5.6069	7.5836 6.3184	6.2553 5.0000	6.4914 5.7955
	6	6.0768 5.6568	7.3741 7.0050	6.1249 5.5782	6.7188 6.0174
	7	6.7351 6.4167	7.5315 6.8997	6.1563 5.6541	6.1249 6.0914
	7.4	6.8633 6.4496	7.4914 6.8997	5.9700 5.3184	6.5836 5.8082
	8.1	6.4367 5.8234	7.4674 6.7103	6.3680 5.8234	6.1761 5.5570
V. vulnificus	3	0.0000 0.0000	0.0000 0.0000	0.0000 0.0000	0.0000 0.0000
	4	2.8282 2.8648	0.0000 0.0000	3.2937 2.7103	4.0531 2.9542
	5	4.9853 4.4834	7.1663 6.9687	4.3862 3.8830	5.3490 4.5071

6	5.1139	5.2131	4.9868	4.8653
	4.6484	4.8509	4.2893	4.4329
7	5.5643	6.5682	5.0000	3.8846
	5.0559	6.1178	4.4225	3.3184
7.4	4.9260	7.2005	5.4094	5.3082
	4.5695	6.7873	4.5071	4.7548
8.1	5.1461	7.4634	5.1357	5.0000
	4.8167	6.5086	4.7410	4.2386

[1]CFU values were log transformed
(± SD) Standard deviation

Table B.24. Statistical comparison of *V. parahaemolyticus* and *V. vulnificus* biofilm biomass[1], biofilm cell[2], cell colonization[1] and cell dispersal[2] values on/from LDPE[3], PP[3] and PS[4] in nutrient rich media compared to nutrient starved.

	Surface Type		**Coefficient**	***p***
V. parahaemolyticus	**LDPE**	**Biofilm Biomass**	0.21	1.00
		Biofilm Cells	-3.5E04	1.00
		Cell Colonization	-0.11	1.00
		Cell Dispersal	6.2E06	1.00
	PP	**Biofilm Biomass**	0.11	1.00
		Biofilm Cells	-1.3E03	1.00
		Cell Colonization	0.04	1.00

		Cell Dispersal	5.1E07	0.98
	PS	**Biofilm Biomass**	0.92	0.64
		Biofilm Cells	3.2E05	1.00
		Cell Colonization	0.03	1.00
		Cell Dispersal	2.6E06	1.00
V. vulnificus	**LDPE**	**Biofilm Biomass**	2.32E02	1.00
		Biofilm Cells	-8.8E03	0.76
		Cell Colonization	2.02E-02	1.00
		Cell Dispersal	1.2E04	1.00
	PP	**Biofilm Biomass**	-0.004	1.00
		Biofilm Cells	-3.8E03	1.00
		Cell Colonization	0.029	1.00
		Cell Dispersal	-6.6E05	1.00
	PS	**Biofilm Biomass**	0.006	1.00
		Biofilm Cells	-4.1E03	1.00
		Cell Colonization	0.02	1.00
		Cell Dispersal	-2.72E-04	1.00

[1]Optical density at 570 nm
[2]CFU values were log transformed
[3]Biofilm biomass and CFU values on plastic divided by total coupon surface area (24 mm^2)
[4]Biofilm biomass and CFU values on plastic divided by total coupon surface area (14 mm^2)

Table B.25. Statistical comparison of *V. parahaemolyticus* and *V. vulnificus* biofilm biomass[1], biofilm cell[2], cell colonization[1] and cell dispersal[2] values on/from LDPE[3], PP[3] and PS[4] at 37°C compared to 25°C.

	Surface Type		Coefficient	*p*
V. parahaemolyticus	**LDPE**	**Biofilm Biomass**	0.22	1.00
		Biofilm Cells	-7.2E02	1.00
		Cell Colonization	-0.13	1.00
		Cell Dispersal	2.4E07	1.00
	PP	**Biofilm Biomass**	-0.02	1.00
		Biofilm Cells	-1.2E05	1.00
		Cell Colonization	-0.1	0.17
		Cell Dispersal	-2.5E07	1.00
	PS	**Biofilm Biomass**	0.07	1.00
		Biofilm Cells	1.9E04	1.00
		Cell Colonization	-0.06	0.29
		Cell Dispersal	-1.5E07	1.00
V. vulnificus	**LDPE**	**Biofilm Biomass**	1.47E-02	1.00
		Biofilm Cells	1.3E02	1.00
		Cell Colonization	-1.11E-05	1.00
		Cell Dispersal	2.2E06	1.00
	PP	**Biofilm Biomass**	-0.003	1.00
		Biofilm Cells	-7.7E01	1.00

		Cell Colonization	0.005	1.00
		Cell Dispersal	-2.2E06	0.29
	PS	**Biofilm Biomass**	0.03	1.00
		Biofilm Cells	1.4E03	1.00
		Cell Colonization	0.006	1.00
		Cell Dispersal	-1.4E-07	0.78

[1]Optical density at 570 nm
[2]CFU values were log transformed
[3]Biofilm biomass and CFU values on plastic divided by total coupon surface area (24 mm^2)
[4]Biofilm biomass and CFU values on plastic divided by total coupon surface area (14 mm^2)

Table B.26. Statistical comparison of effect of pH on *V. parahaemolyticus* and *V. vulnificus* biofilm biomass[1], biofilm cell[2], cell colonization[1] and cell dispersal[2] values on/from LDPE[3], PP[3] and PS[4].

	Surface Type		**Coefficient**	***p***
V. parahaemolyticus	**LDPE**	**Biofilm Biomass**	0.08*	$\leq$0.01
		Biofilm Cells	2.4E04	1.00
		Cell Colonization	0.005	1.00
		Cell Dispersal	7.1E06	1.00
	PP	**Biofilm Biomass**	0.03	0.74
		Biofilm Cells	1.0E04	1.00
		Cell Colonization	0.02*	$\leq$0.01
		Cell Dispersal	1.3E07*	$\leq$0.05
	PS	**Biofilm Biomass**	0.02	0.09

		Biofilm Cells	4.6E03	1.00
		Cell Colonization	0.01*	≤0.05
		Cell Dispersal	1.0E06	1.00
V. vulnificus	**LDPE**	**Biofilm Biomass**	6.34E-03	0.87
		Biofilm Cells	3.0E02	1.00
		Cell Colonization	8.8E-03*	≤0.05
		Cell Dispersal	7.2E04	1.00
	PP	**Biofilm Biomass**	0.001	1.00
		Biofilm Cells	4.2E01	1.00
		Cell Colonization	0.008*	≤0.05
		Cell Dispersal	-2.0E04	1.00
	PS	**Biofilm Biomass**	0.008	0.59
		Biofilm Cells	4.5E02	1.00
		Cell Colonization	0.008	0.71
		Cell Dispersal	4.06E-04	1.00

[1]Optical density at 570 nm
[2]CFU values were log transformed
[3]Biofilm biomass and CFU values on plastic divided by total coupon surface area (24 mm^2)
[4]Biofilm biomass and CFU values on plastic divided by total coupon surface area (14 mm^2)
*Significant increase (+) /decrease (-) in biofilm biomass/cell colonization or cell dispersal

Table B.27. Statistical comparison of effect of pH on *V. parahaemolyticus* and *V. vulnificus* biofilm biomass[1], biofilm cell[2], cell colonization[1] and cell dispersal[2] values on/from LDPE[3], PP[3] and PS[4] in nutrient rich media compared to nutrient starved.

	Surface Type		**Coefficient**	***p***
V. parahaemolyticus	**LDPE**	**Biofilm Biomass**	-0.07	0.053
		Biofilm Cells	3.2E04	1.00
		Cell Colonization	-0.007	1.00
		Cell Dispersal	-3.3E06	1.00
	PP	**Biofilm Biomass**	-0.02	1.00
		Biofilm Cells	1.5E04	1.00
		Cell Colonization	-0.01	0.27
		Cell Dispersal	-1.1E07	0.37
	PS	**Biofilm Biomass**	-0.01	1.00
		Biofilm Cells	-3.0E04	1.00
		Cell Colonization	-0.01	0.23
		Cell Dispersal	-7.3E05	1.00
V. vulnificus	**LDPE**	**Biofilm Biomass**	-6.41	1.00
		Biofilm Cells	2.2E03	0.11
		Cell Colonization	-8.43	0.27
		Cell Dispersal	-2.6E03	1.00
	PP	**Biofilm Biomass**	-0.001	1.00
		Biofilm Cells	1.3E03	0.41

		Cell Colonization	-0.008	0.28
		Cell Dispersal	6.4E04	1.00
	PS	**Biofilm Biomass**	-0.003	1.00
		Biofilm Cells	1.3E03	1.00
		Cell Colonization	-0.007	1.00
		Cell Dispersal	-2.79E-02	1.00

[1]Optical density at 570 nm
[2]CFU values were log transformed
[3]Biofilm biomass and CFU values on plastic divided by total coupon surface area (24 mm^2)
[4]Biofilm biomass and CFU values on plastic divided by total coupon surface area (14 mm^2)
*Significant increase (+) /decrease (-) in biofilm biomass or cell dispersal

Table B.28. Statistical comparison of effect of pH on *V. parahaemolyticus* and *V. vulnificus* biomass[1], biofilm cell[2], cell colonization[1] and cell dispersal[2] values on/from LDPE[3], PP[3] and PS[4] at 37°C compared to 25°C.

	Surface Type		**Coefficient**	***p***
V. parahaemolyticus	**LDPE**	**Biofilm Biomass**	-0.04	0.62
		Biofilm Cells	-6.1E03	1.00
		Cell Colonization	0.04	0.11
		Cell Dispersal	-3.2E06	1.00
	PP	**Biofilm Biomass**	-0.02	1.00
		Biofilm Cells	1.8E04	1.00
		Cell Colonization	0.03*	≤0.001
		Cell Dispersal	5.9E06	1.00

	PS	**Biofilm Biomass**	-0.02	0.34
		Biofilm Cells	-3.1E03	1.00
		Cell Colonization	0.02*	≤0.01
		Cell Dispersal	5.3E06	0.07
V. vulnificus	**LDPE**	**Biofilm Biomass**	-1.6E-03	1.00
		Biofilm Cells	-3.2E02	1.00
		Cell Colonization	1.49E-04	1.00
		Cell Dispersal	1.1E06	1.00
	PP	**Biofilm Biomass**	0.001	1.00
		Biofilm Cells	2.4E01	1.00
		Cell Colonization	0.001	1.00
		Cell Dispersal	3.7E05	0.051
	PS	**Biofilm Biomass**	-0.006	1.00
		Biofilm Cells	3.1E02	1.00
		Cell Colonization	0.001	1.00
		Cell Dispersal	4.04E-06	0.06

[1]Optical density at 570 nm
[2]CFU values were log transformed
[3]Biofilm biomass and CFU values on plastic divided by total coupon surface area (24 mm^2)
[4]Biofilm biomass and CFU values on plastic divided by total coupon surface area (14 mm^2)
*Significant increase (+) /decrease (-) in biofilm biomass or cell dispersal

Table B.29. Statistical comparison of *V. parahaemolyticus* and *V. vulnificus* biofilm biomass[1], biofilm cell[2], cell colonization[1] and cell dispersal[2] values on/from LDPE[3], PP[3] and PS[4] at 37°C and nutrient starved media compared to 25°C and nutrient rich media.

	Surface Type		**Coefficient**	***p***
V. parahaemolyticus	**LDPE**	**Biofilm Biomass**	-0.22	1.00
		Biofilm Cells	5.1E04	1.00
		Cell Colonization	0.11	1.00
		Cell Dispersal	-3.8E07	1.00
	PP	**Biofilm Biomass**	-0.01	1.00
		Biofilm Cells	9.8E05	1.00
		Cell Colonization	0.11	0.62
		Cell Dispersal	2.2E07	1.00
	PS	**Biofilm Biomass**	-0.03	1.00
		Biofilm Cells	-3.5E05	1.00
		Cell Colonization	0.07	0.61
		Cell Dispersal	1.4E07	1.00
V. vulnificus	**LDPE**	**Biofilm Biomass**	-6.19E-03	1.09
		Biofilm Cells	6.7E03	1.00
		Cell Colonization	9.02E-03	1.00
		Cell Dispersal	-1.9E06	1.00
	PP	**Biofilm Biomass**	0.002	1.00
		Biofilm Cells	5.7E03	1.00

		Cell Colonization	-0.007	1.00
		Cell Dispersal	2.6E06	0.9
	PS	**Biofilm Biomass**	0.03	1.00
		Biofilm Cells	-1.9E03	1.00
		Cell Colonization	-0.002	1.00
		Cell Dispersal	1.45E-07	1.00

[1]Optical density at 570 nm
[2]CFU values were log transformed
[3]Biofilm biomass and CFU values on plastic divided by total coupon surface area (24 mm^2)
[4]Biofilm biomass and CFU values on plastic divided by total coupon surface area (14 mm^2)
*Significant increase (+) /decrease (-) in biofilm biomass or cell dispersal

Table B.30. Statistical comparison of effect of pH on *V. parahaemolyticus* and *V. vulnificus* biofilm biomass[1], biofilm cell[2], cell colonization[1] and cell dispersal[2] values on/from LDPE[3], PP[3] and PS[4] at 37°C and nutrient starved media compared to 25°C and nutrient rich media.

	Surface Type		**Coefficient**	***p***
V. parahaemolyticus	**LDPE**	**Biofilm Biomass**	0.04	1.00
		Biofilm Cells	-3.8E04	1.00
		Cell Colonization	-0.04	0.63
		Cell Dispersal	6.8E06	1.00
	PP	**Biofilm Biomass**	0.015	1.00
		Biofilm Cells	-1.9E4	1.00
		Cell Colonization	-0.04*	≤0.01

		Cell Dispersal	-4.7E06	1.00
	PS	**Biofilm Biomass**	0.009	1.00
		Biofilm Cells	3.9E04	1.00
		Cell Colonization	-0.02*	≤0.05
		Cell Dispersal	-5.5E06	0.35
V. vulnificus	**LDPE**	**Biofilm Biomass**	-9.17E-03	1.00
		Biofilm Cells	-1.3E03	1.00
		Cell Colonization	-1.11E-03	1.00
		Cell Dispersal	-1.1E06	1.00
	PP	**Biofilm Biomass**	-0.002	1.00
		Biofilm Cells	-7.5E02	1.00
		Cell Colonization	-0.001	1.00
		Cell Dispersal	-5.0E05	0.31
	PS	**Biofilm Biomass**	3.0E-04	1.00
		Biofilm Cells	-4.6E02	1.00
		Cell Colonization	-0.002	1.00
		Cell Dispersal	-4.06E-06	0.4

[1]Optical density at 570 nm
[2]CFU values were log transformed
[3]Biofilm biomass and CFU values on plastic divided by total coupon surface area (24 mm^2)
[4]Biofilm biomass and CFU values on plastic divided by total coupon surface area (14 mm^2)
*Significant increase (+) /decrease (-) in biofilm biomass or cell dispersal

Table B.31. Effect of media composition on overall mean biofilm biomass[1] by *V. parahaemolyticus* and *V. vulnificus*.

Species	SGF (25°C) (± SD)	SGF (37°C) (± SD)	SIF (25°C) (± SD)	SIF (37°C) (± SD)	HPLM (25°C) (± SD)	HPLM (37°C) (± SD)
V. parahaemolyticus	0.947	1.106	1.822	1.785	2.980	2.889
	0.296	0.144	0.627	0.339	0.325	0.488
V. vulnificus	0.088	0.137	0.091	0.178	0.491	0.580
	0.059	0.107	0.091	0.111	0.040	0.146

[1]Optical density at 570 nm
(± SD) Standard deviation

Table B.32. Effect of media composition on mean overall final[1] *V. parahaemolyticus* and *V. vulnificus* cell dispersal[2] values.

Species	SGF (25°C) (± SD)	SGF (37°C) (± SD)	SIF (25°C) (± SD)	SIF (37°C) (± SD)	HPLM (25°C) (± SD)	HPLM (37°C) (± SD)
V. parahaemolyticus	0.002	0.000	0.000	0.000	0.013	0.008
	0.001	0.000	0.000	0.000	0.012	0.008
V. vulnificus	0.000	0.000	0.000	0.000	0.030	0.059
	0.000	0.000	0.000	0.000	0.000	0.004

[1]Original starting values were subtracted from final values after exposure.
[2]Optical density at 600 nm
(± SD) Standard deviation

Table B.33. Statistical comparison of *V. parahaemolyticus* and *V. vulnificus* overall biofilm biomass[1] and cell dispersal[2] values in different simulated human medias at 37°C compared to 25°C.

	Media Type		Coefficient	*p*
V. parahaemolyticus	**SGF**	**Biofilm Biomass**	-0.06	1.00
		Cell Dispersal	-0.02	1.00
	SIF	**Biofilm Biomass**	-0.5	1.00
		Cell Dispersal	-0.02	1.00
	HPLM	**Biofilm Biomass**	-0.12	1.00
		Cell Dispersal	-0.03	1.00
V. vulnificus	**SGF**	**Biofilm Biomass**	-0.05	1.00
		Cell Dispersal	-0.04	1.00
	SIF	**Biofilm Biomass**	-0.05	1.00
		Cell Dispersal	-0.04	1.00
	HPLM	**Biofilm Biomass**	0.11	1.00
		Cell Dispersal	-0.01	1.00

[1]Optical density at 570 nm
[2]Optical density at 600 nm
*Significant increase (+) /decrease (-) in biofilm biomass or cell dispersal

Table B.34. Statistical comparison of *V. parahaemolyticus* and *V. vulnificus* overall biofilm biomass[1] and cell dispersal[2] values in different simulated human medias compared to respective MSYE with similar pH.

	Media Type		Coefficient	*p*
V. parahaemolyticus	**SGF**	**Biofilm Biomass**	-0.47	1.00
		Cell Dispersal	-0.04	1.00

	SIF	**Biofilm Biomass**	-0.75	1.00
		Cell Dispersal	-0.04	1.00
	HPLM	**Biofilm Biomass**	1.46	0.35
		Cell Dispersal	-0.03	1.00
V. vulnificus	**SGF**	**Biofilm Biomass**	-0.08	1.00
		Cell Dispersal	-0.03	1.00
	SIF	**Biofilm Biomass**	-0.11	1.00
		Cell Dispersal	-0.03	1.00
	HPLM	**Biofilm Biomass**	0.37*	≤0.05
		Cell Dispersal	-0.001	1.00

[1]Optical density at 570 nm
[2]Optical density at 600 nm
*Significant increase (+) /decrease (-) in biofilm biomass or cell dispersal

Table B.35. Statistical comparison of *V. parahaemolyticus* and *V. vulnificus* overall biofilm biomass[1] and cell dispersal[2] values in different simulated human medias at 37°C compared to MSYE and 25°C.

	Media Type		**Coefficient**	***p***
V. parahaemolyticus	**SGF**	**Biofilm Biomass**	-0.06	1.00
		Cell Dispersal	-0.03	1.00
	SIF	**Biofilm Biomass**	-0.51	1.00
		Cell Dispersal	-0.02	1.00
	HPLM	**Biofilm Biomass**	-0.13	1.00

		Cell Dispersal	-0.03	1.00
V. vulnificus	**SGF**	**Biofilm Biomass**	-0.06	1.00
		Cell Dispersal	-0.04	1.00
	SIF	**Biofilm Biomass**	-0.06	1.00
		Cell Dispersal	-0.04	1.00
	HPLM	**Biofilm Biomass**	0.01	1.00
		Cell Dispersal	-0.01	1.00

[1]Optical density at 570 nm
[2]Optical density at 600 nm

Table B.36. Statistical comparison of *V. vulnificus* overall biofilm biomass[1] and cell dispersal[2] values in different simulated human medias compared to *V. parahaemolyticus*.

	Media Type		**Coefficient**	***p***
V. vulnificus	**SGF**	**Biofilm Biomass**	-1.4*	≤0.01
		Cell Dispersal	-0.01	1.00
	SIF	**Biofilm Biomass**	-1.4*	≤0.01
		Cell Dispersal	-0.01	1.00
	HPLM	**Biofilm Biomass**	-1.4*	≤0.01
		Cell Dispersal	-0.02	1.00

[1]Optical density at 570 nm
[2]Optical density at 600 nm

*Significant increase (+) /decrease (-) in biofilm biomass or cell dispersal

Table B.37. Statistical comparison of *V. vulnificus* overall biofilm biomass[1] and cell dispersal[2] values in different simulated human medias at 37 °C compared to *V. parahaemolyticus* and 25°C.

	Media Type		**Coefficient**	***p***
V. vulnificus	**SGF**	**Biofilm Biomass**	0.04	1.00
		Cell Dispersal	0.02	1.00
	SIF	**Biofilm Biomass**	0.04	1.00
		Cell Dispersal	0.02	1.00
	HPLM	**Biofilm Biomass**	0.04	1.00
		Cell Dispersal	0.02	1.00

[1]Optical density at 570 nm
[2]Optical density at 600 nm
*Significant increase (+) /decrease (-) in biofilm biomass or cell dispersal

Table B.38. Statistical comparison of *V. vulnificus* overall biofilm biomass[1] and cell dispersal[2] values in different simulated human medias compared to MSYE and *V. parahaemolyticus*.

	Media Type		**Coefficient**	***p***
V. vulnificus	**SGF**	**Biofilm Biomass**	0.4	1.00
		Cell Dispersal	0.01	1.00
	SIF	**Biofilm Biomass**	0.6	1.00
		Cell Dispersal	0.01	1.00
	HPLM	**Biofilm Biomass**	-1.1	0.52

		Cell Dispersal	0.03	1.00

[1]Optical density at 570 nm
[2]Optical density at 600 nm
*Significant increase (+) /decrease (-) in biofilm biomass or cell dispersal

Table B.39. Statistical comparison of *V. vulnificus* overall biofilm biomass[1] and cell dispersal[2] values in different simulated human medias at 37°C compared to MSYE, 25°C and *V. parahaemolyticus*.

	Media Type		**Coefficient**	***p***
V. vulnificus	**SGF**	**Biofilm Biomass**	2.5E-04	1.00
		Cell Dispersal	-0.02	1.00
	SIF	**Biofilm Biomass**	0.45	1.00
		Cell Dispersal	-0.02	1.00
	HPLM	**Biofilm Biomass**	0.14	1.00
		Cell Dispersal	0.01	1.00

[1]Optical density at 570 nm
[2]Optical density at 600 nm
*Significant increase (+) /decrease (-) in biofilm biomass or cell dispersal

Table B.40. Effect of media composition on *V. parahaemolyticus* and *V. vulnificus* overall biofilm metabolic activity[1].

Species	**Time (mins)**	**SGF**	**SIF**	**HPLM**
V. parahaemolyticus	0	69553	80945	52938
	15	1	3943	332720

	30	1	5538	404464
	45	1	9409	318552
	60	24	13741	244572
	75	3	17750	208055
	90	82	20823	169183
	105	88	23614	147350
	120	40	25607	126688
	135	174	31055	112723
	150	77	30834	98846
	165	362	35176	89673
	180	89	34803	82599
	195	429	40118	75411
	210	420	40754	69570
	225	459	43518	64180
	240	951	41949	57442
V. vulnificus	0	610318	250145	69480

15	1584	13677	186077
30	1	11518	243303
45	1	11692	323263
60	1	12774	317020
75	1	13360	259164
90	1	14338	225203
105	1	15633	206583
120	1	12691	186356
135	1	15726	172002
150	1	13942	149915
165	1	22481	136072
180	1	13753	122840
195	1	17789	111703
210	1	17098	103603
225	1	17161	97785
240	1	14964	91554

[1]RFU values were divided by corresponding optical density at 600 nm values for normalization.

Table B.41. Effect of media composition on mean biofilm biomass[1] on LDPE[2] by *V. parahaemolyticus* and *V. vulnificus*.

Species	SGF (25°C) (± SD)	SGF (37°C) (± SD)	SIF (25°C) (± SD)	SIF (37°C) (± SD)	HPLM (25°C) (± SD)	HPLM (37°C) (± SD)
V. parahaemolyticus	0.0218	0.0091	0.0220	0.0169	0.0158	0.0057
	0.0077	0.0036	0.0085	0.0059	0.0077	0.0071
V. vulnificus	0.0005	0.0004	0.0003	0.0001	0.0028	0.0056
	0.0000	0.0001	0.0001	0.0001	0.0017	0.0016

[1]Optical density at 570 nm
[2]Biomass values divided by total microplastic surface area (24 mm^2)
(± SD) Standard deviation

Table B.42. Effect of media composition on mean CFUs[1] on LDPE[2] by *V. parahaemolyticus* and *V. vulnificus*.

Species	SGF (25°C) (± SD)	SGF (37°C) (± SD)	SIF (25°C) (± SD)	SIF (37°C) (± SD)	HPLM (25°C) (± SD)	HPLM (37°C) (± SD)
V. parahaemolyticus	0.0000	0.0000	4.6892	0.0000	5.8985	5.4851
	0.0000	0.0000	4.4200	0.0000	5.3655	4.3129
V. vulnificus	0.0000	0.0000	0.0000	0.0000	4.1680	3.8669
	0.0000	0.0000	0.0000	0.0000	3.6705	3.1653

[1]CFU values were log transformed
[2]CFU values divided by total coupon surface area (24 mm^2)
(± SD) Standard deviation

Table B.43. Effect of media composition on mean cell colonization[1] on microplates from LDPE by *V. parahaemolyticus* and *V. vulnificus*.

Species	SGF (25°C) (± SD)	SGF (37°C) (± SD)	SIF (25°C) (± SD)	SIF (37°C) (± SD)	HPLM (25°C) (± SD)	HPLM (37°C) (± SD)
V. parahaemolyticus	0.0756	0.0591	0.0293	0.0549	0.0682	0.0369
	0.0344	0.0090	0.0103	0.0154	0.0083	0.0228
V. vulnificus	0.0009	0.0252	0.0000	0.0220	0.1455	0.2182
	0.0016	0.0112	0.0000	0.0043	0.1023	0.0739

[1]Optical density at 570 nm
(± SD) Standard deviation

Table B.44. Effect of media composition on mean CFUs[1] dispersed from LDPE by *V. parahaemolyticus* and *V. vulnificus*.

Species	SGF (25°C) (± SD)	SGF (37°C) (± SD)	SIF (25°C) (± SD)	SIF (37°C) (± SD)	HPLM (25°C) (± SD)	HPLM (37°C) (± SD)
V. parahaemolyticus	0.0000	0.0000	5.0374	0.0000	7.4260	7.5984
	0.0000	0.0000	4.1799	0.0000	6.6065	6.5455
V. vulnificus	0.0000	0.0000	0.0000	0.0000	5.8902	5.9853
	0.0000	0.0000	0.0000	0.0000	5.3334	5.6065

[1]CFU values were log transformed.
(± SD) Standard deviation

Table B.45. Effect of media composition on mean biofilm biomass[1] on PP[2] by *V. parahaemolyticus* and *V. vulnificus*.

Species	SGF (25°C) (± SD)	SGF (37°C) (± SD)	SIF (25°C) (± SD)	SIF (37°C) (± SD)	HPLM (25°C) (± SD)	HPLM (37°C) (± SD)
V. parahaemolyticus	0.0130	0.0058	0.0237	0.0086	0.0201	0.0102
	0.0025	0.0008	0.0048	0.0012	0.0038	0.0086

V. vulnificus	0.0001	0.0002	0.0000	0.0000	0.0006	0.0018
	0.0002	0.0001	0.0000	0.0000	0.0005	0.0004

[1]Optical density at 570 nm
[2]Biomass values divided by total microplastic surface area (24 mm^2)
(± SD) Standard deviation

Table B.46. Effect of media composition on mean CFUs[1] on PP[2] by *V. parahaemolyticus* and *V. vulnificus*.

Species	**SGF (25°C)** (± SD)	**SGF (37°C)** (± SD)	**SIF (25°C)** (± SD)	**SIF (37°C)** (± SD)	**HPLM (25°C)** (± SD)	**HPLM (37°C)** (± SD)
V. parahaemolyticus	0.0000	0.0000	3.6572	0.0000	5.3245	5.3930
	0.0000	0.0000	2.7997	0.0000	4.5749	4.0206
V. vulnificus	0.0000	0.0000	0.0000	0.0000	3.2033	3.3705
	0.0000	0.0000	0.0000	0.0000	2.4432	2.6205

[1]CFU values were log transformed
[2]CFU values divided by total coupon surface area (24 mm^2)
(± SD) Standard deviation

Table B.47. Effect of media composition on mean cell colonization[1] on microplates from PP by *V. parahaemolyticus* and *V. vulnificus*.

Species	**SGF (25°C)** (± SD)	**SGF (37°C)** (± SD)	**SIF (25°C)** (± SD)	**SIF (37°C)** (± SD)	**HPLM (25°C)** (± SD)	**HPLM (37°C)** (± SD)
V. parahaemolyticus	0.0476	0.0378	0.0340	0.0444	0.0482	0.0381
	0.0039	0.0162	0.0033	0.0045	0.0173	0.0258
V. vulnificus	0.0000	0.0225	0.0000	0.0482	0.0158	0.0436
	0.0000	0.0069	0.0000	0.0501	0.0075	0.0080

[1]Optical density at 570 nm
(± SD) Standard deviation

Table B.48. Effect of media composition on mean CFUs[1] dispersed from PP by *V. parahaemolyticus* and *V. vulnificus*.

Species	SGF (25°C) (± SD)	SGF (37°C) (± SD)	SIF (25°C) (± SD)	SIF (37°C) (± SD)	HPLM (25°C) (± SD)	HPLM (37°C) (± SD)
V. parahaemolyticus	0.0000	0.0000	6.9395	0.0000	7.2710	7.4819
	0.0000	0.0000	6.1288	0.0000	6.1840	6.7410
V. vulnificus	0.0000	0.0000	0.0000	0.0000	4.6056	5.0334
	0.0000	0.0000	0.0000	0.0000	3.9755	3.9842

[1]CFU values were log transformed
(± SD) Standard deviation

Table B.49. Effect of media composition on mean biofilm biomass[1] on PS[2] by *V. parahaemolyticus* and *V. vulnificus*.

Species	SGF (25°C) (± SD)	SGF (37°C) (± SD)	SIF (25°C) (± SD)	SIF (37°C) (± SD)	HPLM (25°C) (± SD)	HPLM (37°C) (± SD)
V. parahaemolyticus	0.0087	0.0132	0.0065	0.0129	0.0256	0.0234
	0.0024	0.0016	0.0015	0.0026	0.0119	0.0072
V. vulnificus	0.0065	0.0014	0.0083	0.0124	0.0021	0.0139
	0.0028	0.0021	0.0012	0.0025	0.0025	0.0070

[1]Optical density at 570 nm
[2]Biomass values divided by total microplastic surface area (14 mm^2)
(± SD) Standard deviation

Table B.50. Effect of media composition on mean CFUs[1] on PS[2] by *V. parahaemolyticus* and *V. vulnificus*.

Species	SGF (25°C) (± SD)	SGF (37°C) (± SD)	SIF (25°C) (± SD)	SIF (37°C) (± SD)	HPLM (25°C) (± SD)	HPLM (37°C) (± SD)
V. parahaemolyticus	0.0000	0.0000	2.1010	0.0000	4.3405	4.6271
	0.0000	0.0000	1.8713	0.0000	3.5557	3.3143
V. vulnificus	0.0000	0.0000	1.6555	0.0000	3.9809	5.9985
	0.0000	0.0000	1.4604	0.0000	3.1819	5.6387

[1]CFU values were log transformed.
[2]CFU values divided by total coupon surface area (14 mm^2)
(± SD) Standard deviation

Table B.51. Effect of media composition on mean cell colonization[1] on microplates from PS by *V. parahaemolyticus* and *V. vulnificus*.

Species	SGF (25°C) (± SD)	SGF (37°C) (± SD)	SIF (25°C) (± SD)	SIF (37°C) (± SD)	HPLM (25°C) (± SD)	HPLM (37°C) (± SD)
V. parahaemolyticus	0.0000	0.0250	0.0071	0.0412	0.0401	0.0882
	0.0000	0.0072	0.0063	0.0082	0.0327	0.0320
V. vulnificus	0.0010	0.0297	0.0013	0.0497	0.0298	0.1950
	0.0017	0.0119	0.0022	0.0190	0.0262	0.1344

[1]Optical density at 570 nm
(± SD) Standard deviation

Table B.52. Effect of media composition on mean CFUs[1] dispersed from PS by *V. parahaemolyticus* and *V. vulnificus*.

Species	SGF (25°C) (± SD)	SGF (37°C) (± SD)	SIF (25°C) (± SD)	SIF (37°C) (± SD)	HPLM (25°C) (± SD)	HPLM (37°C) (± SD)
V. parahaemolyticus	0.0000	0.0000	5.5141	0.0000	6.1760	6.0000
	0.0000	0.0000	4.8466	0.0000	5.8406	5.7157
V. vulnificus	0.0000	0.0000	0.0000	0.0000	5.2648	5.9378
	0.0000	0.0000	0.0000	0.0000	4.4998	5.4912

[1]CFU values were log transformed.
(± SD) Standard deviation

Table B.53. Statistical comparison of *V. parahaemolyticus* and *V. vulnificus* biofilm biomass[1], biofilm cell[2], cell colonization[1] and cell dispersal[2] values on/from LDPE[3], PP[3] and PS[4] in different simulated human medias compared to respective MSYE with similar pH.

	Surface Type	Media Type		Coefficient	*p*
V. parahaemolyticus	**LDPE**	**SGF**	**Biofilm Biomass**	0.28	0.92
			Biofilm Cells	-1.6E05	1.00
			Cell Colonization	-0.1	1.00
			Cell Dispersal	-4.0E07	1.00

PP	**SGF**	**Biofilm Biomass**	0.11	1.00
		Biofilm Cells	-3.4E04	1.00
		Cell Colonization	-0.02	1.00
		Cell Dispersal	-4.2E07	1.00
PS	**SGF**	**Biofilm Biomass**	0.07	0.3
		Biofilm Cells	-5.2E03	1.00
		Cell Colonization	-0.04	1.00
		Cell Dispersal	-4.2E06	1.00
LDPE	**SIF**	**Biofilm Biomass**	0.28	0.88
		Biofilm Cells	-1.1E05	1.00
		Cell Colonization	-0.14	1.00
		Cell Dispersal	-4.0E07	1.00
PP	**SIF**	**Biofilm Biomass**	0.37	0.12
		Biofilm Cells	-3.0E4	1.00
		Cell Colonization	-0.04	1.00
		Cell Dispersal	-3.3E07	1.00
PS	**SIF**	**Biofilm Biomass**	0.04	1.00
		Biofilm Cells	-5.1E03	1.00

			Cell Colonization	-0.03	1.00
			Cell Dispersal	-3.9E06	1.00
	LDPE	**HPLM**	**Biofilm Biomass**	0.13	1.00
			Biofilm Cells	6.3E05	0.22
			Cell Colonization	-0.12	1.00
			Cell Dispersal	-1.3E07	1.00
	PP	**HPLM**	**Biofilm Biomass**	0.27	0.27
			Biofilm Cells	1.7E05	1.00
			Cell Colonization	-0.02	1.00
			Cell Dispersal	-2.4E07	1.00
	PS	**HPLM**	**Biofilm Biomass**	0.31*	≤0.01
			Biofilm Cells	1.6E04	0.35
			Cell Colonization	2.0E-03	1.00
			Cell Dispersal	-2.7E06	1.00
V. vulnificus	**LDPE**	**SGF**	**Biofilm Biomass**	-0.02	1.00
			Biofilm Cells	-1.5E02	1.00
			Cell Colonization	-0.03	1.00
			Cell Dispersal	-1.6E05	1.00

PP	**SGF**	**Biofilm Biomass**	-0.007	1.00
		Biofilm Cells	-2.39E02	1.00
		Cell Colonization	-0.02	1.00
		Cell Dispersal	-2.8E05	1.00
PS	**SGF**	**Biofilm Biomass**	0.06*	≤0.01
		Biofilm Cells	-1.6E03	1.00
		Cell Colonization	-0.02	1.00
		Cell Dispersal	-1.3E05	1.00
LDPE	**SIF**	**Biofilm Biomass**	-0.02	1.00
		Biofilm Cells	-1.5E02	1.00
		Cell Colonization	-0.03	1.00
		Cell Dispersal	-1.6E05	1.00
PP	**SIF**	**Biofilm Biomass**	-0.01	1.00
		Biofilm Cells	-2.39E02	1.00
		Cell Colonization	-0.02	1.00
		Cell Dispersal	-2.8E05	1.00
PS	**SIF**	**Biofilm Biomass**	0.09*	≤0.01
		Biofilm Cells	-1.6E03	1.00

		Cell Colonization	-0.02	1.00
		Cell Dispersal	-1.5E05	1.00
LDPE	**HPLM**	**Biofilm Biomass**	0.04	1.00
		Biofilm Cells	1.3E04*	≤0.01
		Cell Colonization	0.11	0.15
		Cell Dispersal	6.1E05	1.00
PP	**HPLM**	**Biofilm Biomass**	0.006	1.00
		Biofilm Cells	1.3E03	0.76
		Cell Colonization	-0.003	1.00
		Cell Dispersal	-2.5E05	1.00
PS	**HPLM**	**Biofilm Biomass**	0.05*	≤0.05
		Biofilm Cells	7.8E03	1.00
		Cell Colonization	0.01	1.00
		Cell Dispersal	3.4E04	1.00

[1]Optical density at 570 nm
[2]CFU values were log transformed
[3]Biofilm biomass and CFU values on plastic divided by total coupon surface area (24 mm^2)
[4]Biofilm biomass and CFU values on plastic divided by total coupon surface area (14 mm^2)
*Significant increase (+) /decrease (-) in biofilm biomass or cell dispersal

Table B.54. Statistical overall comparison of *V. parahaemolyticus* and *V. vulnificus* biofilm biomass[1], biofilm cell[2], cell colonization[1] and cell dispersal[2] values on/from LDPE[3], PP[3] and PS[4] at 37°C compared to 25°C.

	Surface Type		Coefficient	*p*
V. parahaemolyticus	**LDPE**	**Biofilm Biomass**	0.03	1.00
		Biofilm Cells	-7.9E04	1.00
		Cell Colonization	0.09	1.00
		Cell Dispersal	-2.3E07	1.00
	PP	**Biofilm Biomass**	-0.03	1.00
		Biofilm Cells	1.2E05	1.00
		Cell Colonization	0.08	1.00
		Cell Dispersal	9.7E06	1.00
	PS	**Biofilm Biomass**	-0.03	1.00
		Biofilm Cells	6.7E02	1.00
		Cell Colonization	0.05	1.00
		Cell Dispersal	1.7E07	1.00
V. vulnificus	**LDPE**	**Biofilm Biomass**	8.0E-03	1.00
		Biofilm Cells	-1.2E03	1.00
		Cell Colonization	-2.0E-03	1.00
		Cell Dispersal	3.1E06	1.00

PP	**Biofilm Biomass**	0.01	1.00
	Biofilm Cells	1.83E02	1.00
	Cell Colonization	0.02	1.00
	Cell Dispersal	1.3E06	1.00
PS	**Biofilm Biomass**	-0.004	1.00
	Biofilm Cells	1.7E03	1.00
	Cell Colonization	0.01	1.00
	Cell Dispersal	6.3E06	1.00

[1]Optical density at 570 nm
[2]CFU values were log transformed
[3]Biofilm biomass and CFU values on plastic divided by total coupon surface area (24 mm^2)
[4]Biofilm biomass and CFU values on plastic divided by total coupon surface area (14 mm^2)
*Significant increase (+) /decrease (-) in biofilm biomass or cell dispersal

Table B.55. Statistical comparison of *V. parahaemolyticus* and *V. vulnificus* biofilm biomass[1], biofilm cell[2], cell colonization[1] and cell dispersal[2] values on/from LDPE[3], PP[3] and PS[4] in different simulated human medias at 37°C compared to MSYE and 25°C.

	Surface Type	**Media Type**		**Coefficient**	***p***
V. parahaemolyticus	**LDPE**	**SGF**	**Biofilm Biomass**	-0.33	1.00
			Biofilm Cells	7.9E05	1.00
			Cell Colonization	-0.11	1.00
			Cell Dispersal	2.3E07	1.00

PP	**SGF**	**Biofilm Biomass**	-0.12	1.00
		Biofilm Cells	-1.2E05	1.00
		Cell Colonization	-0.09	1.00
		Cell Dispersal	-9.7E06	1.00
PS	**SGF**	**Biofilm Biomass**	0.09	0.4
		Biofilm Cells	-6.7E02	1.00
		Cell Colonization	-0.02	1.00
		Cell Dispersal	-1.7E07	1.00
LDPE	**SIF**	**Biofilm Biomass**	-0.15	1.00
		Biofilm Cells	3.0E05	1.00
		Cell Colonization	-0.07	1.00
		Cell Dispersal	2.3E07	1.00
PP	**SIF**	**Biofilm Biomass**	-0.31	0.53
		Biofilm Cells	-1.2E05	1.00
		Cell Colonization	-0.07	1.00
		Cell Dispersal	-1.8E07	1.00
PS	**SIF**	**Biofilm Biomass**	0.12	0.19
		Biofilm Cells	-8.0E02	1.00

			Cell Colonization	-0.02	1.00
			Cell Dispersal	-1.8E07	1.00
	LDPE	**HPLM**	**Biofilm Biomass**	-0.27	1.00
			Biofilm Cells	-4.1E05	1.00
			Cell Colonization	-0.12	1.00
			Cell Dispersal	3.6E07	1.00
	PP	**HPLM**	**Biofilm Biomass**	-0.18	1.00
			Biofilm Cells	-8.3E04	1.00
			Cell Colonization	-0.09	1.00
			Cell Dispersal	1.9E06	1.00
	PS	**HPLM**	**Biofilm Biomass**	1.0E-03	1.00
			Biofilm Cells	1.9E04	0.57
			Cell Colonization	-2.0E-03	1.00
			Cell Dispersal	-1.8E07	1.00
V. vulnificus	**LDPE**	**SGF**	**Biofilm Biomass**	-0.01	1.00
			Biofilm Cells	1.2E03	1.00
			Cell Colonization	0.02	1.00
			Cell Dispersal	-3.1E06	1.00

PP	**SGF**	**Biofilm Biomass**	-0.01	1.00
		Biofilm Cells	-1.8E02	1.00
		Cell Colonization	2.0E-04	1.00
		Cell Dispersal	-1.3E06	1.00
PS	**SGF**	**Biofilm Biomass**	0.04	0.11
		Biofilm Cells	-1.7E03	1.00
		Cell Colonization	0.01	1.00
		Cell Dispersal	-6.3E06	1.00
LDPE	**SIF**	**Biofilm Biomass**	-0.01	1.00
		Biofilm Cells	1.2E03	1.00
		Cell Colonization	0.02	1.00
		Cell Dispersal	-3.1E06	1.00
PP	**SIF**	**Biofilm Biomass**	-9.0E-03	1.00
		Biofilm Cells	-1.8E02	1.00
		Cell Colonization	0.02	1.00
		Cell Dispersal	-1.3E06	1.00
PS	**SIF**	**Biofilm Biomass**	0.06*	≤0.05
		Biofilm Cells	-1.7E03	1.00

		Cell Colonization	0.03	1.00
		Cell Dispersal	-6.3E06	1.00
LDPE	**HPLM**	**Biofilm Biomass**	0.06	1.00
		Biofilm Cells	-6.1E03	0.17
		Cell Colonization	0.07	1.00
		Cell Dispersal	-2.9E06	1.00
PP	**HPLM**	**Biofilm Biomass**	0.04	1.00
		Biofilm Cells	5.6E02	1.00
		Cell Colonization	5.00E-03	1.00
		Cell Dispersal	-1.2E06	1.00
PS	**HPLM**	**Biofilm Biomass**	0.16*	≤0.001
		Biofilm Cells	5.9E04*	≤0.01
		Cell Colonization	0.15	0.19
		Cell Dispersal	-5.7E06	1.00

[1]Optical density at 570 nm
[2]CFU values were log transformed
[3]Biofilm biomass and CFU values on plastic divided by total coupon surface area (24 mm^2)
[4]Biofilm biomass and CFU values on plastic divided by total coupon surface area (14 mm^2)
*Significant increase (+) /decrease (-) in biofilm biomass or cell dispersal

Table B.56. Statistical comparison of *V. vulnificus* biofilm biomass[1], biofilm cell[2], cell colonization[1] and cell dispersal[2] values on/from LDPE[3], PP[3] and PS[4] in different simulated human medias compared to *V. parahaemolyticus*.

	Surface Type	Media Type		Coefficient	*p*
V. vulnificus	**LDPE**	**SGF**	**Biofilm Biomass**	-0.21	0.12
			Biofilm Cells	-1.5E05	1.00
			Cell Colonization	-0.14	0.29
			Cell Dispersal	-4.0E07	0.28
	PP	**SGF**	**Biofilm Biomass**	-0.19*	≤0.05
			Biofilm Cells	-3.4E04	1.00
			Cell Colonization	-0.05	1.00
			Cell Dispersal	-4.2E07	1.00
	PS	**SGF**	**Biofilm Biomass**	-0.019	1.00
			Biofilm Cells	-5.3E03	1.00
			Cell Colonization	-0.02	1.00
			Cell Dispersal	-4.1E06	1.00
	LDPE	**SIF**	**Biofilm Biomass**	-0.21	0.12
			Biofilm Cells	-1.3E05	1.00
			Cell Colonization	-0.14	0.29

		Cell Dispersal	-4.0E07	0.28
PP	**SIF**	**Biofilm Biomass**	-0.19*	≤0.05
		Biofilm Cells	-3.4E04	1.00
		Cell Colonization	-0.05	1.00
		Cell Dispersal	-4.2E07	1.00
PS	**SIF**	**Biofilm Biomass**	-0.02	1.00
		Biofilm Cells	-3.3E03	1.00
		Cell Colonization	-0.02	1.00
		Cell Dispersal	-4.1E06	1.00
LDPE	**HPLM**	**Biofilm Biomass**	-0.21	0.12
		Biofilm Cells	-1.3E05	1.00
		Cell Colonization	-0.14	0.28
		Cell Dispersal	-4.0E07	0.28
PP	**HPLM**	**Biofilm Biomass**	-0.19*	≤0.05
		Biofilm Cells	-3.4E04	1.00
		Cell Colonization	-0.05	1.00
		Cell Dispersal	-4.2E07	1.00
PS	**HPLM**	**Biofilm Biomass**	-0.01	1.00

			Biofilm Cells	-3.5E3	1.00
			Cell Colonization	-0.02	1.00
			Cell Dispersal	-4.1E06	1.00

[1]Optical density at 570 nm
[2]CFU values were log transformed
[3]Biofilm biomass and CFU values on plastic divided by total coupon surface area (24 mm^2)
[4]Biofilm biomass and CFU values on plastic divided by total coupon surface area (14 mm^2)
*Significant increase (+) /decrease (-) in biofilm biomass or cell dispersal

Table B.57. Statistical comparison of *V.* biofilm biomass[1], biofilm cell[2], cell colonization[1] and cell dispersal[2] values on/from LDPE[3], PP[3] and PS[4] at 37 °C compared to *V. parahaemolyticus* and 25°C.

	Surface Type	**Media Type**		**Coefficient**	***p***
V. vulnificus	**LDPE**	**SGF**	**Biofilm Biomass**	-0.02	1.00
			Biofilm Cells	7.6E04	1.00
			Cell Colonization	-0.09	1.00
			Cell Dispersal	2.6E07	1.00
	PP	**SGF**	**Biofilm Biomass**	0.06	1.00
			Biofilm Cells	-1.1E05	1.00
			Cell Colonization	-0.06	1.00
			Cell Dispersal	-8.4E06	1.00

PS	**SGF**	**Biofilm Biomass**	0.03	1.00
		Biofilm Cells	1.1E03	1.00
		Cell Colonization	-0.03	1.00
		Cell Dispersal	-1.1E07	1.00
LDPE	**SIF**	**Biofilm Biomass**	-0.02	1.00
		Biofilm Cells	7.8E05	1.00
		Cell Colonization	-0.09	1.00
		Cell Dispersal	2.6E07	1.00
PP	**SIF**	**Biofilm Biomass**	0.06	1.00
		Biofilm Cells	-1.2E05	1.00
		Cell Colonization	-0.06	1.00
		Cell Dispersal	-8.4E06	1.00
PS	**SIF**	**Biofilm Biomass**	0.03	1.00
		Biofilm Cells	1.1E03	1.00
		Cell Colonization	-0.03	1.00
		Cell Dispersal	-1.1E07	1.00
LDPE	**HPLM**	**Biofilm Biomass**	-0.018	1.00
		Biofilm Cells	7.8E04	1.00

		Cell Colonization	-0.09	1.00
		Cell Dispersal	2.6E07	1.00
PP	**HPLM**	**Biofilm Biomass**	0.06	0.12
		Biofilm Cells	-1.1E05	1.00
		Cell Colonization	-0.06	1.00
		Cell Dispersal	-8.4E06	1.00
PS	**HPLM**	**Biofilm Biomass**	0.03	1.00
		Biofilm Cells	1.0E03	1.00
		Cell Colonization	-0.03	1.00
		Cell Dispersal	-1.1E07	1.00

[1]Optical density at 570 nm
[2]CFU values were log transformed
[3]Biofilm biomass and CFU values on plastic divided by total coupon surface area (24 mm^2)
[4]Biofilm biomass and CFU values on plastic divided by total coupon surface area (14 mm^2)
*Significant increase (+) /decrease (-) in biofilm biomass or cell dispersal

Table B.58. Statistical comparison of *V. vulnificus* biofilm biomass[1], biofilm cell[2], cell colonization[1] and cell dispersal[2] values on/from LDPE[3], PP[3] and PS[4] in different simulated human medias compared to MSYE and *V. parahaemolyticus*.

	Surface Type	**Media Type**		**Coefficient**	***p***
V. vulnificus	**LDPE**	**SGF**	**Biofilm Biomass**	-0.3	0.56

		Biofilm Cells	1.5E05	1.00
		Cell Colonization	0.06	1.00
		Cell Dispersal	4.0E07	1.00
PP	**SGF**	**Biofilm Biomass**	-0.11	1.00
		Biofilm Cells	3.4E04	1.00
		Cell Colonization	2.0E-03	1.00
		Cell Dispersal	4.2E07	1.00
PS	**SGF**	**Biofilm Biomass**	-0.01	1.00
		Biofilm Cells	3.5E03	1.00
		Cell Colonization	0.02	1.00
		Cell Dispersal	4.1E06	1.00
LDPE	**SIF**	**Biofilm Biomass**	-0.3	0.52
		Biofilm Cells	1.1E05	1.00
		Cell Colonization	0.11	1.00
		Cell Dispersal	4.0E07	1.00
PP	**SIF**	**Biofilm Biomass**	-0.4*	≤0.05
		Biofilm Cells	3.0E04	1.00
		Cell Colonization	0.01	1.00

		Cell Dispersal	3.3E07	1.00
PS	**SIF**	**Biofilm Biomass**	0.04	0.93
		Biofilm Cells	3.4E03	1.00
		Cell Colonization	0.01	1.00
		Cell Dispersal	3.7E06	1.00
LDPE	**HPLM**	**Biofilm Biomass**	-0.09	1.00
		Biofilm Cells	-6.2E05	0.08
		Cell Colonization	0.21	0.71
		Cell Dispersal	1.4E07	1.00
PP	**HPLM**	**Biofilm Biomass**	-0.03	0.12
		Biofilm Cells	-1.7E05	1.00
		Cell Colonization	0.02	1.00
		Cell Dispersal	2.3E07	1.00
PS	**HPLM**	**Biofilm Biomass**	-0.26*	≤0.001
		Biofilm Cells	-8.8E03	1.00
		Cell Colonization	0.01	1.00
		Cell Dispersal	2.8E06	1.00

[1]Optical density at 570 nm
[2]CFU values were log transformed

[3]Biofilm biomass and CFU values on plastic divided by total coupon surface area (24 mm^2)
[4]Biofilm biomass and CFU values on plastic divided by total coupon surface area (14 mm^2)
*Significant increase (+) /decrease (-) in biofilm biomass or cell dispersal

Table B.59. Statistical comparison of *V. vulnificus* biofilm biomass[1], biofilm cell[2], cell colonization[1] and cell dispersal[2] values on/from LDPE[3], PP[3] and PS[4] in different simulated human medias at 37°C compared to MSYE, 25°C and *V. parahaemolyticus*.

	Surface Type	**Media Type**		**Coefficient**	***p***
V. vulnificus	**LDPE**	**SGF**	**Biofilm Biomass**	0.31	1.00
			Biofilm Cells	-7.9E04	1.00
			Cell Colonization	0.13	1.00
			Cell Dispersal	-2.7E07	1.00
	PP	**SGF**	**Biofilm Biomass**	0.11	1.00
			Biofilm Cells	1.2E05	1.00
			Cell Colonization	0.09	1.00
			Cell Dispersal	8.4E06	1.00
	PS	**SGF**	**Biofilm Biomass**	-0.03	1.00
			Biofilm Cells	-1.1E03	1.00
			Cell Colonization	0.04	1.00

		Cell Dispersal	1.1E07	1.00
LDPE	**SIF**	**Biofilm Biomass**	0.13	1.00
		Biofilm Cells	-2.9E04	1.00
		Cell Colonization	0.09	1.00
		Cell Dispersal	-2.7E07	1.00
PP	**SIF**	**Biofilm Biomass**	0.3	0.34
		Biofilm Cells	1.2E05	1.00
		Cell Colonization	0.1	1.00
		Cell Dispersal	1.7E07	1.00
PS	**SIF**	**Biofilm Biomass**	-0.03	1.00
		Biofilm Cells	-9.3E02	1.00
		Cell Colonization	0.05	1.00
		Cell Dispersal	1.2E07	1.00
LDPE	**HPLM**	**Biofilm Biomass**	0.32	1.00
		Biofilm Cells	4.0E05	1.00
		Cell Colonization	0.19	1.00
		Cell Dispersal	-4.0E07	1.00
PP	**HPLM**	**Biofilm Biomass**	0.22	0.94

		Biofilm Cells	8.4E04	1.00
		Cell Colonization	0.09	1.00
		Cell Dispersal	-3.2E06	1.00
PS	**HPLM**	**Biofilm Biomass**	0.16*	≤0.05
		Biofilm Cells	4.0E04*	≤0.05
		Cell Colonization	0.15	1.00
		Cell Dispersal	1.2E07	1.00

[1]Optical density at 570 nm
[2]CFU values were log transformed.
[3]Biofilm biomass and CFU values on plastic divided by total coupon surface area (24 mm^2)
[4]Biofilm biomass and CFU values on plastic divided by total coupon surface area (14 mm^2)
*Significant increase (+) /decrease (-) in biofilm biomass or cell dispersal.

Table B.60. Effect of media composition on *V. parahaemolyticus* and *V. vulnificus* biofilm and cell dispersal estimated c-di-GMP concentrations (ng/µL) at 37°C.

Species	**MSYE (Biofilm)** **(± SD)**	**MSYE (Dispersal)** **(± SD)**	**SIF (Biofilm)** **(± SD)**	**SIF (Dispersal)** **(± SD)**	**HPLM (Biofilm)** **(± SD)**	**HPLM (Dispersal)** **(± SD)**
V. parahaemolyticus	0.15	0.00	4.92	2.78	0.06	0.00
	0.24	0.00	2.64	2.88	0.15	0.00
V. vulnificus	0.44	0.00	6.99	7.61	0.86	0.07
	0.40	0.00	3.76	3.92	0.22	0.17

(± SD) Standard deviation

Table B.61. Statistical comparison of *V. parahaemolyticus* and *V. vulnificus* c-di-GMP concentrations within biofilms and within dispersal cell states in different medias.

Species	Cell State	Media Comparison	*p*
V. parahaemolyticus	Biofilm	SIF vs MSYE*	≤0.01
		SIF vs HPLM*	≤0.01
		MSYE vs HPLM	0.86
	Dispersal	SIF vs MSYE	0.08
		SIF vs HPLM	0.08
		MSYE vs HPLM	1.00
V. vulnificus	Biofilm	SIF vs MSYE*	≤0.01
		SIF vs HPLM*	≤0.01
		MSYE vs HPLM	0.09
	Dispersal	SIF vs MSYE*	≤0.01
		SIF vs HPLM*	≤0.01
		MSYE vs HPLM	0.12

*Significant difference in c-di-GMP concentrations between medias

Table B.62. Statistical comparison of *V. parahaemolyticus* and *V. vulnificus* c-di-GMP concentrations between biofilm and dispersal cell states within different medias.

Species	Media	*p*
V. parahaemolyticus	MSYE	0.28
	SIF	0.41
	HPLM	0.68
V. vulnificus	MSYE*	≤0.05
	SIF	1.00
	HPLM*	≤0.001

*Significant difference in c-di-GMP concentrations between biofilm and dispersal cell states in this media

Supplementary Figures and Tables

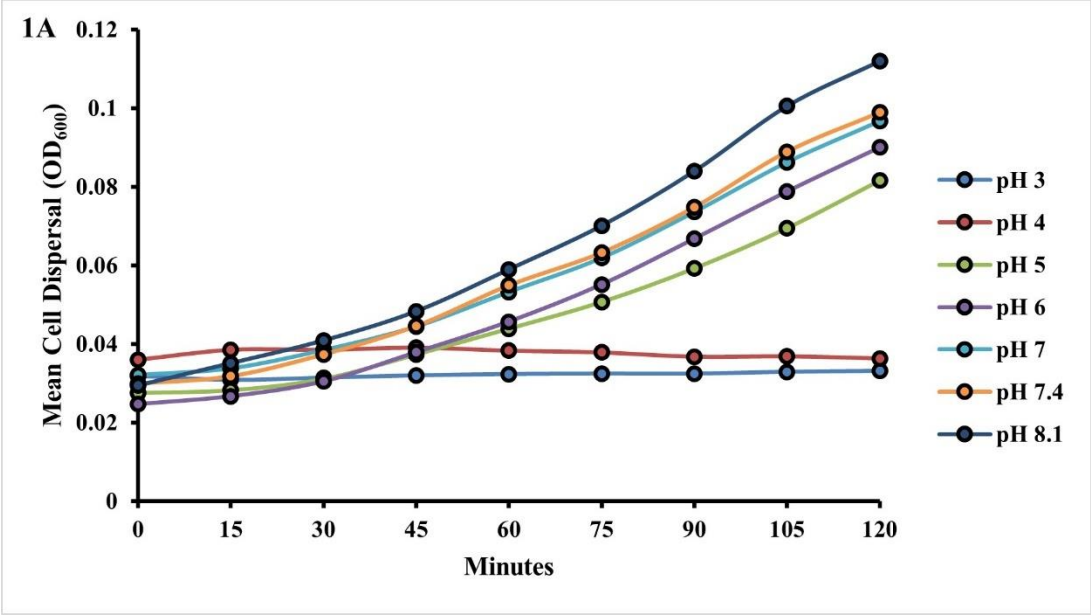

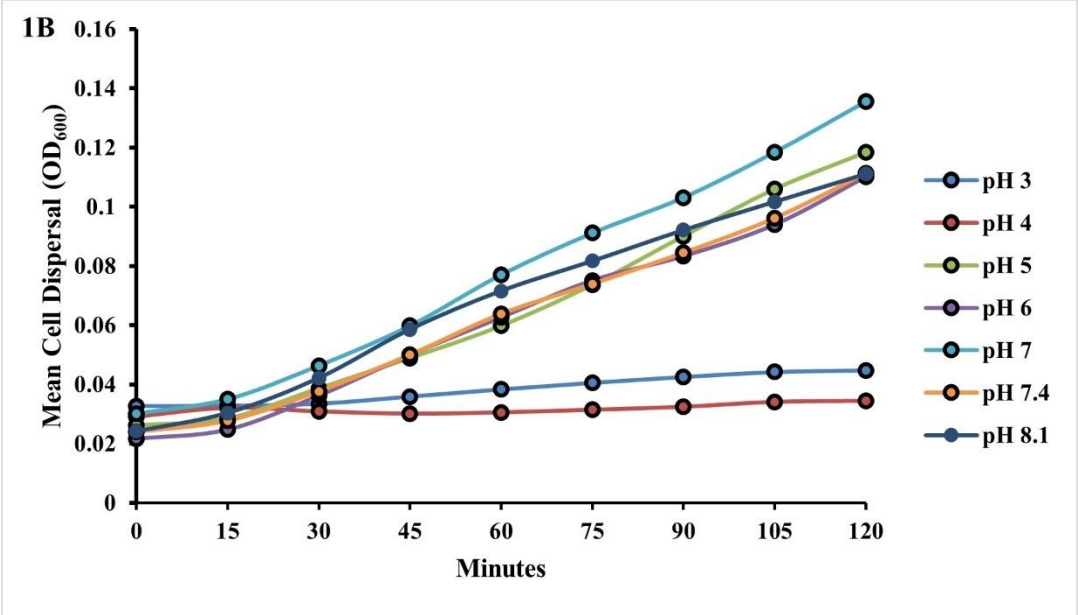
1B
Mean Cell Dispersal (OD600)
0.16
0.14
0.12
0.1
0.08
0.06
0.04
0.02
0
0
15
30
45
60
75
90
105
120
Minutes
pH 3
pH 4
pH 5
pH 6
pH 7
pH 7.4
pH 8.1

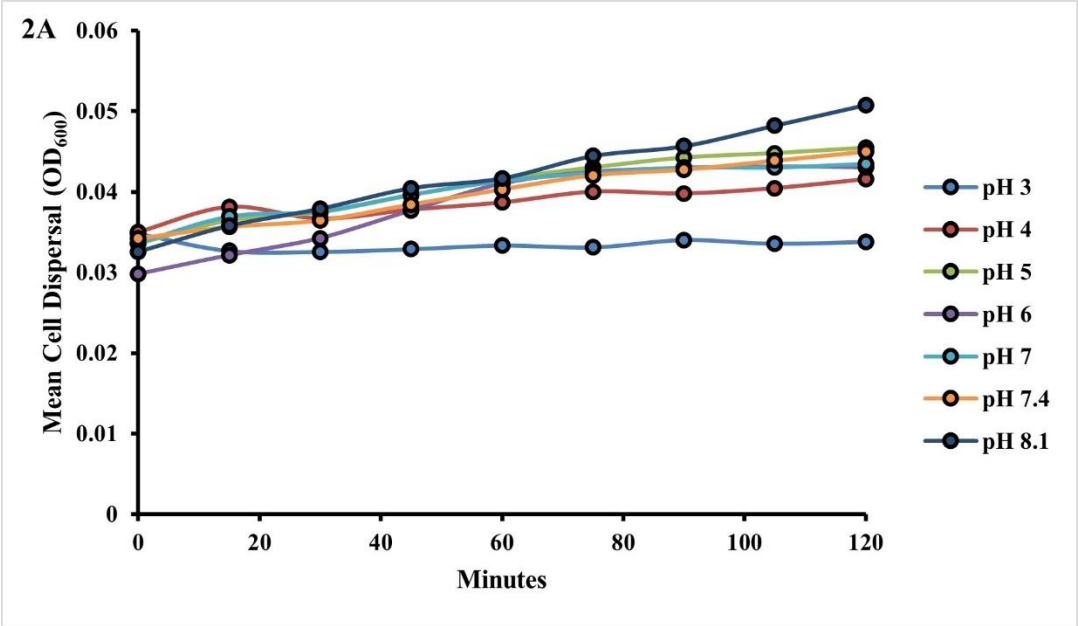
2A
Mean Cell Dispersal (OD600)
0.06
0.05
0.04
0.03
0.02
0.01
0
0
20
40
60
80
100
120
Minutes
pH 3
pH 4
pH 5
pH 6
pH 7
pH 7.4
pH 8.1

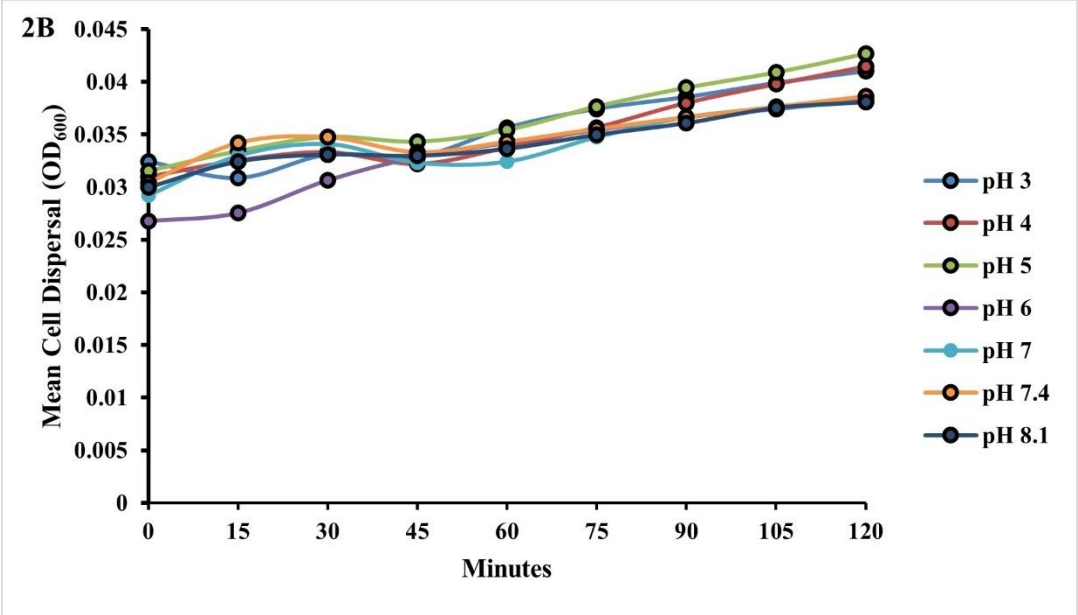

Figure B.1. *V. parahaemolyticus* and *V. vulnificus* cell dispersal (OD_{600}) over time at different pH and temperature in nutrient rich media. Comparison of cell dispersal (means of all biological triplicates and three independent experiments) after 2- hour exposure between *V. parahaemolyticus* at 25 °C (**1A**) and 37°C (**1B**) and *V. vulnificus* at 25 °C (**2A**) and 37°C (**2B**).

Table B.63. *V. parahaemolyticus* and *V. vulnificus* mean cell dispersal[1] values over time at different pH and temperature in nutrient rich media.

Species	Temp	Time (mins)	pH 3	pH 4	pH 5	pH 6	pH 7	pH 7.4	pH 8.1
V. parahaemolyticus	25°C	0	0.0319	0.0360	0.0276	0.0247	0.0321	0.0299	0.0294
	25°C	15	0.0309	0.0386	0.0282	0.0267	0.0338	0.0318	0.0351
	25°C	30	0.0314	0.0386	0.0311	0.0304	0.0384	0.0373	0.0409
	25°C	45	0.0320	0.0391	0.0373	0.0379	0.0444	0.0446	0.0483

	25°C	60	0.0323	0.0383	0.0439	0.0457	0.0532	0.0549	0.0590
	25°C	75	0.0324	0.0379	0.0507	0.0551	0.0619	0.0632	0.0701
	25°C	90	0.0324	0.0368	0.0592	0.0668	0.0736	0.0748	0.0840
	25°C	105	0.0329	0.0369	0.0694	0.0788	0.0862	0.0889	0.1006
	25°C	120	0.0331	0.0363	0.0816	0.0900	0.0967	0.0989	0.1120
V. parahaemolyticus	37°C	0	0.0327	0.0291	0.0261	0.0217	0.0301	0.0240	0.0241
	37°C	15	0.0328	0.0321	0.0284	0.0248	0.0350	0.0278	0.0303
	37°C	30	0.0334	0.0309	0.0387	0.0362	0.0463	0.0377	0.0421
	37°C	45	0.0359	0.0301	0.0489	0.0500	0.0598	0.0500	0.0586
	37°C	60	0.0383	0.0306	0.0598	0.0627	0.0770	0.0638	0.0716
	37°C	75	0.0406	0.0314	0.0737	0.0751	0.0911	0.0739	0.0817
	37°C	90	0.0426	0.0324	0.0901	0.0833	0.1031	0.0844	0.0921
	37°C	105	0.0442	0.0341	0.1060	0.0940	0.1184	0.0961	0.1017
	37°C	120	0.0448	0.0344	0.1184	0.1101	0.1356	0.1112	0.1111
V. vulnificus	25°C	0	0.0063	0.0091	0.0091	0.0118	0.0082	0.0082	0.0083
	25°C	15	0.0066	0.0086	0.0091	0.0120	0.0081	0.0091	0.0081

	25°C	30	0.0061	0.0086	0.0114	0.0140	0.0097	0.0102	0.0093
	25°C	45	0.0060	0.0081	0.0130	0.0179	0.0121	0.0131	0.0117
	25°C	60	0.0064	0.0081	0.0164	0.0240	0.0169	0.0173	0.0162
	25°C	75	0.0071	0.0079	0.0216	0.0313	0.0240	0.0262	0.0229
	25°C	90	0.0070	0.0078	0.0286	0.0392	0.0341	0.0358	0.0300
	25°C	105	0.0068	0.0077	0.0353	0.0488	0.0467	0.0499	0.0401
	25°C	120	0.0064	0.0078	0.0439	0.0602	0.0560	0.0573	0.0537
V. vulnificus	37°C	0	0.0048	0.0057	0.0070	0.0086	0.0058	0.0078	0.0067
	37°C	15	0.0049	0.0058	0.0082	0.0113	0.0072	0.0097	0.0082
	37°C	30	0.0060	0.0056	0.0133	0.0190	0.0127	0.0171	0.0152
	37°C	45	0.0067	0.0051	0.0204	0.0327	0.0277	0.0346	0.0302
	37°C	60	0.0093	0.0052	0.0307	0.0474	0.0524	0.0569	0.0513
	37°C	75	0.0114	0.0054	0.0472	0.0658	0.0753	0.0789	0.0679
	37°C	90	0.0123	0.0056	0.0677	0.0813	0.0901	0.0923	0.0750
	37°C	105	0.0116	0.0060	0.0819	0.0941	0.1008	0.1033	0.0816
	37°C	120	0.0119	0.0062	0.0999	0.1093	0.1131	0.1189	0.0881

[1]Optical density at 600 nm

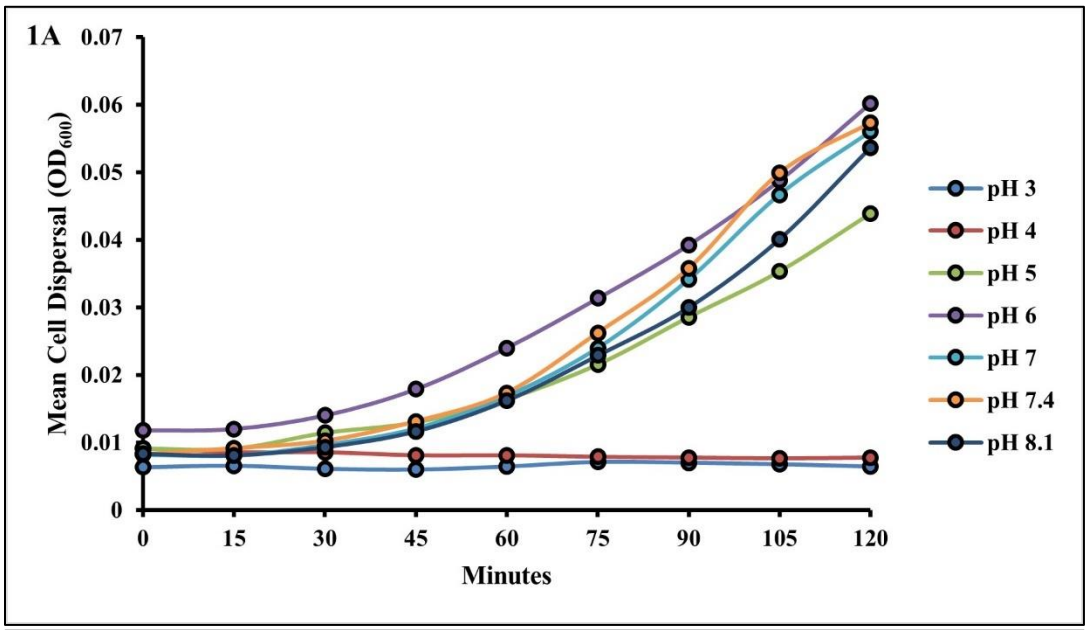

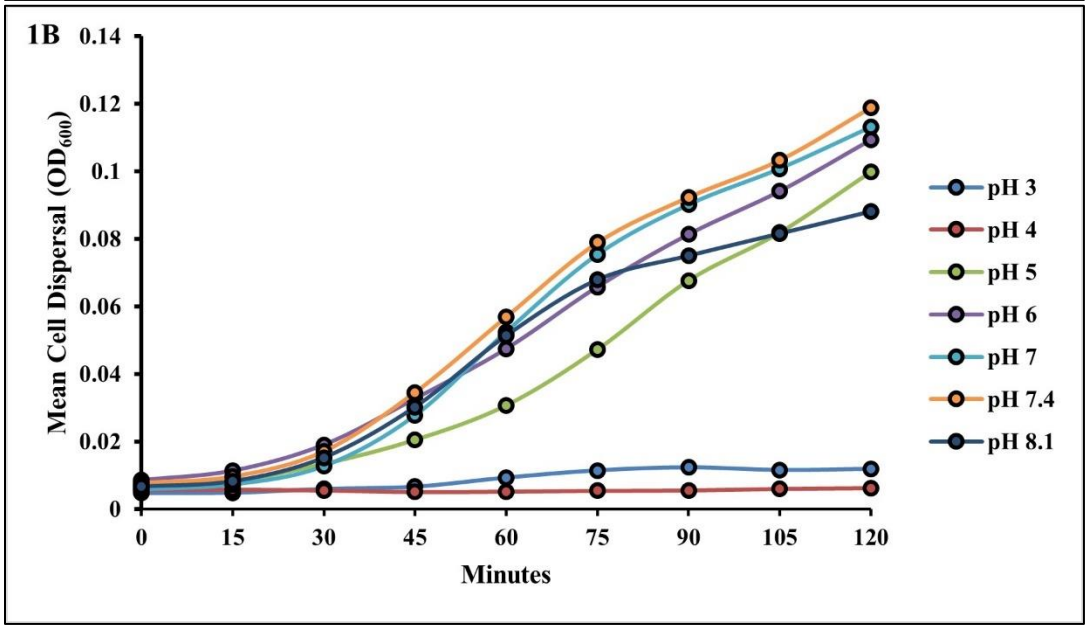

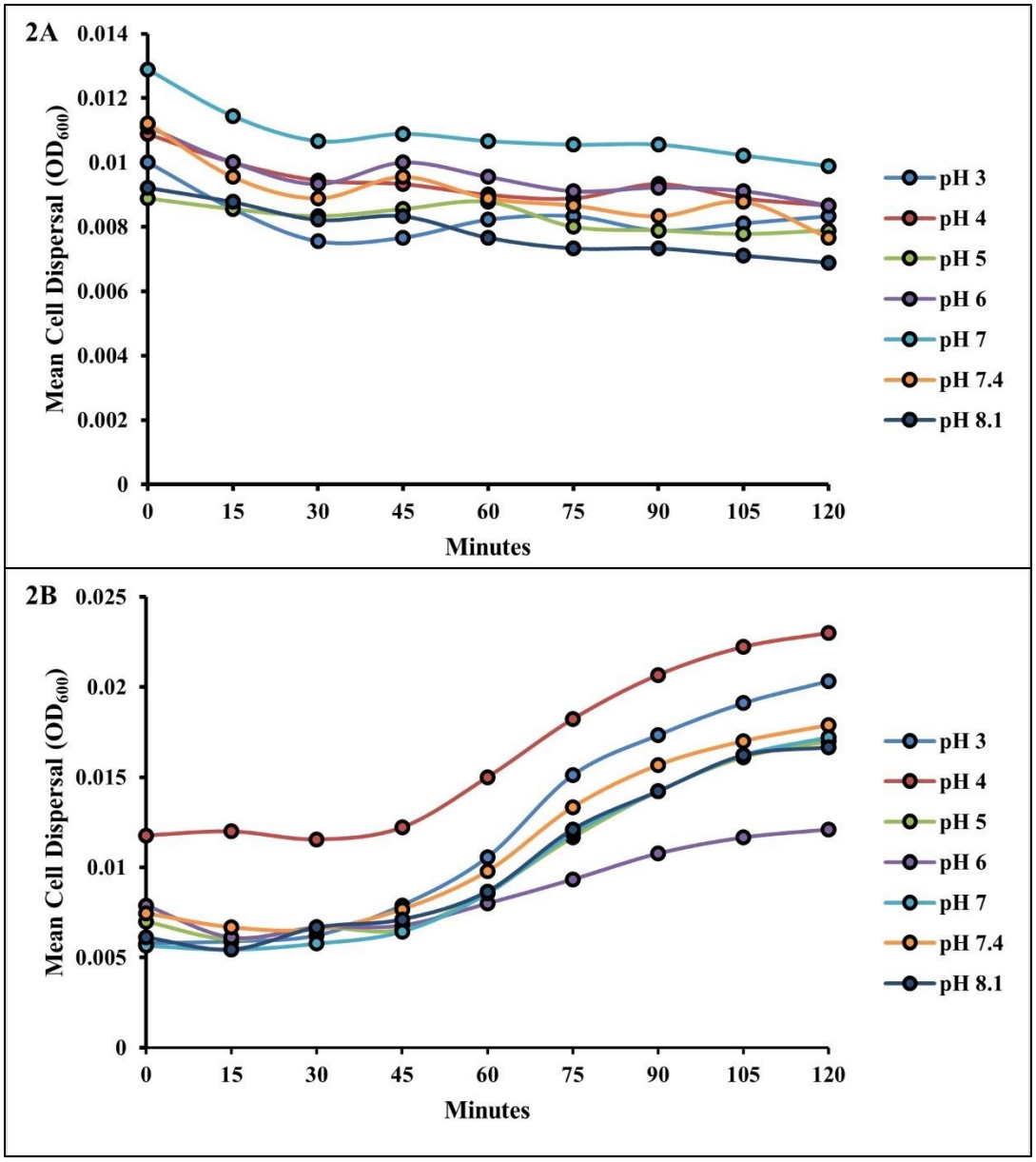

Figure B.2. *V. parahaemolyticus* and *V. vulnificus* cell dispersal (OD_{600}) over time at different pH and temperature in nutrient starved media. Comparison of cell dispersal (means of all biological triplicates and three independent experiments) after 2- hour exposure between *V. parahaemolyticus* at 25 °C (**1A**) and 37°C (**1B**) and *V. vulnificus* at 25 °C (**2A**) and 37°C (**2B**).

Table B.64. *V. parahaemolyticus* and *V. vulnificus* mean cell dispersal[1] values over time at different pH and temperature in nutrient starved media.

Species	Temp	Time (mins)	pH 3	pH 4	pH 5	pH 6	pH 7	pH 7.4	pH 8.1
V. parahaemolyticus	25°C	0	0.0348	0.0350	0.0336	0.0298	0.0337	0.0342	0.0326
	25°C	15	0.0327	0.0381	0.0364	0.0321	0.0369	0.0356	0.0358
	25°C	30	0.0326	0.0367	0.0374	0.0342	0.0376	0.0364	0.0379
	25°C	45	0.0329	0.0378	0.0396	0.0377	0.0396	0.0384	0.0404
	25°C	60	0.0333	0.0387	0.0416	0.0410	0.0413	0.0403	0.0417
	25°C	75	0.0331	0.0400	0.0430	0.0424	0.0423	0.0420	0.0444
	25°C	90	0.0340	0.0398	0.0442	0.0429	0.0430	0.0427	0.0457
	25°C	105	0.0336	0.0404	0.0448	0.0431	0.0430	0.0439	0.0482
	25°C	120	0.0338	0.0416	0.0454	0.0430	0.0434	0.0450	0.0508
V. parahaemolyticus	37°C	0	0.0324	0.0310	0.0316	0.0268	0.0292	0.0304	0.0300
	37°C	15	0.0309	0.0326	0.0334	0.0276	0.0330	0.0342	0.0324
	37°C	30	0.0331	0.0333	0.0348	0.0307	0.0341	0.0348	0.0331
	37°C	45	0.0329	0.0322	0.0343	0.0329	0.0323	0.0333	0.0330

	37°C	60	0.0357	0.0338	0.0354	0.0342	0.0324	0.0343	0.0337
	37°C	75	0.0374	0.0357	0.0377	0.0354	0.0348	0.0356	0.0350
	37°C	90	0.0386	0.0380	0.0394	0.0367	0.0367	0.0367	0.0361
	37°C	105	0.0399	0.0398	0.0409	0.0374	0.0376	0.0377	0.0376
	37°C	120	0.0410	0.0414	0.0427	0.0383	0.0381	0.0387	0.0381
V. vulnificus	25°C	0	0.0100	0.0109	0.0089	0.0111	0.0129	0.0112	0.0092
	25°C	15	0.0086	0.0100	0.0086	0.0100	0.0114	0.0096	0.0088
	25°C	30	0.0076	0.0094	0.0083	0.0093	0.0107	0.0089	0.0082
	25°C	45	0.0077	0.0093	0.0086	0.0100	0.0109	0.0096	0.0083
	25°C	60	0.0082	0.0090	0.0088	0.0096	0.0107	0.0089	0.0077
	25°C	75	0.0083	0.0089	0.0080	0.0091	0.0106	0.0087	0.0073
	25°C	90	0.0079	0.0093	0.0079	0.0092	0.0106	0.0083	0.0073
	25°C	105	0.0081	0.0089	0.0078	0.0091	0.0102	0.0088	0.0071
	25°C	120	0.0083	0.0087	0.0079	0.0087	0.0099	0.0077	0.0069
V. vulnificus	37°C	0	0.0058	0.0118	0.0070	0.0079	0.0057	0.0074	0.0061
	37°C	15	0.0059	0.0120	0.0060	0.0061	0.0054	0.0067	0.0054

37°C	30	0.0062	0.0116	0.0067	0.0067	0.0058	0.0066	0.0067
37°C	45	0.0079	0.0122	0.0066	0.0068	0.0064	0.0077	0.0071
37°C	60	0.0106	0.0150	0.0087	0.0080	0.0086	0.0098	0.0087
37°C	75	0.0151	0.0182	0.0117	0.0093	0.0119	0.0133	0.0121
37°C	90	0.0173	0.0207	0.0142	0.0108	0.0142	0.0157	0.0142
37°C	105	0.0191	0.0222	0.0161	0.0117	0.0162	0.0170	0.0162
37°C	120	0.0203	0.0230	0.0170	0.0121	0.0172	0.0179	0.0167

[1]Optical density at 600 nm

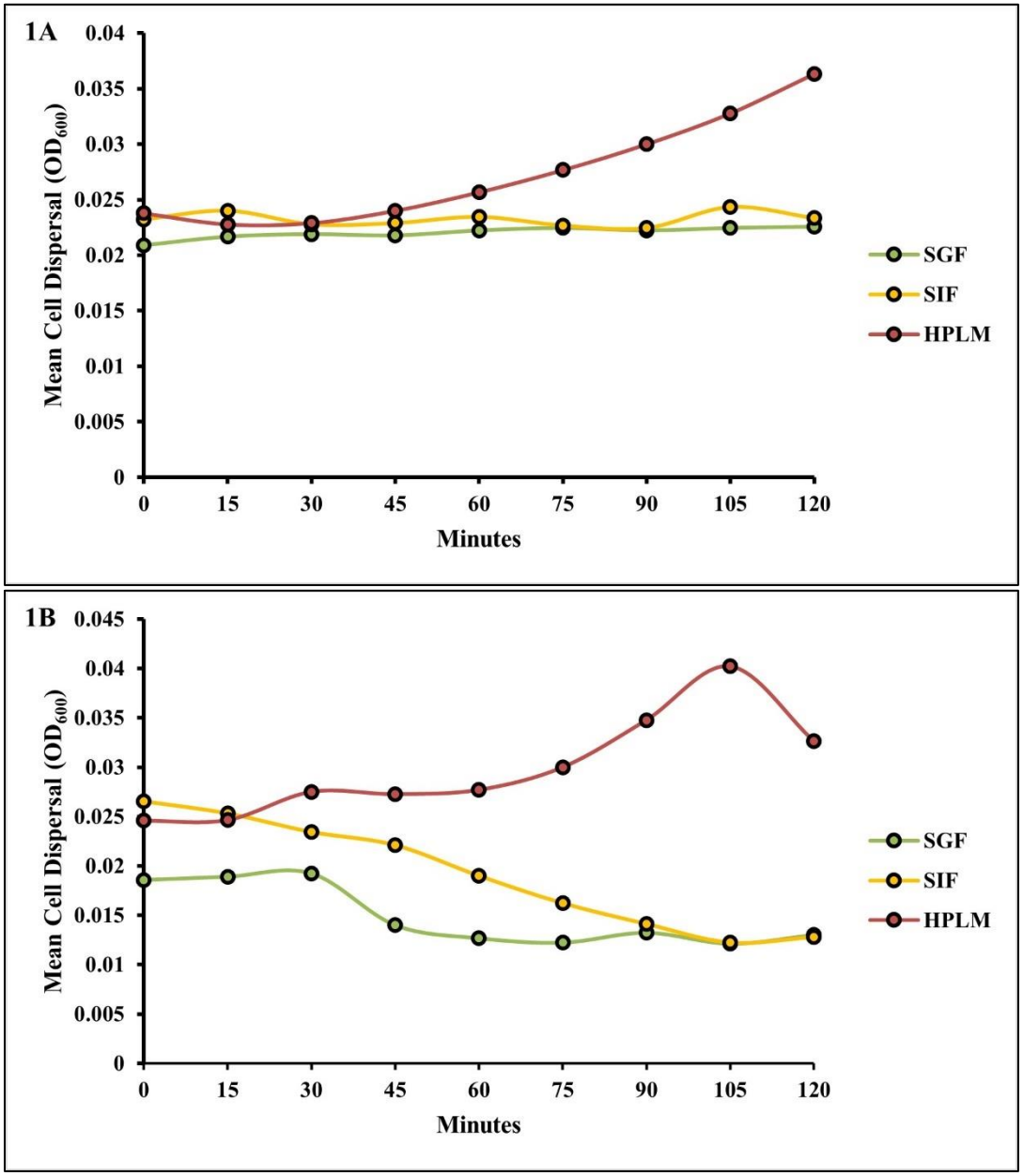

Figure B.3. *V. parahaemolyticus* cell dispersal (OD_{600}) over time at different temperature in simulated human media. Comparison of cell dispersal (means of all biological triplicates and three independent experiments) after 2- hour exposure between *V. parahaemolyticus* at 25 °C (**1A**) and 37°C (**1B**).

Table B.65. *V. parahaemolyticus* mean cell dispersal[1] values over time at different temperature in simulated human media.

Species	Temperature	Time (mins)	SGF	SIF	HPLM
V. parahaemolyticus	25°C	0	0.0209	0.0232	0.0238
	25°C	15	0.0217	0.0240	0.0228
	25°C	30	0.0219	0.0228	0.0229
	25°C	45	0.0218	0.0229	0.0240
	25°C	60	0.0222	0.0234	0.0257
	25°C	75	0.0224	0.0227	0.0277
	25°C	90	0.0222	0.0224	0.0300
	25°C	105	0.0224	0.0243	0.0328
	25°C	120	0.0226	0.0233	0.0363
V. parahaemolyticus	37°C	0	0.0186	0.0266	0.0246
	37°C	15	0.0189	0.0253	0.0247
	37°C	30	0.0192	0.0234	0.0275
	37°C	45	0.0140	0.0221	0.0273
	37°C	60	0.0127	0.0190	0.0277

	37°C	75	0.0122	0.0162	0.0300
	37°C	90	0.0132	0.0141	0.0348
	37°C	105	0.0121	0.0122	0.0402
	37°C	120	0.0130	0.0128	0.0327

[1]Optical density at 600 nm

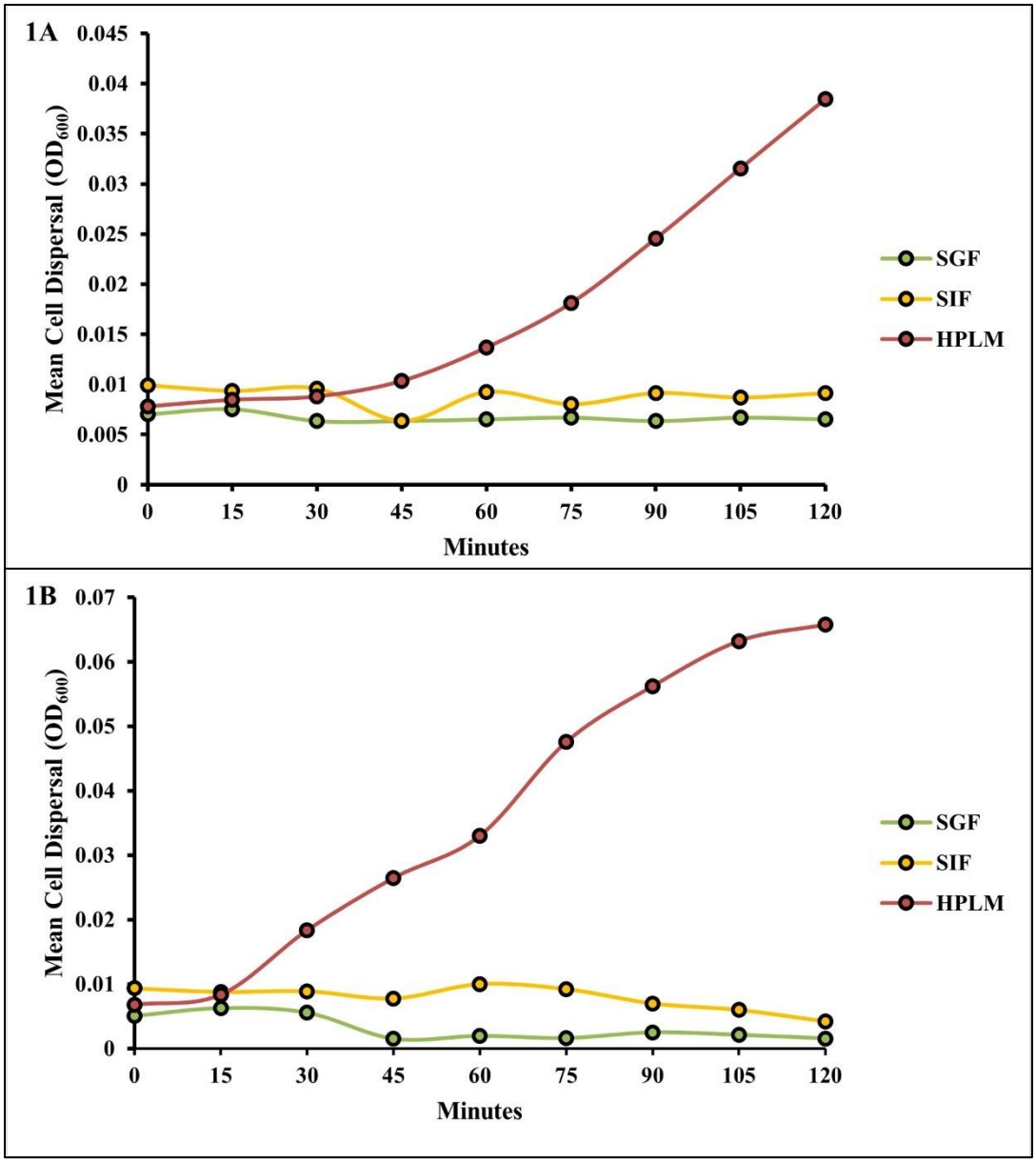

Figure B.4. *V. vulnificus* cell dispersal (OD_{600}) over time at different temperature in simulated human media. Comparison of cell dispersal (means of all biological triplicates and three independent experiments) after 2- hour exposure between *V. vulnificus* at 25 °C (**1A**) and 37°C (**1B**).

Table B.66. *V. vulnificus* mean cell dispersal[1] values over time at different temperatures in simulated human media.

Species	Temperature	Time (mins)	SGF	SIF	HPLM
V. vulnificus	25°C	0	0.0070	0.0099	0.0078
	25°C	15	0.0075	0.0093	0.0084
	25°C	30	0.0063	0.0096	0.0088
	25°C	45	0.0063	0.0063	0.0103
	25°C	60	0.0065	0.0092	0.0137
	25°C	75	0.0067	0.0080	0.0181
	25°C	90	0.0063	0.0091	0.0246
	25°C	105	0.0067	0.0087	0.0316
	25°C	120	0.0065	0.0091	0.0384
V. vulnificus	37°C	0	0.0051	0.0093	0.0068
	37°C	15	0.0063	0.0088	0.0083
	37°C	30	0.0056	0.0089	0.0183
	37°C	45	0.0015	0.0078	0.0264

37°C	60	0.0019	0.0100	0.0330
37°C	75	0.0016	0.0092	0.0476
37°C	90	0.0025	0.0070	0.0562
37°C	105	0.0021	0.0060	0.0632
37°C	120	0.0016	0.0042	0.0658

[1]Optical density at 600 nm

APPENDIX C:

MODELING PH AND TEMPERATURE EFFECTS AS CLIMATIC HAZARDS IN *VIBRIO VULNIFICUS* AND *VIBRIO PARAHAEMOLYTICUS* PLANKTONIC GROWTH AND BIOFILM FORMATION[1]

---

[1]Velez, K. E. C. , Leighton, R. E. , Decho, A. W. , Pinckney, J. L. , & Norman, R. S. (2023). Modeling pH and temperature effects as climatic hazards in *Vibrio vulnificus* and *Vibrio parahaemolyticus* planktonic growth and biofilm formation. GeoHealth, 7, e2022GH000769. 10.1029/2022GH000769

C.1 Abstract

Climate-induced stressors, such as changes in temperature, salinity, and pH, contribute to the emergence of infectious diseases. These changes alter geographical constraint, resulting in increased *Vibrio* spread, exposure, and infection rates, thus facilitating greater *Vibrio*-human interactions. Multiple efforts have been developed to predict *Vibrio* exposure and raise awareness of health risks, but most models only use temperature and salinity as prediction factors. This study aimed to better understand the potential effects of temperature and pH on *V. vulnificus* and *V. parahaemolyticus* planktonic and biofilm growth. *Vibrio* strains were grown in triplicate at 25°, 30°, and 37°C in 96 well plates containing Modified Seawater Yeast Extract modified with CaCl2 at pH's ranging from 5 to 9.6. AMiGA software was used to model growth curves using Gaussian process regression. The effects of temperature and pH were evaluated using randomized complete block analysis of variance, and the growth rates of *V. parahaemolyticus* and *V. vulnificus* were modeled using the interpolation fit on the MatLab Curve Fitting Toolbox. Different optimal conditions involving temperature and pH were observed for planktonic and biofilm *Vibrio* growth within- and between-species. This study showed that temperature and pH factors significantly affect *Vibrio* planktonic growth rates and *V. parahaemolyticus* biofilm formation. Therefore, pH effects must be added to the *Vibrio* growth modeling efforts to better predict *Vibrio* risk in estuarine and coastal zones that can potentially experience the cooccurrence of *Vibrio* and harmful algal bloom outbreak events.

C.2 Plain Language Summary

Changes in temperature, salinity, and pH are increasing *Vibrio*-human interactions in coastal communities. Multiple efforts have been developed to predict *Vibrio* risk, mainly using temperature and salinity measurements. However, more comprehensive models are needed to help inform decision-makers on how to better design policies and create public health awareness. This study looks at how temperature and pH could affect the growth of the potential human bacterial pathogens, *V. vulnificus* and *V. parahaemolyticus*. *Vibrio* strains were grown in triplicate at different temperatures in acidic, neutral, and alkaline conditions (different pH ranges). The effects of temperature and pH were evaluated using randomized complete block analysis of variance, and the growth rates of *V. parahaemolyticus* and *V. vulnificus* were modeled using the MatLab Curve Fitting Toolbox. This study found different optimal conditions for free-living and aggregated *Vibrio* growth within and between species. In addition, this study showed that temperature and pH factors significantly impact *Vibrio* growth. Overall, the pH effects must be added to the *Vibrio* growth modeling efforts to have a more comprehensive model and to better predict *Vibrio* risk in climate change scenarios.

C.3 Introduction

Climate change is causing unprecedented ecological changes and altering infection patterns for diseases sensitive to environmental changes, such as *Vibrio* infections (Epstein, 2001; Mora et al., 2022; Wu et al., 2014). Some hazards resulting from climate change, such as warming, sea level rise, pH decline, floods, and abnormal weather patterns may lead to a potential increase in *Vibrio* infections (Trinanes & Martinez-Urtaza, 2021). The number of cases of vibriosis has been increasing during the

past few decades worldwide, even in regions where environmental conditions had been considered adverse for *Vibrio* proliferation, especially in higher latitude locations (Baker-Austin et al., 2013, 2017, 2018; Newton et al., 2012; Vezzulli et al., 2013). In the United States, the Foodborne Diseases Active Surveillance Network (FoodNet, Tack et al., 2019) has reported increased incidences of *Vibrio* infections. For example, incidence in 2018 increased by 109% compared to 2015–2017, with similar increasing trends observed in previous years. In 2020, the incidence of *Vibrio* decreased by 15% compared to those in 2017–2019 due to the COVID-19 pandemic and the corresponding public health response that limited healthcare-seeking behaviors, healthcare delivery, and human exposure. This decrease in incidence was an abnormal trend, which is expected to change due to the abatement of COVID-19 related restrictions (Tack et al., 2020: Ray et al., 2021; Trinanes & Martinez-Urtaza, 2021). The increase in *Vibrio* spread and infection rates are thought to be a consequence of altered geographical constraints driven by warming seawater temperature, sea-level rise, and changes in salinity associated with climate change (Deeb et al., 2018). This poleward spread is contributing to the increase of human disease burden globally (Baker-Austin et al., 2013, 2018).

Vibrio spp. inhabit estuarine and marine environments and prefer relatively warm water (≥15°C) and low to moderate salinities, where seawater temperature modulates the abundance of *Vibrio* and salinity defines habitat suitability (FAO and WHO, 2020; Marinez-Urtaza et al., 2008; Thompson et al., 2004; Vezzulli et al., 2009; Wang et al., 2020). *Vibrio* spp. can persist in a free-living (planktonic) state in the water column or form biofilms on biotic and abiotic surfaces (Baker-Austin et al., 2018). Biofilm formation depends on many physical, chemical, and biological parameters and is

considered a selective survival strategy for protection against stress, such as changes in temperature, pH variability, low nutrients, and antibiotics (Decho & Gutierrez, 2017; Harjai et al., 2005; Hoštacká et al., 2010; Jefferson, 2004; Yang et al., 2007). Also, some *Vibrio* spp., including *V. parahaemolyticus* and *V. vulnificus*, can enter a viable but non-culturable (VBNC) protective state under unfavorable conditions, where the bacterial metabolism becomes dormant and cells cannot grow under laboratory conditions (Colwell, 2000; Li et al., 2014). VBNC bacterial cells regain their culturability and virulence properties when the conditions become favorable, which may be triggered by changes in temperature and salinity (Oliver, 2010). Studies have demonstrated that VBNC *Vibrio* spp. can cause disease after resuscitation in their respective hosts (Baffone et al., 2003; Colwell, 1996; Sun et al., 2008) Also, another study showed that four *Vibrio* spp. expressed some virulence and toxin genes during the VBNC state (Vora et al., 2005).

Not all *Vibrio* strains are equally pathogenic and can be classified according to biotype and genotype. *V. vulnificus* strains are classified into three biotypes based on their biochemical characteristic: biotype 1 is responsible for human infections (Oliver, 2015), biotype 2 is primarily an eel pathogen (Amaro & Biosca, 1996; Tison et al., 1982), and biotype 3 is a hybrid of biotypes 1 and 2 that can cause wound infections and has been suggested to be geographically restricted to Israel (Bisharat et al., 1999; Zaidenstein et al., 2008). Strains within biotype 1 are commonly grouped into clinical (16S rRNA type B and vcgC) and environmental (16S rRNA type A and vcgE) genotypes (Nilsson et al., 2003; Rosche, Smith, et al., 2005; Rosche, Yano, & Oliver, 2005). Furthermore, the vvhA gene encoding hemolysin/cytolysin is used as a *V. vulnificus* species marker and has been associated with pathogenic strains. Other genes

associated with pathogenic *V. vulnificus* strains are rtxA1, vvpE, viuB, gbpA, and pilin genes (pilA and pilD) (Gavin et al., 2017; Jang et al., 2016; Johnson et al., 1984; Natividad-Bonifacio et al., 2013; Panicker et al., 2004; Paranjpye & Strom, 2005). *V. vulnificus* regulates virulence gene expression by integration of signals during the course of infection. For example, in the early stages of infection in the upper intestine and bloodstream where glucose levels are high, IscR activates the up-regulation of gbpA, prx3, and vvhA and CRP up-regulates the rtxA for survival against stress, intestinal colonization, and dissemination through the host. In later stages of infection, CRP-mediated up-regulation of plpA, vvhA, and vvpE leads to inflammation and disease development (Choi & Choi, 2022). For *V. parahaemolyticus*, strains that carry thermostable direct hemolysin (tdh) and/or thermostable-related hemolysin (trh) genes are often considered pathogenic (Nishibuchi et al., 1992; Shirai et al., 1990). Non-cholera *Vibrio* species, such as *V. parahaemolyticus* and *V. vulnificus*, can cause infection by exposure to contaminated water or consumption of raw or undercooked contaminated seafood. Clinical manifestations include mild and self-limiting gastroenteritis and wound infections that can result in acute septicemia and death (Jones & Oliver, 2009).

Although environmental stressors such as temperature and salinity and *Vibrio* abundance and distribution data are used in current modeling to predict future *Vibrio* exposure risk (Semenza et al., 2017), other key factors have been suggested as contributing to the increase in *Vibrio* cases, such as demographic changes and population growth (Trinanes & Martinez-Urtaza, 2021). Population growth and development in coastal regions have been significantly higher compared to inland areas worldwide, generating pressures on coastal ecosystems due to anthropogenic pollution (Balk

et al., 2009; Crossland et al., 2005; Neumann et al., 2015; Patterson & Hardy, 2008; Small & Nicholls, 2003).

The combination of climate hazards, demographic changes, and population growth in coastal areas has been suggested as key factors in the increase in *Vibrio*-human interactions (Archer et al., 2023; Froelich & Daines, 2020). But the potential for infection is more complex due to the variation in pathogenicity across species and even strains. Furthermore, little is known about how changing environmental parameters, such as pH and exposure to other potentially co-occurring biological hazards, such as harmful algal blooms (HABs), can shift or change *Vibrio* abundance, distribution, and pathogenicity in estuaries and marine environments. The limited studies that have addressed *Vibrio*-Phytoplankton interaction have shown a high correlation between *Vibrio* and phytoplankton abundance (Main et al., 2015; Rosales et al., 2022; Turner et al., 2009). These studies suggest that the correlation may be due to the combination of changes in environmental parameters and the production of algal exudate that activates *Vibrio* biofilm formation pathways. There is also a limited understanding of how changing ocean pH can affect the abundance of *Vibrio* species. Non-cholera *Vibrio* spp. have the capability to grow in a broad pH range from 5 to 10 and have been shown to develop resistance to acid inactivation in the VBNC state, adding to the complexity of the situation (Nowakowska & Oliver, 2013; Wong & Wang, 2004).

Changing environmental parameters in coastal areas, including temperature and pH, might led to the generation of new areas with ideal conditions for *Vibrio* growth. Future climate change scenarios project warmer, less saline, and more acidic coastal water. The ocean surface warming has accelerated in the last decade to 0.280 ± 0.068°C

per decade and is expected to increase more than 4°C by 2100. Meanwhile, the ocean pH has declined by 0.1 since the industrial revolution and is projected to decline by 0.1–0.4 pH units by the end of 2100 in the open ocean (Garcia-Soto et al., 2021). Coastal regions are more dynamic than the open ocean, with environmental parameters differing according to geographical locations, morphology, freshwater influx, and other environmental and anthropogenic pressures (Cloern et al., 2016). Biogeochemical processes in coastal zones can lead to seasonal pH variation and even daily changes higher than 1 pH unit, where daytime photosynthesis drives high levels of dissolved oxygen and pH and nighttime respiration drives decreased dissolved oxygen concentration and pH values (Baumann et al., 2015; Provoost et al., 2010; Raven et al., 2020; Wallace et al., 2014). Baumann and Smith (2018) used long-term monitoring data from the National Estuarine Research Reserve System (NERRS) to evaluate pH and oxygen fluctuation in 16 US nearshore sites and found that dissolved oxygen, as a result of metabolic processes, and salinity have a high correlation with pH fluctuations. Furthermore, in areas that have an extensive network of intertidal salt marshes, such as the ACE Basin and North Inlet NERRS sites (South Carolina, USA), pH fluctuations can be correlated with tidal and diurnal cycles. Dense cyanobacteria blooms in these dynamic ecosystems can also increase water column pH > 9 due to metabolically-driven decreases in dissolved CO2 to less than 1 μmol per liter (Adams et al., 2022; Huisman et al., 2018). Changes in environmental parameters not only affect the growth and distribution of *Vibrio* species but may also alter their gene expression, resulting in enhanced virulence profiles (Billaud et al., 2022; Correa Velez & Norman, 2021; Pazhani et al., 2021; Williams et al., 2014). To understand the changing abundances of *Vibrio* spp. under

natural conditions and to develop better models to predict future climate change impacts, it is necessary to determine how environmental stressors, such as pH and temperature, can affect *Vibrio* in their different forms of growth (planktonic and biofilm states). This study examined the potential effects of temperature and pH on non-cholera *Vibrio* planktonic and biofilm growth using *V. vulnificus* and *V. parahaemolyticus* as models of opportunistic pathogens. A better understanding of how clinical and environmental strains respond to coupled climatic hazards will aid in the development of more precise models to predict potential *Vibrio* exposure and increase awareness of health risk in coastal regions.

C.4 Materials and Methods

Bacterial Strains and Growth Conditions

To examine the effect of pH and temperature on bacterial growth in planktonic and biofilm states, reference clinical and environmental strains of *V. vulnificus* and *V. parahaemolyticus* (Table 1) were grown at three temperatures (25°, 30°, and 37°C) and 11 pH's ranging from 5.0 to 9.6. The pH and temperatures were selected to encompass a range of natural conditions encountered by *V. vulnificus* and *V. parahaemolyticus*. The average sea surface temperature in warm coastal areas susceptible to *Vibrio* proliferation is between 25°C to 30°C, whereas a human host temperature is 37°C. *Vibrio* can survive in pH ranges from 5 to 10. The pH of the water column fluctuates between 7.2 and 8.1 under most environmental conditions, with photosynthesis-driven alkaline conditions (≥9.2) often occurring during cyanobacterial bloom events. The pH in human-host conditions is 6.5–7.5 in saliva and decreases to 2–6.5 in the gastrointestinal tract. For free-living or planktonic growth, *Vibrio* strains were grown in 96 well plates containing

three replicates of Modified Seawater Yeast Extract (MSYE; Oliver & Colwell, 1973) supplemented with calcium chloride (CaCl2; 1.8 g/L), pH adjusted using 1M Sodium Hydroxide (NaOH) or 1M Hydrochloric acid (HCl), and a final salinity of 30 ± 0.5 g/kg. In each experimental condition, diluted 1:10 overnight fresh cultures (8 hr) were used as inocula. Optical density (OD600) of each replicate was measured hourly to determine bacterial growth over 24 hr using a Victor X3 plate reader (PerkinElmer, Waltham, MA, USA). Gaussian process regression was performed on background-subtracted OD data to model growth curves, and model-predicted ODs were used to estimate growth parameters for each treatment using AMiGA software (Midani et al., 2021). For biofilm formation assays, tissue culture-treated 96-well polystyrene microplates were used under each environmental condition without additional modifications.

Crystal Violet Staining Assay

The biomass of *V. parahaemolyticus* and *V. vulnificus* biofilms was estimated using crystal violet staining according to O'Toole (2011), with slight modifications. Briefly, after 0, 6, 12, 24, 36 hr of growth, planktonic cells were removed from the 96-well microplates before gently washing with 1× phosphate buffer saline (PBS) three times. After washing, 100% methanol (MeOH) was added to the plates to fix the biofilms to the plates. After 20 min of incubation at room temperature, MeOH was removed and the plates were allowed to air-dry to eliminate any MeOH residue. The biofilms were stained with 0.1% (wt/vol) crystal violet for 15 min at room temperature, and a second wash was performed three times using 1× PBS to remove the non-bound dye. The stained and washed biofilms were air-dried overnight, and 30% acetic acid was added to dissolve the bound crystal violet for 15 min. The solubilized crystal violet acetic acid solution was

then transferred to a new 96-well polystyrene microplate and the optical density of each well was measured at 570 nm using a SpectraMax M3 plate reader (Molecular Devices, San Jose, CA, United States). These OD measurements were used to estimate the biofilm growth parameters for each treatment using AMiGA software.

Modeling and Statistical Analysis

The growth rates of *V. parahaemolyticus* and *V. vulnificus* obtained from the AMiGA analysis for each combination of factors (pH and temperature) were modeled using the interpolation fit function using the liner method in the MatLab Curve Fitting Toolbox (v. R2022b, 9.13.0.2049777). The interpolation method estimated the values between known data points, which involves the construction of a function f that matches given data values, yi, at given data sites, xi, in the sense that f(xi) = yi, all i. For the statistical analysis, a randomized complete block design analysis of variance (RCB-ANOVA) was performed using SPSS Statistics (v. 28.0.1.0) to evaluate the effects of temperature and pH on bacterial growth rate using the strain as a blocking factor. Ryan, Einot, Gabriel, and Welsch (R-E-G-W F) multiple comparisons of means were used to determine aposteriori differences among the factor combinations. The level of significance was set at $p < 0.05$. Interaction (profile) plots were generated using the general linear method, univariate function in SPSS software. The data used for both analyses are available at Mendeley data via https://doi.org/10.17632/xxkkkbx3hg.1.

C.5 Results

Vibrio Modeling Reveals That Optimal Growth Conditions Vary Between Planktonic and Biofilm States

Vibrio modeling using the interpolate method revealed that optimal pH and temperature conditions vary between strain and state of growth. *V. vulnificus* strains associated with disease in humans and animals showed optimal growth rates at 37°C and at pH's between 6.5 and 8.5 during planktonic growth (Figures 1a and 1b, left), with the highest growth rate at pH 7.1 for ATCC 27562 and pH 8.3 for ATCC 33147. In comparison, the environmental isolates of *V. vulnificus* (Figures 1c and 1d, left) exhibited growth throughout a wider range of conditions, suggesting greater adaptation to varying environmental conditions. Higher growth rates were observed at 36ºC and pH 7.0 for the NOAA 48 strain and 32°C and pH 6.9 for the NOAA 155 strain. During biofilm growth, the optimal conditions in terms of pH and temperature were opposite from those observed during planktonic growth (Figure 1, right Panel). The greatest biofilm formation for *V. vulnificus* strains associated with disease were observed at 25ºC and pH 7.5 for ATCC 27562, and 26°C and pH 5.4 for ATCC 33147. Similar patterns were observed for the environmental strains, where optimal growth conditions were 25°C and pH 5.2 for the NOAA 48 strain and 30°C and pH 7.9 for the NOAA 155 strain.

All *V. parahaemolyticus* strains in planktonic growth (Figure 2 left panel) exhibited increased growth at temperatures between 36.6–36.8°C and pH ranging from neutral to acidic: 7.1 (strain 48057), 6.4 (C12), 5.9 (17802), and 5.7 (4.1PR). In contrast, optimal biofilm formation for all strains was observed at lower temperatures, from 25.2–30°C and pH ranges similar to those of planktonic cells (Figure 2 right panel). Modeling *V. parahaemolyticus* growth during both planktonic and biofilm mode of growth showed similar strain-level patterns based on pH, where higher biofilm biomass developed in pH's ranging from neutral to acidic. However, different temperature optimums were

observed for clinical and environmental strains, whereas the planktonic environmental strain patterns showed higher growth rates throughout a wider temperature range (26°C–37°C) compared with the clinical strains, suggesting better adaptability to changes in temperature.

pH and Temperature Have Significant Effects on *Vibrio* spp. Planktonic Growth Rates

A randomized complete block design model multifactor analysis of variance (RCB-ANOVA) was used to determine the effect of pH (11 levels) and temperature (3 levels) on growth rates of *V. vulnificus* and *V. parahaemolyticus* strains using strain as the blocking factor (4 levels) as shown in Table 2. Each factor combination has three replicates. For *V. vulnificus* planktonic growth, the RCB-ANOVA indicated that temperature and pH had a significant effect on the bacterial planktonic growth rate ($F_{2,360} = 101.239$, $p < 0.001$; $F_{10,360} = 61.619$, $p < 0.001$). There was also a significant block effect (strain, $F_{3,360} = 7.608$, $p < 0.001$) and a significant interaction between temperature and pH ($F_{20,360} = 6.620$, $p < 0.001$). A similar trend was observed in *V. parahaemolyticus* planktonic ANOVA results, temperature ($F_{2,360} = 125.346$, $p < 0.001$) and pH ($F_{10,360} = 44.774$, $p < 0.001$) and showed a significant effect on the growth rate. The interaction factor between temperature and pH and the blocking factor effect on growth rate was also highly significant ($F_{20,360} = 2.408$, $p < 0.001$; $F_{3,360} = 16.706$, $p < 0.001$).

Additionally, the RCB-ANOVA results of *V. vulnificus* biofilm growth indicated that temperature had a significant effect on growth rate ($F_{2,294} = 11.161$, $p < 0.001$). However, pH, the interaction factor (temperature * pH), and blocking effects were not significant ($F_{2, 294} = 1.044$, $p = 0.406$; $F_{20,294} = 1.091$, $p = 0.358$; $F_{3,294} = 2.158$, $p = 0.093$).

For *V. parahaemolyticus* biofilm formation, the RCB-ANOVA revealed that temperature ($F_{2,360} = 33.443$, $p < 0.001$) and pH ($F_{10,360} = 5.516$, $p < 0.001$) had a significant effect on biofilm growth. There was a significant block effect (strain, $F_{3,360} = 28.322$, $p < 0.001$), but the interaction between temperature and pH was not significant ($F_{20,360} = 1.374$, $p = 0.132$).

Figure 3. illustrates the results of interaction plots for *V. vulnificus* and *V. parahaemolyticus* strains showing planktonic and biofilm growth rates. RCB-ANOVA suggests a significant interaction on planktonic growth rates in both *Vibrio* species and a significant effect of independent factors. These results indicate that the response to pH differed depending on the incubation temperature. The lines in the planktonic interaction profiles (Figure 3, left panel) were not parallel and converged, showing interaction. In *V. vulnificus* (Figure 3, panel a, left), the plot indicates interactions at pH < 6.0 and >9.0, where the pH drives the interaction. In comparison, temperature influences the interaction between pH 6.4 and 9.0, where higher temperatures showed higher growth rates. In the *V. parahaemolyticus* interaction plot (panel b, left), pH has a greater effect on the interaction at pH < 5.5 and >8.2. The temperature contributes more to the interaction in pH between 5.5 and 8.0, where higher temperatures exhibited higher growth rates.

Vibrio biofilm growth patterns showed no significant interaction, but the lines converge at some points due to the significance of the independent factors (Figure 3, right panel). RCB-ANOVA indicated that temperature significantly affected *V. vulnificus* growth rates; this is illustrated in the interaction plot where the blue line (25°C) converges with other temperatures at multiple points (Figure 3, panel a, right). A similar trend was observed in the *V. parahaemolyticus* profile plot, wherein temperature and pH

significantly affected the growth rate, but this interaction was not significant. The red line (37°C) intercepted with the green (30°C) and blue (25°C) lines throughout multiple points (different pH values), which explained the significance of the Individual factors and the difference in response between conditions.

C.6 Discussion and Conclusions

Climate change is contributing to the successful emergence of human pathogenic diseases, including *Vibrio* infections (Edelson et al., 2022; Landrigan et al., 2020). *Vibrio* are expanding their geographical distribution toward the poles, and their abundances have increased during the past decade (Baker-Austin et al., 2018). At the same time, global temperature changes, increased eutrophication, and elevated pCO_2 have also enhanced cyanobacterial HAB growth rates, resulting in more frequent HAB occurrence within ecosystems that are conducive to *Vibrio* proliferation (O'Neil et al., 2012; Paerl & Paul, 2012; Suikkanen et al., 2013; Visser et al., 2016). Within these estuarine and coastal zone ecosystems, pH changes have become more frequent and driven, in part, by the increasing occurrence and metabolic activities of HABs, where localized pH can fluctuate from acidic ($pH < 6$) to alkaline levels ($pH > 9$) (Adams et al., 2022; Zepernick et al., 2021). High biomass blooms cause increases in pH (during daylight) due to the rapid cellular intake of CO_2, resulting in an advantage to cyanobacteria, which possess carbon-concentrating mechanics that provide a competitive advantage to growing in low CO_2 and high pH (Sandrini et al., 2016; Wells et al., 2020). While multiple models have been developed to predict future risks of *Vibrio* outbreaks, the models do not consider pH or the pH changes in the water column due to co-

occurrence of HABs as factors in *Vibrio* growth (Dickinson et al., 2013; Froelich et al., 2013; Semenza et al., 2017).

The results of the present study suggest that pH effects should be added to the *Vibrio* growth modeling efforts to better predict *Vibrio* risk in estuarine and coastal zones. The pH of these zones can be influenced by multiple environmental factors, including anormal weather patterns, influx of natural or man-made chemical nutrients, and co-occurrence of *Vibrio* and HAB outbreak events. Different optimal growth conditions in terms of temperature and pH were observed for planktonic and biofilm non-cholera *Vibrio* growth within and between species generating different modeling patterns (Figures 1 and 2). In addition, this study found that *Vibrios* could have multiple optimal growth conditions that depend on the mode of growth and their interaction with different stressors, including temperature and pH. These findings also suggest that *Vibrio* may express adaptive responses, switching between planktonic to biofilm and vise-versa to resist temperature and pH stressors, potentially increasing bacterial survival under climate change scenarios and increasing *Vibrio*-human interactions. Future transcriptomic studies are needed to understand the *Vibrio* adaptative responses and metabolic pathways expressed under different climate conditions.

Vibrio modeling showed that the bacterial response to acidic and alkaline conditions could vary between strains and species. The ability of *Vibrio* spp. to adapt to pH changes is an essential factor to consider in bacteria-host interactions. Previous studies have documented that *V. vulnificus* can adapt to acidic conditions and become acid resistant by breaking down lysine to cadaverine, which is regulated by the *cadBA* operon (Rhee et al., 2002, 2005). Cadaverine can also act as a superoxide

radical scavenger that provides tolerance to oxidative stress (Kang et al., 2007). The link between acid and oxidant stress tolerance may enhance bacterial survival in transitioning between the environment to a human host. Studies have demonstrated that pre-exposure to slightly acidic environments increases *V. vulnificus* acid tolerance and may increase resistance to other stresses (Bang & Drake, 2005). The expression of cross-protective mechanisms in *V. vulnificus* is often regulated by the sigma factor RpoS (σ^S) and, after nutrient starvation, can induce cross-protective effects against oxidative stress (Rosche, Smith, et al., 2005; Rosche, Yano, & Oliver, 2005). Studies have also reported the expression of cross-protection in *V. parahaemolyticus* strains. For example, *V. parahaemolyticus* showed enhanced survival at lower pH (4.4) after exposure to mildly acidic conditions (pH 5.5) and showed cross-protection against low salinity and temperature (Wong et al., 1998). *V. parahaemolyticus* also developed cross-protection after exposure to alkaline conditions (pH 9.0), where adapted cells were found to increase resistance to heat, crystal violet, deoxycholic acid, and hydrogen peroxide (Koga et al., 2002). Furthermore, the production of Kanagawa hemolysin by *V. parahaemolyticus* has been related to lower pH ranges, where the hemolysin production increased (Cherwonogrodzky & Clark, 1981). These studies, in addition to the present work, suggest that *V. vulnificus* and *V. parahaemolyticus* can adapt, survive, and grow under a broad pH range from pH 5 to 9.5.

This study also shows that temperature and pH factors significantly affect the planktonic growth rate of *Vibrio* spp. and the formation of *V. parahaemolyticus* biofilms (Table 2, Figure 3). Previously, the effect of temperature and pH was evaluated in *Pseudomonas aeruginosa*, *Klebsiella pneumoniae*, and *V. cholerae*, where increased

pH significantly affected biofilm formation in all species and strains tested (Hostacka et al., 2010). A recent study reported that *V. vulnificus* biofilm biomass in clinical strains is higher than in environmental isolates at 24°C, with the greatest biofilm biomass of all strains observed at pH 5.5 and 24°C as compared to 30° and 37°C (Çam & Brinkmeyer, 2020). However, Çam and Brinkmeyer (2020) reported that the *V. vulnificus* biofilm growth rate was lowest for environmental strains at pH 5.5, whereas the clinical strains showed no difference between pH 5.5, 7.5 and 8.5, suggesting tolerance to acidic and alkaline conditions. In the case of *V. parahaemolyticus,* greater biofilm formation has been documented at 25°C compared to 15°C and 37°C (Song et al., 2017). Furthermore, another study showed greater biofilm formation and production of exoprotease and autoinducer-2 in food and food contact surfaces at temperatures between 25°C and 37°C (Han et al., 2016).

The relationship between temperature and growth rate has been reported in multiple studies examining *V. vulnificus* and *V. parahaemolyticus*, where increased temperature resulted in increased planktonic growth (Kim et al., 2016; Mudoh et al., 2014; Sheikh, John, et al., 2022; Sheikh, Najiah, et al., 2022; Sullivan & Neigel, 2018). The increase in *V. parahaemolyticus* growth at higher temperatures has been correlated with a shorter generation time, a shorter lag time (Kim et al., 2012), and a faster growth rate (Fernandez-Piquer et al., 2011). In *V. vulnificus*, this positive effect of temperature was also correlated with a higher growth rate and a short lag time at 22°C and 30°C (Wang & Gu, 2005). Another study reported a positive correlation between temperature and growth under conditions from 11°C to 36°C, where the optimum growth rate, the shortest lag time, and the highest density were observed at 36°C (Kim

et al., 2012). *Vibrio* incidence also has been positively associated with temperature after HABs during warmer months. Greenfield et al. (2017) suggested that HABs in retention pond systems were associated with *V. vulnificus* and *V. parahaemolyticus* increases when the water temperature was >10°C. After two cyanobacteria bloom events, the *Vibrio* incidence increased from non-detectable to 6.82×10^2 copies/100 mL and 1.17×10^3 copies/100 mL of *V. parahaemolyticus* and 5.10 and 5.16×10^3 copies/100 mL of *V. vulnificus*. The findings outlined by Greenfield et al. (2017) support the adaptability of *Vibrio* spp. as suggested by our modeling where regardless of the strain variability, the bacteria may survive at different temperatures and pH ranges. These observations and our models suggest a potential to respond to environmental changes and exhibit a higher virulence profile. Higher temperatures can enhance *Vibrio* planktonic growth and serve as a selective pressure for strains with higher virulence potential, allowing for more effective host invasion (Vezzulli et al., 2020). Future studies are needed to assess the interaction between *Vibrio* and HABs and how changes in environmental parameters, such as changes in pH, can strengthen their co-occurrence and selection for pathogenic *Vibrio* strains in real-time environmental conditions.

Overall, the data suggest that non-cholera *Vibrio*, such as *V. vulnificus* and *V. parahaemolyticus*, are capable of adapting to temperature and pH changes in coastal zones and switching between growth modes, increasing their potential to survive under climate change scenarios. While multiple efforts have been developed to create models to predict *Vibrio* exposure and raise awareness of health risk, most models employ water temperature and salinity to predict the potential risk (Brumfield et al., 2021). This study revealed that pH also plays an important role in the adaptive response

of *Vibrio* spp., which can increase the virulence potential of environmental isolates. For example, potential exposure to different pH ranges during HAB events, where water pH can fluctuate over diel and tidal cycles, combined with other climatic hazards, can lead to an increase in the distribution, abundance, and virulence of *Vibrio* spp., contributing to the increase of *Vibrio*-human interactions in coastal regions. Future studies are needed to assess simulated climate change conditions and multiple stressors to better understand how climate change can influence *Vibrio* outbreaks and to develop better models to predict future risk of exposure to *Vibrio* with enhanced virulence profiles. This study provides a new perspective that could be integrated into existing models to help decision makers inform those individuals whose risk of infection is high.

C.7 References

Adams, H., Smith, S. A., Reeder, S., Appleton, E., Leinweber, B., Forbes, S., et al. (2022). Characterizing and mitigating cyanobacterial blooms in drinking water reservoirs.

Journal American Water Works Association, 114(4), 26–38. https://doi.org/10.1002/awwa.1901

Amaro, C., & Biosca, E. G. (1996). *Vibrio vulnificus* biotype 2, pathogenic for eels, is also an opportunistic pathogen for humans. Applied and Environmental Microbiology, 62(4), 1454–1457. https://doi.org/10.1128/aem.62.4.1454-1457.1996

Archer, E. J., Baker-Austin, C., Osborn, T. J., Jones, N. R., Martínez-Urtaza, J., Trinanes, J., et al. (2023). Climate warming and increasing *Vibrio vulnificus* infections in

North America. Scientific Reports, 13(1), 3893. https://doi.org/10.1038/s41598-023-28247-2

Baffone, W., Citterio, B., Vittoria, E., Casaroli, A., Campana, R., Falzano, L., & Donelli, G. (2003). Retention of virulence in viable but non-culturable halophilic *Vibrio* spp. International Journal of Food Microbiology, 89(1), 31–39. https://doi.org/10.1016/s0168-1605(03)00102-8

Baker-Austin, C., Oliver, J. D., Alam, M., Ali, A., Waldor, M. K., Qadri, F., & Martinez-Urtaza, J. (2018). *Vibrio* spp. infections. Nature Reviews Disease Primers, 4(1), 8–19. https://doi.org/10.1038/s41572-018-0005-8

Baker-Austin, C., Trinanes, J., Gonzalez-Escalona, N., & Martinez-Urtaza, J. (2017). Non-cholera *Vibrio*s: The microbial barometer of climate change. Trends in Microbiology, 25(1), 76–84. https://doi.org/10.1016/j.tim.2016.09.008

Baker-Austin, C., Trinanes, J., Taylor, N., Hartnell, R., Siitonen, A., & Martinez-Urtaza, J. (2013). Emerging *Vibrio* risk at high latitudes in response to ocean warming. Nature Climate Change, 3(1), 73–77. https://doi.org/10.1038/nclimate1628

Balk, D., Montgomery, M. R., McGranahan, G., Kim, D., Mara, V., Todd, M., et al. (2009). Mapping urban settlements and the risks of climate change in Africa, Asia and South Americ. In J. M. Guzmán, G. Martine, G. McGranahan, D. Schensul, & C. Tacoli (Eds.), Population dynamics and climate change (pp. 80–103). United Nations Population Fund, International Institute for Environment and Development.

Bang, W., & Drake, M. A. (2005). Acid adaptation of *Vibrio vulnificus* and subsequent impact on stress tolerance. Food Microbiology, 22(4), 301–309. https://doi.org/10.1016/j.fm.2004.09.006

Baumann, H., & Smith, E. M. (2018). Quantifying metabolically driven ph and oxygen fluctuations in US nearshore habitats at diel to interannual time scales. Estuaries and Coasts, 41(4), 1102–1117. https://doi.org/10.1007/s12237-017-0321-3

Baumann, H., Wallace, R. B., Tagliaferri, T., & Gobler, C. J. (2015). Large natural pH, CO2, and O2 fluctuations in a temperate tidal salt marsh on diel, seasonal, and interannual time scales. Estuaries and Coasts, 38(1), 220–231. https://doi.org/10.1007/s12237-014-9800-y

Billaud, M., Seneca, F., Tambutté, E., & Czerucka, D. (2022). An increase of seawater temperature upregulates the expression of *Vibrio parahaemolyticus* virulence factors implicated in adhesion and biofilm formation. Frontiers in Microbiology, 13, 840628. https://doi.org/10.3389/ fmicb.2022.840628

Bisharat, N., Agmon, V., Finkelstein, R., Raz, R., Ben-Dror, G., Lerner, L., et al. (1999). Clinical, epidemiological, and microbiological features of *Vibrio vulnificus* biogroup 3 causing outbreaks of wound infection and bacteraemia in Israel. Israel *Vibrio* Study Group. Lancet (London, England), 354(9188), 1421–1424. https://doi.org/10.1016/s0140-6736(99)02471-x

Brumfield, K. D., Usmani, M., Chen, K. M., Gangwar, M., Jutla, A. S., Huq, A., & Colwell, R. R. (2021). Environmental parameters associated with incidence and transmission of pathogenic *Vibrio* spp. Environmental Microbiology, 23(12), 7314–7340. https://doi. org/10.1111/1462-2920.15716

Çam, S., & Brinkmeyer, R. (2020). The effects of temperature, pH, and iron on biofilm formation by clinical versus environmental strains of *Vibrio vulnificus*. Folia Microbiologica, 65(3), 557–566. https://doi.org/10.1007/s12223-019-00761-9

Cherwonogrodzky, J. W., & Clark, A. G. (1981). Effect of pH on the production of the Kanagawa hemolysin by *Vibrio parahaemolyticus*. Infection and Immunity, 34(1), 115–119. https://doi.org/10.1128/iai.34.1.115-119.1981

Choi, G., & Choi, S. H. (2022). Complex regulatory networks of virulence factors in *Vibrio vulnificus*. Trends in Microbiology, 30(12), 1205– 1216. https://doi.org/10.1016/j.tim.2022.05.009

Cloern, J. E., Abreu, P. C., Carstensen, J., Chauvaud, L., Elmgren, R., Grall, J., et al. (2016). Human activities and climate variability drive fast-paced change across the world's estuarine-coastal ecosystems. Global Change Biology, 22(2), 513–529. https://doi.org/10.1111/gcb.13059

Colwell, R. R. (1996). Global climate and infectious disease: The cholera paradigm. Science, 274(5295), 2025–2031. https://doi.org/10.1126/ science.274.5295.2025

Colwell, R. R. (2000). Viable but non-culturable bacteria: A survival strategy. Journal of Infection and Chemotherapy: Official Journal of the Japan Society of Chemotherapy, 6(2), 121–125. https://doi.org/10.1007/pl00012151

Correa Velez, K. E., & Norman, R. S. (2021). Transcriptomic analysis reveals that municipal wastewater effluent enhances *Vibrio vulnificus* growth and virulence potential. Frontiers in Microbiology, 12, 754683. https://doi.org/10.3389/fmicb.2021.754683

Crossland, C., Baird, D., Ducrotoy, J. P., Lindeboom, H., Buddemeier, R., Dennison, W. C., et al. (2005). The coastal zone—A domain of global interaction. In C. Crossland, H. Kremer, H. Lindeboom, J. Marshall Crossland, & M. A. Tissier (Eds.), Coastal fluxes in the Anthropocene (pp. 1–37). Springer.

Decho, A. W., & Gutierrez, T. (2017). Microbial extracellular polymeric substances (EPSs) in ocean systems. Frontiers in Microbiology, 8, 922. https://doi.org/10.3389/fmicb.2017.00922

Deeb, R., Tufford, D., Scott, G. I., Moore, J. G., & Dow, K. (2018). Impact of climate change on *Vibrio vulnificus* abundance and exposure risk. Estuaries and Coasts, 41(8), 2289–2303. https://doi.org/10.1007/s12237-018-0424-5 Dickinson, G., Lim, K. Y., & Jiang, S. C. (2013). Quantitative microbial risk assessment of pathogenic vibrios in marine recreational waters of Southern California. Applied and Environmental Microbiology, 79(1), 294–302. https://doi.org/10.1128/AEM.02674-12

Edelson, P. J., Harold, R., Ackelsberg, J., Duchin, J. S., Lawrence, S. J., Manabe, Y. C., et al. (2022). Climate change and the epidemiology of infectious diseases in the United States. Clinical infectious diseases. Advance Online Publication. ciac697. https://doi.org/10.1093/cid/ciac697

Epstein, P. R. (2001). Climate change and emerging infectious diseases. Microbes and Infection, 3(9), 747–754. https://doi.org/10.1016/ s1286-4579(01)01429-0 FAO and WHO. (2020). Risk assessment tools for *Vibrio parahaemolyticus* and *Vibrio vulnificus* associated with seafood. In Microbiological risk assessment series No. 20.

Fernandez-Piquer, J., Bowman, J. P., Ross, T., & Tamplin, M. L. (2011). Predictive models for the effect of storage temperature on *Vibrio parahaemolyticus* viability and counts of total viable bacteria in Pacific oysters (Crassostrea gigas). Applied and Environmental Microbiology, 77(24), 8687–8695. https://doi.org/10.1128/AEM.05568-11

Froelich, B., Bowen, J., Gonzalez, R., Snedeker, A., & Noble, R. (2013). Mechanistic and statistical models of total *Vibrio* abundance in the Neuse River Estuary. Water Research, 47(15), 5783–5793. https://doi.org/10.1016/j.watres.2013.06.050

Froelich, B. A., & Daines, D. A. (2020). In hot water: Effects of climate change on *Vibrio*-human interactions. Environmental Microbiology, 22(10), 4101–4111. https://doi.org/10.1111/1462-2920.14967

Garcia-Soto, C., Cheng, L., Caesar, L., Schmidtko, S., Jewett, E. B., Cheripka, A., et al. (2021). An overview of Ocean climate change indicators: Sea surface temperature, ocean heat content, ocean pH, dissolved oxygen concentration, Arctic sea ice extent, thickness and volume, sea level and strength of the AMOC (Atlantic Meridional Overturning Circulation). Frontiers in Marine Science, 8, 642372. https://doi.org/10.3389/ fmars.2021.642372

Gavin, H. E., Beubier, N. T., & Satchell, K. J. (2017). The effector domain region of the *Vibrio vulnificus* MARTX toxin confers biphasic epithelial barrier disruption and is essential for systemic spread from the intestine. PLoS Pathogens, 13(1), e1006119. https://doi.org/10.1371/ journal.ppat.1006119

Greenfield, D. I., Gooch Moore, J., Stewart, J. R., Hilborn, E. D., George, B. J., Li, Q., et al. (2017). Temporal and environmental factors driving *Vibrio vulnificus* and *V.*

parahaemolyticus populations and their associations with harmful algal blooms in South Carolina detention ponds and receiving tidal creeks. GeoHealth, 1(9), 306–317. https://doi.org/10.1002/2017GH000094

Han, N., Mizan, M. F. R., Jahid, I. K., & Ha, S. (2016). Biofilm formation by *Vibrio parahaemolyticus* on food and food contact surfaces increases with rise in temperature. Food Control, 70, 161–166. https://doi.org/10.1016/j.foodcont.2016.05.054

Harjai, K., Khandwahaa, R. K., Mittal, R., Yadav, V., Gupta, V., & Sharma, S. (2005). Effect of pH on production of virulence factors by biofilm cells of Pseudomonas aeruginosa. Folia Microbiologica, 50(2), 99–102. https://doi.org/10.1007/BF02931455

Hostacká, A., Ciznár, I., & Stefkovicová, M. (2010). Temperature and pH affect the production of bacterial biofilm. Folia Microbiologica, 55(1), 75–78. https://doi.org/10.1007/s12223-010-0012-y

Huisman, J., Codd, G. A., Paerl, H. W., Ibelings, B. W., Verspagen, J. M. H., & Visser, P. M. (2018). Cyanobacterial blooms. Nature Reviews Microbiology, 16(8), 471–483. https://doi.org/10.1038/s41579-018-0040-1

Jang, K. K., Gil, S. Y., Lim, J. G., & Choi, S. H. (2016). Regulatory characteristics of *Vibrio vulnificus* gbpA gene encoding a mucin-binding protein essential for pathogenesis. Journal of Biological Chemistry, 291(11), 5774–5787. https://doi.org/10.1074/jbc.M115.685321

Jefferson, K. K. (2004). What drives bacteria to produce a biofilm? FEMS Microbiology Letters, 236(2), 163–173. https://doi.org/10.1016/j. femsle.2004.06.005

Johnson, D. E., Calia, F. M., Musher, D. M., & Goree, A. (1984). Resistance of *Vibrio vulnificus* to serum bactericidal and opsonizing factors: Relation to virulence in suckling mice and humans. The Journal of Infectious Diseases, 150(3), 413–418. https://doi.org/10.1093/infdis/150.3.413

Jones, M. K., & Oliver, J. D. (2009). *Vibrio vulnificus*: Disease and pathogenesis. Infection and Immunity, 77(5), 1723–1733. https://doi. org/10.1128/IAI.01046-08

Kang, I. H., Kim, J. S., Kim, E. J., & Lee, J. K. (2007). Cadaverine protects *Vibrio vulnificus* from superoxide stress. Journal of Microbiology and Biotechnology, 17(1), 176–179.

Kim, C. M., Ahn, Y. J., Kim, S. J., Yoon, D. H., & Shin, S. H. (2016). Temperature change induces the expression of vuuA encoding vulnibactin receptor and crp encoding cyclic AMP receptor protein in *Vibrio vulnificus*. Current Microbiology, 73(1), 54–64. https://doi.org/10.1007/ s00284-016-1026-8

Kim, Y. W., Lee, S. H., Hwang, I. G., & Yoon, K. S. (2012). Effect of temperature on growth of *Vibrio parahaemolyticus* [corrected] and *Vibrio vulnificus* in flounder, salmon sashimi, and oyster meat. International Journal of Environmental Research and Public Health, 9(12), 4662–4675. https://doi.org/10.3390/ijerph9124662

Koga, T., Katagiri, T., Hori, H., & Takumi, K. (2002). Alkaline adaptation induces cross-protection against some environmental stresses and morphological change in *Vibrio parahaemolyticus*. Microbiological Research, 157(4), 249–255. https://doi.org/10.1078/0944-5013-00160

Landrigan, P. J., Stegeman, J. J., Fleming, L. E., Allemand, D., Anderson, D. M., Backer, L. C., et al. (2020). Human health and ocean pollution. Annals of Global Health, 86(1), 151. https://doi.org/10.5334/aogh.2831

Li, L., Mendis, N., Trigui, H., Oliver, J. D., & Faucher, S. P. (2014). The importance of the viable but non-culturable state in human bacterial pathogens. Frontiers in Microbiology, 5, 258. https://doi.org/10.3389/fmicb.2014.002583

Main, C. R., Salvitti, L. R., Whereat, E. B., & Coyne, K. J. (2015). Community-level and species-specific associations between phytoplankton and particle-associated *Vibrio* species in Delaware's Inland Bays. Applied and Environmental Microbiology, 81(17), 5703–5713. https://doi. org/10.1128/AEM.00580-15

Martinez-Urtaza, J., Lozano-Leon, A., Varela-Pet, J., Trinanes, J., Pazos, Y., & Garcia-Martin, O. (2008). Environmental determinants of the occurrence and distribution of *Vibrio parahaemolyticus* in the rias of Galicia, Spain. Applied and Environmental Microbiology, 74(1), 265–274. https://doi.org/10.1128/AEM.01307-07

Midani, F. S., Collins, J., & Britton, R. A. (2021). AMiGA: Software for automated analysis of microbial growth assays. mSystems, 6(4), e00508. https://doi.org/10.1128/mSystems.00508-21

Mora, C., McKenzie, T., Gaw, I. M., Dean, J. M., von Hammerstein, H., Knudson, T. A., et al. (2022). Over half of known human pathogenic diseases can be aggravated by climate change. Nature Climate Change, 12(9), 869–875. https://doi.org/10.1038/s41558-022-01426-1

Mudoh, M. F., Parveen, S., Schwarz, J., Rippen, T., & Chaudhuri, A. (2014). The effects of storage temperature on the growth of *Vibrio parahaemolyticus* and organoleptic properties in oysters. Frontiers in Public Health, 2, 45. https://doi.org/10.3389/fpubh.2014.00045

Natividad-Bonifacio, I., Fernández, F. J., Quiñones-Ramírez, E. I., Curiel-Quesada, E., & Vázquez-Salinas, C. (2013). Presence of virulence markers in environmental *Vibrio vulnificus* strains. Journal of Applied Microbiology, 114(5), 1539–1546. https://doi.org/10.1111/jam.12149

Neumann, B., Vafeidis, A. T., Zimmermann, J., & Nicholls, R. J. (2015). Future coastal population growth and exposure to sea-level rise and coastal flooding—A global assessment. PLoS One, 10(6), e0131375. https://doi.org/10.1371/journal.pone.0118571

Newton, A., Kendall, M., Vugia, D. J., Henao, O. L., & Mahon, B. E. (2012). Increasing rates of vibriosis in the United States, 1996-2010: Review of surveillance data from 2 systems. Clinical Infectious Diseases, 54(0 5), S391–S395. https://doi.org/10.1093/cid/cis243

Nilsson, W. B., Paranjype, R. N., DePaola, A., & Strom, M. S. (2003). Sequence polymorphism of the 16S rRNA gene of *Vibrio vulnificus* is a possible indicator of strain virulence. Journal of Clinical Microbiology, 41(1), 442–446. https://doi.org/10.1128/JCM.41.1.442-446.2003

Nishibuchi, M., Fasano, A., Russell, R. G., & Kaper, J. B. (1992). Enterotoxigenicity of *Vibrio parahaemolyticus* with and without genes encoding thermostable direct

hemolysin. Infection and Immunity, 60(9), 3539–3545. https://doi.org/10.1128/iai.60.9.3539-3545.1992

Norman, R., & Correa Velez, K. E. (2022). Modeling pH and temperature effects as climatic hazards in *Vibrio vulnificus* and *Vibrio parahaemolyticus* planktonic growth and biofilm formation. In Mendeley data, V1. https://doi.org/10.17632/xxkkkbx3hg.1

Nowakowska, J., & Oliver, J. D. (2013). Resistance to environmental stresses by *Vibrio vulnificus* in the viable but nonculturable state. FEMS Microbiology Ecology, 84(1), 213–222. https://doi.org/10.1111/1574-6941.12052

Oliver, J. D. (2010). Recent findings on the viable but non-culturable state in pathogenic bacteria. FEMS Microbiology Reviews, 34(4), 415–425. https://doi.org/10.1111/j.1574-6976.2009.00200.x

Oliver, J. D. (2015). The biology of *Vibrio vulnificus*. Microbiology Spectrum, 3(3). https://doi.org/10.1128/microbiolspec.VE-0001-2014 Oliver, J. D., & Colwell, R. R. (1973). Extractable lipids of gram-negative marine bacteria: Phospholipid composition. Journal of Bacteriology, 114(3), 897–908. https://doi.org/10.1128/jb.114.3.897-908.1973

O'Neil, J. M., Davis, T. W., Burford, M. A., & Gobler, C. J. (2012). The rise of harmful cyanobacteria blooms: Potential role of eutrophication and climate change. Harmful Algae, 14, 313–334. https://doi.org/10.1016/j.hal.2011.10.027

O'Toole, G. A. (2011). Microtiter dish biofilm formation assay. Journal of Visualized Experiments: JoVE(47), 2437. https://doi.org/10.3791/2437

Paerl, H. W., & Paul, V. J. (2012). Climate change: Links to global expansion of harmful cyanobacteria. Water Research, 46(5), 1349–1363. https://doi.org/10.1016/j.watres.2011.08.002

Panicker, G., Myers, M. L., & Bej, A. K. (2004). Rapid detection of *Vibrio vulnificus* in shellfish and Gulf of Mexico water by real-time PCR. Applied and Environmental Microbiology, 70(1), 498–507. https://doi.org/10.1128/AEM.70.1.498-507.2004

Paranjpye, R. N., & Strom, M. S. (2005). A *Vibrio vulnificus* type IV pilin contributes to biofilm formation, adherence to epithelial cells, and virulence. Infection and Immunity, 73(3), 1411–1422. https://doi.org/10.1128/IAI.73.3.1411-1422.2005

Patterson, M., & Hardy, D. (2008). Economic drivers of change and their oceanic-coastal ecological impact. In M. Patterson & B. C. Glavovic (Eds.), Ecological economics of the oceans and coasts (pp. 187–209).

Edward Elgar Publishing. Pazhani, G. P., Chowdhury, G., & Ramamurthy, T. (2021). Adaptations of *Vibrio parahaemolyticus* to stress during environmental survival, host colonization, and infection. Frontiers in Microbiology, 12, 737299. https://doi.org/10.3389/fmicb.2021.737299

Provoost, P., van Heuven, S., Soetaert, K., Laane, R. W. P. M., & Middelburg, J. J. (2010). Seasonal and long-term changes in pH in the Dutch coastal zone. Biogeosciences, 7(11), 3869–3878. https://doi.org/10.5194/bg-7-3869-2010

Raven, J. A., Gobler, C. J., & Hansen, P. J. (2020). Dynamic CO2 and pH levels in coastal, estuarine, and inland waters: Theoretical and observed effects on harmful algal blooms. Harmful Algae, 91, 101594. https://doi.org/10.1016/j.hal.2019.03.012

Ray, L. C., Collins, J. P., Griffin, P. M., Shah, H. J., Boyle, M. M., Cieslak, P. R., et al. (2021). Decreased incidence of infections caused by pathogens transmitted commonly through food during the COVID-19 Pandemic—Foodborne diseases active surveillance network, 10 U.S. Sites, 2017–2020. Morbidity and Mortality Weekly Report, 70(38), 1332–1336. https://doi.org/10.15585/mmwr.mm7038a4

Rhee, J. E., Kim, K. S., & Choi, S. H. (2005). CadC activates pH-dependent expression of the *Vibrio vulnificus* cadBA operon at a distance through direct binding to an upstream region. Journal of Bacteriology, 187(22), 7870–7875. https://doi.org/10.1128/JB.187.22.7870-7875.2005

Rhee, J. E., Rhee, J. H., Ryu, P. Y., & Choi, S. H. (2002). Identification of the cadBA operon from *Vibrio vulnificus* and its influence on survival to acid stress. FEMS Microbiology Letters, 208(2), 245–251. https://doi.org/10.1111/j.1574-6968.2002.tb11089.x

Rosales, D., Ellett, A., Jacobs, J., Ozbay, G., Parveen, S., & Pitula, J. (2022). Investigating the Relationship between nitrate, total dissolved nitrogen, and phosphate with abundance of pathogenic *Vibrio*s and harmful algal blooms in Rehoboth Bay, Delaware. Applied and Environmental Microbiology, 88(14), e0035622. https://doi.org/10.1128/aem.00356-22

Rosche, T. M., Smith, D. J., Parker, E. E., & Oliver, J. D. (2005). RpoS involvement and requirement for exogenous nutrient for osmotically induced cross protection in *Vibrio vulnificus*. FEMS Microbiology Ecology, 53(3), 455–462. https://doi.org/10.1016/j.femsec.2005.02.008 Rosche, T. M., Yano, Y., & Oliver, J. D. (2005). A rapid and simple PCR analysis indicates there are two subgroups

of *Vibrio vulnificus* which correlate with clinical or environmental isolation. Microbiology and Immunology, 49(4), 381–389. https://doi.org/10.1111/j.1348-0421.2005. tb03731.x

Sandrini, G., Tann, R. P., Schuurmans, J. M., van Beusekom, S. A., Matthijs, H. C., & Huisman, J. (2016). Diel variation in gene expression of the CO2-concentrating mechanism during a harmful cyanobacterial bloom. Frontiers in Microbiology, 7, 551. https://doi.org/10.3389/ fmicb.2016.00551

Semenza, J. C., Trinanes, J., Lohr, W., Sudre, B., Löfdahl, M., Martinez-Urtaza, J., et al. (2017). Environmental suitability of *Vibrio* infections in a warming climate: An early warning system. Environmental Health Perspectives, 125(10), 107004. https://doi.org/10.1289/EHP2198

Sheikh, H., John, A., Musa, N., Abdulrazzak, L. A., Alfatama, M., & Fadhlina, A. (2022). *Vibrio* spp. and their *Vibrio*cin as a *Vibrio*sis control measure in aquaculture. Applied Biochemistry and Biotechnology, 194(10), 4477–4491. https://doi.org/10.1007/s12010-022-03919-3

Sheikh, H. I., Najiah, M., Fadhlina, A., Laith, A. A., Nor, M. M., Jalal, K. C. A., & Kasan, N. A. (2022). Temperature upshift mostly but not always enhances the growth of *Vibrio* species: A systematic review. Frontiers in Marine Science, 9, 959830. https://doi.org/10.3389/ fmars.2022.959830

Shirai, H., Ito, H., Hirayama, T., Nakamoto, Y., Nakabayashi, N., Kumagai, K., et al. (1990). Molecular epidemiologic evidence for association of thermostable direct hemolysin (TDH) and TDH-related hemolysin of *Vibrio parahaemolyticus* with

gastroenteritis. Infection and Immunity, 58(11), 3568–3573. https://doi.org/10.1128/iai.58.11.3568-3573.1990

Small, C., & Nicholls, R. J. (2003). A global analysis of human settlement in coastal zones. Journal of Coastal Research, 19(3), 584–599.

Song, X., Ma, Y., Fu, J., Zhao, A., Guo, Z., Malakar, P. K., et al. (2017). Effect of temperature on pathogenic and non-pathogenic *Vibrio parahaemolyticus* biofilm formation. Food Control, 73(Part B), 485–491. https://doi.org/10.1016/j.foodcont.2016.08.041

Suikkanen, S., Pulina, S., Engström-Öst, J., Lehtiniemi, M., Lehtinen, S., & Brutemark, A. (2013). Climate change and eutrophication induced shifts in northern summer plankton communities. PLoS One, 8(6), e66475. https://doi.org/10.1371/journal.pone.0066475

Sullivan, T. J., & Neigel, J. E. (2018). Effects of temperature and salinity on prevalence and intensity of infection of blue crabs, Callinectes sapidus, by *Vibrio* cholerae, *V. parahaemolyticus*, and *V. vulnificus* in Louisiana. Journal of Invertebrate Pathology, 151, 82–90. https://doi. org/10.1016/j.jip.2017.11.004

Sun, F., Chen, J., Zhong, L., Zhang, X. H., Wang, R., Guo, Q., & Dong, Y. (2008). Characterization and virulence retention of viable but non-culturable *Vibrio* harveyi. FEMS Microbiology Ecology, 64(1), 37–44. https://doi.org/10.1111/j.1574-6941.2008.00442.x

Tack, D. M., Marder, E. P., Griffin, P. M., Cieslak, P. R., Dunn, J., Hurd, S., et al. (2019). Preliminary incidence and trends of infections with pathogens transmitted commonly through food—Foodborne diseases active surveillance network, 10

U.S. sites, 2015–2018. MMWR. Morbidity and Mortality Weekly Report, 68(16), 369–373. https://doi.org/10.15585/mmwr.mm6816a2

Tack, D. M., Ray, L., Griffin, P. M., Cieslak, P. R., Dunn, J., Rissman, T., et al. (2020). Preliminary incidence and trends of infections with pathogens transmitted commonly through food—Foodborne diseases active surveillance network, 10 U.S. sites, 2016–2019. Morbidity and Mortality Weekly Report, 69(17), 509–514. https://doi.org/10.15585/mmwr.mm6917a1

Thompson, J. R., Randa, M. A., Marcelino, L. A., Tomita-Mitchell, A., Lim, E., & Polz, M. F. (2004). Diversity and dynamics of a North Atlantic coastal *Vibrio* community. Applied and Environmental Microbiology, 70(7), 4103–4110. https://doi.org/10.1128/AEM.70.7.4103-4110.2004

Tison, D. L., Nishibuchi, M., Greenwood, J. D., & Seidler, R. J. (1982). *Vibrio vulnificus* biogroup 2: New biogroup pathogenic for eels. Applied and Environmental Microbiology, 44(3), 640–646. https://doi.org/10.1128/aem.44.3.640-646.1982

Trinanes, J., & Martinez-Urtaza, J. (2021). Future scenarios of risk of *Vibrio* infections in a warming planet: A global mapping study. The Lancet Planetary Health, 5(7), e426–e435. https://doi.org/10.1016/S2542-5196(21)00169-8

Turner, J. W., Good, B., Cole, D., & Lipp, E. K. (2009). Plankton composition and environmental factors contribute to *Vibrio* seasonality. The ISME Journal, 3(9), 1082–1092. https://doi.org/10.1038/ismej.2009.50

Vezzulli, L., Baker-Austin, C., Kirschner, A., Pruzzo, C., & Martinez-Urtaza, J. (2020). Global emergence of environmental non-O1/O139 *Vibrio* cholerae infections

linked with climate change: A neglected research field? Environmental Microbiology, 22(10), 4342–4355. https://doi. org/10.1111/1462-2920.15040

Vezzulli, L., Colwell, R. R., & Pruzzo, C. (2013). Ocean warming and spread of pathogenic vibrios in the aquatic environment. Microbial Ecology, 65(4), 817–825. https://doi.org/10.1007/s00248-012-0163-2

Vezzulli, L., Pezzati, E., Moreno, M., Fabiano, M., Pane, L., Pruzzo, C., & Consortium, V. S. (2009). Benthic ecology of *Vibrio* spp. and pathogenic *Vibrio* species in a coastal Mediterranean environment (La Spezia Gulf, Italy). Microbial Ecology, 58(4), 808–818. https://doi. org/10.1007/s00248-009-9542-8

Visser, P. M., Verspagen, J. M. H., Sandrini, G., Stal, L. J., Matthijs, H. C. P., Davis, T. W., et al. (2016). How rising CO2 and global warming may stimulate harmful cyanobacterial blooms. Harmful Algae, 54, 145–159. https://doi.org/10.1016/j.hal.2015.12.006

Vora, G. J., Meador, C. E., Bird, M. M., Bopp, C. A., Andreadis, J. D., & Stenger, D. A. (2005). Microarray-based detection of genetic heterogeneity, antimicrobial resistance, and the viable but non-culturable state in human pathogenic *Vibrio* spp. Proceedings of the National Academy of Sciences of the United States of America, 102(52), 19109–19114. https://doi.org/10.1073/pnas.0505033102

Wallace, R. B., Baumann, H., Grear, J. S., Aller, R. C., & Gobler, C. J. (2014). Coastal ocean acidification: The other eutrophication problem. Estuarine, Coastal and Shelf Science, 148, 1–13. https://doi.org/10.1016/j.ecss.2014.05.027

Wang, X., Liu, J., Liang, J., Sun, H., & Zhang, X. H. (2020). Spatiotemporal dynamics of the total and active *Vibrio* spp. populations throughout the Changjiang estuary in

China. Environmental Microbiology, 22(10), 4438–4455. https://doi.org/10.1111/1462-2920.15152

Wang, Y., & Gu, J. D. (2005). Influence of temperature, salinity and pH on the growth of environmental Aeromonas and *Vibrio* species isolated from Mai Po and the inner deep bay nature reserve Ramsar site of Hong Kong. Journal of Basic Microbiology, 45(1), 83–93. https://doi. org/10.1002/jobm.200410446

Wells, M. L., Karlson, B., Wulff, A., Kudela, R., Trick, C., Asnaghi, V., et al. (2020). Future HAB science: Directions and challenges in a changing climate. Harmful Algae, 91, 101632. https://doi.org/10.1016/j.hal.2019.101632

Williams, T. C., Blackman, E. R., Morrison, S. S., Gibas, C. J., & Oliver, J. D. (2014). Transcriptome sequencing reveals the virulence and environmental genetic programs of *Vibrio vulnificus* exposed to host and estuarine conditions. PLoS One, 9(12), e114376. https://doi.org/10.1371/ journal.pone.0114376

Wong, H. C., Peng, P. Y., Han, J. M., Chang, C. Y., & Lan, S. L. (1998). Effect of mild acid treatment on the survival, enteropathogenicity, and protein production in *Vibrio parahaemolyticus*. Infection and Immunity, 66(7), 3066–3071. https://doi.org/10.1128/IAI.66.7.3066-3071.1998

Wong, H. C., & Wang, P. (2004). Induction of viable but nonculturable state in *Vibrio parahaemolyticus* and its susceptibility to environmental stresses. Journal of Applied Microbiology, 96(2), 359–366. https://doi.org/10.1046/j.1365-2672.2004.02166.x

Wu, X., Tian, H., Zhou, S., Chen, L., & Xu, B. (2014). Impact of global change on transmission of human infectious diseases. Science China Earth Sciences, 57(2), 189–203. https://doi.org/10.1007/s11430-013-4635-0

Yang, L., Barken, K. B., Skindersoe, M. E., Christensen, A. B., Givskov, M., & Tolker-Nielsen, T. (2007). Effects of iron on DNA release and biofilm development by *Pseudomonas aeruginosa*. Microbiology, 153(Pt 5), 1318–1328. https://doi.org/10.1099/mic.0.2006/004911-0

Zaidenstein, R., Sadik, C., Lerner, L., Valinsky, L., Kopelowitz, J., Yishai, R., et al. (2008). Clinical characteristics and molecular subtyping of *Vibrio vulnificus* illnesses, Israel. Emerging Infectious Diseases, 14(12), 1875–1882. https://doi.org/10.3201/eid1412.080499

Zepernick, B. N., Gann, E. R., Martin, R. M., Pound, H. L., Krausfeldt, L. E., Chaffin, J. D., & Wilhelm, S. W. (2021). Elevated pH conditions associated With Microcystis spp. blooms decrease viability of the cultured diatom *Fragilaria crotonensis* and natural diatoms in Lake Erie. Frontiers in Microbiology, 12, 598736. https://doi.org/10.3389/fmicb.2021.598736

Table C.1. *Vibrio* Strains Used in This Study

Strain ID	Type	Source	Location	Characteristics
V. vulnificus NBRC 15645 = ATCC 27562	Clinical	Human	Florida, USA	Type strain, 16S type B, biotype 1
			Human blood	
V. vulnificus ATCC 33147	Environmental	Eel	Japan	16S type A, biotype 2
			Diseased eel	
V. vulnificus NOAA48	Environmental	Water	South Carolina, USA	16S type A
			ACE Basin, 28°C, 26 g/kg, pH = 7.8	
V. vulnificus NOAA155	Environmental	Water	South Carolina, USA	16S type B, *pilF* positive
			Winyah Bay, 28°C, 10 g/kg, pH = 7.3	
V. parahaemolyticus ATCC 17802	Clinical	Human	Japan	tlh/trh
			Shirasu food poisoning	
V. parahaemolyticus 48057 (BEI NR-21990)	Clinical	Human	Washington, USA	tlh/tdh/trh,
			Clinical case of food poisoning	serotype O4:K12

Strain ID	Type	Source	Location	Characteristics
V. parahaemolyticus C12	Environmental	Water	South Carolina, USA	tlh
			Winyah Bay, Oyster Landing,	
			22°C, 34 g/kg, pH = 7.6	
V. parahaemolyticus 4.1PR	Environmental	Oyster	Cabo Rojo, PR	tlh
			Boquerón, 28°C, 35 g/kg, pH = 8	

Table C.2. Randomized Complete Block ANOVA Results for Effects of Temperature and pH in *Vibrio* spp.

Vibrio species			**Sum of squares**	**df**	**Mean square**	**F value**	**Pr (>F)**	**Partial eta squared**
Planktonic Growth	*Vibrio vulnificus*	Strain (block)	1.917	3	0.639	7.608	<0.001 [a]	0.060
		Temperature	17.004	2	8.502	101.239	<0.001 [a]	0.360

Vibrio species		Sum of squares	df	Mean square	F value	Pr (>F)	Partial eta squared
	pH	51.746	10	5.175	61.619	<0.001 [a]	0.631
	Temperature [a] pH	11.118	20	0.556	6.620	<0.001 [a]	0.269
	Error	30.232	360	0.084			
Vibrio parahaemolyticus	Strain (block)	5.083	3	1.694	16.706	<0.001 [a]	0.122
	Temperature	25.424	2	12.712	125.346	<0.001 [a]	0.411
	pH	45.407	10	4.541	44.774	<0.001 [a]	0.554
	Temperature [a] pH	4.884	20	0.244	2.408	<0.001 [a]	0.118
	Error	36.509	360	0.101			
	Strain (block)	24.523	3	8.174	2.158	0.093	0.022

	Vibrio species		**Sum of squares**	**df**	**Mean square**	**F value**	**Pr (>F)**	**Partial eta squared**
Biofilm Growth	*Vibrio vulnificus*	Temperature	84.573	2	42.286	11.161	<0.001 [a]	0.071
		pH	39.560	10	3.956	1.044	0.406	0.034
		Temperature [a] pH	82.672	20	4.134	1.091	0.358	0.069
		Error	1113.890	294	3.789			
	Vibrio parahaemolyticus	Strain (block)	358.521	3	119.507	28.322	<0.001 [a]	0.191
		Temperature	282.231	2	141.116	33.443	<0.001 [a]	0.157
		pH	232.738	10	23.274	5.516	<0.001 [a]	0.133
		Temperature [a] pH	115.935	20	5.797	1.374	0.132	0.071
		Error	1519.034	360	4.220			

Note. Growth Rate. Independent factors: temperature, pH; Dependent variable: growth rate; Block factor: strain.

[a] Significant: $p < 0.05$.

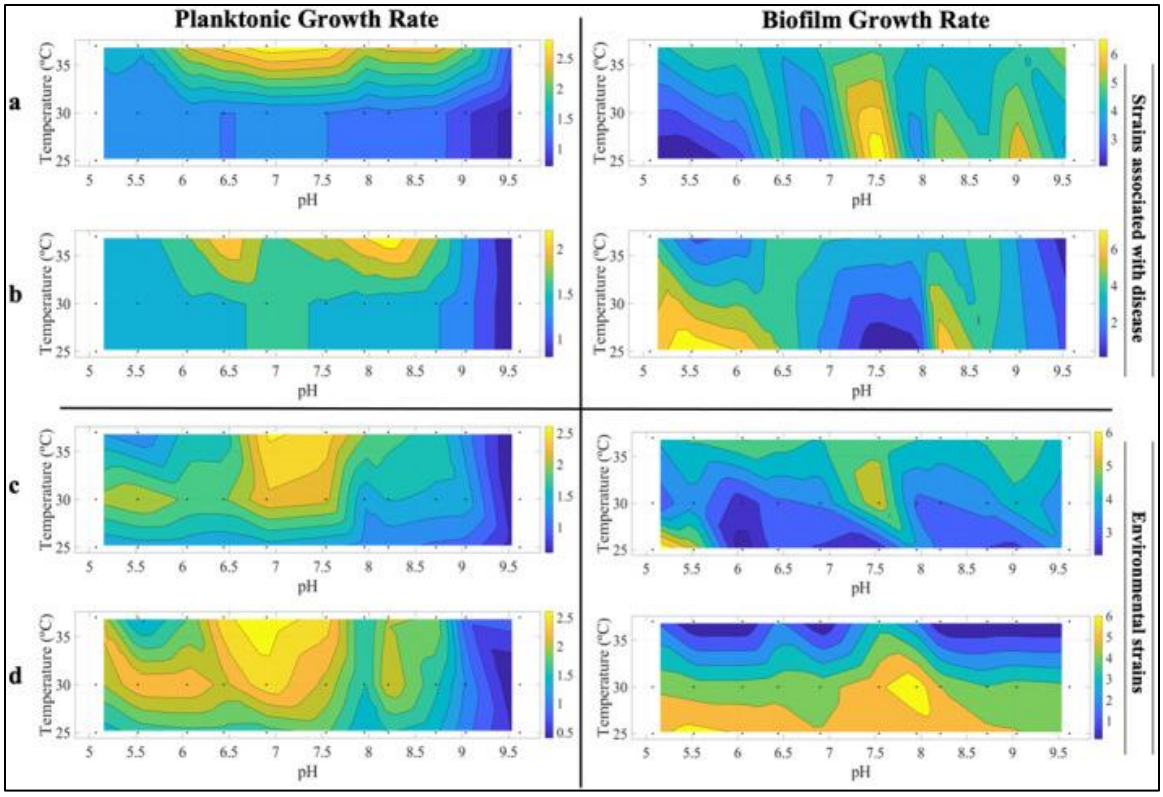

Figure C.1. Modeling of bacterial growth rates in planktonic and biofilm stages of *V. vulnificus* strains at different temperatures and pH ranges. Strains associated with disease in humans and animals are shown in panels a (*V. vulnificus* NBRC 15645 = ATCC 27562) and b (*V. vulnificus* ATCC 33147). Environmental strains are shown in panels c (*V. vulnificus* NOAA 48) and d (*V. vulnificus* NOAA 155). Growth rates are calculated as (ddtlnOD) with yellow representing higher growth rates and blue representing lower growth rates.

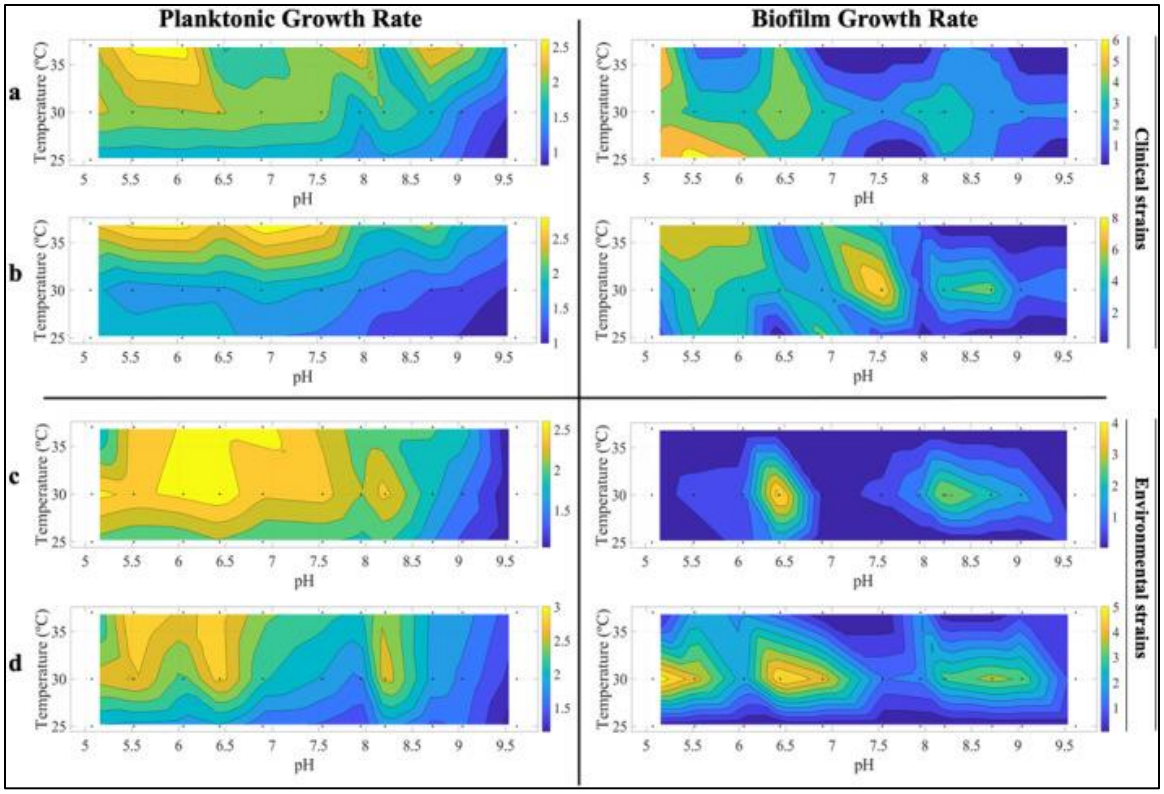

Figure C.2. Modeling of bacterial growth rates in planktonic and biofilm stages of *V. parahaemolyticus* strains at different temperatures and pH ranges. Clinical reference strains are shown in panels a (*V. parahaemolyticus* ATCC 17802) and b (*V. parahaemolyticus* 48057). The environmental strains are shown in panels c (*V. parahaemolyticus* C12) and d (*V. parahaemolyticus* 4.1PR). Growth rates are calculated as (ddtlnOD) with yellow representing higher growth rates and blue representing lower growth rates.

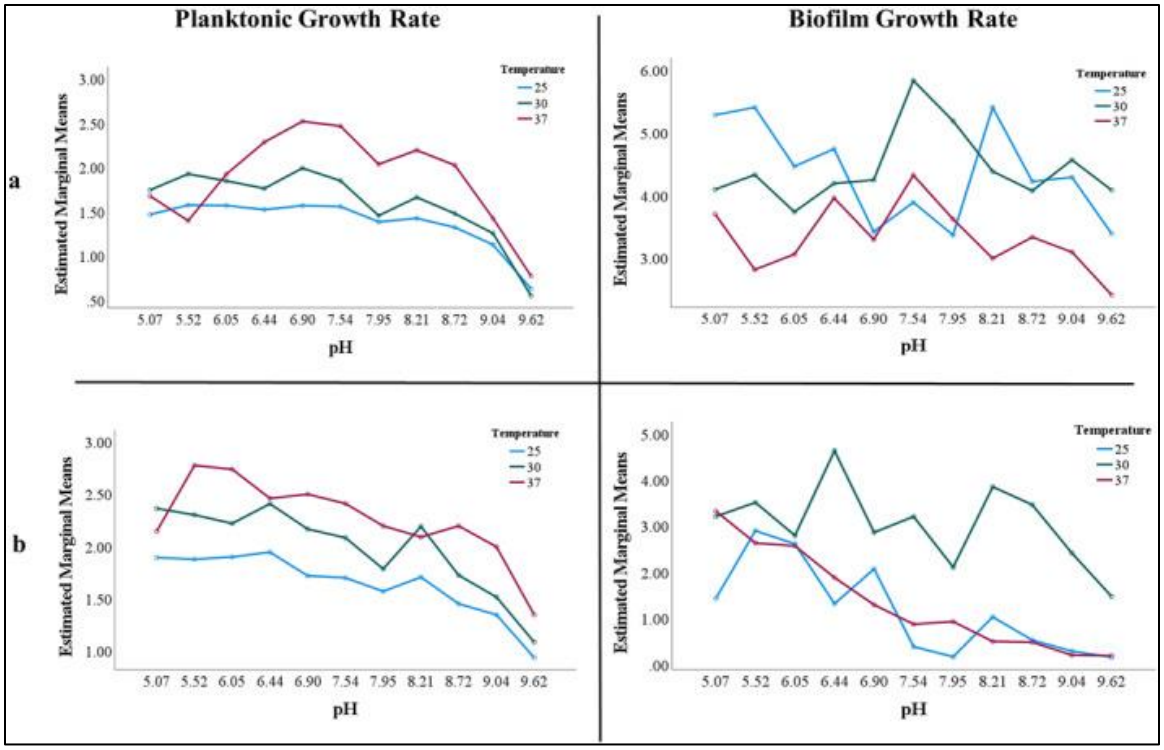

Figure C.3. Interaction plots of the estimated marginal means of growth rate in planktonic and biofilm stages of *Vibrio* spp. at different temperatures and ranges of pH. Panel a shows *V. vulnificus* strains, and Panel b shows *V. parahaemolyticus* strains. The line colors represent the different temperatures: 25ºC (blue), 30°C (green), and 37°C (red). The estimated marginal means of the growth rate are expressed in ddtlnOD.

Permission to Reprint: